ISSN 0973-3302

JOURNAL OF ACOUSTICAL SOCIETY OF INDIA

Volume 37 Number 1 January 2010

A Quarterly Publication of the JASI
http://www.acousticsindia.org

JASI

Journal of Acoustical Society of India

The Refereed Journal of the Acoustical Society of India (JASI)

The Journal of Acoustical Society of India is a refereed journal of the Acoustical Society of India **(ASI)**. The **ASI** is a non-profit national society founded in 31st July, 1971. The primary objective of the society is to advance the science of acoustics by creating an organization that is responsive to the needs of scientists and engineers concerned with acoustics problems all around the world.

Manuscripts of articles, technical notes and letter to the editor should be submitted to the Chief Editor. Copies of articles on specific topics listed above should also be submitted to the respective Associate Scientific Editor. Manuscripts are refereed by at least two referees and are reviewed by Publication Committee (all editors) before acceptance. On acceptance, revised articles with the text and figures scanned as separate files on a diskette should be submitted to the Editor by express mail. Manuscripts of articles must be prepared in strict accordance with the author instructions.

All information concerning subscription, new books, journals, conferences, etc. should be submitted to Chief Editor:

Acoustics Section, National Physical Laboratory, Dr. KS Krishnan Road, New Delhi 110 012,
Tel: +91.11.4560.9319, Fax: +91.11.4560.9310, e-mail: mahavir@nplindia.org

Annual subscription price including mail postage is Rs. 2000/= for institutions, companies and libraries and Rs. 2000/= for individuals who are not **ASI** members. The Journal of Acoustical Society of India will be sent to **ASI** members free of any extra charge. Requests for specimen copies and claims for missing issues as well as address changes should be sent to the Editorial Office:

Acoustics Section, National Physical Laboratory, Dr. KS Krishnan Road, New Delhi 110 012,
Tel: +91.11.4560.9319, Fax: +91.11.4560.9310, e-mail: mahavir@nplindia.org

ISSN 0973-330

Printed at Alpha Printers, BG-2/38C, Paschim Vihar, New Delhi-110063 Tel.: 9811848335. JASI is sent to ASI members free of charge.

JASI

Journal of Acoustical Society of India (JASI)

A quarterly publication of the Acoustical Society of India

Volume 37, Number 1, January 2010

EDITORIAL

ARTICLES

INFORMATION

Sound Transmission through Building Enclosures

This article deals with sound transmission through building enclosures including different forms of predominantly lightweight wall construction. It gives guidance on how walls comprising a number of separate elements can be assessed. Sound transmission from outside to inside be covered. Although many aspects are common to sound transmission from inside to outside the reader should also see BS EN 12354-4:2000 if they are concerned with containment of sound within a building.

The performance of a wall or roof has to be considered in terms of the internal spaces. The aim is to provide a building envelope that gives the required sound pressure levels within a room or other internal space. The noise level within a room will depend on the amount of sound energy transmitted through the wall and interreflection of sound inside the room. The room effect is usually determined by the amount of sound absorbing material in the room. Sound transmission of an assembly of components can be calculated provided the wall can be analysed as discrete areas, for each of which the Sound Reduction Index is known.

This applies to windows in walls and collections of windows but note that sound transmission through interface components such a joining mullions between windows may not be known.

Sound transmission through a whole wall is established by calculating an apparent sound reduction index (SRI) for the wall. This is used to determine the difference in sound between the outside and inside. The procedure is to calculate the sound power reduction for each element of the wall. The total sound power reduction can then be calculated and converted to an apparent sound reduction index.

When sound of intensity 1W/m^2 falls on a wall, the sound power (in watts) transmitted by an element is given by:

$$W_i = S_i 10^{-\frac{R_i}{10}}$$

where

S_i is the area of an element (m^2)

R_i is the Sound Reduction Index of that element (dB)

Mahavir Singh

Journal of Acoustical Society of India : Vol. 37, No. 1, 2010 (pp. 3-8)

Acoustic Material Characterization Using Inverse and Simulation Techniques and Its Validation

S.K. Jain and S. Raju
The Automotive Research Association of India, NVH & CAE Department, Vetal Hill, Off Paud Road, Kothrud, City Pune 411 038, INDIA
jain.nvh@araiindia.com and sraju.nvh@araiindia.com

ABSTRACT

Acoustic materials are generally poro-elastic in nature. A number of attempts have been made to simulate, predict and optimize the various parameters of acoustic material for different applications particularly for multi-layer composite materials. There are number of commercially available softwares based on Finite Element and Transfer Matrices to carry out this sort of work. Among these, two software viz. Virtual Lab and NOVA based on Biot's Model are well known. Both the softwares require nine intrinsic material properties as input viz. five acoustic - Flow Resistivity, Porosity, Tortuosity, Viscous Characteristic Length and Thermal Characteristic Length and four physical - Density, Young's Modulus, Loss Factor and Poisson's Ratio. All these parameters are difficult to measure in the absence of standardized procedure except for Flow Resistivity and Density. Remaining parameters are determined by individual laboratories working in this area using their own methods. To overcome this problem, an inverse characterization technique is being used in recent times for computing five acoustic parameters using the Sound Absorption Coefficient (SAC) measured in an impedance tube as per ISO 10534-2. This paper presents comparison of these five parameters predicted by inverse characterization and also physical validation of three parameters, which were possible to measure. The results of a study carried out to understand the consistency of measurement with respect to sample-to-sample variation, sample preparation and mounting methodology and lab-to-lab variations on SAC are also presented and discussed.

1. INTRODUCTION

Porous materials such as foams and fibers have many applications for passive noise control in automotive, aircraft and building acoustics. It is necessary for the noise control engineer to have means to predict the sound absorption of the material at the design stage itself so that many combinations can be tried out and the best possible ones can be arrived at before making prototypes. There are already commercially available software such as the VIOLINS module of VIRTUAL LAB of LMS and NOVA of ESI, which can simulate and predict the acoustic characteristics of the material such as absorption coefficient, surface impedance and transmission loss, even for multi-layer acoustic material. These softwares can effectively be used in a cost and time effective manner to optimize the acoustic design of systems. Both the softwares are based on Biot's Model for the 2-phase porous material and mixed displacement formulation. VIOLINS uses a 3-D Finite Element approach combined with a Boundary Element procedure in order to assess the radiated acoustic field[1]. NOVA uses a transfer matrix method with correction for finite size effects in the mid and high frequencies while it adopts a similar procedure like VIOLINS at low frequencies[2]. Because of the use of the Biot's theory, both the softwares require nine intrinsic material properties as input acoustic viz. Flow Resistivity, Porosity, Tortuosity, Viscous Characteristic Length (VCL) and Thermal Characteristic Length (TCL) and physical viz. Bulk density, Young's Modulus, Loss Factor and Poisson's Ratio. This in turn calls for individual test rigs for determining physically the properties, which many times are complicated. However, the major bottleneck is that there is no standardized procedure available for determining these properties, except for Flow Resistivity (ISO 9053) [3]. Presently determination of the remaining eight properties is carried out by individual laboratories working in this area using their own methods and no standardized procedure is in sight.

To overcome this problem, a technique called inverse characterization is used in recent times, where it is possible to compute the five acoustic parameters based on the measured sound absorption coefficient in an impedance tube as per ISO 10534-2[4]. One such software, which is commercially available, is FOAM-X of ESI. Some more groups such as Ferrara University, Italy, are working in this area as this looks an attractive solution to the difficult problem of material characterization. FOAM-X uses an inverse algorithm to identify the porous material properties using a non-linear best fit algorithm. Genetic algorithm based method is used by Ferrara University in Italy[5].

As a result, the characterization process relies heavily on the accuracy of experimental data on the absorption coefficient and surface impedance. The accuracy of this technique is affected by the quality and homogeneity of the material samples, their environmental and operational conditions during the experiments, the quality of setup, measured frequency range and frequency resolution and the material preparation and mounting method. These conditions and measurement apparatus can vary from lab to lab and their effect on the measured values of the sound absorption coefficient is not much reported.

2. METHODOLOGY

Round robin tests for sound absorption coefficient were carried out in four labs viz. University of Ferrara, Italy, B&K, Denmark, Mecanum Numerik Solution (MNS), Canada and ARAI, India. The materials were two types - PU foam of two different densities of 32 kg/m3 and 40 kg/m3 (A and B) and fibrous of two different densities of 24 kg/m3 and 45 kg/m3 (C and D). Specimens of these materials have been cut individually by the labs from adequate size sheets provided by ARAI to fit the diameters of the impedance tube. The diameter of impedance tube, measurement method, sample preparation procedure and method of mounting the sample in the labs are detailed in Table I. The measurements were carried out as per ISO 10534-2 and compared. Further to this, the inverse characterization methods by FOAM-X and Genetic algorithm were used to calculate the five parameters based on the measured sound absorption coefficient. This was compared with three physical parameters viz. flow resistivity, Porosity and Tortuosity, which were possible to measure. Further these five inverse parameters were used as input to VIOLINS and NOVA for prediction of sound absorption coefficient and compared with experimental results.

Table 1. Comparison of different test conditions in the four labs

Laboratory	Impedance tube dia, mm	Measured frequency range, Hz	Frequency resolution, Hz	Temp, ^{0}C / Humidity, %	Material preparation
ARAI, India	100 & 29	112 - 3152	16	29-30 / 45-50	Die cutting
Ferrara, Italy	45	125 - 4389	43	20-22 / 45-50	Rotating blade
B&K, Denmark	100 & 29	100 - 6400	2	15-20 / 50-60	Die cutting
MNS, Canada	45	260 - 4227	5	22-23 / 40-44	Die cutting

Comparison of Sound Absorption Coefficient and Inverse Characterization Techniques

In order to compare the two techniques available for inverse characterization, the same four materials, two foams (A and B) and two fibrous (C and D) were used. The sound absorption coefficient characteristics used for FOAM-X were measured in all four labs, while those used for Genetic algorithm, were measured in Ferrara and ARAI. Fig 1 to fig 4 shows the comparison of sound absorption results measured in each lab for sample A, B, C and D respectively. There are sensible differences in sound absorption characteristics between the four labs due to sample-to-sample variation (even though it was cut from the same sheet), measured frequency range and sample preparation and mounting, diameter of standing wave tube and signal processing method. This is not surprising as similar differences have been reported in literature[6].

In order to validate the five parameters predicted by inverse characterization, three parameters viz. Flow Resistivity, Porosity and Tortuosity could be physically measured as mentioned earlier.

Table II compares the five acoustic parameters predicted by FOAM-X and Genetic algorithms along with the three physically measured parameters. These techniques make use of non linear best-fit algorithms to determine the best solution to minimize a cost function calculated by means of a prediction model. They do not take into account the cause of variation in sound absorption during measurement. So in the inverse procedure the software will try to find global solutions for all parameters in the bounds provided inside the softwares on

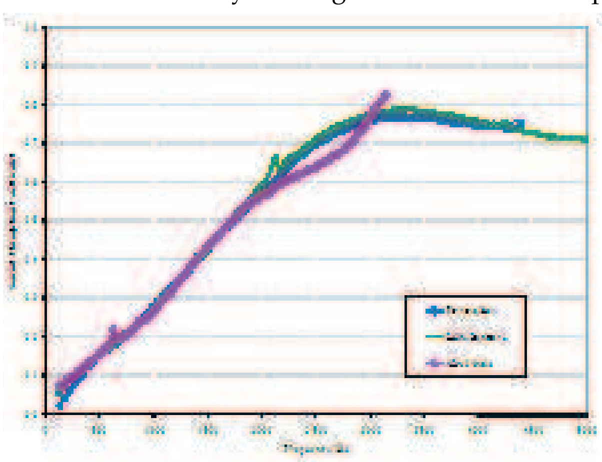

Fig. 1. Comparison of measured sound absorption in three labs of sample A

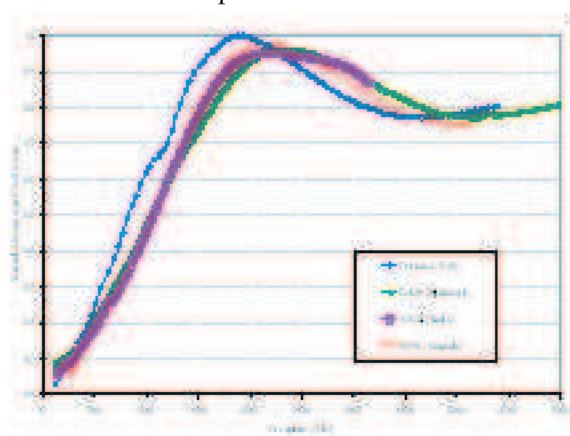

Fig. 2. Comparison of measured sound absorption in four labs of sample B

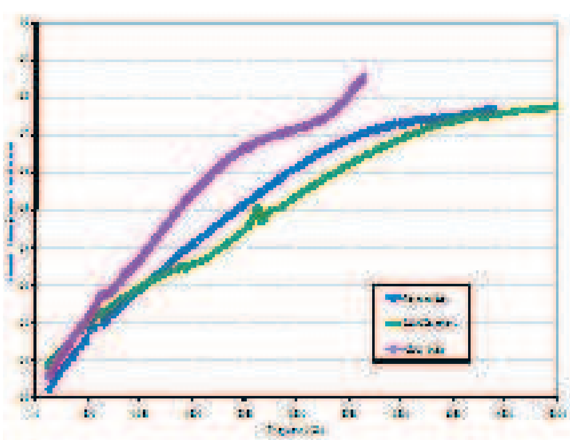

Fig. 3. Comparison of measured sound absorption in three labs of sample C

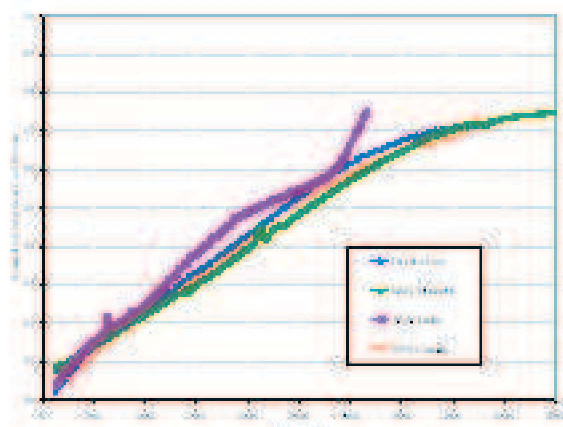

Fig. 4. Comparison of measured sound absorption in four labs of sample D

all parameters.

High variations in flow resistivity values obtained from both the FOAM X and Genetic algorithms are observed. A maximum of 200% is seen in case of foam - Ferrara results for sample A and B&K results for sample B. In case of felt, there is 147 % variation in two inverse results for B&K for sample C. Porosity of all the materials predicted is one or near to one. This may be because of the highly porous nature as seen from the measured porosity. Good correlation in tortuosity values for all the materials are observed except for sample B. The maximum variation between the inverse values is 74 % for ARAI result for sample B. When the measured flow resistivity, porosity, tortuosity and sound absorption coefficient were used as input for inverse characterization, it minimizes the error in remaining two parameters viz. VCL and TCL. Over all, B&K results are showing values near to physically measured for sample A and D, for sample B FOAM X is nearer while Genetic algorithm for sample C.

Another way of comparing the inverse characterization is to compare the measured sound absorption coefficient, used as an input to VIOLINS and NOVA. Figure 5 to 8 compares the input sound absorption coefficient and the predicted one with the five parameters obtained by inverse characterization by both FOAM-X and Genetic algorithms for Ferrara results. There are no significant variations seen for all the four materials using both the softwares.

Table 2. Comparison between physically measured and inversely determined parameters using FOAM X and Genetic Algorithms

Measurements Techniques		Flow resistivity, Ns/m^4		Porosity		Tortuosity		VCL, µm		TCL, µm	
		Sample A (PU Foam 32 kg/m^3 25 mm thick)									
		FOAM X	Genetic	FOAM X	Genetic	FOAM X	Genetic	FOAM X	Genetic	FOAM X	Genetic
Physical Measurements		8443		0.98		1.24		-		-	
Inverse Characterization	Ferrara, Italy	1622	4918	1	1	1.23	1.27	131	137	252	249
	B&K, Denmark	8354	7244	1	1	1.17	1.24	137(155)	161	322(315)	254
	ARAI, India	11045	12013	1	0.84	1	1.12	333	316	337	316
		Sample B (PU Foam 40 kg/m^3 25 mm thick)									
		FOAM X	Genetic	FOAM X	Genetic	FOAM X	Genetic	FOAM X	Genetic	FOAM X	Genetic
Physical Measurements		24119		0.98		1.76			-		-
Inverse Characterization	Ferrara, Italy	36386	21398	1	1	2.22	1.82	61	44	438	266
	B&K, Denmark	26799	8874	1	1	2.01	1.56	295(107)	60	375(314)	301
	ARAI, India	19364	20489	0.89	0.92	1.38	2.4	49	345	297	345
	MNS, Canada	10451	8789	0.86	1	1.62	1.66	82(63)	63	223(402)	307
		Sample C (Soft PET Felt 24 kg/m^3 32 mm thick)									
		FOAM X	Genetic	FOAM X	Genetic	FOAM X	Genetic	FOAM X	Genetic	FOAM X	Genetic
Physical Measurements		4788		0.98		1.01		-		-	
Inverse Characterization	Ferrara, Italy	6084	6634	1	1	1	1.06	559	147	561	203
	B&K, Denmark	2172	5373	1	1	1	1	270(400)	169	270(400)	239
	ARAI, India	7387	5842	1	0.99	1	1.19	290	275	290	274
		Sample D (Hard Felt 45 kg/m^3 22 mm thick)									
		FOAM X	Genetic	FOAM X	Genetic	FOAM X	Genetic	FOAM X	Genetic	FOAM X	Genetic
Physical Measurements		6734		0.99		1.03		-		-	
Inverse Characterization	Ferrara, Italy	6257	3229	0.97	1	1.08	1.07	165	122	246	206
	B&K, Denmark	7085	6364	1	1	1	1	270(260)	129	270(260)	236
	ARAI, India	10485	14057	1	1	1	1.3	254	288	257	292
	MNS, Canada	5435	5931	0.99	1	1	1.02	208(229)	165	358(346)	294

* The numbers in parenthesis indicates the values when measured flow resistivity, porosity, tortuosity and sound absorption coefficient were used as inputs for inverse characterization

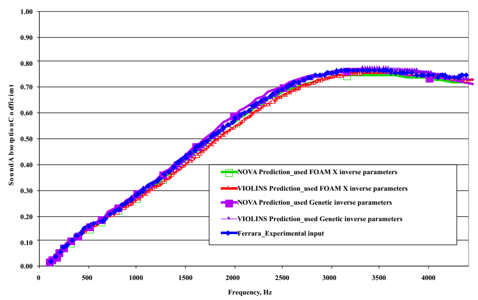

Fig. 5. Comparison between measured and predicted sound absorption for Ferrara of sample A

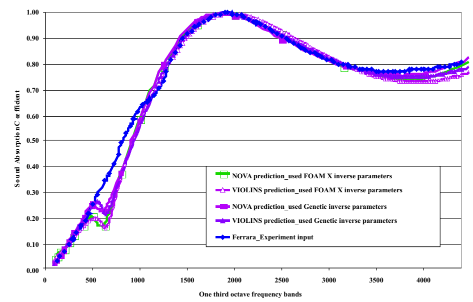

Fig. 6. Comparison between measured and predicted sound absorption for Ferrara of sample B

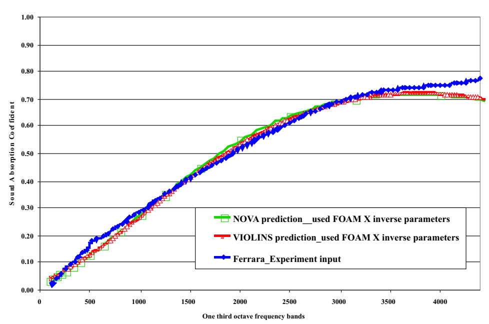

Fig. 7. Comparison between measured and predicted sound absorption for Ferrara of sample C

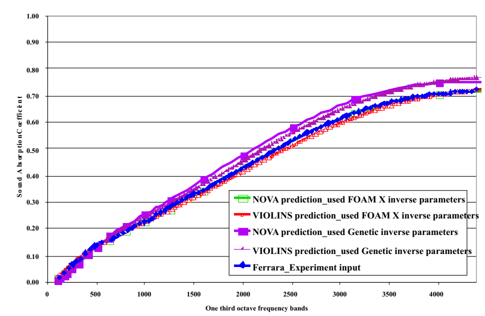

Fig. 8. Comparison between measured and predicted sound absorption for Ferrara of sample D

3. CONCLUSION

It was found that using six parameters viz. five acoustic and density are adequate to predict the sound absorption coefficient using Biot's model of porous material instead of the nine parameters, which are required for the available software today viz. VIOLINS and NOVA. These five acoustic parameters can be found out by inverse characterization for which softwares are getting evolved. Typical ones are FOAM-X and Genetic Algorithm from Ferrara University. These are found to be reasonably accurate. However, a better understanding of the physical parameters and their correlation to the software is required before they can be used effectively. This can provide a quick solution for design optimization of acoustic systems using the commercially available simulation software instead of going through the difficult process of determining all the nine parameters physically. In any case, standardized procedures for the measurement of the parameters have to be evolved, which is not in sight. A parametric study of the various parameters involved in the determination of sound absorption coefficient, its sensitivity and methods of control to ensure repeatability of results would go a long way in this methodology.

4. ACKNOWLEDGMENT

The authors would like to thank Director, ARAI and colleagues of NVH and CAE department for their support. They would also like to thank

- Mr. Paresh Shravage, Department of Engineering, Universita di Ferrara, Via Saragat, Italy
- Dr. Yunseon Ryu of Bruel & Kjaer, Denmark
- Prof. Noureddine Atalla, Mecanum Numerik Solution, Sherbrooke University, Canada
- Mr. Trevor Edwards, ESI group, France
- Mr. Vaibhav, ESI, India

for the experimental and simulation support for this work.

5 REFERENCES

[1] J.P. COYTTE and T.J. COATS, "VIOLINS-A Modeling Tool for Layered Materials", Society of Automotive Engineers Paper no. 980947.

[2] Literature on Nova, Multi-layered material acoustic simulation and design, ESI Group.

[3] ISO: 9053, "1991. Acoustics - Materials for acoustical applications - Determination of airflow resistivity".

[4] ISO: 10534-2, 1998. "Acoustics - Determination of sound absorption coefficient and impedance in impedance tubes".

[5] BONFIGLIO, PAOLO and POMPOLI, FRANCESCO, 2007. "Comparison of different inversion techniques for determining physical parameters of porous media", 19th International Congress on Acoustics, Madrid.

[6] V. KRILL HOROSHENKOV and AMIR KHAN, 2006. "Reproducibility experiments on measuring acoustical properties of rigid-frame porous media (round-robin tests)", ICSV 13, Vienna.

Journal of Acoustical Society of India : Vol. 37, No. 1, 2010 (pp. 9-14)

Design of a Single Suspension Element Passive Radiator for Compact Entertainment Speakers

Nachiketa Tiwari
Indian Institute of Technology, Kanpur, 208 016, India
e-mail: ntiwari@iitk.ac.in

ABSTRACT

Ports, also known as acoustic-mass elements are frequently used to enhance the bass response of entertainment speakers. While the appeal of ports lies in their simple design, no moving parts, high long term reliability, and low cost, they have limitations in terms of their size and also their suboptimal transient response. Also, the sound produced through these elements is not clean enough because of port noise attributable to turbulent fluid flow especially at high volume velocities. In contrast speakers which use passive radiators produce very clean sound and offer superior transient response due to high damping properties of their suspension elements. However, these acoustic elements cost more vis-a-vis ports, and their traditional designs are not necessarily compact enough either. In this paper, a passive radiator design is proposed which addresses these two limitations, and also does not compromise on other performance attributes. Unlike a traditional passive radiator which uses two suspension elements, the proposed design uses a single suspension element, thereby reducing the overall cost of the element and also makes it more compact. In this design process, due care was taken to ensure the stability of the proposed design given that it uses only one suspension elements.

1. DESCRIPTION OF THE PROBLEM

Acoustic mass elements, also known as ports, have been extensively used in entertainment speaker systems to enhance the bass response of the audio system [1]. Such systems are called bass reflex enclosures, where the port acts as a second "diaphragm" which is driven by the back side of the acoustic transducer pressure. Figure 1 shows the schematic of a representative bass reflex system. The port enhances the bass response of the system particularly at a frequency dependent on the value of acoustic-mass, and the compliance of the enclosed volume, Vo. However, numerical analysis of such systems through lumped parameter approach [2] shows that the size of the port increases with reduction in tuning frequency. Further, ports have suboptimal transient response because they have low damping properties. Finally, the signal-to-noise ratio of sound coming from ports is not acceptable particularly at high power levels because of turbulence conditions existing in port corresponding to high volume velocities.

These challenges, as they relate to performance attributes of the speaker, get sufficiently resolved if the port gets replaced by an actual diaphragm, i.e. passive radiator. This is shown in Fig. 2. Here, the diaphragm which has a moving mass m, and which radiates sound, is mounted on a 'surround' - a suspension element. The diaphragm is also connected to another suspension element, 'spider', through a thin barrel shaped 'bobbin'. Together, these two suspension elements ensure that the diaphragm is tuned for pistonic motion at appropriate frequencies, and also that the diaphragm does not exhibit rocking due to its natural mode of vibration below a

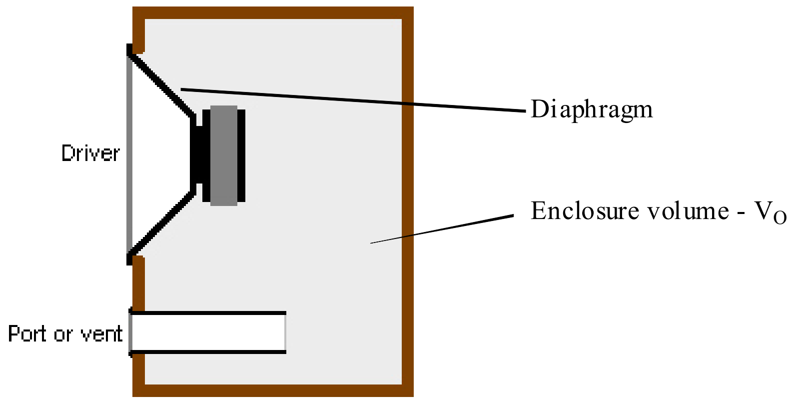

Fig. 1. Schematic Representation of Bass-Reflex Enclosure with a Port
(Source: http://upload.wikimedia.org/wikipedia/en/d/db/Bass_reflex_spk.PNG)

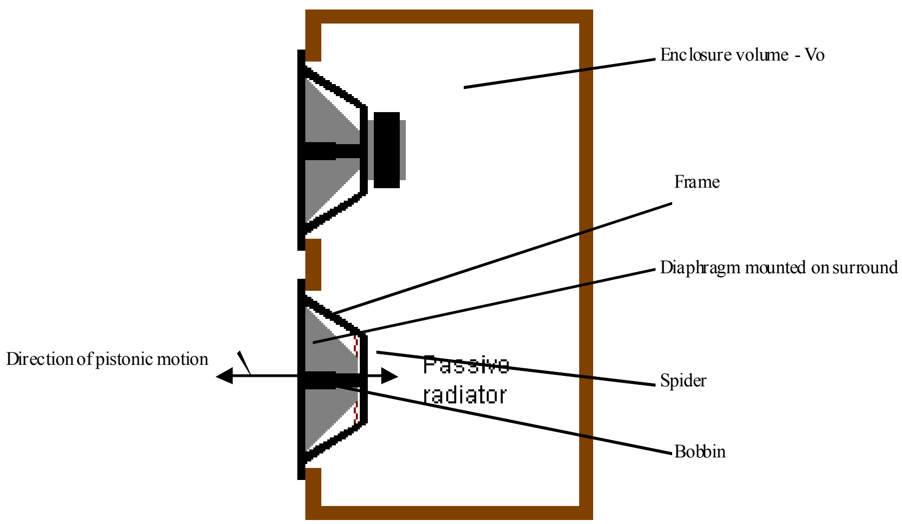

Fig. 2. Schematic Representation of Bass-Reflex Enclosure with a Passive Radiator
(Source: http://en.wikipedia.org/wiki/File:Passive_radiator_enclosure.gif)

pre-determined frequency. The direction of pistonic motion is shown in Fig. 2, and the rocking motion happens around an axis which is normal through the plane of paper and passes through the geometric centre of diaphragm. The entire passive radiator assembly is mounted on a 'frame', which in turn is attached to the speaker box.

In such a design, the transient response of the passive radiator is superb because the radiator is typically suspended by elastomeric springs with high damping properties. Also, such a design has no port noise whatsoever. However, such designs are more expensive, complex to manufacture, and also not sufficiently compact. In this paper, a simpler design is proposed which addresses these two concerns, and yet requires only one suspension element.

2. DESIGN PARAMETERS AND CONSTRAINTS

While developing such a design, the following considerations were taken into account:

- The diaphragm will not exhibit rocking mode in the operating bandwidth of the radiator, which is f1 - f2

Hz. This requirement is different than that used for developing conventional passive radiators, because in the latter design, rocking mode is avoided below a particular frequency number. In other words, the value of f1 for conventional designs is 0 Hz.

- The passive radiator will behave linearly within its operational excursion limits.
- It will not exhibit creep over a period of time due to gravity forces induced by moving mass of diaphragm.

The overall Thiele-Small parameters for the passive radiator were acquired by constructing a lumped parameter model of the entire loudspeaker as described in [1], specifying acoustic and input power targets, and solving the constructed model iteratively so that the set of Thiele-Small parameters for the radiator were technologically achievable, and reflected a cost effective design. Using such a process, the following parameters were extracted from the lumped parameter model as inputs to the detailed design of passive radiator.

Suspension stiffness (k): 2500 N/m	Moving mass (m): 68 gm
Radiating area (A): 0.01 m^2	Overall depth of passive radiator assembly: 25 mm
Operating bandwidth: 50 Hz - 120 Hz	Peak-to-peak excursion of diaphragm: 32 mm

These parameters were used to construct several alternative geometries for the passive radiator. In the next section, the details of the final converged design are presented.

3. DESIGN DETAILS

Figure 3 shows an isometric view of the proposed design with the nominal length and width of the radiating part of the surround. Figure 4 is a cross-section view of the assembly when it is cut along its longer line of symmetry. The passive radiator is made up to two parts - an elastomeric surround, and a metallic plate. While the surround provides stiffness to the element, the metallic plate, which can be thickened appropriately to achieve the desired moving mass target, provides bulk of the moving mass for the passive radiator. In the design proposed, the surround-roll has a midplane radius of 15 mm at its long end, and 12 mm at its narrow end. This variation of roll radius ensures that the surround does not buckle during excursion at its long end. Further, the material of the surround is carefully chosen so that it does not exhibit significant softening during operational temperature range of system. Further, whatever thermal softening is seen by the elastomer due to temperature effects, it is small in percentage terms when the overall stiffness of the speaker is considered, because the volume of the box also adds up to the overall stiffness seen by the passive radiator.

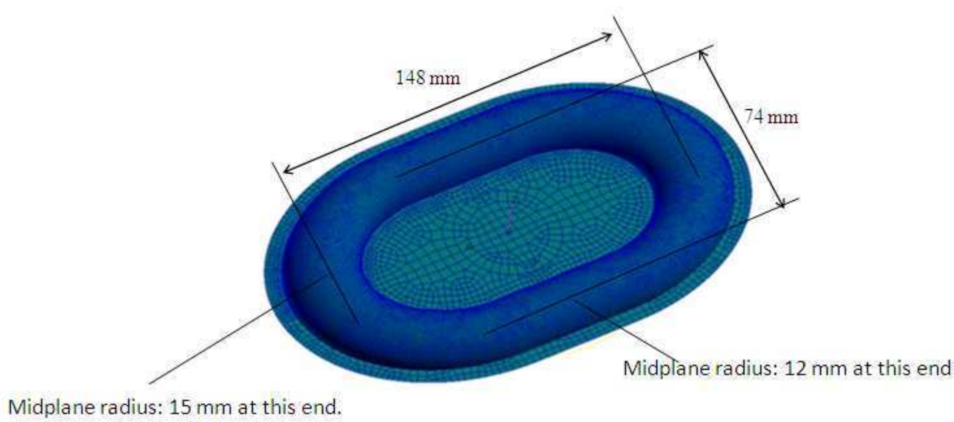

Fig. 3. An isometric view of the proposed design

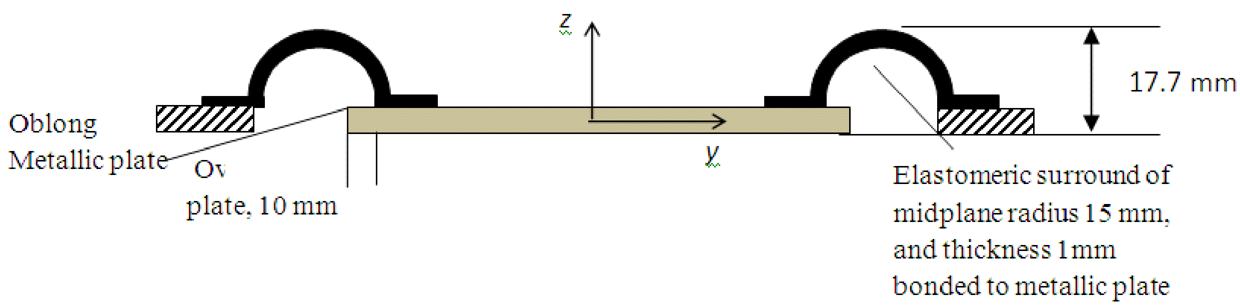

Fig. 4. A cross sectional view of proposed design (along the longer line of symmetry)

Also, it is seen in Figure 4 that the metallic plate overhangs the surround role by 10 mm on each side. The amount of overhang has been iteratively determined to ensure that the rocking mode of the surround does not fall between the operating bandwidth of the passive radiator. To increase the rocking frequency of the design, the value of overhang can be reduced, and vice versa. This is so because as the value of overhang increases, so does the plate's rotational moment of inertia, which in turn reduces the rocking frequency. Any rocking which occurs in excess of 80 Hz (which is the higher limit of radiator's operational bandwidth) can be neglected, because the contribution by the radiator to the SPL in the room will be very small, and also because the amplitude of these rocking motions will be small due to significant amount of damping present in the system. Finally, we note that the overall thickness of this design is 17.7 mm. This is shown in Fig. 4. For a dual suspension design, this value would have exceeded the design envelope by approximately 20 mm.

4. RESULTS FROM NUMERICAL SIMULATIONS

Figure 5 shows load-deflection response of the proposed design. Here we observe that the system behaves linearly in the range ±18 mm. This is consistent with our excursion requirement for linear range, which is ±16 mm. Also, the overall stiffness of the system in this range is 2670 N/m. This value is about 7% higher that our desired target stiffness value of 2500 N/m, and thus is acceptable. Figure 6 shows the pistonic mode of the passive radiator in free air at 30.2 Hz. From this value, and the predicted stiffness value of 2670 N/mm, we back calculate the moving mass of the design to be 74 gm. Once again, this value is reasonably close to its target value of 67 gm. In actual box, where such passive radiators are typically mounted, the air stiffness is significantly

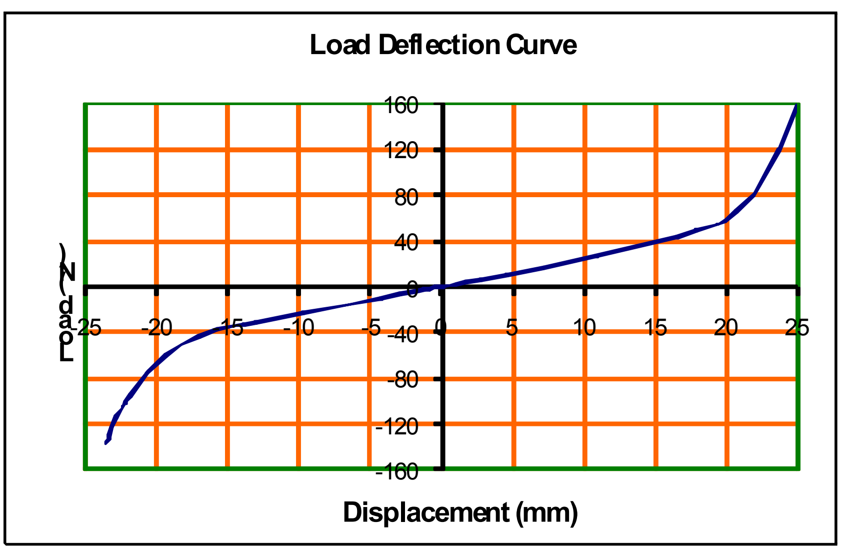

Fig. 5. Load-Deflection Response for Single Suspension Design

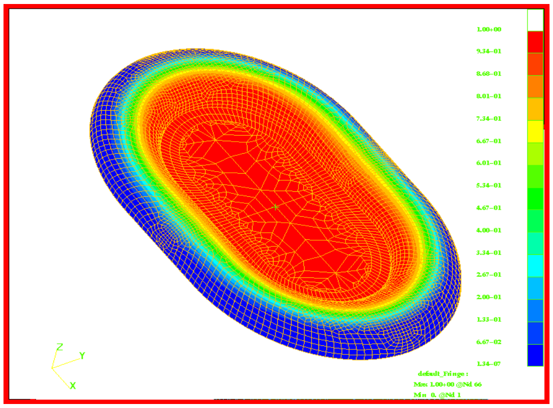

Fig. 6. Pistonic mode in free air at 30.2 Hz

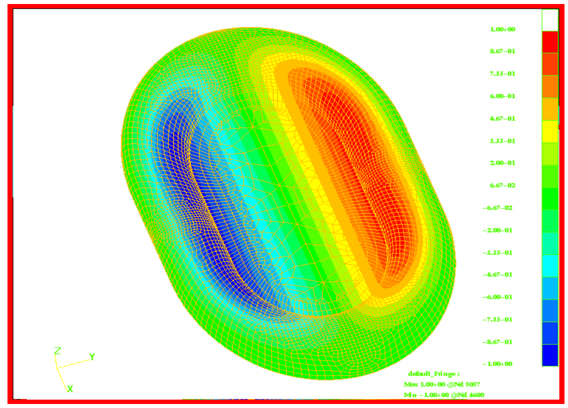

Fig. 7. First rocking frequency at 40 Hz

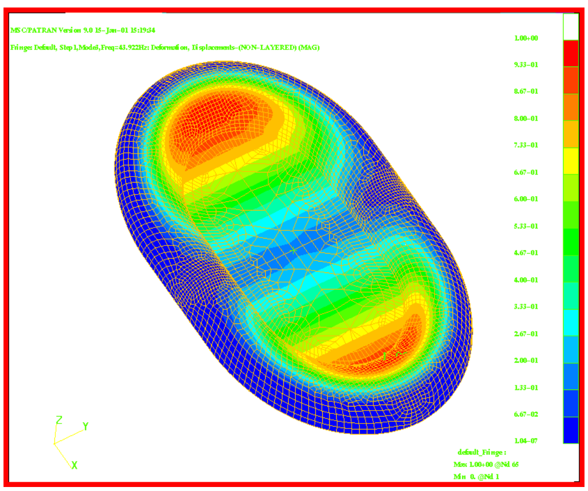

Fig.8. Second rocking frequency at 44 Hz

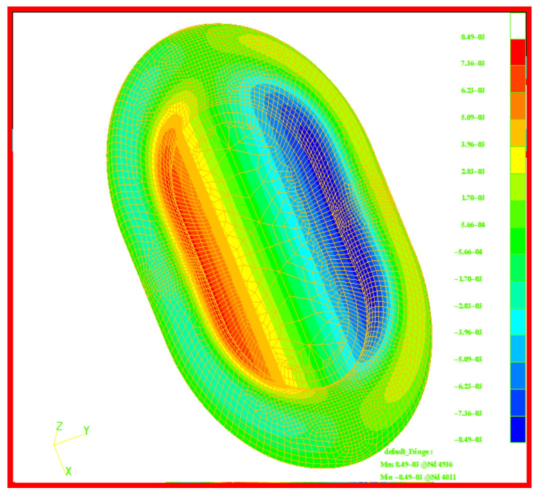

Fig. 9. First Third rocking frequency at 140 Hz

higher than that of the rubber surround. For instance, in lumped parameter model developed, air stiffness was found to be 7500 N/m. Hence the total stiffness seen by the passive radiator would be 10,167 N/m, and in such a box, the passive radiator would resonate pistonically at 59 Hz.

Next we look at the design's rocking frequencies and modes. The first three of these frequencies, as computed by FEA code, are 40 Hz, 44 Hz, and 140 Hz. These modes have been achieved by carefully calibrating the value of overhang of the plate. We observe that while the first two rocking modes, are below the operating bandwidth of the passive radiator, the third mode lies appreciably upwards of 120 Hz, which is radiator's operational bandwidth's upper limit. Thus, we have shown the feasibility of a passive radiator design which uses only one suspension element, and still remains stable in its operational bandwidth.

Figure 10 shows the buckling response of the surround when it is moved 16 mm in positive z direction as per the axis convention shown in Fig. 4. As per numerical prediction, buckling starts occurring at -0.83 times this displacement value. Thus, when the surround moves -13.3 mm in negative z direction, surround starts buckling. However, the fringe plot for buckling pattern depicted in Fig. 10 shows that the nature of this buckling is extremely local. Given that the material of the surround is elastomeric, we do not anticipate material cracking due to this local buckling. Further, such a small buckling phenomenon will not in any fundamental way alter the overall radiating area of surround, thereby adversely impacting the SPL emanating

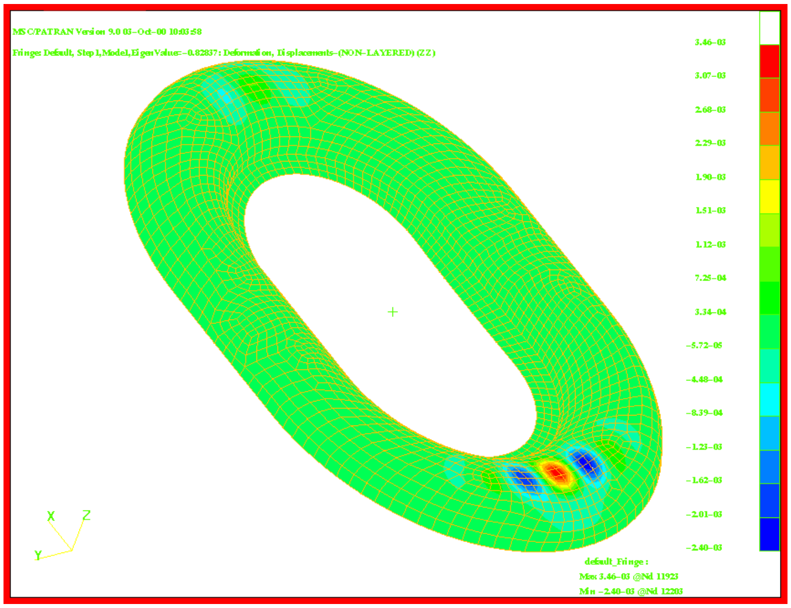

Fig.10. Buckling response of surround

from the passive radiator. Hence, we can safely conclude that this local buckling does not warrant any significant concern.

Finally, we look at the creep response of the design. This is important because the rubber element sees a continual 1-g load associated with a mass of 74 grams. This load is attributable to the hanging moving mass, which is impressed upon by Earth's gravitational pull. For this, three static FEA analyses were conducted, where the passive radiator was subjected to 1-g inertial loads in x, y, and z directions. The stress plots for such an analysis showed that the surround experiences very low levels of stresses when subjected to 1-g loads. The maximum stress values reported by FE analysis were 22.5, 30.2, and 67.0 kPa, for x, y, and z directions, respectively. We infer from these data that such low levels of stresses will not induce significant creep deformation in the system.

5. RESULTS AND CONCLUSION

We have shown by detailed analysis that it is feasible to design a passive radiator which has only one suspension element. Such a design meets all the requirements of the application from functional standpoints. Such a design is significantly compact vis-a-vis the traditional two suspension element design, and is also dynamically stable within the operating bandwidth of the passive radiator. It also meets all other requirements as they relate to creep, thermal stability, and buckling.

6. REFERENCES

[1] L. L. BERANEK, 1993. *Acoustics*, Acoustical Society of America, Woodbury, NY, 240-258.
[2] M. BRUNEAU, 2007. *Fundamentals of Acoustics*, Brijbasi Art Press, Noida, UP, India, 577-625.

Journal of Acoustical Society of India : Vol. 37, No. 1, 2010 (pp. 15-19)

Ultrasonic and Spectroscopic Studies of Binary Mixtures Benzaldehyde + Benzyl Chloride and Benzyl Chloride + 2-Butanone

A.J. Clement Lourduraj[1] and I. Johnson[2]
[1]*Lecturer in Physics, St. Joseph's College (Autonomous), Trichirappaali - 620 002*
e-mail : ajeevaclement @ yahoo.co.in
[2]*Reader in Physics, St. Joseph's College (Autonomous), Trichirappaali - 620 002*
e-mail : jnaadarsh @ hotmail.com

ABSTRACT

This paper reports the experimental densities, sound velocities and viscosities of the binary mixtures Benzaldehyde + Benzyl Chloride and Benzyl Chloride + 2-Butanone which have been measured at 308.15K for the entire range of mole fraction. From these data, excess volume (VE) have been calculated. Experimental and computed results are used to study the type and nature of inter and intra molecular interactions between the mixing components. Even though these types of studies exist in the literature there is no confirmation for the observed excess properties through other non-ultrasonic techniques. For the confirmation of the excess properties FTIR spectra have been taken for various compositions of those mixtures. This FTIR study gives supportive evidences for the results obtained through the excess volume study.

1. INTRODUCTION

The present work is a continuation of our earlier studies of thermodynamic and physico-chemical properties of non-aqueous binary and ternary liquid mixtures[1]. The present investigation is concerned with the study of the binary systems Benzaldehyde + Benzyl Chloride and Benzyl Chloride + 2-Butanone for their entire composition range. A deeper knowledge of mixing properties of such multicomponent liquid system is essential in many industrial applications, such as design calculation, mass transfer, fluid flow etc[3]. The present work reports densities, viscosities and speeds of sound for the system measured at 308.15K. From these data excess volume VE, have been calculated. FTIR spectra have been taken for some ranges of mole fractions of liquid mixtures and pure liquids.

2. EXPERIMENTAL MATERIALS

High - purity spectroscopic and HPLC grade chemicals of Benzaldehyde, Benzyl Chloride and 2-Butanone were obtained from Merck Co. Their purities were 99.5 % or better and no further purification was done. The chemicals were stored over molecular sieves. The verification of the purity of the chemicals was realized by ascertaining the consistency of the values of density, viscosity and ultrasonic velocity at 298.15K which were reasonably in accordance with the values found in the literature.

3. MEASUREMENTS

Densities of liquids and their mixtures were measured at 308.15K with specific gravity bottle method. The results of density are accurate to ± 0.0002 gcm^{-3}. An electronic digital balance is used to measure the mass of the liquids within an accuracy of ± 0.001g. The viscosities of the pure liquids and their mixtures were measured using an ostwald's viscometer. The flow times are measured within an accuracy of ± 0.01sec. The speed of sound in the mixture has been measured by an ultrasonic interferometer of frequency 2MHz. The speed of sound values is accurate to ± $2 m.s^{-1}$. The measurements have been carried out in a constant temperature bath at 308.15K within an accuracy of ± 0.01K. FTIR spectra were taken for the liquid mixtures in a FTIR spectrum photometer (Perklin Elmer Co. model 1605) by using the KBr pellet method[4].

4. RESULTS AND DISCUSION

In the case of Benzaldehyde + Benzyl Chloride mixture, the VE is maximum negative for 0.4 mole fraction of Benzaldehyde. The maximum negative in excess volume is due to dipole-dipole interaction which has been supported by earlier workers. It is also due to the interstitial accommodation of one type of molecule into other. In the case of Benzyl Chloride + 2-Butanone mixture, the VE is maximum positive for 0.5 mole fraction of Benzyl Chloride which shows the presence of dispersion type interaction which has also been supported by earlier researchers. The FTIR spectrum taken shows a change in the frequency value or the presence of a new frequency value for 0.4 mole fraction of Benzaldehyde (from Fig. - 1 and Table - 2, 0.4 of Benzaldehyde + 0.6 of Benzyl Chloride) and for 0.5 mole fraction of Benzyl Chloride (from Fig. - 2 and Table - 4, 0.5 of Benzyl Chloride + 0.5 of 2-Butanone). From literature (W. Kemp, 1990, Organic Spectroscopy) it has been found that change in

Table 1. Determination of mole fraction, velocity, viscosity and density for benzaldehye + benzyl chloride

Mole Fraction (Benzyl Chloride)	Velocity (m/sec)	Viscosity (10^{-3} $N.s/m^2$)	Density (10^{-3} kg/m^3)	Excess Volume (10^6 m^3)
1	1098	1.2505	1.0884	0.0000
0.9431	1091	1.2456	1.0845	-2.5465
0.8787	1084	1.2390	1.0530	-2.8298
0.7722	1079	1.2278	1.0330	-6.1554
0.6928	1071	1.2207	1.0312	-9.9335
0.5847	1064	1.1941	1.0145	-13.5023
0.4800	1059	1.1803	0.9617	-12.3778
0.3841	1053	1.1066	0.8409	0.7056
0.2694	1048	1.1029	0.8105	0.8931
0.1455	1040	1.0733	0.7698	3.4387
0	1033	0.8033	0.7567	0.0000

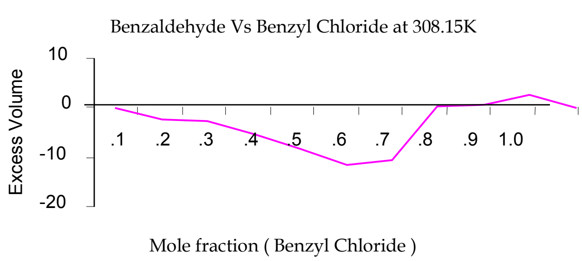

Fig. 1. Excess volume

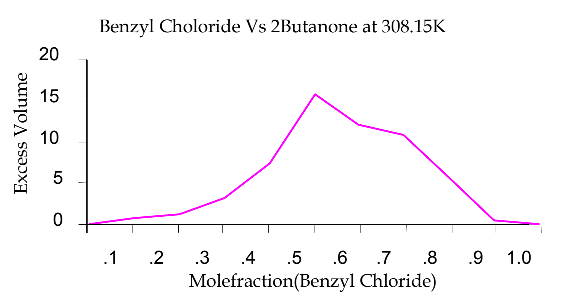

Fig. 2. Excess volume

Table 2. Observations of FTIR spectrum of benzaldehyde + benzyl chloride

1 (Ben) + 0(BC) cm^{-1}	0.9(Ben) + 0.1(BC) cm^{-1}	0.8(Ben) + 0.2(BC) cm^{-1}	0.7(Ben) + 0.3(BC) cm^{-1}	0.6 Ben) + 0.4(BC) cm^{-1}	0.5(Ben) + 0.5(BC) cm^{-1}	*0.4 (Ben) + 0.6(BC) cm^{-1}	0.3(Ben) + 0.7(BC) cm^{-1}	0.2(Ben) + 0.8(BC) cm^{-1}	0.1(Ben) + 0.9(BC) cm^{-1}	0(Ben) + 1(BC) cm^{-1}
3392.11	3390.83	3392.16	3390.58	3390.66	3437.67	3439.86	3439.42	3443.18	3447.49	3444.32
3068.94	3071.24	3069.01	3066.47	3068.18	3069.79	3066.36	3067.86	3073.15	3073.48	3065.58
2818.39	2819.15	2818.59	2818.69	2818.64	2818.57	3033.97*	2963.51	2819.75	2962.70	3033.08
2738.32	2738.60	2738.17	2737.93	2737.89	2737.87	2817.73	2817.20	2737.67	2817.92	2960.77
2332.07	2550.16	1978.74	2549.23	2550.12	2362.73	2737.26	2736.97	2545.69	2736.78	2866.83
2139.72	2365.30	1910.83	2363.98	2361.64	1970.64	2361.84	2359.43	2359.20	2540.68	2361.42
1982.52	2140.47	1822.87	1973.32	1976.28	1700.91	1965.84	1962.60	1960.10	2358.99	1954.65
1910.62	2027.14	1701.95	1908.74	1911.15	1597.14	1701.17	1701.42	1698.89	1958.06	1887.33
1826.09	1980.33	1595.96	1820.52	1821.69	1495.11	1596.78	1597.63	1495.36	1699.03	1807.15
1702.46	1913.14	1453.08	1700.74	1700.47	1452.75	1495.51	1494.80	1452.09	1648.19	1699.23
1596.07	1823.61	1394.45	1596.05	1595.83	1397.50	1453.28	1452.57	1400.26	1495.12	1637.89
1454.14	1700.22	130681	1492.75	1494.04	1277.16	1393.06	1393.77	1271.31	1452.03	1495.29
1392.52	1596.65	1205.67	1452.81	1451.93	1205.39	1310.13*	1268.98	1204.83	1398.17	1452.48
1308.46	1492.91	1167.92	1394.61	1397.26	1168.03	1269.20	1204.22	1168.03	1268.72	1394.35
1204.67	1454.23	1110.72	1281.16	1281.88	1073.45	1204.36	1166.43	1074.55	1204.97	1266.53
1167.04	1396.15	1072.84	1205.18	1205.43	1020.97	1166.79	1074.02	1024.51	1167.05	1207.06
1108.93	1285.60	1016.10	1167.95	1168.71	927.05	1072.78	1022.76	928075	1074.60	1160.38
1072.68	1205.95	925.48	1111.33	1112.48	823.92	1023.51	925.20	815.57	1025.73	1073.70
1012.18	1169.01	825.54	1072.00	1072.39	746.94	925.94	821.29	747.40	926.73	1027.37
922.30	1112.44	746.88	1022.32	1018.08	696.10	824.59	747.14	695.95	813.02	925.88
826.10	1072.61	693.96	927.04	927.95	557.83	746.84	694.86	557.54	695.77	810.75
747.24	1015.51	652.64	825.21	824.10	453.48	696.19	559.14	458.71	559.03	760.56
689.23	926.88	555.32	746.76	746.52		559.12	456.26		462.79	696.69
650.77	824.81	451.12	695.33	695.80		453.69				559.46
450.84	746.45		556.59	553.80						464.81
	694.76		452.04	451.58						
	652.82									
	548.34									
	450.72									

* Maximum shift in the frequency has been observed.

Table 3. Determination of mole fraction, velocity, viscosity and density for benzyl chloride + 2-butanone

Mole Fraction (Benzyl Chloride)	Velocity (m/sec)	Viscosity (10^{-3} N.s/m^2)	Density (10^{-3} kg/m^3)	Excess Volume (10^6 m^3)
1	1193	1.2825	1.0404	0.0000
0.8925	1164	1.0901	0.9896	0.7166
0.8228	1125	1.0064	0.9560	1.2859
0.7394	1122	0.8759	0.9069	3.1996
0.6671	1111	0.7868	0.8488	7.2985
0.5695	1075	0.7546	0.7607	15.4517
0.4847	1029	0.6297	0.7480	11.9093
0.4106	994	0.6261	0.7256	10.6990
0.2972	976	0.4902	0.7092	5.4485
0.1956	946	0.4688	0.6945	0.5195
0	922	0.3278	0.6118	0.0000

Table 4. Observations of FTIR Spectrum of Benzyl Chloride + 2-Butanone

1 (Ben) + 0(2but) cm^{-1}	0.9(Ben) + 0.1(2but) cm^{-1}	0.8(Ben) + 0.2(2but) cm^{-1}	0.7(Ben) + 0.3(2but) cm^{-1}	0.6(Ben) + 0.4(2but) cm^{-1}	*0.5(Ben) + 0.5(2but) cm^{-1}	0.4(Ben) + 0.6(2but) cm^{-1}	0.3(Ben) + 0.7(2but) cm^{-1}	0.2(Ben) + 0.8(2but) cm^{-1}	0.1(Ben) + 0.9(2but) cm^{-1}	0(Ben) + 1(2but) cm^{-1}
3394.11	3392.13	3396.11	3396.05	3393.76	3393.99	3399.05	3446.56	3446.41	3450.46	3449.47
3072.11	3067.40	3070.63	3069.41	3067.49	3066.72	3069.09	2984.11	3069.90	2985.42	2987.29
2818.42	2818.44	2818.50	2818.69	2818.81	2981.95*	2983.47	2819.21	2984.67	2668.13	2552.77
2738.34	2738.20	2738.21	2738.46	2738.32	2818.73	2819.42	2738.64	2823.30	2558.32	2370.90
2372.89	2367.01	2373.11	2329.91	2331.93	2738.47	2738.97	1984.33	2736.41	1916.64	2339.69
2330.26	2332.27	2330.79	2138.94	1982.81	2405.59*	1983.33	1703.56	2670.86	1690.02	2098.22
2235.79	2236.38	2235.76	1983.09	1912.98	2329.51	1705.87	1596.96	2558.19	1419.42	1724.52
2139.83	2139.34	2139.03	1911.55	1825.18	2138.99	1596.94	1454.30	1917.31	1324.68	1453.62
2026.52	2027.08	2027.29	1826.24	1703.44	2027.34	1453.55	1391.35	1698.20	1289.26	1374.94
1982.86	1983.03	1983.09	1703.53	1595.99	1984.22	1387.82	1311.01	1597.56	1176.11	1289.16
1911.14	1910.17	1911.42	1597.13	1454.20	1911.03	1309.35	1204.29	1451.42	1126.20	1172.99
1826.50	1826.27	1825.70	1453.99	1391.37	1826.92	1204.37	1169.24	1418.90	1073.49	1024.90
1701.69	1702.00	1701.38	1391.81	1310.66	1703.87	1170.93	1110.76	1288.32	1025.96	938.37
1596.72	1655.24	1654.81	1308.28	1204.91	1596.18	1109.88	1073.33	1174.81	934.40	752.00
1454.12	1595.90	1596.48	1204.32	1168.61	1454.61	1012.35	1016.45	1124.97	805.24	708.66
1392.85	1454.70	1454.41	1168.77	1109.98	1391.15	935.87	933.56	1072.21	750.45	593.27
1308.72	1392.10	1392.53	1109.33	1072.58	1310.20	826.54	826.81	1024.29	707.39	548.46
1204.25	1310.13	1310.26	1073.80	1015.10	1203.83	747.69	747.32	933.60	594.50	
1166.91	1204.12	1204.34	1011.83	930.45	1168.19	691.22	689.04	821.56	547.41	
1109.92	1166.83	1166.82	925.28	826.77	1106.93	650.64	650.21	746.48		
1073.38	1108.54	1109.80	825.98	747.39	1073.17	451.50	451.46	706.48		
1012.73	1072.28	1072.43	747.33	689.11	1011.61			654.22		
922.40	1012.18	1012.95	690.05	650.24	928.64			547.54		
826.07	923.43	923.24	651.03	451.16	826.38			450.85		
746.86	826.70	826.64	451.19		747.78					
688.87	747.06	746.91			689.19					
650.60	688.70	688.63			650.30					
450.67	650.23	650.17			451.17					
	450.89	450.96								

* Maximum shift in the frequency has been observed.

the frequency value or the presence of a new frequency value in the FTIR spectrum is due to the above said molecular interaction. So, the FTIR spectrum study gives an additional evidence for the observed molecular interactions through excess volume study.

5. LITERARTURE CITED

Periodicals:

[1] I. JOHNSON, M. KALIDOSS and R. SRINIVASAMOORTHY, 2001, Acoustical investigation of some binary and ternary liquid mixtures, Proceedings of the 17th International congress on Acoustics (ROME), *Physical Acoustics -Part B*, **1**, 12-13.

[2] J.D. PANDEY and ASHOK KUMAR, 1994. Ultrasonic velocity in pure liquids, *Journal of Pure and Applied Ultrasonics*, **16**, 63-68.

[3] S. VISWANATHAN and M. ANAND RAO, 2000. *Journal of Chem. Eng.*, Data - **45**, 764 - 770.

[4] A. MUKHERJEE and S. KAMILA et al, 1999. *Acoustics Letters (U.K).*, **23**, 17 - 24.

[5] M. KALIDOSS, I. JOHNSON and R. SRINIVASAMOORTHY, 1999. *J. Acoust. Soc. Ind.*, **27**, 319.
[6] M. KALIDOSS and R. SRINIVASAMOORTHY, 1997. *J. Pure Appl. Ultrason.*, **19**, 9.
[7] C.V. SURYANARAYANA and S. KUPPUSAMY, 1979. *J. Acous. Soc. Ind.*, **7**, 131.
[8] R.J. FORT AND W.R. MOORE, 1965. *Trans. Faraday Society*, **61**, 2102-2107.
[9] E. ZOREBSKI and A. ZAK -Z., 1999. *Physikalische Chemie.Bd.*, **210,S.**, 223-233.

Books:

[1] Riddick.J.A., Bunger W.B., Sanako T.K., 1986, Organic solvents. Physical properties and methods of purification (Techniques of Chemistry) 4thed, Wiley-Interscience, New York.
[2] Weissberger, 1955, Technique of Organic Chemistry, Vol. VII, Organic solvents. Physical properties and methods of purification, 2nded, Inter-science publisher, New York.
[3] Handbook of Chemistry and Physics, 1984, The Chemical Rubber company, Cleveland, Ohio, USA.
[4] Robert M. Silverstein and Francis X. Webster, 1998, Spectrometric identification of organic compounds, John Wiley & Sons, Singapore.

Journal of Acoustical Society of India : Vol. 37, No. 1, 2010 (pp. 20-24)

Study of Molecular Interaction and Association in Binary Mixture of Dehpa (Di-(2-Ethyl-Hexyl) Phosphoric Acid) with N-Butyl Chloride at Different Temperatures

***Rita Paikaray and Sujata Mishra**
Department of Physics, Ravenshaw University, Cuttack
**e-mail: r_ paikaray @ rediffmail.com*

ABSTRACT

The behaviour of binary mixture of DEHPA (Di-(2-ethyl-hexyl) phosphoric acid) with n-Butyl chloride has been studied at different temperatures (30ºC, 35ºC, 40ºC, 45ºC). Experimentally determined values of ultrasonic velocity (C) and density (ρ) are used to calculate various derived parameters like isentropic compressibilities (K_s), intermolecular free length (L_f), acoustic impedance (Z), relative association(RA).Excess values of some derived parameters like excess isentropic compressibilities (K^E_S), excess acoustic impedance (Z^E) are also calculated at different temperatures. Variation of these parameters with temperature gives significant interpretation in a mixture of two polar liquids. The results explain the nature and strength of molecular interaction between the components.

1. INTRODUCTION

The range and strength of molecular interaction in liquid mixture can be obtained by ultrasonic technique as it serves as a very important tool for investigation of molecular structure of matter. Liquid -Liquid solvent extraction technology finds extensive use in different industrial processes like hydro metallurgy, petroleum and petro chemical processing, organo-chemical and pharmaceutical production, food and fuel industries etc.

DEHPA is one of the most widely used characterized extractant in the atomic-energy industry. It is used for extraction of many transuranic elements (z>92) like plutonium, americium and curium etc. from environmental samples like sea water, sediments and marine materials. It is also used for extraction of uranium, vanadium, beryllium, yttrium, cobalt, zinc, rare earths and other valuable metals [1]. Extraction efficiency of extractants can be improved by mixing it with organic diluents and modifiers. In nuclear energy industry, the common extractants are used with mixtures with polar and non-polar diluents to give greater phase dispersal and rapid phase disengagements [2]. In view of above, we have undertaken the ultrasonic studies to investigate the basic properties of DEHPA by mixing with a polar solvent (n-Butyl chloride) at different temperatures (30ºC, 35ºC, 40ºC, 45ºC) and at frequency of 1MHZ. n-Butyl chloride is used as a solvent, an alkylating agent in organo synthesis, organo metallic compound manufacturing. Moreover, literature survey indicates that no ultrasonic study on this binary system has been reported. In the present paper, we have estimated acoustic parameters such as isentropic compressibility, intermolecular free length, acoustic impedance, relative association, excess isentropic compressibility and excess acoustic impedance for mixture of DEHPA with n-Butyl chloride at different temperatures in order to understand the molecular interaction and association between the component molecules and effect of temperature on them.

2. THEORETICAL CONSIDERATIONS

The experimentally measured values of ultrasonic velocity (C) and density (ρ) are used to calculate the acoustic parameters such as isentropic compressibilities (K_s), intermolecular free length (L_f), acoustic impedance (Z), relative association(R_A) and their excess values using the following expressions [3,4]

$$K_s = 1/\rho C^2 \tag{1}$$

$$L_f = K (k_s)^{1/2} \tag{2}$$

$$Z = \rho_C = (\rho_A X_A + \rho_B X_B)\ C \tag{3}$$

$$R_A = (\rho/\rho_o)\ (C_o/C)^{\ 1/3} \tag{4}$$

$$K^E_S = K_s\ (mix) - X_A K_s\ (A) + X_B K_{S(B)} \tag{5}$$

$$Z^E = Z\ (mix) - (X_A\ Z_A + X_B\ Z_B) \tag{6}$$

Where X_A and X_B are mole fractions of DEHPA and n-Butyl chloride, ρ_o = density of DEHPA, C_0 = Ultrasonic velocity in pure DEHPA at a particular temperature, ρ = density of mixture. K is the temperature dependant constant, having value (93.875 + 0.375 T) x 10^{-8}, T being the absolute temperature [4].

3. EXPERIMENTAL

In the present study, the chemical used are of analytical grade (spectro-chem. Lab) India purified by standard procedure [5, 6]. Density was determined by using a single capillary pyknometer of bulb capacity 25cm^3 at different temperatures. Ultrasonic velocity in pure liquids and binary mixtures were measured by using a single crystal variable path ultrasonic interferometer (Model Mx^{-3}, Mittal Enterprises) at frequency 1MHz and at different temperatures and concentrations. The temperature of the sample was maintained constant at different values (30ºC, 35ºC, 40ºC, 45ºC) by using thermostatically controlled water bath with a precision of ± 0.1ºC. The purity of sample was checked by comparing the measured value of density with that of literature value.

3. RESULTS AND DISCUSSION

The experimentally measured ultrasonic velocity in pure liquids of DEHPA and n-Butyl chloride with their density values at different temperatures are determined. The density values of DEHPA at different temperature determined by us are in good agreement with the literature Values [1]. It is found that the ultrasonic velocity values and density of pure components decreases with increase of temperature.

The various thermodynamic parameters like isentropic compressibilities (K_s), intermolecular free length (L_f), acoustic impedance (Z), relative association (R_A), excess isentropic compressibility ($K_S{}^E$) and excess acoustic impedance (Z^E) are estimated using equations 1-6 at different temperatures.

From Fig-1, it is clear that the dependence of the velocity on temperature shows a linear decrease with increasing temperature and a linear increase with the increase in concentration of DEHPA. The trend in ultrasonic velocity values in this system indicates stronger interaction between DEHPA and n- Butyl chloride. This complexion is concentration dependent [8]. It is observed that at lower concentration region of DEHPA, velocity increases slowly and at higher concentration region it increases sharply. This gives rise to a denser packing of molecules and intermolecular complex formation is taking place in the high DEHPA concentration region. Considering the effect of temperature, it is very clear that the interaction between DEHPA and n-Butyl chloride decreases with increase of temperature and the solution becomes more and more loosely packed which results decrease in ultrasonic velocity.

From Fig. 2, it is evident that Z values increases with the increase in concentration of DEHPA. The increase of Z values with solute concentration can be attributed to the effective solute- solvent interaction. When temperature increases Z values decreases at a particular concentration.

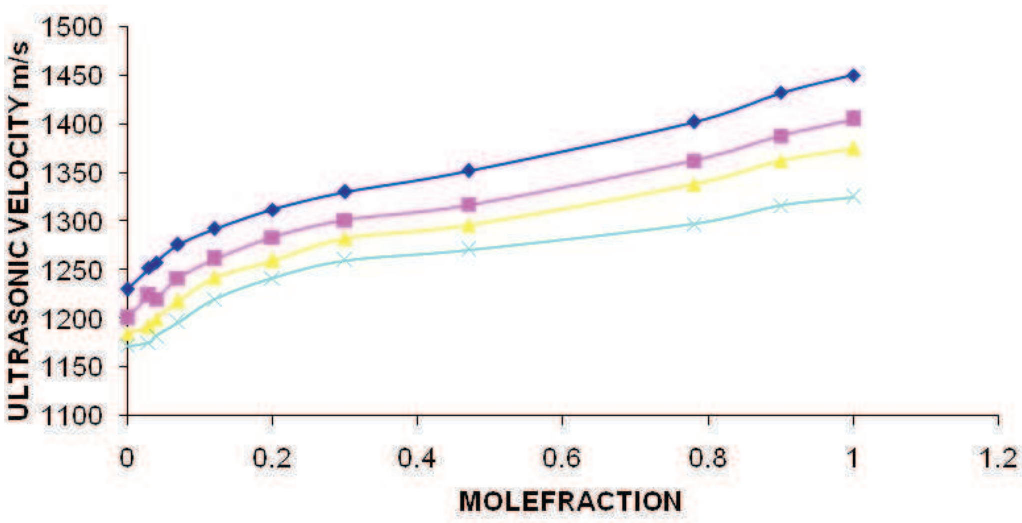

Fig. 1. Variation of ultrasonic velocity with molefraction of dehpa at different temperature

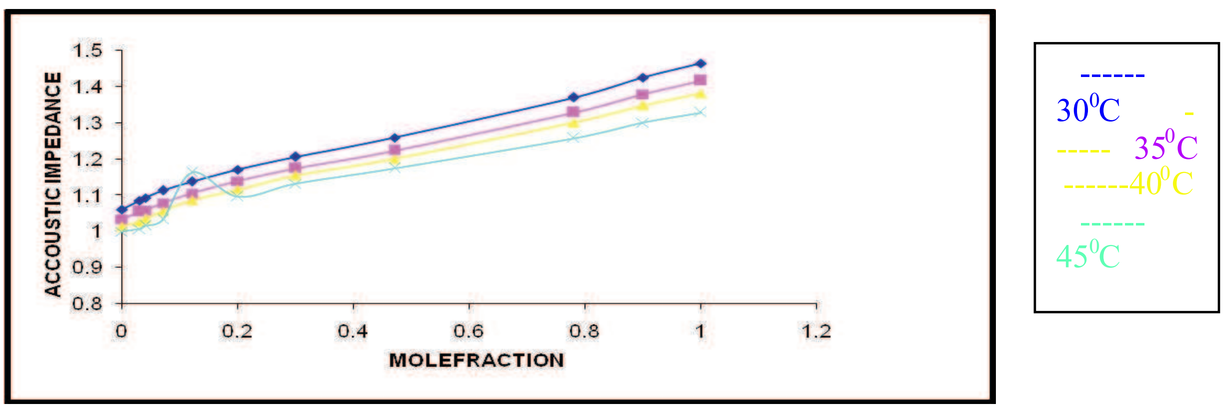

Fig. 2. Variation of accoustic impedance with mole fraction at different temperature

Figure 3 shows that free length (L_f) values decreases with increase in concentration of DEHPA and increases with increase of temperature. This decrease in Lf with concentration suggests the presence of strong solute-solvent interactions. A similar type of behavior has been reported by Kalyanasundaram and co-workers [9] in the ultrasonic velocity study on poly Methylacrylate in DMF solutions at different temperatures. As the intermolecular free length is found to be a predominant factor in determining the nature of sound velocity variation in liquid mixtures [7], such variation can be interpreted in terms of specific interaction between different sizes of molecules.

The variation of excess isentropic compressibility (K_S^E) with mole fraction of DEHPA at different temperatures is presented in Fig. 4. The isentropic compressibility is a measure of ease with which the system can be compressed. The excess isentropic compressibility is negative over the entire composition range of mixture investigated in the present study. The negative values of excess isentropic compressibility suggests that liquid mixture is less compressible than the pure liquids and molecules in the mixture are more tightly bound in the liquid mixture than in pure liquids[10]. Thus in the present study negative values of excess isentropic compressibility indicate strong specific interaction between component molecules and interstitial accommodation of smaller molecules in the voids created by bigger molecules[7,11].

The value of ZE is positive over entire composition range, investigated in the present study as shown in the Fig 5. It agrees with the result from KES. Similar type of result have been obtained for the system of DIBK & bromobenzene [2]. Several workers [12] in there study of ZE reported that more than one type of interaction may be present in any given system. Here DEHPA molecules are polar and in addition with n-Butyl chloride (which is also polar) they can accept as well as donate electrons. Hence the dipole-dipole and acceptor-donor

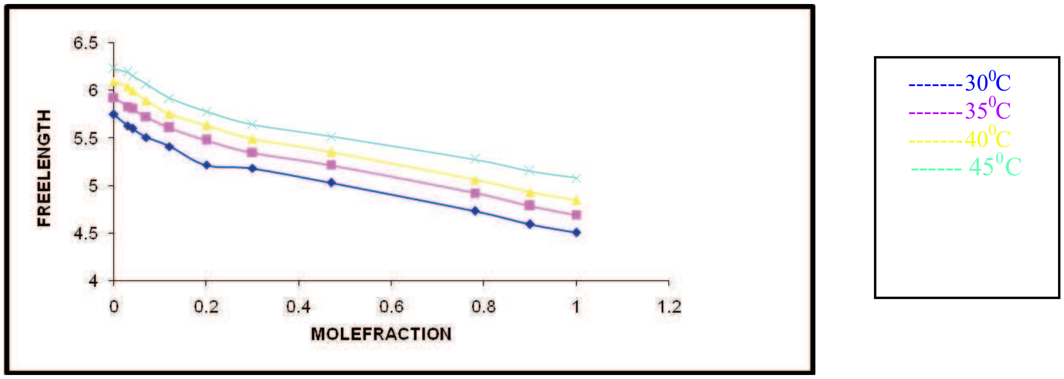

Fig. 3. Variation of freelength with mole fraction of dehpa at different temperature

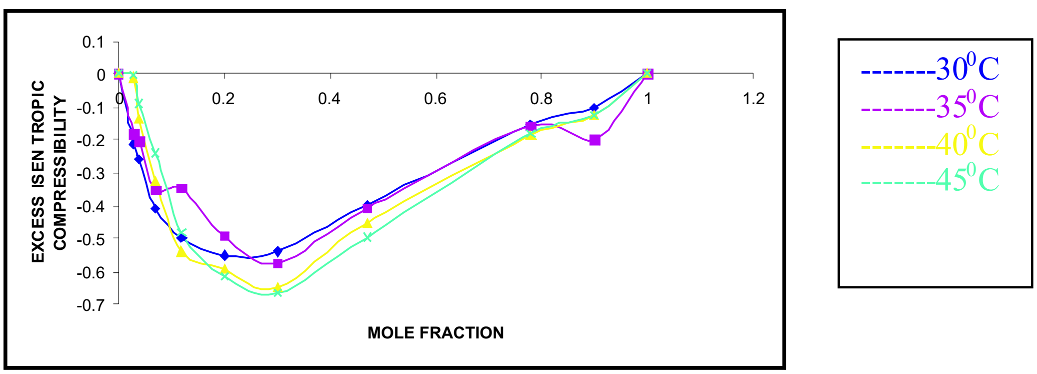

Fig. 4. Variation of excess isentropic compressibility with mole fraction at different temperature

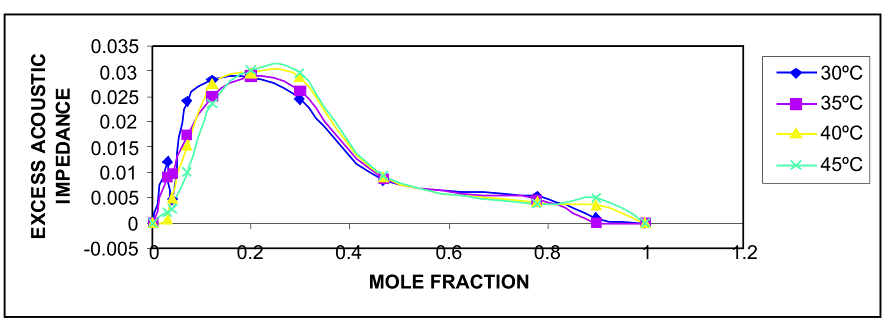

Fig. 5. Variation of excess acoustic impedance with mole fraction at different temperaturure

type interaction are also possible in addition. The relative association (R_A) is found to increase with the increase in molar concentration of DEHPA. This signifies that unlike interactions are relatively stronger compared to like interactions. When temperature increases it is showing some irregular trend in lower concentration region of DEHPA. Similar reports are available on literature for mixtures containing some polythene and I-propanol [13].

5. CONCLUSION

Ultrasonic velocity studies on the system of binary mixture of DEHPA with n- Butyl chloride show that when concentration of DEHPA increases, more rigid structure is formed due to bonding between the unlike molecules through dipole-dipole interaction. Isentropic compressibility found to decrease with concentration at a given temperature. Ultrasonic velocity found to decrease with increase of temperature, when temperature increases free length also increases, resulting a loosely packed molecular structure. So acoustic parameters are highly affected at different temperatures. This indicates DEHPA shows non- ideal behavior when mixed with organic diluents, which is in close agreement with the literature [1].

6. REFERENCES

[1] N. SWAIN, S.K. SINGH, D. PANDA and V. CHAKRAVORTHY, 2001. *Journal of Molecular Liquid,* **94** , 233-248.
[2] S. ACHARYA, R. PAIKARAY and G.C. MOHANTY, 2003. *Indian Journal of Pure & applied physics,* **41,** 855-857.
[3] R.P. THAKUR and N.K. GUPTA, 1985. *Acoustica*, 53, 59.
[4] B. JACOBSON, 1952. *J.chem. Physics,* **20**, 927.
[5] Voget AI, Text Book of practical organic chemistry Third edition. (Longmans, London), (1951).
[6] A. WEISSBERGER, Techniques of organic chemistry 1955. (Interscience, New York), vol.VII.
[7] S. ANURADHA, S. PREMA and K. RAJAGOPAL, 2005. *J.Pure Appl. Ultrasonic,* **27**, 49.
[8] V. KANNAPPAN and INDRA GANDHI, 2007. *Indian Journal of pure and applied physics,* **45**, 221.
[9] S. KALYANSUNDARAM, A. MANUEL STEPHAN and A.J. GOPALAN, 1995. *J. Polym. Mater* **12**,177.
[10] D. SRAVANA KUMAR and D. KRISHNA RAO, 2007. *Indian Journal of Pure and applied Physics,* **45**, 210.
[11] R. MEHRA and M. PANCHALI, 2006. *Indian journal of Phys,* 80,195.
[12] S. PRAKASH, N. PRASAD, R. SINGH and D. PRAKASH , 1975. *Acoustica* **34**, 121.
[13] J. PAL, GURUCHARAN DASS and J. HARSH KUMAR, 2001. *Pure- Appl. Ultrasonic*, **23**,10.

Journal of Acoustical Society of India : Vol. 37, No. 1, 2010 (pp. 25-32)

Evaluation of Excess Internal Pressures, Excess Free Volumes and Other Excess Thermodynamic Parameters of Formamide + 1-Butanol, 2-Butanol, 1,3-Butanediol and 1,4-Butanediol Mixtures from Ultrasonic Speed and Density Data

A.K. Nain[1*], P. Chaudhary[1] and A.K. Srivastava[2]

[1]*Department of Chemistry, Dyal Singh College (University of Delhi), Lodi Road, New Delhi - 110 003, India*

[2]*Department of Chemistry, University of Allahabad, Allahabad - 211 002, U.P., India*

**e-mail: ak_nain@yahoo.co.in*

ABSTRACT

The internal pressures, π_i, free volumes, V_f, excess internal pressures, π^E_i, excess free volumes, V^E_f, excess free energy, G^E, excess enthalpy, H^E and excess entropy, S^E of mixing for the binary mixtures of formamide with 1-butanol, 2-butanol, 1,3-butanediol and 1,4-butanediol have been calculated using the experimental ultrasonic speed and density data over the whole composition range at 298.15 K by using regular solution theory. The results have been interpreted in terms of intermolecular interactions between the component molecules in the mixture. The variations of these excess properties with composition indicate that the formamide-alkanol interaction in these mixtures follows the order: 1-butanol > 2-butanol > 1,3-butanediol > 1,4-butanediol. It is observed that the order of interactions in these mixtures depends upon the number and position of hydroxyl groups in these alkanol molecules. The FA-alkanol interaction decreases with increase in the number of hydroxyl groups and when hydroxyl group is attached to the β- or γ-carbon atom in the alkanol molecule.

1. INTRODUCTION

The excess thermodynamic properties such as excess internal pressure, excess free volume, excess free energy, excess enthalpy and excess entropy have been found to provide useful information regarding intermolecular interactions between the component molecules of the binary liquid mixtures. Whatever the model chosen for the liquid state, the cohesive forces are of primary importance. Internal pressure, π_i [$= (\partial E/\partial V)_T$] of a fluid is the volume derivative of the internal energy of the fluid at constant temperature. It is the resultant of the forces of attraction and of repulsion between the constituents in a liquid medium. Internal pressure has gained significant interest by chemists, physicists and chemical engineers in past, as it provides a measure of explaining molecular interactions, internal structure, clustering phenomenon, ionic interactions and dipolar interactions. Internal pressure has been subject of active interest among several researchers in the past [1-13].

In the present study, the internal pressures, π_i, free volumes, V_f excess internal pressures, π_i^E, excess free volumes, V^E_f excess free energy, G^E, excess enthalpy, H^E and excess entropy, S^E of mixing for the binary mixtures of formamide with 1-butanol, 2-butanol, 1,3-butanediol and 1,4-butanediol have been evaluated from ultrasonic speed, u and density, ρ data over the whole composition range expressed by mole fraction, x_1 of formamide at 298.15 K by using regular solution theory. The experimental data of ultrasonic speed, u and density, ρ of these binary mixtures have been taken from our previous studies [14,15]. The variations of these parameters with composition of the mixtures are discussed in terms of molecular interactions in these mixtures.

2. THEORY

The internal pressure of a fluid is related to the thermal pressure coefficient (P/T)V by the following well-known thermodynamic equation of state

$$\pi_i = \left(\frac{\partial E}{\partial V}\right)_T = T\left(\frac{\partial P}{\partial T}\right)_V - P = T\left(\frac{\alpha_p}{k_T}\right) - P \tag{1}$$

where p is the isobaric expansivity and k_T is the isothermal compressibility of the mixture. For most of the liquids, the thermal pressure coefficient multiplied by absolute temperature, i.e., $T(\alpha p/k_T)$ is very high so that the external pressure P becomes negligible in comparison [12,16,17] therefore it may be neglected in the Eq.(1) in the present calculations. Thus, the internal pressure can be shown to be equal to [12,16,17]

$$\pi_{nt} = \alpha_p T/k_T \tag{2}$$

The V_f of the mixtures are calculated from the relation [18,19]

$$V_f = \frac{RT}{(P+\pi_i)} \tag{3}$$

since P is very small as compared to π_i, it has been neglected in the Eq.(3) in the present calculations. k_T, is calculated using the well-known thermodynamic relation

$$k_T = k_s + \frac{TV\alpha_p^2}{C_p} \tag{4}$$

where $k_s[= 1/(u^2)]$ is isentropic compressibility, V is the molar volume and C_p is the heat capacity of the mixture. The p values for the mixtures were evaluated from temperature dependence of density data and C_p values for the mixtures have been calculated by using the relation

$$C_p = x_1 C_{p,1} + x_2 C_{p,2} \tag{5}$$

The π_i^E and V_F^E of binary mixtures have been calculated using the relation

$$Y^E = Y - (x_1 Y_1 + x_2 Y_2) \tag{6}$$

where Y is π_i or V_f and subscripts 1 and 2 refers to pure formamide and alkanol/alkanediol, respectively. The excess enthalpies, H^E and excess entropies, S^E are calculated from π_i and V_f by using the following relations based on regular solution theory [18,19]

$$H^E = \pi_i V - \left[x_1 \pi_{i,1} V_1 + x_2 \pi_{i,2} V_2\right] \tag{7}$$

$$S^E = R\left[x_1 \ln V_{f,1} + x_2 \ln V_{f,2} - \ln V_f\right] \tag{8}$$

The excess free energy, G^E of mixtures is given by the relation

$$G^{E} = H^{E} - TS^{E} \tag{9}$$

The values of π_i^E, V_F^E, H^E, S^E and G^E were fitted to a Redlich-Kister20 type polynomial equation

$$Y^{E} = x_1(1-x_1)\sum_{i=0}^{n} A_i(1-2x_1)^i \tag{10}$$

where Y E is π_i^E or V_F^E or H^E or S^E or G^E. The values of coefficients, Ai in Eq. (10) were evaluated by using least-squares method with all points weighted equally.

3. RESULTS AND DISCUSSION

The values of u, ρ, π_i, V_f, π_i^E, V_f^E, G^E, H^E and S^E for the binary mixtures of formamide with 1-butanol, 2-butanol, 1,3-butanediol and 1,4-butanediol as functions of mole fraction, x_1 of formamide at 298.15 K are listed in Table 1. The values of various parameters, C_p, α, k_s and k_T of pure liquids at 298.15 K used in the calculations are listed in Table 2. The values of coefficients, A_i of Eq.(10) for the excess functions and the corresponding standard deviations, $\sigma(Y^E)$ are listed in Table 3. The variations π_i^E, V_f^E, G^E, H^E and S^E with composition of the mixtures, along with smoothed values using Eq.(10) at 298.15 K are presented graphically in Figs. 1-5. The results shown in Fig. 1 indicate that the π_i^E values are negative over entire mole fraction range for all the four systems investigated. The magnitude of π_i^E values follows the sequence: 1-butanol > 2-butanol > 1,3-butanediol > 1,4-butanediol. Fig. 2 indicate that V_f^E values are negative for formamide + 1-butanol/2-butanol and positive for formamide +1,3-butanediol/1,4-butanediol mixtures over the entire mole fraction range. The magnitude of V_f^E values follows the sequence: 1-butanol <2-butanol <1,3-butanediol <1,4-butanediol. The observed trends in V_f^E values for these mixtures indicate the presence of specific interactions between formamide and alkanol molecules, whereas weak interactions between formamide and alkanediol molecules.

In pure state, formamide molecules are strongly self-associated through extensive three-dimensional network of hydrogen bonds, through its three hydrogen bond donors (3 H-atoms) and three acceptors (two lone pairs of electrons at oxygen and one at nitrogen atom) [21]. Alkanol molecules are polar and self-associated through hydrogen bonding of their hydroxyl groups [22], whereas alkanediol molecules are self-associated through inter- and intra- hydrogen bonding [23]. Mixing of formamide with alkanols would induce mutual dissociation of the hydrogen bonded structures present in pure liquids with subsequent formation of (new) H-bonds (C=O .... H -O) between proton-acceptor oxygen atom (with two lone pair of electrons) of C=O group of formamide and hydrogen atom of - OH group(s) of alkanol molecules. Equally important is the formation of H-bond of the type (N-H ...... O- H) between hydrogen atoms of NH_2 groups of formamide and oxygen atom of OH group(s) of alkanol molecules, leading to a contraction in volume, which should result in negative V_f^E values.

The observed negative V_f^E values for formamide + 1-butanol/2-butanol mixtures (Fig. 2) can be considered due to formation of hydrogen bonding between formamide and 1-butanol/2-butanol molecules that leads to more closer packing of molecules resulting in a contraction in volume of the mixture, and hence, decreasing the free volume of the mixture leading to negative V_f^E values. But opposite to our expectation, the positive trends are observed in V_f^E values for formamide + 1,3-butanediol/1,4-butanediol mixtures (Fig. 2) over whole composition range. It has been pointed [22,23] that intramolecular hydrogen bonding in multihydroxylic alkanols considerably influences the formation of intermolecular hydrogen bonding, i.e., the proportion of hydroxyl groups available for intermolecular hydrogen bonding with formamide molecules in the mixture will be smaller in case of alkanediols than those available in alkanols. This leads to the formation of loosely packed hydrogen bonded aggregates between unlike molecules in formamide + 1,3-butanediol/1,4-butanediol mixtures as compared to those in formamide + 1-butanol/2-butanol mixtures, which results in an expansion in volume, i.e., increase in the free volume of the mixture leading to positive V_f^E values. The trends observed in π_i^E and V_f^E values indicate that the order of interactions in these binary mixtures follows the sequence:

Table 1. The values of u, ρ, π_i, V_f, π_i^E, V_F^E, G^E, H^E and S^E as a function of mole fraction, x_1 of formamide for formamide + alkanol/alkanediol binary mixtures at 298.15 K.

x_1	u $(m\,s^{-1})$	ρ $(kg\,m^{-3})$	π_i $(10^8\,N\,m^{-2})$	V_f $(10^{-6}\,m^3\,mol^{-1})$	π_i^E $(10^8\,N\,m^{-2})$	V_F^E $(10^{-6}\,m^3\,mol^{-1})$	G^E $(kJ\,mol^{-1})$	H^E $(kJ\,mol^{-1})$	S^E $(J\,mol^{-1}\,K^{-1})$
Formamide + 1-butanol									
0.0000	1242.6	805.54	2.974	8.335	0.000	0.000	0.000	0.000	0.000
0.1093	1281.2	821.69	3.188	7.776	-0.075	-0.130	0.700	0.700	0.001
0.2057	1315.3	838.08	3.389	7.315	-0.128	-0.214	1.212	1.212	0.001
0.3138	1353.7	859.20	3.630	6.828	-0.171	-0.278	1.660	1.661	0.002
0.4104	1388.3	881.08	3.863	6.417	-0.193	-0.310	1.941	1.944	0.008
0.5115	1424.6	907.63	4.123	6.012	-0.199	-0.320	2.094	2.099	0.017
0.6124	1461.0	938.71	4.402	5.631	-0.186	-0.306	2.087	2.096	0.029
0.7081	1495.5	973.49	4.684	5.292	-0.157	-0.269	1.907	1.919	0.040
0.8123	1533.1	1018.90	5.009	4.949	-0.107	-0.204	1.491	1.505	0.047
0.9086	1567.9	1070.04	5.320	4.660	-0.050	-0.116	0.863	0.875	0.040
1.0000	1601.0	1129.00	5.611	4.418	0.000	0.000	0.000	0.000	0.000
Formamide + 2-butanol									
0.0000	1212.6	802.28	2.818	8.797	0.000	0.000	0.000	0.000	0.000
0.1043	1243.5	817.54	2.992	8.284	-0.117	-0.056	0.395	0.366	-0.098
0.2043	1274.8	834.16	3.177	7.802	-0.211	-0.101	0.733	0.682	-0.172
0.3056	1308.0	853.39	3.383	7.326	-0.288	-0.133	1.015	0.946	-0.229
0.4083	1343.4	875.92	3.615	6.857	-0.343	-0.153	1.229	1.149	-0.266
0.5093	1380.4	901.79	3.870	6.405	-0.370	-0.162	1.363	1.281	-0.278
0.6063	1418.1	931.01	4.144	5.982	-0.367	-0.160	1.402	1.323	-0.265
0.7068	1459.9	967.13	4.462	5.555	-0.329	-0.147	1.330	1.263	-0.225
0.8042	1503.4	1009.60	4.809	5.155	-0.255	-0.121	1.116	1.068	-0.161
0.9024	1550.5	1062.47	5.197	4.770	-0.142	-0.075	0.701	0.678	-0.079
1.0000	1601.0	1129.00	5.611	4.418	0.000	0.000	0.000	0.000	0.000
Formamide + 1,3-butanediol									
0.0000	1523.4	1000.08	3.691	6.716	0.000	0.000	0.000	0.000	0.000
0.1061	1521.7	1005.17	3.761	6.591	-0.134	0.119	-0.113	-0.177	-0.213
0.2004	1518.2	1010.47	3.822	6.485	-0.253	0.229	-0.285	-0.407	-0.407
0.3068	1518.3	1017.51	3.922	6.320	-0.358	0.309	-0.349	-0.517	-0.563
0.4026	1519.5	1025.04	4.030	6.151	-0.434	0.360	-0.386	-0.586	-0.671
0.5033	1524.6	1034.50	4.179	5.932	-0.478	0.373	-0.333	-0.548	-0.720
0.6046	1531.3	1046.06	4.359	5.687	-0.493	0.361	-0.275	-0.490	-0.723
0.7013	1542.5	1059.62	4.581	5.411	-0.456	0.306	-0.144	-0.336	-0.645
0.8073	1559.5	1078.34	4.888	5.071	-0.352	0.210	0.019	-0.123	-0.475
0.9058	1580.2	1100.82	5.241	4.730	-0.189	0.095	0.129	0.058	-0.239
1.0000	1601.0	1129.00	5.611	4.418	0.000	0.000	0.000	0.000	0.000
Formamide + 1,4-butanediol									
0.0000	1605.6	1012.64	4.084	6.069	0.000	0.000	0.000	0.000	0.000
0.1052	1592.6	1016.50	4.105	6.039	-0.140	0.143	-0.331	-0.401	-0.236
0.1988	1579.2	1020.37	4.121	6.016	-0.267	0.275	-0.663	-0.798	-0.451
0.3041	1568.5	1025.94	4.169	5.946	-0.379	0.378	-0.861	-1.049	-0.632
0.4002	1560.2	1032.15	4.232	5.858	-0.463	0.449	-0.979	-1.206	-0.761
0.5009	1553.9	1040.14	4.324	5.733	-0.525	0.491	-1.024	-1.277	-0.849
0.6022	1551.3	1050.18	4.454	5.565	-0.549	0.490	-0.970	-1.229	-0.869
0.6992	1556.0	1062.31	4.640	5.342	-0.511	0.427	-0.752	-0.986	-0.784
0.8051	1565.5	1079.46	4.903	5.056	-0.410	0.316	-0.477	-0.657	-0.607
0.9050	1580.5	1101.04	5.226	4.743	-0.239	0.168	-0.196	-0.298	-0.339
1.0000	1601.0	1129.00	5.611	4.418	0.000	0.000	0.000	0.000	0.000

Table 2. The values of various parameters of pure liquids at 298.15 K used in the calculations

Liquid	C_p ($J\ mol^{-1}\ K^{-1}$)	α_p ($10^{-3}\ K^{-1}$)	k_s ($10^{-10}\ m^2\ N^{-1}$)	k_T ($10^{-10}\ m^2\ N^{-1}$)
Formamide	107.8	0.775	3.4556	4.1183
1-Butanol	177.03	0.938	8.0399	9.4034
2-Butanol	198.03	0.910	8.4769	9.6288
1,3-Butanediol	218.4	0.586	4.3086	4.7305
1,4-Butanediol	200.9	0.587	4.8306	4.2859

Table 3. Coefficients, A_i of Eq.(10) and standard deviations, (σY^E) for formamide + alkanol/alkanediol binary mixtures at different temperatures

Excess property	A_0	A_1	A_2	A_3	A_4	(σY^E)
			Formamide + 1-butanol			
π_i^E (10^8 N m^{-2})	-0.7963	-0.0200	0.1016	-0.1170	0.0992	0.0002
V_F^E (10^{-6} m^3 mol^{1})	-1.2807	0.0049	-0.0895	0.0397	-0.0654	0.0003
G^E (kJ mol^{1})	8.3391	-1.8711	0.5380	-0.1552	0.1700	0.0006
H^E (kJ mol^{-1})	8.3595	-1.9287	0.5912	-0.1993	0.2055	0.0008
S^E (J mol^{-1} K^{-1})	0.0642	-0.2017	0.1825	-0.1293	0.1248	0.0004
			Formamide + 2-butanol			
π_i^E (10^8 N m^{-2})	-1.4752	0.3091	0.0266	-0.1229	0.0649	0.0003
V_F^E (10^{-6} m^3 mol^{1})	-0.6455	0.0811	-0.1367	0.1152	0.0207	0.0003
G^E (kJ mol^{1})	5.4150	-1.9126	0.9613	-0.6305	0.1124	0.0009
H^E (kJ mol^{-1})	5.0842	-1.9040	0.9944	-0.6839	0.1725	0.0014
S^E (J mol^{-1} K^{-1})	-1.1119	0.0460	0.1684	-0.2102	0.0721	0.0004
			Formamide + 1,3-butanediol			
π_i^E (10^8 N m^{-2})	-1.9145	0.6528	-0.2015	-0.2213	0.5596	0.0016
V_F^E (10^{-6} m^3 mol^{1})	1.4993	-0.0320	-0.1074	0.1837	-0.5787	0.0027
G^E (kJ mol^{1})	-1.3714	-1.1079	0.5079	-0.8765	2.8069	0.0118
H^E (kJ mol^{-1})	-2.2318	-0.9338	0.4778	-0.9878	3.1043	0.0128
S^E (J mol^{-1} K^{-1})	-2.8877	0.5922	-0.0756	-0.3678	0.9848	0.0037
			Formamide + 1,4-butanediol			
π_i^E (10^8 N m^{-2})	-2.0991	0.8289	-0.1336	-0.0775	0.1252	0.0033
V_F^E (10^{-6} m^3 mol^{1})	1.9625	-0.3450	-0.2423	0.1684	-0.1480	0.0047
G^E (kJ mol^{1})	-4.0932	-0.4653	1.1889	-0.7019	0.9028	0.0208
H^E (kJ mol^{-1})	-5.1053	-0.1714	1.2288	-0.7620	0.9511	0.0231
S^E (J mol^{-1} K^{-1})	-3.3939	0.9958	0.0985	-0.2296	0.2381	0.0066

1-butanol > 2-butanol > 1,3-butanediol > 1,4-butanediol, which is in agreement with the results reported in our earlier work [14,15].

The values of G^E and H^E (Figs. 3 and 4) values are positive for formamide + 1-butanol/2-butanol and negative for formamide + 1,3-butanediol/1,4-butanediol mixtures over the entire mole fraction range, except for small positive values for formamide + 1,3-butanediol mixtures at higher formamide mole fractions. The magnitude of G^E and H^E values for these mixtures follows the sequence: 1-butanol > 2-butanol > 1,3-butanediol > 1,4-butanediol, which in turn indicate the order of interactions in these mixtures. The S^E values are positive for formamide + 1-butanol and negative for formamide + 2-butanol/1,3-butanediol/1,4-butanediol mixtures over the entire mole fraction range (Fig. 5), and follow the order: 1-butanol > 2-butanol > 1,3-butanediol > 1,4-butanediol. These trends in S^E also indicate that the order of interactions in these mixtures follows the sequence: 1-butanol > 2-butanol > 1,3-butanediol > 1,4-butanediol. This further supports the trends exhibited by π_i^E, V_f^E, G^E and H^E values with composition of the mixtures.

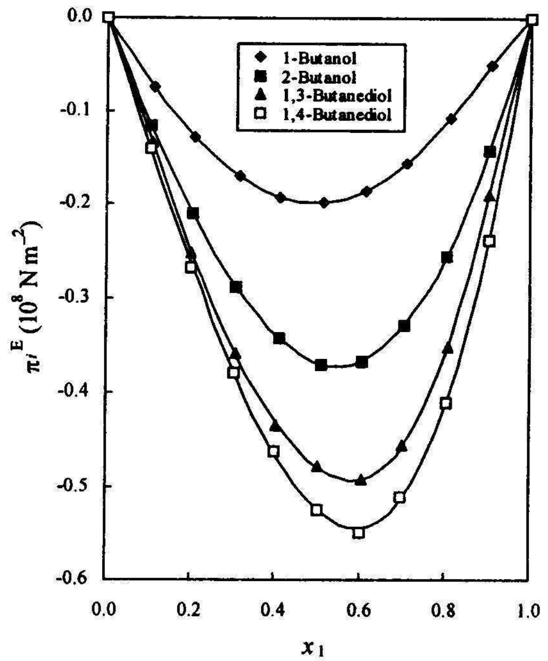

Fig. 1. Variation of excess internal pressure, π_i^E with mole fraction, x_1 of formamide for the binary mixtures at 298.15 K. The points show experimental values and curves show smoothed values using Eq. (10)

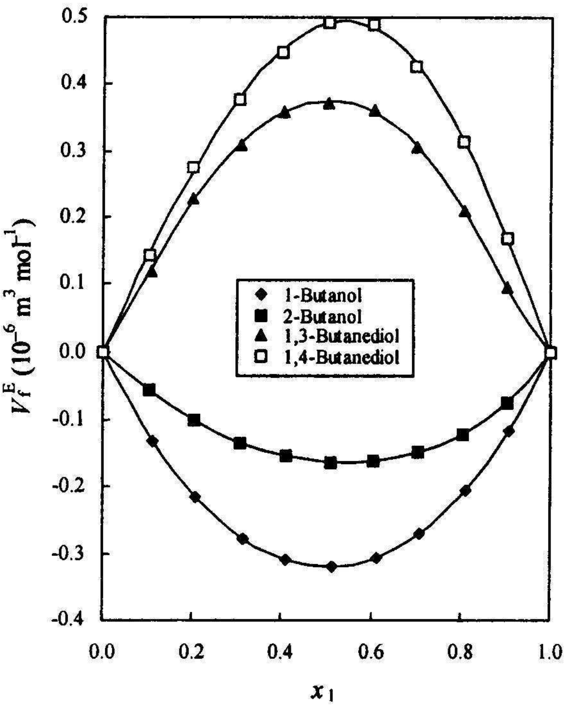

Fig. 2. Variation of excess free volume, V_f^E with mole fraction, x_1 of formamide for the binary mixtures at 298.15 K. The points show experimental values and curves show smoothed values using Eq. (10)

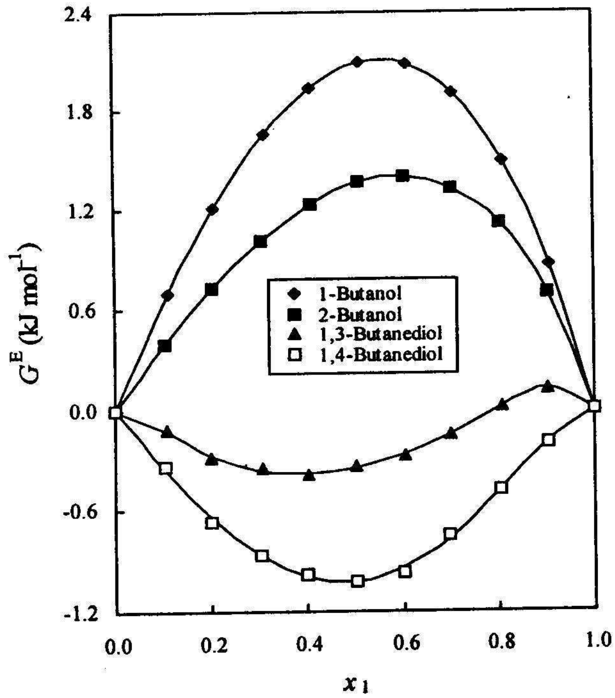

Fig. 3. Variation of excess free energy, G^E with mole fraction, x_1 of formamide for the binary mixtures at 298.15 K. The points show experimental values and curves show smoothed values using Eq. (10)

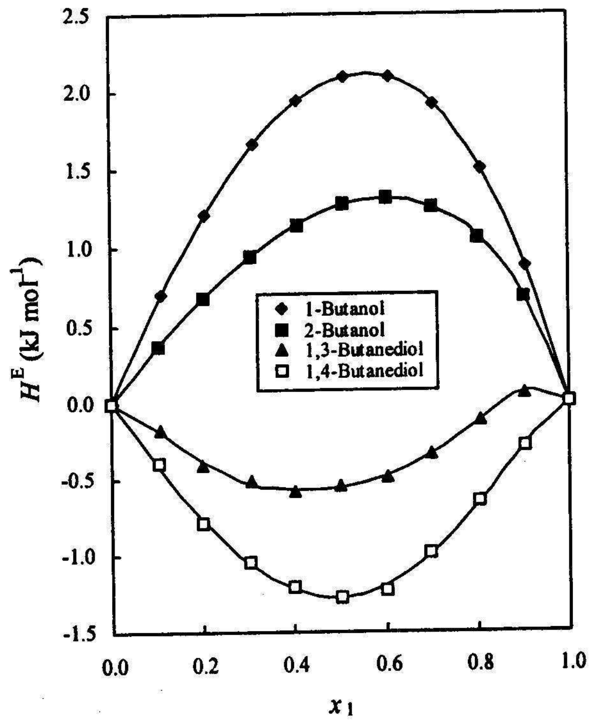

Fig. 4. Variation of excess enthalpy, H^E with mole fraction, x_1 of formamide for the binary mixtures at 298.15 K. The points show experimental values and curves show smoothed values using Eq. (10)

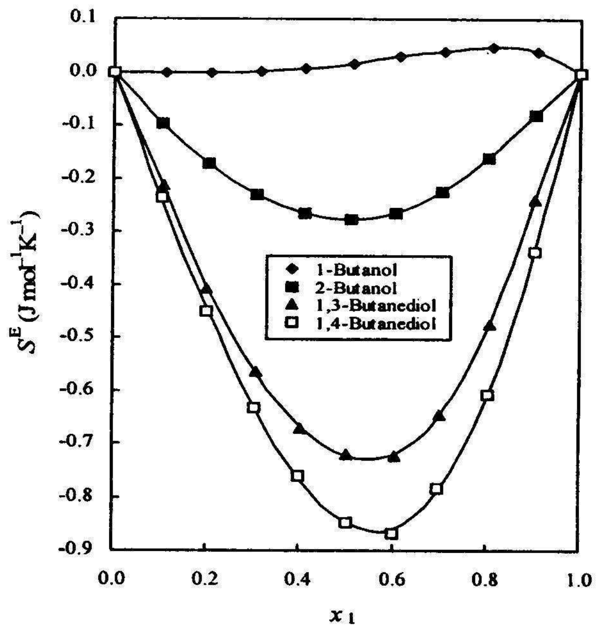

Fig. 5. Variation of excess entropy, S^E with mole fraction, x_1 of formamide for the binary mixtures at 298.15 K. The points show experimental values and curves show smoothed values using Eq. (10)

4. REFERENCES

[1] J.H. HILDEBRAND and R.L. SCOTT, 1962. Regular Solutions, Prentice Hall, Englewood Cliffs, New Jersey.

[2] E.B. BAGLEY, T.P. NELSON and J.M. SCIGLIANO, 1973. *J. Phys. Chem.*, **77**, 2794.

[3] D.R. ROSSEINSKY, 1977. *J. Phys. Chem.*, **81**, 1578.

[4] J.A.R. RENUNCIO, G.J.F. BREEDVELD and J.M. PRAUSNITZ, 1977. *J. Phys. Chem.*, **81**, 324.

[5] A.K. NAIN, D. CHAND, P. CHANDRA and J.D. PANDEY, 2009., *Phys. Chem. Liq.*, **47**, 195.

[6] A.F.M. BARTON, 1971. *Chem. Rev.*, **75**, 731; *J. Chem. Edu.*, **48**, 156.

[7] C.V. SURYANARAYANA, 1976., *J. Acoust. Soc. India*, **4**, 75.

[8] M.R.J. DACK, 1975., *Aust. J. Chem.*, **28**, 1643; *Chem. Soc. Rev.*, **4**, 211.

[9] A. ALI and M. TARIQ, 2006. *J. Chem. Res. (s)*, 261.

[10] J.D. PANDEY, 1980. *J. Chem. Soc., Faraday Trans. II*, **76**, 1215.

[11] J.D. PANDEY and S.N. SRIVASTAVA, 1991. *Acoust. Lett.*, **6**, 91.

[12] J.D. PANDEY, S.K. SHUKLA, J. CHHABRA and R. DEY, 2004. *J. Indian Chem. Soc.*, **81**, 962.

[13] A.K. NAIN, D. CHAND, P. CHAUDHARY and A.K. SRIVASTAVA, 2008. *J. Acoust. Soc. India*, **35**, 23.

[14] A.K. NAIN, 2007. *J. Solution Chem.*, **36**, 497.

[15] A.K. NAIN, 2008. *Fluid Phase Equilib.*, **265**, 46.

[16] J.D. PANDEY, R.K. SHUKLA, A.K. SHUKLA and R.D. Rai, 1988. *J. Chem. Soc., Faraday Trans. I*, **84**, 1873.

[17] J.D. PANDEY, G.P. DUBEY, B.P. SHUKLA and S.N. DUBEY, 1993. *J. Pure Appl. Ultrason.*, **15**, 33.

18][J.H. HILDEBRAND, 1947. *J. Chem. Phys.*, **15**, 225.

[19] J.H. HILDERBRAND and R.L. SCOTT, 1964. The Solubility of Non-electrolytes, 3rd ed., Dover Publications, New York.

[20] O. Redlich and A. T. Kister, 1948. *Ind. Eng. Chem.*, **40**, 345.

[21] B. GARCIA, R. ALCALDE, J.M. LEAL and J.M. MATOS, 1996. *J. Chem. Soc., Faraday Trans.*, **92**, 3347.

[22] Y. MARCUS, 1977. Introduction to Liquid State Chemistry, Wiley Interscience, New York.

[23] G.A. KRESTOV, 1991. Thermodynamics of Solvation, Ellis-Horwood Ltd., England.

Journal of Acoustical Society of India : Vol. 37, No. 1, 2010 (pp. 33-36)

Ultrasonic and Spectroscopic Studies of Ternary Mixture Ethyl Acetate + 2-Butanone + Hexane

A.J. Clement Lourduraj[1] and I. Johnson[2]
[1]*Lecturer in Physics, St. Joseph's College (Autonomous), Trichirappaali - 620 002*
e-mail : ajeevaclement @ yahoo.co.in
[2]*Reader in Physics, St. Joseph's College (Autonomous), Trichirappaali - 620 002*
e-mail : jnaadarsh @ hotmail.com

ABSTRACT

This paper reports the experimental densities, sound velocities and viscosities of the Ternary mixtures Ethyl Acetate + 2-Butanone + Hexane which have been measured at 308.15K for the entire range of mole fraction. From these data, excess volume (VE) have been calculated. Experimental and computed results are used to study the type and nature of inter and intra molecular interactions between the mixing components. Even though these types of studies exist in the literature there is no confirmation for the observed excess properties through other non-ultrasonic techniques. For the confirmation of the excess properties FTIR spectra have been taken for various compositions of those mixtures. This FTIR study gives supportive evidences for the results obtained through the excess volume study.

1. INTRODUCTION

The present work is a continuation of our earlier studies of thermodynamic and physico-chemical properties of non-aqueous ternary liquid mixtures [1]. The present investigation is concerned with the study of the ternary systems Ethyl Acetate + 2-Butanone + Hexane for their entire composition range. A deeper knowledge of mixing properties of such multicomponent liquid system is essential in many industrial applications, such as design calculation, mass transfer, fluid flow etcv[3]. The present work reports densities, viscosities and speeds of sound for the system measured at 308.15K. From these data excess volume VE, have been calculated. FTIR spectra have been taken for some ranges of mole fractions of liquid mixtures and pure liquids.

2. EXPERIMENTAL MATERIALS

High - purity spectroscopic and HPLC grade chemicals of Ethyl Acetate, 2-Butanone and Hexane were obtained from Merck Co. Their purities were 99.5 % or better and no further purification was done. The chemicals were stored over molecular sieves. The verification of the purity of the chemicals was realized by ascertaining the consistency of the values of density, viscosity and ultrasonic velocity at 298.15K which were reasonably in accordance with the values found in the literature.

3. MEASUREMENTS

Densities of liquids and their mixtures were measured at 308.15K with specific gravity bottle method. The results of density are accurate to ± 0.0002 gcm-3. An electronic digital balance is used to measure the mass of the liquids within an accuracy of ± 0.001g. The viscosities of the pure liquids and their mixtures were measured using an ostwald's viscometer. The flow times are measured within an accuracy of ± 0.01sec. The speed of sound in the mixture has been measured by an ultrasonic interferometer of frequency 2MHz. The speed of sound values is accurate to ± 2m.s-1. The measurements have been carried out in a constant temperature bath at 308.15K within an accuracy of ± 0.01K. FTIR spectra were taken for the liquid mixtures in a FTIR spectrum photometer (Perklin Elmer Co. model 1605) by using the KBr pellet method[4].

4. RESULTS AND DISCUSION

In the case of Ethyl Acetate + 2-Butanone + Hexane mixture, the VE is maximum positive (0.4 of Ethyl Acetate + 0.1 of 2-Butanone + 0.5 of Hexane mixture) and maximum negative (0.4 of Ethyl Acetate + 0.2 of 2-Butanone + 0.4 of Hexane mixture) for 0.4 mole fraction of Ethyl Acetate. The maximum positive in excess volume shows

Table 1. Determination of mole fraction, velocity, viscosity and density for Ethyl Acetate + 2-Butanone + Hexane

S.No.	EA	2B	Hex	Viscosity $N.sm^{-2}$	Velocity ms^{-1}	Density $x\ 10^{-3}\ kgm^{-3}$	Excess Volume $(10^6\ m^3)$
1	0.1004	0.1064	0.7932	0.00027	776	0.6801	1.1455
2	0.2034	0.1077	0.6889	0.00051	776	0.6840	4.2055
3	0.3058	0.1071	0.5871	0.00030	777	0.7095	3.4345
4	0.4054	0.1065	0.4881	0.00027	779	0.7458	1.1685
5	0.5057	0.1063	0.3880	0.00059	796	0.7568	3.1167
6	0.6043	0.1062	0.2895	0.00032	796	0.7919	1.6435
7	0.7038	0.1060	0.1902	0.00032	799	0.8246	0.9083
8	0.7989	0.1054	0.0957	0.00061	802	0.8271	3.9882
9	0.2026	0.2094	0.5880	0.00027	780	0.7030	3.0542
10	0.3041	0.2079	0.4880	0.00027	783	0.7330	1.8216
11	0.4055	0.1065	0.4880	0.00053	783	0.7283	3.9256
12	0.4047	0.2075	0.3878	0.00033	807	0.8156	-6.1612
13	0.5043	0.2063	0.2894	0.00031	799	0.7987	-0.4303
14	0.6030	0.2069	0.1901	0.00062	821	0.8000	2.9601
15	0.6989	0.2054	0.0957	0.00034	837	0.8297	2.583
16	0.3048	0.3060	0.3892	0.00031	792	0.7512	1.361
17	0.4488	0.2084	0.3428	0.00057	803	0.7710	1.4096
18	0.5025	0.4008	0.0967	0.00038	825	0.8063	3.2908

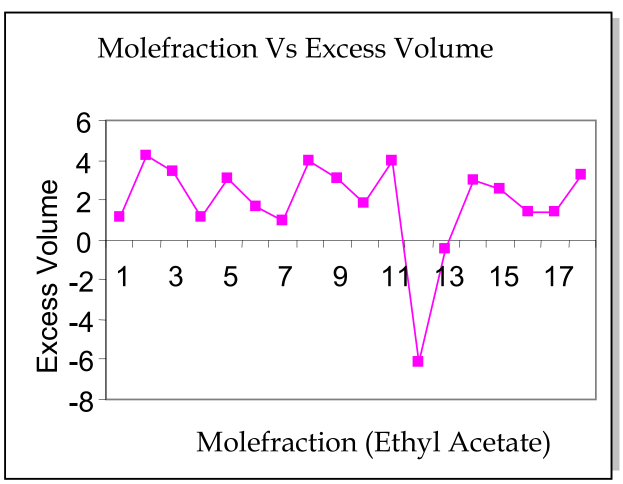

Fig. 1. Excess volume (ethyl acetate + 2-butanone + hexane)

Table 2. Observations of FTIR Spectrum of Ethyl Acetate + 2-Butanone + Hexane

S1 (Cm^{-1})	S2 (Cm^{-1})	S3 (Cm^{-1})	S4 (Cm^{-1})	S5 (Cm^{-1})	S6 (Cm^{-1})	S7 (Cm^{-1})	S8 (Cm^{-1})	S9 (Cm^{-1})
3925.08	3920.42	3922.32	3459.19	3443.38	3921.92	3451.66	3820.17	3922.83
3445.96	3440.28	3794.87	2963.90	2961.38	3441.22	2999.34	3441.43	3815.17
2966.78	2966.24	3457.13	2832.28	2831.71	2978.74	2832.46	2831.80	3439.58
2832.19	2831.80	2961.99	2719.35	2718.65	2832.19	2719.92	2720.98	2963.05
2720.35	2721.64	2832.02	2375.56	1599.10	2720.26	2373.04	2367.12	2831.80
2359.43	1598.26	2719.74	1601.38	1461.09	2364.66	1714.61	1598.86	2720.66
1599.65	1360.15	2376.47	1463.43	1362.27	1599.06	1598.94	1465.75	2369.69
1361.93	773.57	1599.22	1362.84	1241.28	1362.03	1427.18	1361.26	1598.12
1022.04	610.23	1362.02	1241.47	774.69	1242.25	1362.70	1241.58	1360.81
774.63		1228.66	1065.56	613.93	1061.83	1226.38	773.45	1122.61
614.51		774.51	774.90		774.45	1094.54	604.21	773.98
		612.42	612.29		614.72	1057.11		613.73
						905.57		
						774.95		
						611.99		
						532.24		

S1- (EA)0.1004+ (2B)0.1064+ (Hex)0.7932, S2-(EA)0.2034 +(2B)0.1077+ (Hex)0.6889
S3- (EA)0.3058+ (2B)0.1071+(Hex)0.5871, S4-(EA)0.4054+ (2B)0.1065+(Hex)0.4881
S5- (EA)0.5057 +(2B)0.1063+ (Hex)0.3880, S6-(EA)0.6043 +(2B)0.1062 +(Hex)0.2895
S7- (EA)0.7038 +(2B)0.1060+ (Hex)0.1902, S8-(EA)0.7989 +(2B)0.1054 +(Hex)0.0957
S9- (EA)0.2026+ (2B)0.2094+ (Hex)0.5880

S10 (Cm^{-1})	S11 (Cm^{-1})	S12 (Cm^{-1})	S13 (Cm^{-1})	S14 (Cm^{-1})	S5 (Cm^{-1})	S16 (Cm^{-1})	S17 (Cm^{-1})	S18 (Cm^{-1})
3925.24	3919.64	3921.81	3922.83	3931.86	3920.48	3924.15	3923.33	3452.55
3800.40	*3439.12	3438.16	3445.58	3440.19	3788.96	3434.53	3787.28	2987.45
3444.85	*2832.01	*2989.65	2832.13	2831.82	3438.89	2978.96	3451.48	2833.02
2966.09	2722.24	2831.96	2721.10	2721.68	2991.14	2830.51	2981.69	2721.76
2832.26	*2375.34	2722.18	2368.82	2366.92	2832.10	2723.85	2833.58	2480.09
2721.11	1596.57	*1759.91	1598.01	1596.80	2725.86	2365.51	2724.87	2090.67
1598.52	1359.28	1597.41	1361.14	1359.07	2365.04	2163.66	2093.13	1759.67
1361.11	1243.14	*1463.92	774.38	1121.18	2104.88	1596.72	1760.87	1597.19
1244.51	1119.90	1360.37	611.94	1026.21	1760.57	1464.73	1596.84	1461.30
774.34	773.88	1243.11		773.90	1596.95	1358.40	1463.96	1366.24
609.92	610.79	1116.38		607.79	1464.87	1244.05	1364.08	1242.78
		1056.50			1359.05	1117.08	1242.70	1172.34
		774.04			1243.08	1048.04	1172.52	1056.45
		609.81			1056.19	773.34	1056.50	934.26
					773.60	607.34	933.98	843.84
					610.28		773.09	774.40
							615.80	603.88

S10 - (EA)0.3041+(2B)0.2079+(Hex)0.4880, S11 - (EA)0.4055+(2B)0.1065+(Hex)0.4880
S12 - (EA)0.4047+(2B)0.2075+(Hex)0.3878, S13 - (EA)0.5043+(2B)0.2063+(Hex)0.2894
S14 - (EA)0.6030+(2B)0.2069+(Hex)0.1901, S15 - (EA)0.6989+(2B)0.2054+(Hex)0.0957
S16 - (EA)0.3048+(2B)0.3060+(Hex)0.3892, S17 - (EA)0.4488+(2B)0.2084+(Hex)0.3428
S18 - (EA)0.5025+(2B)0.4008+(Hex)0.0967
* Maximum shift in the frequency has been observed.

the presence of dispersion type interaction and maximum negative in excess volume is due to dipole-dipole interaction. It is also due to the interstitial accommodation of one type of molecule into other. The FTIR spectrum taken shows a drastic change in the frequency value or the presence of a new frequency value for 0.4 mole fraction of Ethyl Acetate (0.4 of Ethyl Acetate + 0.1 of 2-Butanone + 0.5 of Hexane mixture and 0.4 of Ethyl Acetate + 0.2 of 2-Butanone + 0.4 of Hexane mixture). So, the FTIR spectrum study gives an additional evidence for the observed molecular interactions through excess volume study.

5. LITERARTURE CITED

Periodicals

[1] I. JOHNSON, M. KALIDOSS and R. SRINIVASAMOORTHY, 2001, Acoustical investigation of some binary and ternary liquid mixtures, Proceedings of the 17th International congress on Acoustics (ROME), *Physical Acoustics -Part B*, **1**, 12-13.

[2] J.D. PANDEY and ASHOK KUMAR, 1994, Ultrasonic velocity in pure liquids, *Journal of Pure and Applied Ultrasonics*, **16**, 63-68.

[3] S. VISWANATHAN and M. ANAND RAO, 2000. *Journal of Chem. Eng*., Data - **45**, 764-770.

[4] A. MUKHERJEE and S. KAMILA et al, 1999. *Acoustics Letters* (*U.K*)., **23**, 17-24.

[5] M. KALIDOSS, I. JOHNSON and R. SRINIVASAMOORTHY, 1999. *J. Acoust. Soc. Ind*., **27**, 319.

[6] M. KALIDOSS and R. SRINIVASAMOORTHY, 1997. *J. Pure Appl. Ultrason*., **19**, 9.

[7] C.V. SURYANARAYANA and S. KUPPUSAMY, 1979, *J. Acous. Soc. Ind.*, **7**, 131.

[8] R.J. FORT and W.R. MOORE, 1965. *Trans. Faraday society*, **61**, 2102-2107.

[9] E. ZOREBSKI and A. ZAK -Z., 1999. *Physikalische chemie.Bd*., **210 S**, 223-233.

Books:

[1] Riddick.J.A., Bunger W.B., Sanako T.K., 1986, Organic solvents. Physical properties and methods of purification (Techniques of Chemistry) 4thed, Wiley-Interscience, New York.

[2] Weissberger, 1955, Technique of Organic Chemistry, Vol. VII, Organic solvents. Physical properties and methods of purification, 2nded, Inter-science publisher, New York.

[3] Handbook of Chemistry and Physics, 1984, The Chemical Rubber company, Cleveland, Ohio, USA.

[4] Robert M. Silverstein and Francis X. Webster, 1998, Spectrometric identification of organic compounds, John Wiley & Sons, Singapore.

Journal of Acoustical Society of India : Vol. 37, No. 1, 2010 (pp. 37-40)

Vowel Duration as an Acoustic Cue in Garhwali Hindi Dialect of Uttarakhand

R.K. Upadhyay, S.K. Adhikari, Manoj Riyal, Sharad Agarwal, Sanjay Kumar and Manila Chauhan

Department of Physics, Government P.G. College, Rishikesh
Dist. Dehradun - 249 201 (Uttarakhand) India

ABSTRACT

This paper presents a study of vowel duration of fifteen stop consonants of Garhwali Hindi syllables abutted with ten vowels / Λ, a, I, i, U, u, e, ε, O, ɔ / for tokens spoken in isolation by 15 adult male and 15 adult female speakers. Garhwali Hindi is a regional dialect of Uttarakhand. It has been found that vowel duration for voiced consonants is greater than the vowel duration for voiceless consonants. The average duration for all vowels followed by voiced consonants is largest for the labial followed by velar and dental respectively and the order for voiceless consonant is retroflex followed by dental, velar and labial sounds.

1. INTRODUCTION

In linguistics, vowel length is the perceived duration of a vowel sound. Vowel length (steady state vowel + VC transition) is measured from the spectrograph or by some speech software. Vowels are described in terms of relative position of the tongue (high, mid, low) the relative position of the lips (spread, round, un round), the position of soft plate (closed, opened), the phonemic length of vowel (short, long), the tenseness of the articulator (lax, tense) and the relative pitch of the vowel (high, mid, low). Acoustically vowels are characterized by formant pattern, spectrum, duration and fundamental frequency.

2. METHOD

Participants: Fifteen male and fifteen female in the age range of 16-30 years participated in a study. None of the subjects had any significant history of ENT, speech or hearing problems.

Procedure: The subjects were instructed to read the token written on the flash card as naturally as possible. The recording was done in partial acoustically treated room for individual subjects by presenting one flash card at a time using a SANYO voice activated recording system (TRC-860C). This was connected to the computer (Pentium IV) having PRAAT Speech software. The speech signal was digitized at the sampling frequency of 16 kHz.

3. RESULTS AND DISCUSSION

Aspirated Sounds for male

The Table:1: shows the vowel duration for voice and voiceless consonants. The ranges of vowel duration for aspirated voiced and voiceless consonant are from 138.31 to 256.79 m sec. and 113.83 to 242.04 msec respectively.

Table 1. Effect of aspiration on vowel duration (in m sec.) for voice and voiceless consonants in isolation for male speakers

Vowel	Voice					Voiceless				
	Labial	Dental	Retrof-lex	Velar	Average Values	Labial	Dental	Retrof-lex	Velar	Average Values
/ʌ/	138.31	151.56	–	149.41	146.43	133.17	125.21	179.32	113.83	137.88
/a/	239.32	245.02	–	177.47	220.60	190.83	208.91	188.49	172.79	190.26
/I/	154.32	169.00	–	168.65	163.99	128.77	148.77	150.71	154.20	145.61
/i/	197.48	206.78	–	207.73	204.00	156.25	189.28	181.14	190.38	179.26
/U/	202.67	157.37	–	159.14	173.06	142.91	147.25	143.76	137.55	142.87
/u/	196.25	201.30	–	228.61	208.72	162.52	151.21	157.63	172.84	161.05
/e/	196.36	191.49	–	184.44	190.76	159.86	161.53	172.44	160.45	163.57
/ɛ/	254.76	223.92	–	256.79	245.16	204.93	207.65	201.76	242.04	214.10
/O/	229.95	224.49	–	206.24	220.23	228.30	229.20	183.81	206.01	211.83
/ɔ/	234.7	217.69	–	221.72	224.70	205.85	201.08	213.17	208.91	207.25
Avg.	204.42	198.86	–	196.02	199.77	171.34	177.01	177.22	175.9	175.37

It has been found that vowel duration for voiced consonants (Avg. 199.77 m sec.) is greater than the vowel duration of for voiceless consonants (Avg. 175.37m sec).The ratio of average durations for voiced to voiceless ending from 1.04 to 1.3 and average ratio is 1.14 whereas difference of the same variations varies from 8.4 to 47.67 m sec and average difference is 24.40 m sec. Study effect of place of articulation on vowel duration was studied by analyzing the data presenting in Table:1:. It has been found that the average duration for all vowels followed by voiced consonants is largest for the labial (Avg. 204.42 m sec.) followed in descending order by velar (Avg. 196.02 m sec) and dental (Avg. 198.86 m sec.) sounds. The order for voiceless consonant is retroflex (Avg. 177.22 m sec.) followed by dental (Avg. 177.01m sec.), velar (Avg. 175.9 m sec.) and labial (Avg. 171.34 m sec.) sounds.

Unaspirated Sounds for male The Table:2: shows the vowel duration for voice and voiceless consonants. The ranges of vowel duration for unaspirated voiced and voiceless consonant are from 153.23 to 305.59 m sec. and 128.62 to 235.19 m sec. respectively.

Table 2. Effect of aspiration on vowel duration (in m sec.) for voice and voiceless consonants in isolation for male speakers

Vowel	Voice					Voiceless				
	Labial	Dental	Retrof-lex	Velar	Average Values	Labial	Dental	Retrof-lex	Velar	Average Values
/ʌ/	170.05	153.23	177.64	163.54	167.12	128.62	145.69	157.11	144.73	144.04
/a/	221.91	207.23	267.40	224.35	230.22	201.95	197.18	228.22	217.81	211.04
/I/	182.23	166.35	194.93	165.08	177.25	157.93	160.59	197.38	158.73	168.66
/i/	204.53	209.17	207.74	219.61	210.26	201.21	180.97	182.57	215.64	195.1
/U/	199.03	161.68	185.04	168.82	178.64	155.71	150.88	160.74	148.11	153.86
/u/	244.44	194.90	201.73	220.38	215.36	172.10	166.60	191.01	180.20	177.48
/e/	215.14	197.38	227.36	231.92	217.95	167.90	159.19	191.52	171.80	172.60
/ɛ/	231.27	247.22	241.88	273.56	248.48	202.76	235.19	225.68	233.35	224.13
/O/	232.55	209.44	214.41	238.30	223.68	226.85	202.82	206.96	222.10	214.68
/ɔ/	219.56	236.21	305.59	227.51	247.22	199.66	229.08	227.07	195.02	212.71
Avg. Values	212.07	198.28	222.37	213.31	211.51	181.47	182.70	196.83	188.82	187.43

It has been found from that vowel duration for voiced consonants (Avg. 211.51 m sec.) is greater than the vowel duration of for voiceless consonants (Avg. 187.43 m sec).

The ratio of average durations for voiced to voiceless ending from 1.04 to 1.64 and average value is 1.18 whereas difference of the same variations varies from 9 to 45.35 m sec. and average value is 22.08 m sec.

In this study, effect of place of articulation on vowel duration was studied by analyzing the data presenting in table. It has been found that the average duration for all vowels followed by voiced consonants are largest for the retroflex (Avg. 222.37 m sec.) followed in descending order by velar (Avg. 213.31 m sec) labial (212.07 m sec) and dental (Avg. 198.28 m sec.) sounds. The order for voiceless consonant is retroflex (Avg. 196.83 m sec.) followed by velar (Avg. 188.82m sec.), dental (Avg. 182.7 m sec.) and labial (Avg. 181.47 m sec.) sounds.

The average vowel duration for all categories of stops is maximum for retroflex (Avg. 198.81 m sec) followed by velar (Avg.193.51m sec), labial (Avg. 192.33 m sec) and dental (Avg. 189.21 m sec.) sounds.

Aspirated sounds for female speakers

The Table:3: shows the vowel duration for voice and voiceless consonants. The ranges of vowel duration for aspirated voiced and voiceless consonant are from 119.16 to 277.65 m sec. and 101.81 to 262.95 m sec. respectively. It has been found from table that vowel duration for voiced consonants (Avg. 198.55 m sec.) is greater than the vowel duration of for voiceless consonants (Avg. 184.1 m sec). The ratio of average durations for voiced to voiceless ending from 1.01to1.19 and average ratio is 1.09 whereas difference of the same variations varies from 1.3 to 23.63 m sec and average difference is 14 .45 m sec.

Effect of place of articulation on vowel duration was studied by analyzing the data presenting in table:3:. It has been found that the average duration for all vowels followed by voiced consonants is largest for the labial (Avg. 206.80 m sec.) followed in descending order by velar (Avg. 196.98 m sec) and dental (Avg. 191.88 m sec.) sounds. The order for voiceless consonant is retroflex (Avg. 189.44 m sec.) followed by velar (Avg. 183.64 m sec.), dental (Avg. 181.92 m sec.) and labial (Avg. 181.4 m sec.) sounds.

Unaspirated sounds for female speakers

Table-4 shows the vowel duration for voice and voiceless consonants. The ranges of vowel duration for unaspirated voiced and voiceless consonant are from 125.25 to 300.71 m sec. and 117.14 to 274.46 m sec. respectively. It has been found from Table-4 that vowel duration for voiced consonants (Avg. 209.7 m sec.) is

Table 3. Effect of aspiration on vowel duration (in m sec.) for voice and voiceless consonants in isolation for female speakers

Vowel	Voice					Voiceless				
	Labial	Dental	Retroflex	Velar	Average Values	Labial	Dental	Retroflex	Velar	Average Values
/Λ/	155.83	147.38	–	161.08	154.76	127.39	115.66	136.63	144.86	131.13
/a/	257.62	238.49	–	254.83	250.31	234.33	234.57	220.07	242.14	232.78
/I/	153.82	134.06	–	121.17	136.35	136.69	117.58	103.41	101.81	114.87
/i/	235.99	171.26	–	189.83	199.03	161.79	158.09	188.46	170.43	169.69
/U/	119.16	128.91	–	125.08	124.39	106.00	125.81	134.06	114.80	120.17
/u/	143.08	147.33	–	143.99	144.80	142.27	141.08	152.03	138.35	143.43
/e/	237.18	209.92	–	209.54	218.88	217.41	200.82	228.71	204.45	212.85
/ε/	269.16	239.30	–	241.83	250.10	237.99	230.04	247.49	233.74	237.32
/O/	253.17	247.44	–	244.79	248.47	246.00	244.91	237.18	222.89	237.75
/ɔ/	242.94	254.68	–	277.65	258.42	204.17	250.57	246.35	262.95	241.01
Avg. Values	206.80	191.88	–	196.98	198.55	181.4	181.92	189.44	183.64	184.10

Table 4. Effect of aspiration on vowel duration (in m sec.) for voice and voiceless consonants in isolation for female speakers

Vowel	Voice					Voiceless				
	Labial	Dental	Retrof-lex	Velar	Average Values	Labial	Dental	Retrof-lex	Velar	Average Values
/ʌ/	136.00	164.71	205.08	145.91	162.93	127.82	158.66	136.00	122.89	136.34
/a/	228.89	247.75	272.81	271.05	255.12	216.77	238.19	252.52	263.16	242.66
/I/	141.66	133.16	154.07	145.81	143.67	134.50	132.02	133.81	122.03	130.59
/i/	237.75	221.99	197.16	192.91	212.20	150.98	202.11	171.08	184.08	177.06
/U/	157.67	125.25	154.35	117.58	138.71	117.14	124.35	135.53	116.00	123.00
/u/	183.95	154.42	181.49	158.97	169.72	155.78	147.17	177.65	133.84	153.36
/e/	239.05	211.62	245.25	224.03	229.99	219.77	199.89	237.81	205.93	215.85
/ε/	256.86	233.12	292.06	261.84	260.97	219.63	216.30	274.46	248.84	239.81
/O/	274.54	230.30	298.91	225.69	257.36	265.25	227.19	255.65	218.23	241.58
/ɔ/	242.04	251.75	300.71	270.71	266.30	241.92	245.33	225.15	247.07	239.37
Avg.	209.04	197.41	209.58	201.45	209.70	184.86	189.02	199.97	186.21	189.97

greater than the vowel duration of for voiceless consonants (Avg. 189.97 m sec).

The ratio of average durations for voiced to voiceless is ending from 1.05 to 1.2 and average value is 1.11whereas difference of the same variations varies from 12.46 to 35.14 m sec. and average value is 19.74 m sec.

Effect of place of articulation on vowel duration was studied by analyzing the data presenting in Table-4. It has been found that the average duration for all vowels followed by voiced consonants are largest for the retroflex (Avg. 209.58 m sec.) followed in descending order by labial (Avg. 209.04 m sec) velar (201.45 m sec) and dental (Avg. 197.41 m sec.) sounds. The order for voiceless consonant is retroflex (Avg. 199.97 m sec.) followed by dental (Avg. 189.02m sec.), velar (Avg. 186.21 m sec.) and labial (Avg. 184.86 m sec.) sounds.

The average vowel duration for all categories of stops is maximum for retroflex (Avg. 199.75 m sec) followed by labial (Avg.195.53m sec), velar (Avg. 192.07 m sec) and labial (Avg. 190.06 m sec.) sounds.

4. ACKNOWLEDGEMENT

Financial assistance provided by the Uttarakhand Council for Science and Technology to the authors is gratefully acknowledged.

5. REFERENCES

[1] M. SEEMA, T. JAYAKUMAR and P.S. KALAISELVI, 2005. "The effect of Speaking Sample Duration on Fundamental Frequency, *J. Acoust. Soc. India*", **14**, 330-332.
[2] COKER and N. UMEDAN, 1969. "Vowel duration and pitch prominence", *J. Acoust. Soc. Am.*, **47**, 94(A).
[3] T. CHIBA and M. KAJIYAMA, 1941. "The Vowel - Its Nature and Structure".
[4] D.B. FRY, 195. "Duration and Intensity as physical correlates to stress", *J. Acoust. Soc. Am.*, **27**, 765 -768.
[5] B.P. BOGERT, 1953. "On the bandwidth of Vowel formants", *J. Acoust. Soc. Am.*, 2**5**, 791 - 792.
[6] C.F. HOCKETT and A.S. HOVSE , 1957. "Estimation of formant band width from measurements of Transient response of the vocal tract", *J. of speech and Hearing Research*, 309-315.
[7] B.P. BOGERT, 1953. "On the bandwidth of Vowel formants", *J. Acoust. Soc. Am.*, **25**, 791 - 792.
[8] C.F. HOCKETT and A.S. HOVSE, 1957. "Estimation of formant band width from measurements of Transient response of the vocal tract". *J. of Speech and Hearing*.

Acoustical Society of India
(Regn. No. 65-1971)

Executive Council (2010-12)

Announcement

NSA 2010

Rishikesh . Uttarakhand . November 11-13
www.nsa2010.gpgcrishikesh.com

Important Dates

Important dates for NSA 2010

Call for Abstracts	April 2010
Submission of Abstract Deadline	15 May 2010 Extended to 30th May Late abstract submission till 15 June
Notification of Abstract acceptance	15 July 2010
Submission of Full Papers Deadline	15 September 2010
Registration Deadline	15 September 2010
Program Available	1 November 2010
NSA Symposia	11-13 November 2010

INFORMATION FOR AUTHORS

ARTICLES

The Journal of Acoustical Society of India (JASI) is a refereed publication published quarterly by the Acoustical Society of India (ASI). JASI includes refereed articles, technical notes, letters-to-the-editor, book review and announcements of general interest to readers.

Articles may be theoretical or experimental in nature. But those which combine theoretical and experimental approaches to solve acoustics problems are particularly welcome. Technical notes, letters-to-the-editor and announcements may also be submitted. Articles must not have been published previously in other engineering or scientific journals. Articles in the following are particularly encouraged: applied acoustics, acoustical materials, active noise & vibration control, bioacoustics, communication acoustics including speech, computational acoustics, electro-acoustics and audio engineering, environmental acoustics, musical acoustics, non-linear acoustics, noise, physical acoustics, physiological and psychological acoustics, quieter technologies, room and building acoustics, structural acoustics and vibration, ultrasonics, underwater acoustics.

Authors whose articles are accepted for publication must transfer copyright of their articles to the ASI. This transfer involves publication only and does not in any way alter the author's traditional right regarding his/her articles.

PREPARATION OF MANUSCRIPTS

All manuscripts are refereed by at least two referees and are reviewed by the Publication Committee (all editors) before acceptance. Manuscripts of articles and technical notes should be submitted for review electronically to the Chief Editor by e-mail or by express mail on a disc. JASI maintains a high standard in the reviewing process and only accept papers of high quality. On acceptance, revised articles of all authors should be submitted to the Chief Editor by e-mail or by express mail.

Text of the manuscript should be double-spaced on A4 size paper, subdivided by main headings-typed in upper and lower case flush centre, with one line of space above and below and sub-headings within a section-typed in upper and lower case understood, flush left, followed by a period. Sub-sub headings should be italic. Articles should be written so that readers in different fields of acoustics can understand them easily. Manuscripts are only published if not normally exceeding twenty double-spaced text pages. If figures and illustrations are included then normally they should be restricted to no more than twelve-fifteen.

The first page of manuscripts should include on separate lines, the title of article, the names, of authors, affiliations and mailing addresses of authors in upper and lowers case. Do not include the author's title, position or degrees. Give an adequate post office address including pin or other postal code and the name of the city. An abstract of not more than 200 words should be included with each article. References should be numbered consecutively throughout the article with the number appearing as a superscript at the end of the sentence unless such placement causes ambiguity. The references should be grouped together, double spaced at the end of the article on a separate page. Footnotes are discouraged. Abbreviations and special terms must be defined if used.

EQUATIONS

Mathematical expressions should be typewritten as completely as possible. Equation should be numbered consecutively throughout the body of the article at the right hand margin in parentheses. Use letters and numbers for any equations in an appendix: Appendix A: (A1, (A2), etc. Equation numbers in the running text should be enclosed in parentheses, i.e., Eq. (1), Eqs. (1a) and (2a). Figures should be referred to as Fig. 1, Fig. 2, etc. Reference to table is in full: Table 1, Table 2, etc. Metric units should be used: the preferred from of metric unit is the System International (SI).

REFERENCES

The order and style of information differs slightly between periodical and book references and between published and unpublished references, depending on the available publication entries. A few examples are shown below.

Periodicals:

[1] S.R. Pride and M.W. Haartsen, 1996. Electroseismic wave properties, *J. Acoust. Soc. Am.*, **100** (3), 1301-1315.

[2] S.-H. Kim and I. Lee, 1996. Aeroelastic analysis of a flexible airfoil with free play non-linearity, *J. Sound Vib.*, **193** (4), 823-846.

Books:

[1] E.S. Skudzryk, 1968. *Simple and Comlex Vibratory Systems*, the Pennsylvania State University Press, London.

[2] E.H. Dowell, 1975. *Aeroelasticity of plates and shells*, Nordhoff, Leyden.

Others:

[1] J.N. Yang and A. Akbarpour, 1987. Technical Report NCEER-87-0007, Instantaneous Optimal Control Law For Tall Buildings Under Seismic Excitations.

SUMISSIONS

All materials from authors should be submitted in electronic form to the JASI Chief Editor: Dr Mahavir Singh, Acoustics Section, National Physical Laboratory, Dr. K. S. Krishnan Road, New Delhi-110 012 (email: mahavir@nplindia.org Tel: +91-11-4560.9319, Fax: +91-11-4560.9310). For the item to be published in a given issue of a journal, the manuscript must reach the Chief Editor at least twelve week before the publication date.

SUMISSION OF ACCEPTED MANUSCRIPT

On acceptance, revised articles should be submitted in electronic form to the JASI Chief Editor (mahavir@nplindia.org).

JASI

Journal of Acoustical Society of India

The Refereed Journal of the Acoustical Society of India (JASI)

The Journal of Acoustical Society of India is a refereed journal of the Acoustical Society of India **(ASI)**. The **ASI** is a non-profit national society founded in 31st July, 1971. The primary objective of the society is to advance the science of acoustics by creating an organization that is responsive to the needs of scientists and engineers concerned with acoustics problems all around the world.

Manuscripts of articles, technical notes and letter to the editor should be submitted to the Chief Editor. Copies of articles on specific topics listed above should also be submitted to the respective Associate Scientific Editor. Manuscripts are refereed by at least two referees and are reviewed by Publication Committee (all editors) before acceptance. On acceptance, revised articles with the text and figures scanned as separate files on a diskette should be submitted to the Editor by express mail. Manuscripts of articles must be prepared in strict accordance with the author instructions.

All information concerning subscription, new books, journals, conferences, etc. should be submitted to Chief Editor:

Acoustics Section, National Physical Laboratory, Dr. KS Krishnan Road, New Delhi 110 012,
Tel: +91.11.4560.9319, Fax: +91.11.4560.9310, e-mail: mahavir@nplindia.org

Annual subscription price including mail postage is Rs. 2000/= for institutions, companies and libraries and Rs. 2000/= for individuals who are not **ASI** members. The Journal of Acoustical Society of India will be sent to **ASI** members free of any extra charge. Requests for specimen copies and claims for missing issues as well as address changes should be sent to the Editorial Office:

Acoustics Section, National Physical Laboratory, Dr. KS Krishnan Road, New Delhi 110 012,
Tel: +91.11.4560.9319, Fax: +91.11.4560.9310, e-mail: mahavir@nplindia.org

ISSN 0973-330

Printed at Alpha Printers, BG-2/38C, Paschim Vihar, New Delhi-110063 Tel.: 9811848335. JASI is sent to ASI members free of charge.

JASI

Journal of Acoustical Society of India (JASI)

A quarterly publication of the Acoustical Society of India

Volume 37, Number 2, April 2010

EDITORIAL

ARTICLES

INFORMATION

How does a Fibrous Product Improve the Acoustic Performance of a Wall?

The reason why a double-leaf partition gives better sound insulation when its cavity is filled with a fibrous product is known. Many theoretical and experimental studies have been performed to investigate the effects of porous-mineral wool products in walls. From these studies we can draw the conclusion that there are three basic reasons why the sound reduction index (R) or Sound Transmission Loss (TL) of a double-leaf wall improves when glass wool is used in the cavity.

- The resonance frequency of the mass-spring-mass system is shifted to a lower value.
- The glass wool dampens sound waves transmitted through the wall.
- The glass wool dampens lateral standing sound waves in the cavity of the wall.

Each one of these reasons is discussed in more detail in the following paragraphs.

Shift of resonance frequency: All double walls have a resonance frequency caused by the mass-spring-mass system. At this frequency, the Sound Transmission Loss of the wall decreases. For most partitions, this resonance occurs at a frequency below 200 Hz. The frequency at which this resonance occurs is dependant on the mass per unit area of the leaf material and the stiffness of the spring, which is the air space. The mass is usually provided by gypsum wallboard on both sides. The stiffness of the spring is given by the distance between the leaves and the dynamic properties of the enclosed air. When glass wool rolls or batts are placed in the cavity between the leaves, the mass-air-mass / mass-spring-mass resonance frequency shifts lower, which causes an increase of the overall sound insulation properties of the wall. The shift of the resonance of the mass-spring-mass system to a lower frequency is caused by the reduced dynamic stiffness of the cavity / spring filled with glass wool. Glass wool rolls and batts are very effective at causing the resonance frequency of lightweight cavity walls to shift lower, resulting in higher sound insulation.

Damping of sound waves: In double-leaf lightweight walls, sound is transmitted from one leaf to the other via the cavity. As the sound waves pass through a fibrous material, friction occurs between the sound wave and the surface of the individual fibres of the insulation product. This friction causes some of the sound field energy to be converted into heat. With the conversion of acoustic energy into heat, there is less sound energy transmitted through the wall. The thicker the insulation product, the more energy of the sound field is converted into heat, resulting in an increase of the sound insulation. The best acoustic performing construction is obtained when the cavity is filled a damping material. Glass wool rolls and batts will give the most economical way maximising acoustic performance.

Lateral damping: In the air cavity between the two leaves of a lightweight partition, resonance of lateral sound waves occurs. These resonance frequencies are the results of standing waves due to the wall dimensions and the distance between the studs inside the wall. At the resonance frequencies, the sound Reduction Index or Sound Transmission loss of a wall decreases. When the cavity is filled with a damping material, hence glass wool, these lateral standing sound waves are reduced due to the conversion of acoustical energy into heat generated by friction. Converting sound energy into heat energy causes the damping of both lateral standing waves inside the cavity and of sound waves transmitted via the cavity across the wall. Filling the cavity with glass wool rolls or batts reduces the negative influence of standing waves and results in the best overall acoustic performance.

Mahavir Singh

Journal of Acoustical Society of India : Vol. 37, No. 2, 2010 (pp. 45-50)

Prediction of the Effective Loss Factor of Acoustically Lagged Pipes

M. Vamsikanth* and M.L. Munjal
Facility for Research in Technical Acoustics (FRITA)
Department of Mechanical Engineering, Indian Institute of Science, Bangalore - 560 012
**e-mail: munjal@mecheng.iisc.ernet.in*

ABSTRACT

The use of lined/lagged plates, sheet metal components, pipes and ducts is very common in the industry. Apart from having good sound absorbing capacity, these laggings should also have high damping to prevent transmission of vibration to the outer impervious layer, where it can be radiated as sound. To serve this purpose, the effective loss factor of the composite structure may be enhanced using visco-elastic layers like bitumen-based melt sheets. Our basic focus here is to determine composite loss factor of the multilayered shells consisting of intermediate visco-elastic layers by making use of the transfer matrix method and impedance approach.

1. INTRODUCTION

Pipes of the exhaust systems of I.C. engines and compressors are often lagged acoustically on the outside in order to reduce break-out noise. However, break-out noise is known to depend on the resonant flexural vibration of the duct walls excited by the acoustical field inside. This resonant vibration can be reduced by means of structural damping. Whether this damping would come from the porous layer or only from the viscoelastic layer is investigated in this paper.

2. ANALYSIS

Fig. 1 shows the schematic of an acoustically lagged pipe with an intermediate visco-elastic layer. For a plane acoustic wave propagating radially outward, the state variables p_1 and u_1 on the inside can be related to p_5 and u_5 on the outside (Fig. 1) by means of the transfer matrix relation [1]:

$$\begin{bmatrix} p_1 \\ u_1 \end{bmatrix} = \begin{bmatrix} 1 & Z_{12} \\ 0 & 1 \end{bmatrix} \begin{bmatrix} 1 & Z_{23} \\ 0 & 1 \end{bmatrix} \begin{bmatrix} T_{11} & T_{12} \\ T_{21} & T_{22} \end{bmatrix} \begin{bmatrix} 1 & Z_{45} \\ 0 & 1 \end{bmatrix} \begin{bmatrix} p_5 \\ u_5 \end{bmatrix} \tag{1}$$

where Z_{12} is the lumped impedance of the inner pipe wall, Z_{23} is the lumped impedance of the visco-elastic layer, T_{11}, T_{12}, T_{21}, T_{22}, are the transfer matrix elements for the porous layer (expressed in terms of cylindrical functions), and Z_{45} is the lumped impedance of the outer metal jacket.

Lumped impedance of the inner pipe wall may be written as [2]

$$Z_{12} = j\omega I + \frac{1}{j\omega C} \tag{2}$$

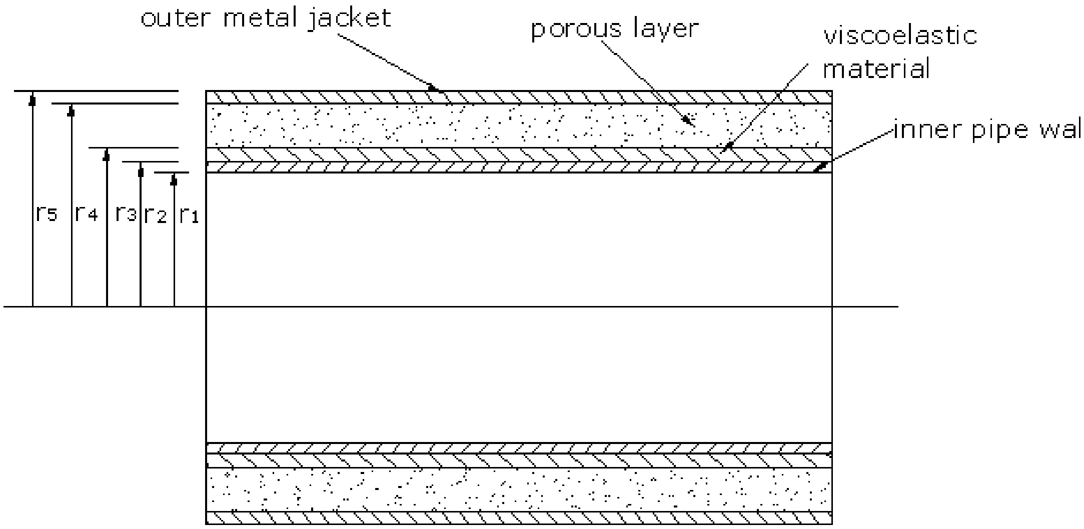

Fig. 1. An acoustically lagged pipe with an intermediate visco-elastic layer

where

inertance, $I = \rho_{12} t_{12} \left\{ 1 + \left(\frac{0.025}{r_1} \right)^2 \right\}$,

compliance, $C = \frac{r_1}{E_{12}} \left[\frac{r_2^{\,2} + r_1^{\,2}}{r_2^{\,2} - r_1^{\,2}} + \upsilon_{12} \right]$

ν_{12} is the Poisson's ratio, E_{12} is the Young's modulus in Pa, and ρ_{12} is the density of the inner pipe wall material in kg/m^3, respectively. r_1, r_2 are the inner and outer radii of the inner pipe wall in m, and $t_{12}=r_2-r_1$ is the thickness of the inner pipe wall in m.

Lumped impedance of the viscoelastic layer is given by [2]

$$Z_{23} = j\omega m_{23} + \frac{K}{j\omega}$$

$$= j\omega \rho_{23} t_{23} + \frac{E_R}{j\omega\, t_{23}} + \frac{\eta\, E_R}{\omega\, t_{23}} \qquad (3)$$

where, ω is the circular frequency in rad/s, $m_{23}= r_{23}t_{23}$ is the density per unit area of the viscoelastic material in kg/m^2, ρ_{23} is the density of the viscoelastic material in kg/m^3, $t_{23}=r_3,r_2$ is the thickness of the viscoelastic layer in m, K is the complex stiffness in N/m, E_R is the storage modulus in Pa, and η is the loss factor of the viscoelastic material.

Transfer matrix elements of the porous layer are given by [3]

$$T_{11} = (X/\det)(J_{1,4}N_{0,3} - J_{0,3}N_{1,4}) \qquad (4)$$

$$T_{12} = (1/\det)(J_{0,4}N_{0,3} - J_{0,3}N_{0,4}) \qquad (5)$$

$$T_{21} = \left(X^2/\det\right)\left(J_{1,3}N_{1,4} - J_{1,4}N_{1,3}\right) \tag{6}$$

$$T_{22} = \left(X/\det\right)\left(J_{1,3}N_{0,4} - J_{0,4}N_{1,3}\right) \tag{7}$$

where J and N denote Bessel function and Neumann function, respectively,

$$X \equiv j\frac{k_{rp}}{Y_p k_p}, \det \equiv X\left(J_{1,4}N_{0,4} - J_{0,4}N_{1,4}\right), \tag{8}$$

$$J_{1,4} \equiv J_1\left(k_{rp}r_4\right), \quad J_{0,4} \equiv J_0\left(k_{rp}r_4\right), \quad N_{1,3} \equiv N_1\left(k_{rp}r_3\right), \text{etc.} \tag{9}$$

Y_p is complex characteristic impedance of the porous layer in kg/(m[2]s) [1,4]:

$$Y_p = \rho_o c_o \sqrt{\left[1 - j\frac{R_p}{\rho_o \omega}\right]} \tag{10}$$

where, R_p is the flow resistivity of the porous layer in kg/(m[3]s), ρ_0 is the density of the fluid entrapped in the pores in kg/m[3], and c_0 is the sound speed in the fluid entrapped in the pores in m/s. K_p is the complex wave number of the porous layer, per m:

$$k_p = k_o \sqrt{\left[1 - j\frac{R_p}{\rho_o \omega}\right]} \tag{11}$$

$k_o = \omega/c_0$ is the wave number, and

$k_{rp} = \left(k_p{}^2 - k_z{}^2\right)^{1/2}$ = radial component of K_p

Lumped impedance of the outer metal jacket is purely inertial:

$$Z_{45} = j\omega\rho_{45}t_{45} \tag{12}$$

where

ρ_{45} is the density in kg/m[3], and t_{45}, r_5-r_5-r_4 is the thickness of the outer jacket in m.

Using Eqs. (2)-(11) in Eq. (1), and multiplying out the constituent transfer matrices, one gets

$$\begin{bmatrix} p_1 \\ u_1 \end{bmatrix} = \begin{bmatrix} T_{11}^* & T_{12}^* \\ T_{21}^* & T_{22}^* \end{bmatrix} \begin{bmatrix} p_5 \\ u_5 \end{bmatrix} \tag{13}$$

and then the total impedance of the wall to the plane waves inside the pipe is given by:

$$Z_w = \frac{p_1}{u_1} = \frac{T_{11}^* Z_o + T_{12}^*}{T_{21}^* Z_o + T_{22}^*} \tag{14}$$

where,

,

is the radiation impedance [6] (15)

$k_{ro} = \sqrt{k_o^2 - k_z^2}$, and subscript 'o ' indicates "outside medium".

The common axial component of the wave number, k_z, in the inner medium, composite pipe and the outer medium, is given by [2]

$$k_z = k_i \left(1 - 2j \frac{\rho_i c_i}{Z_w k_i r_1} \right)^{1/2} \tag{16}$$

where, $k_i = \omega / c_i$, c_i is the velocity of sound, and ρ_i is the density of the inside medium. Solving Eqs. (14) and (16) iteratively, the wall impedance Z_w is obtained.

The composite loss factor of the lagged pipe is then given by

$$\eta_c = \frac{\mathrm{Re}\,(Z_w)}{\mathrm{Im}\,(Z_w)} \tag{17}$$

$T_{21}^* =$ $Z_o =$

3. RESULTS AND CONCLUSION

Fig. 2 shows the variation of the composite loss factor (for a lagged pipe with intermediate visco-elastic layer) and the loss factor of the visco-elastic material, vem (curve fitting the data measured from the experiments [7]).

The following data have been used for plotting the curves in Fig. 2.

Properties of the outer and the inner medium (air):

$\rho_o = 1.2\ \mathrm{kg/m^3},\ c_o = 340\ \mathrm{m/s},\ \rho_i = 1.2\ \mathrm{kg/m^3},\ c_i = 340\ \mathrm{m/s}$

Dimensions of the lagged pipe (see Fig. 1):

$r_1 = 0.1\ \mathrm{m},\ r_2 = 0.101\ \mathrm{m},\ r_3 = 0.102\ \mathrm{m},\ r_4 = 0.152\ \mathrm{m},\ r_5 = 0.153\ \mathrm{m}$

Properties of the inner steel pipe:

$\rho_{12} = 7600\ \mathrm{kg/m^3},\ E_{12} = 206\ \mathrm{GPa},\ \mu_{12} = 0.27$

Properties of the viscoelastic material (vem) layer:

$\rho_{23} = 1830\ \mathrm{kg/m^3}$, and are given by the equations [7]:

$$\eta = -0.05534 f^3 + 0.167 f^2 - 0.171 f + 0.443 \tag{18}$$

$$E_R = 0.1084 f^3 - 0.5196 f^2 + 1.1224 f + 1.1518,\ \ \mathrm{GPa} \tag{19}$$

where f is in kHz.

Flow resistivity of the porous layer:

$$R_p = 10000\ \text{kg}/(\text{m}^3\text{s})$$

Properties of the outer aluminium jacket:

$$\rho_{12} = 2700\ \text{kg}/\text{m}^3,\ \ E_{12} = 71.6\ \text{GPa},\ \ \mu_{12} = 0.34$$

For plane wave propagation inside the pipe, the maximum (cut-off) frequency (corresponding to diameter of 0.1 m) would be 1990 Hz, which lies within the stiffness controlled region. Hence, because of the high stiffness behavior of the pipe, the two loss factor curves (that is the composite and the individual for the vem) shown in Fig. 2 are very close to each other. However, this would not be the case for an acoustically lined flat plate with visco-elastic layer in-between, the vibration of which would be mass-controlled. This is borne out by Fig. 3, which shows the composite loss factor of the corresponding flat plate, along with the loss factor of the visco-elastic (damping) material as a function of frequency.

It may be noted from Fig. 2 that for the lagged pipe considered here, the composite loss factor is almost equal to the loss factor of the visco-elastic material. This is significant inasmuch as for a corresponding lined flat plate (with the thicknesses of the individual layers being same as those in the case of the lagged pipe), the composite loss factor is quite less (of the order of 0.05) as compared to that of the visco-elastic material. Thus, it would be a good practice to apply a layer of visco-elastic material on the pipe before lagging it acoustically on the outside (or lining it acoustically on the inside).

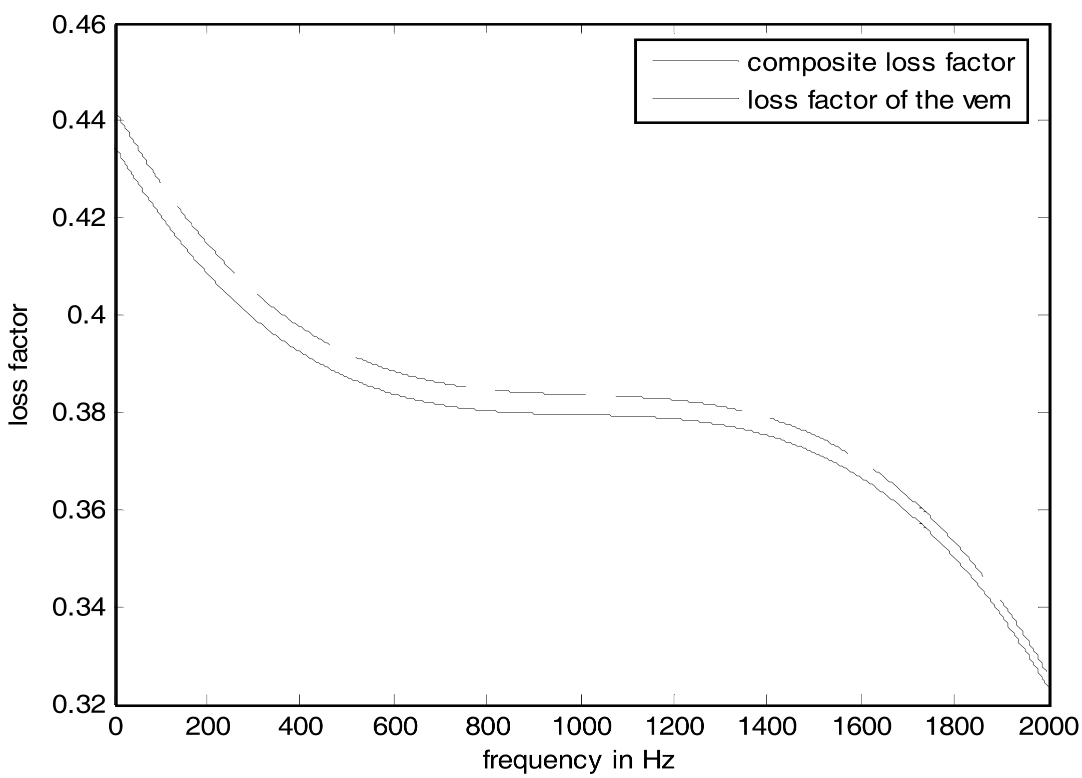

Fig. 2. Composite loss factor of a lagged pipe and the loss factor of the visco-elastic material

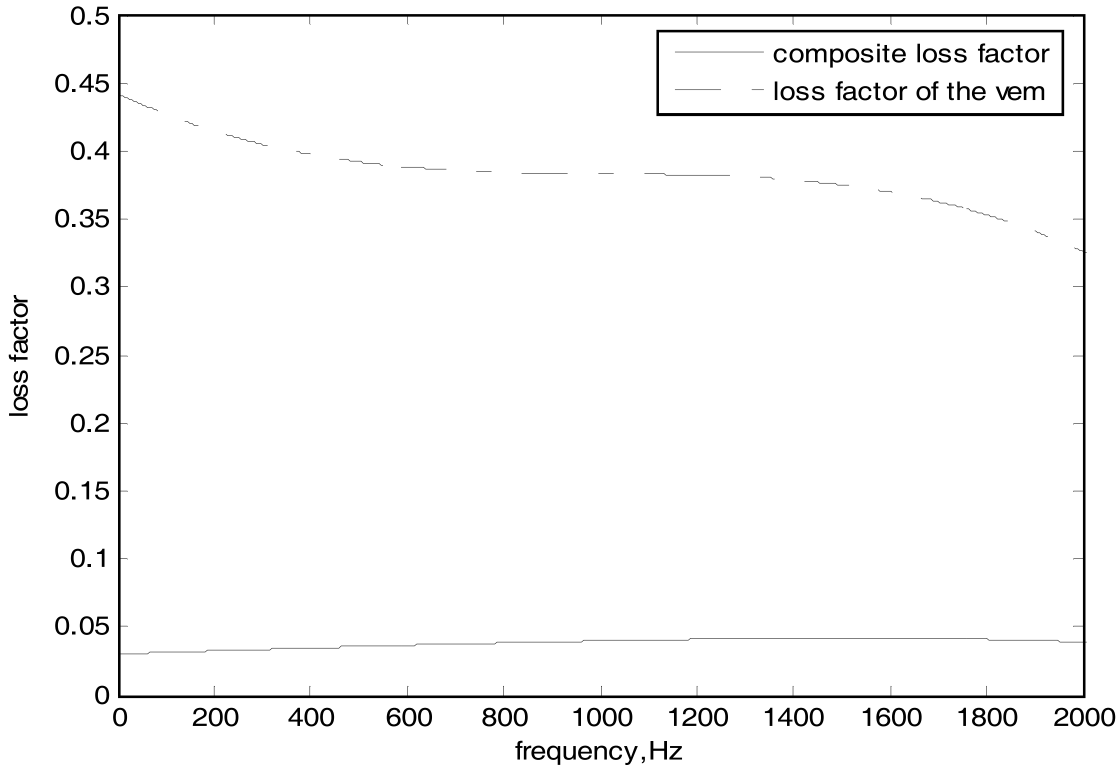

Fig. 3. Composite loss factor of a lined flat plate and the loss factor of the visco-elastic material

4. REFERENCES

[1] M.L. MUNJAL, 1987. Acoustics of Ducts and Mufflers, John Wiley, New York.

[2] M.L. MUNJAL and P.T. THAWANI, 1996. Acoustic Performance of Hoses - A Parametric Study, *Noise Control Engineering Journal*, **44**, 274-280.

[3] M.L. MUNJAL, 1997. Acoustic Analysis and Parametric Studies of Lagged Pipes, *Noise Control Engineering Journal*, **45(3)**, 113-118.

[4] L.L. BERANEK, 1947. Acoustical Properties of Homogeneous, Isotropic Rigid Tiles and Flexible Blankets, *Journal of the Acoustical Society of America*, **19(4)**, 556-568.

[5] A.D. NASHIF, D.I.G. JONES and J.P. HENDERSON, 1985. Vibration Damping, John Wiley, New York.

[6] V. EASWARAN and M.L. MUNJAL, 1995. A Note on the Effect of Wall Compliance on Lowest Order Mode Propagation in Fluid-filled/Submerged Impedance Tubes, *Journal of the Acoustical Society of the America*, **97**, 3494-3501.

[7] M. VAMSIKANTH, June 2008. Evaluation of Vibro-acoustic Properties of Linings, ME dissertation, Indian Institute of Science, Bangalore.

Journal of Acoustical Society of India : Vol. 37, No. 2, 2010 (pp. 51-56)

Computation of Noise Levels due to Elevated Structures

R. Kalai Selvi and A. Ramachandraiah
Acoustics Laboratory, Department of Civil Engineering, IIT Madras, Chennai - 600 036
e-mail : kalaiarchi@gmail.com, btar@iitm.ac.in

ABSTRACT

There is a considerable growth of noise pollution due to excessive presence of moving vehicles more specifically in urban conglomerates. The solutions for noise reduction in such environments are bit difficult especially inside an urban environment. To avoid congestion of traffic-streams introduction of flyovers in the traffic flow happens to be a common feature in many urban centers. Through introduction of flyovers an increase or decrease in noise pollution parameters takes place. They change the soundscape of the city considerably. In this paper an evaluation of these parameters (Lden, Ld, Ln) for an existing flyover of a given geometry has been analyzed using a noise mapping software called soundplan. Noise maps have been developed for a typical flyover in Chennai to show the effects of noise propagation. Noise maps serve as good acoustic tools for visualizing the noise impact. They enable to establish the city soundscape.

1. INTRODUCTION

The Chennai city experiences great traffic volume moving daily. In such cities the urban noise buildup is quite huge. To reduce the congestion of traffic the introduction of flyovers has become a great necessity. Hence large numbers of flyovers have come up in the city and the topographic feature of Chennai is embedded with many flyovers. In this study the effect of noise due to presence of flyover and how the grade separators affects the three dimensional propagation of traffic noise into its neighborhood are highlighted. Noise levels depend on the rates of flow of the different types of passing vehicles, the mean speed of the traffic, the gradient and width of the flyover, the nature of the flow, the type and conditions of the road surface, the weather, the characteristics of the physical surroundings, and the position of the point of observation in relation to the road. Lesser information is available on the effects of gradients or modified topography on road traffic noise especially with flyovers. In some studies [1&2] it is reported that there is a progressive increase in heavy vehicle noise from 2 to 5dB (A) as the gradient or slope of the pavements increase from 2 to 7%.

2. METHODOLOGY

The methodology to evaluate the noise is described further. The basic noise level is calculated from the traffic parameters for a certain reference distance as shown in the Figs. (1a & 1b). The noise level from the road decays with distance. While calculating the contribution of flyover if only a section of the road is to be calculated, the level from the section is described by deducting 10*log (segment angle/180) the geometrical from the flyover distance are established as shown in Figs. (1) and (2). When coming to curved roads or flyovers, it is to be divided into series of smaller sections which are considered to be straight as they deviate from straight by less than 10% of the receiver distance D (for a separation of 5D being the distance between the two end points of segments considered) from the nearest point. A flow chart to describe computation is shown in Fig. (2).

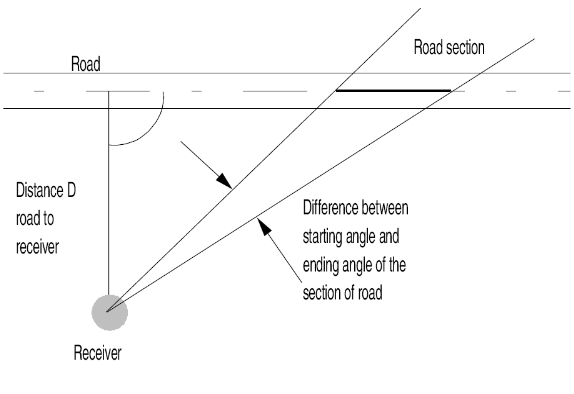

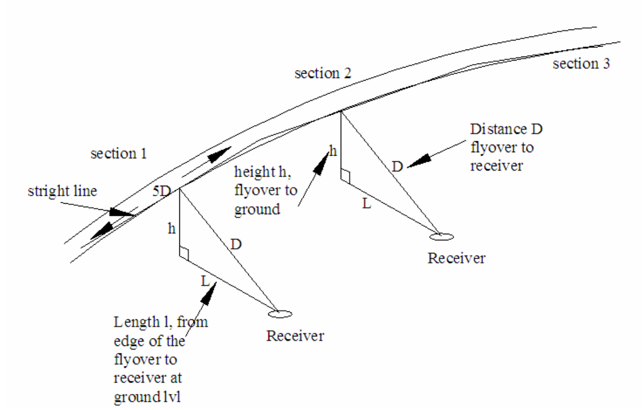

Fig. I a. Angle method for road sections - for straight roads

Fig. I b. Angle method for road sections for curved flyovers or bridges

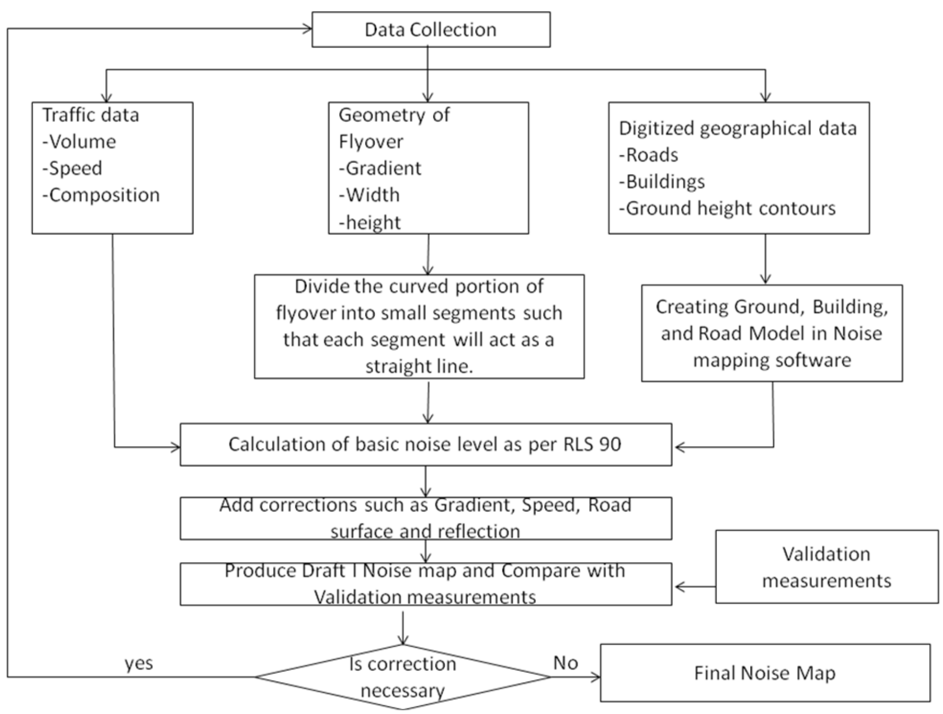

Fig. 2. Flow chart indicating the calculation of noise levels

A three dimensional model of the flyovers is developed initially. Firstly the local topography of the surrounding areas of flyovers is modeled. Subsequently the roads which are lying underneath the flyover are also considered for their contribution towards the noise level at the point of investigation. The other parameters considered are the road width, geometry of flyover, vehicle flow rate, Percentage of heavy vehicles (vehicles with un-laden weight > 1525Kg), mean vehicle speed, gradient of flyover and the road characteristics. The buildings around the flyover are also modeled to study the propagation. Heights of the buildings are estimated with the help of aerial photographs (Google earth) by measuring the heights of the shadows. Wherever there is lack of information on height of buildings it is considered as 8m high as specified in the toolkit 15.2 [3].

The calculations for flyover noise are made in accordance with the methodology prescribed in RLS 90 [4]. The RLS 90 specifications rate (rating level) the sound level at the receiver location for the day (6.00 AM to 10PM) and night (10.00PM to 6.006AM) time ranges for the evaluation of the resulting sound impact. Computations are made to evaluate the noise levels at different heights with respect to flyover.

3. NOISE MEASUREMENTS

A total number of 15 measurements have been selected around the flyover. Some typical measurements are represented in Fig. (3). The measured values are tabulated in Table (2). In these locations field measurements of L10, L50, L90 and Leq are monitored around the flyover using the Norsonic sound level meter type 118. The sound level meter is calibrated prior to each measurement using a sound calibrator type 1251. Sound level meter is mounted on a tripod at 1.2 m above the ground level for the surrounding measurements and in few locations the SLM is mounted 1.2 m above the flyover.

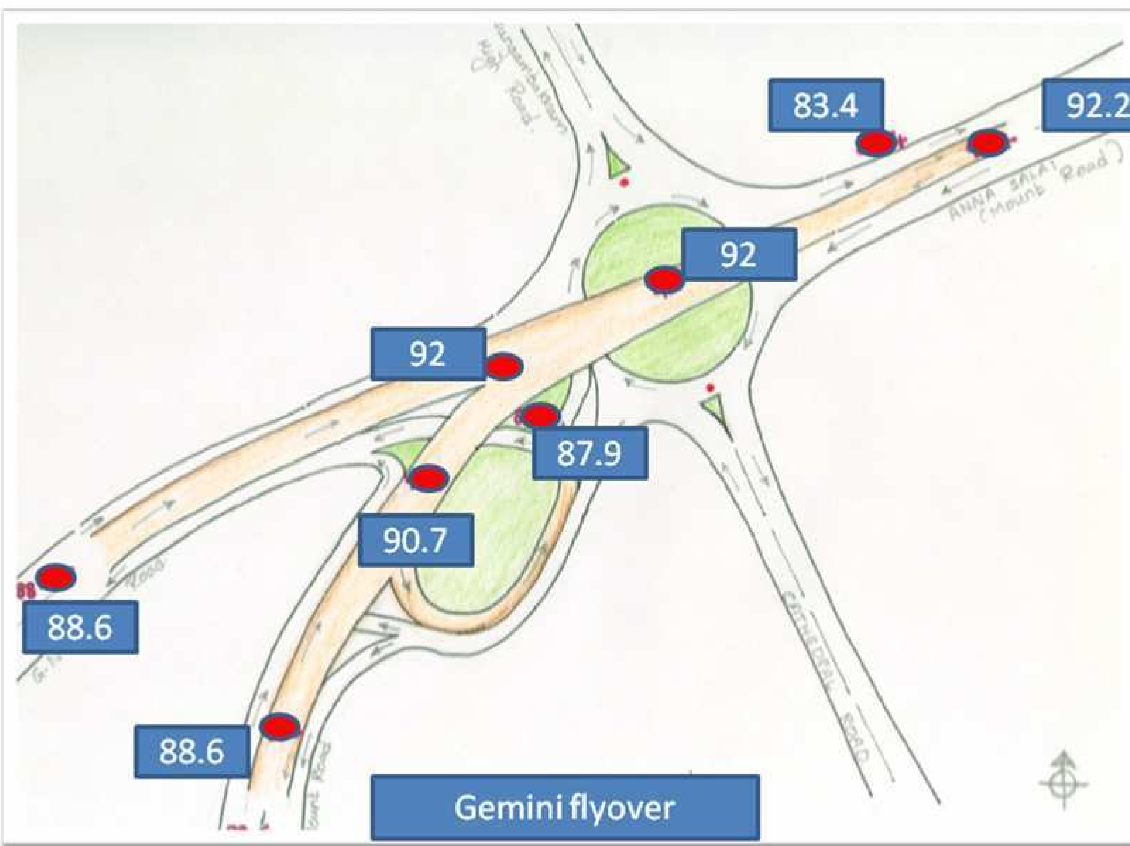

Fig. 3. Plan of Gemini flyover along with measured leq noise levels

4. RESULTS AND DISCUSSION

Figures (4) to (6) show the noise map of flyover considered and its surrounding areas using the soundplan. The noise load distribution map show contour lines (with a difference of 4dB) of day time equivalent noise levels Leq (dB(A)). This map summarizes results of long term measurements (Leq 24hr). It shows the spread of noise from flyover to the adjacent areas and also shows variation of noise contour with the height, geometry and operation conditions of the flyover.

Fig. 4. Noise map of Gemini flyover and its surroundings

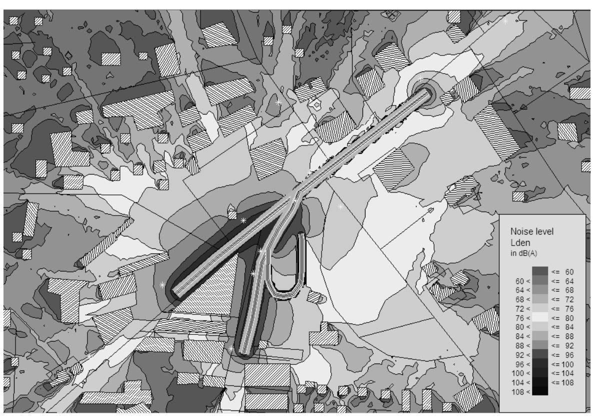

Fig. 5. Result showing the noise levels contributed by flyover alone

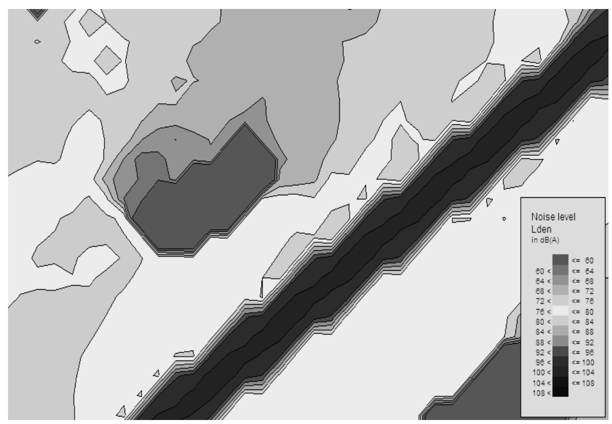

Fig. 6. Results showing the slightly lower noise levels adjacent to flyover

It is seen (Table (1)) that the traffic noise levels Increase vertically with respect to height of the flyover. Fig. (4) shows the noise levels decrease immediately by 3 to 7 dB along the sides of the flyover and then increase. This is due to the shadow effect of flyover geometry. The shadow zone depends on the size and shape of the flyover and it also depends upon height of the physical barrier which presents on the sides of the bridge. Fig. (7) shows the formation of the shadow zone. As the noise level from road/flyover decays with distance the neighborhood areas experiences marginally lower noise levels of the order of 3 to 5 dB(A).

5. VALIDATION OF THE MODEL

The validation of the model is carried out by comparing the measured values with the predicted through the noise map. Table (2) shows the comparison between the Predicted and measured values. (r^2= 0.882)

Table 1. Predicted Lden & Ld values at different heights with respect to flyover

S. No	Location	Lden @Gvl dB(A)	Ld @Gvl dB(A)	Lden @1m dB(A)	L d @1m dB(A)	Lden @5m dB(A)	Ld @5m dB(A)	Lden @10m dB(A)	L d @10m dB(A)	Lden @15m dB(A)	Ld @ 15m dB(A)
1	Location 1	87.3	84.5	88.6	85.8	90.4	87.6	90.4	87.6	89.2	86.4
2	Location 2	92.5	89.4	93.9	91	94	91.1	93.2	90.3	92.6	89.6
3	Location 3	78.6	75.3	78	74.7	78.6	75.3	83.9	80.5	88.8	85.3
4	Location 4	96.1	93	102	99	98.2	95.2	96.1	93	94.8	91.6
5	Location 5	96.8	93.3	97.2	93.6	94.7	91.2	92.8	89.2	91.7	88.2
6	Location 6	93.4	89.8	88.7	85.2	90	86.4	93.4	89.9	93.2	89.7
7	Location 7	89.8	86.2	91.5	87	92.1	88.5	91.4	87.8	90.6	87.1
8	Location 8	88	84.5	89.5	85.9	90.1	86.6	92	88.5	92.6	89
9	Location 9	84.2	82.1	86.1	84	87.2	85.2	86.7	84.6	85.9	83.8
10	Location 10	78.1	74.8	77.8	74.6	78.5	75.2	82.1	78.7	86.9	83.4
11	Location 11	82.9	80.2	84.2	81.5	86.7	84	87.2	84.3	87	84.1
12	Location 12	94.5	91.4	94.8	91.7	94.8	91.8	94.2	91.1	94.2	90.8
13	Location 13	92.9	89.4	91.8	88.3	93.7	90.2	93.7	90.2	93.3	89.8
14	Location 14	88.5	84.7	89.2	85.5	91.2	87.5	91.2	87.5	91.6	87.9
15	Location 15	86	82	87.3	83.3	89.2	85.2	89.2	85.2	89	85

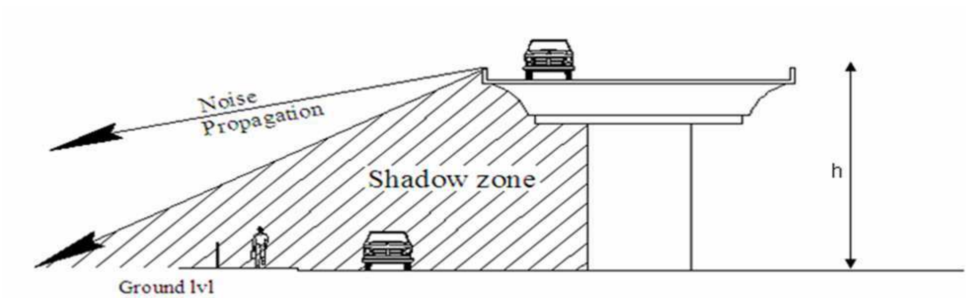

Fig. 7. Noise propagation form the flyover

Table 2. Predicted and measured Leq values

S.No	Location	Leq dB (A) Predicted	Measured	Difference
1	Location 1	87.3	86.7	0.6
2	Location 2	92.5	91	0.5
3	Location 3	78.6	83	-4.4
4	Location 4	96.1	92	4.1
5	Location 5	96.8	90.2	4.6
6	Location 6	93.4	92	1.4
7	Location 7	89.8	89	0.8
8	Location 8	88	88.7	-0.7
9	Location 9	84.2	88.6	-4.4
10	Location 10	78.1	83.3	-5.2
11	Location 11	85.9	92.2	-2.3
12	Location 12	94.5	90.2	4.3
13	Location 13	92.9	90	2.9
14	Location 14	88.5	88.6	-0.1
15	Location 15	86	88	-2

Fig. 8. Correlation chart between measured and predicted Leq values

6. CONCLUSION

This paper illustrates a methodology to predict the noise levels due to elevated structures which are becoming common features in many urban conglomerates. Both the vertical noise gradient and the horizontal spread of the noise due to flyover could be studied with this methodology. The presence of flyover reduces the congestion and signals resulting in a continuous flow of the traffic. It is seen that it provides to an average noise reduction of 3 to 10dB (A) of Leq in the immediate vicinity of road traffic. The difference in noise levels of the upstream and downstream vehicles moving on the flyover can exhibit a difference of 3dB. Subsequent areas beyond the shadow zone also get benefited in terms of noise reduction by virtue of distance attenuation. Some more studies are under investigations and experiments are carried out at other flyovers.

7. REFERENCES

[1] J. BLITZ, 1974. Traffic noise measurements on urban main roads with gradients, *J. sound and vibration,* **37**, 311-319.

[2] B.G. GROVER and J. BLITZ, 1971. The effects of gradients on road traffic noise, *Revista de Acustica*, Madrid **2**, 69-72.

[3] European Commission Working Group Assessment of Exposure to Noise (WG-AEN) Position Paper "Good Practice Guide for Strategic Noise Mapping and the Production of Associated Data on Noise Exposure" Version 1, 2003.

[4] Richtlinien fuÈ r den LaÈ rmschutz an Straûen (RLS-90) (Guidelines for Noise Protection on Streets)- RLS 90/DIN 18005 - 1990.

Journal of Acoustical Society of India : Vol. 37, No. 2, 2010 (pp. 57-64)

Acoustic Study for Recognition of Hindi Stop Consonants in Initial Position of /CVC/ Syllables

R.P. Sharma*, O. Farooq[2], I. Khan[1] and S.K. Gupta[1]
Department of Electronics Engineering, NIMS University, Jaipur, India
[1]Department of Physics, AMU Aligarh, India
[2]Department of Electronics Engineering, AMU Aligarh, India
**e-mail: sharmarp77@gmail.com*

ABSTRACT

This paper deals with the study of various acoustic properties for the recognition of the Hindi unaspirated stop consonants in the initial position in a consonant-vowel-consonant (CVC) context. A total of eight stop consonant classes of different place of articulations have been taken in initial position of CVC syllables. Acoustic parameters such as burst duration (BD), burst frequency (BF), voice onset time (VOT), Duration of second formant transition (F2D) are used as features for recognition of the stop consonants. A discriminant analysis based classifier was implement using quadratic function and the classification results obtained show that these features can be effectively used for the recognition of Hindi stop consonants.

1. INTRODUCTION

The stop sounds, / p /, / t /, / t. /, / k /, / b /, / d /, / d. /, / g / are produced by a complex movements in the vocal tract. With the nasal cavity closed, a rapid closure and or opening are affected at some points in the oral cavity. Behind the point of closure a pressure is built which is suddenly released when the closure is released.

Several researchers have examined the roles played by acoustic cues in the identification of consonants of various categories occupying different positions in a syllable (VC, CV, VCV, CVC, etc.). Among the consonants, stops are of particular importance as they have many important acoustic features

The stop consonants in initial position of syllables preceding a vowel are cued by various acoustic attributes such as frequency of bursts, onset of the periodic laryngeal vibration or glottal pulsing and the articulatory events associated with the release of the consonant burst and onset frequency of formant transition etc.

Cooper et al., [1] conducted an experiment to evaluate the role of synthetic burst at specific frequencies placed before synthetic vowels to distinguish among / p, t, k / . Their results shows that the frequency position of burst plus steady-state vowel could serve as a cue, through not necessarily as a completely sufficient one, for the identification of / p, t, k /.

Halle, Hughes, and Radely [2] analyzed the spectral properties of stop bursts containing in a number of isolated monosyllabic words. They found that the three classes of stops associated with different points of articulation. The bilabial stops have a primary concentration of energy in the low frequencies (500 - 1500 Hz) , the postdental stops have either a flat spectrum or one in which the higher frequencies (above 4000 Hz) predominate , aside from an energy concentration in the region of 500 Hz and in case of the palatal and velar stops, concentration of energy is in intermediate frequency regions (500 - 4000 Hz).

In a series of studies by Lisker & Abramson [3,4] have argued that the interval of time measured from the release of an initial stop to the onset of periodicity, denoted as voice onset time (VOT) is the critical acoustic cue underlying voicing distinctions. In order to do so, we have to consider the timing of the moment of voice onset (that is: the timing of the start of vocal cord vibration). They proposed to take the start of the release of the plosive as a reference time. When the value of this reference time is zero, then a moment following the release will have a positive time, and a moment preceding the release will have a negative time. Thus, Voice onset time (VOT) is the moment at which the vocal cords start to vibrate, measured in reference to the time of release of the plosive. They also reported that VOT fails to distinguish between voiced unaspirated and aspirated stops.

Cole and Scott [5] in an experiment with natural CV sounds found that the energy spectrum which accompanies the noise portion burst (release plus aspiration) of a stop consonant in initial position of syllable contains invariant perceptual information . But Dorman et. al. , [6] found that the burst and transition act in a complementary manner in identifying the initial voiced stops / b , d , g / .

Ohde and Sharf [7] performed experiments with natural stops to evaluate the relative importance of burst and the vowel transition in initial position of CV syllables. They found that burst carries the heaviest load for the identification of unvoiced stops; they also observed that the vowel transition plus steady state vowel is significant to identify unvoiced stops. They further observed that the burst of the initial stop carries sufficient information for the identification of vowels.

Winitz et. al., [8] found that the duration of VOT , was symmetrically altered for English stops. For unvoiced stops VOT was reduced to half the distance between the voiced and unvoiced cognate, VOT was made equivalent to the voiced cognate, and the vocalic portion preceded the release and aspiration segments by 20 msec. It may be concluded that aspiration is the primary perceptual cue in the detection of voicing, and that VOT operates as a relatively unimportant secondary cue.

Abramson [9] suggested that VOT is merely one of a large set of interrelated acoustic consequences of variation in the relative timing of glottal and oral gestures. It is often necessary to be able to identify the onset of voicing on the basis of an acoustic analysis alone.

Banneau et. al. , [10] reported an experiment on the identification of stops from CVC and CV syllables. The experiment shows that the cues provided by burst onsets under any degree of invariance , are not quite sufficient . First, stop identification can be slightly improved by a foreknowledge of the following vowel. Secondly, the presence of short segment of the following vowel is necessary for perfect stop identification.

Manish, Jaseph, Andrew, and Michael [11] study the VOT and burst frequency of four velar stop consonants in Gujarati. They found that, voiced stops had significantly higher burst frequencies than unvoiced stops. There was no significant difference between mean burst frequencies of the aspirated and unaspirated stops. Also the difference in mean VOT as a function of voicing and aspiration were examined. A significant voicing by aspiration effect was found for VOT. The two voiced stops, while not significantly different from each other, had significantly shorter VOTs than unvoiced stops. The aspirated / kh / had a significantly longer VOT than the unaspirated / k / .

Alexander, et.al., [12] compared five commonly used methods for determining the onset of voicing of syllable -initial consonants. Measurements of voicing onset were made based on the onset of periodicity in the acoustic waveform, and on spectrographic measures of the onset of a voicing bar (f0), the onset of first formant (F1), second formant (F2), and third formant (F3). Results suggested that the presence of aspiration in a syllable decreased the accuracy and increased the variability of spectrogram based measurements, but did not strongly affect measurements made from the acoustic waveform. Overall, the acoustic waveform provided the most accurate estimate of voicing onset.

It is observed that several studies have been carried out so far to find out the cues for the identification of the stop consonants of various categories occupying different positions in a syllable (VC, CV, VCV, CVC, etc.).

But most of these studies are for English and other languages (i.e. two or three category languages). While Hindi, an Indo-Aryan language which has four manner categories of stops- voiceless unaspirated, voiced unaspirated, voiceless aspirated and voiced aspirated at four place of articulation- biabial, dental, post alveolar (retroflex stops), and velar [13]. Thus acoustic study of Hindi stop consonants in the CVC syllables was undertaken.

Another reason of attention to stops is due to their difficulty in the phoneme recognition task. This is due to their non-stationary characteristics, which is difficult to capture using Fourier analysis. To overcome this problem, wavelet transform has been proposed which can process non-stationary signals and has multi-resolution capabilities [14].

In this paper time domain as well as frequency domain acoustic parameters of Hindi speech has been studied for the task of phoneme classification. Due to the non-availability of any standard Hindi speech database, first a database was prepared and then various acoustic parameters were studied. Acoustic parameters such as VOT, burst duration, formant transition, frequency of burst and formant transition were measured. Further, these extracted parameters were used as features for recognition of the stop consonants using a quadratic discriminant function based classifier.

2. DATABASE PREPARATION

Five speakers, three males and two females, volunteered as speakers for the experiment. The speakers ranged in age group of 20 to 25 years. None of them had a history of speech, language, or hearing pathology. All speakers had Hindi as their native language and were bilinguals in the sense that they had part of their education through English as their language of instruction.

Eight initial unaspirated consonants, both voiceless and voiced, /p/, /t/, /t./, /k/, /b/, /d/, /d./, /g/ and 4 final unaspirated voiceless consonants /p/, /t/, /t./, /k/ abutted 3 vowel sounds /a/, /i/, /u/ to obtain 8 x 3 x 4 = 96 CVC syllables. Some of these syllables were non-sensible. From among these syllables three randomized lists containing 32 words each were prepared. The purpose of randomizing the words in the list was to avoid context effects, which would be associated with an unvarying order.

Each item was read by the speakers in carrier phrase "/ dekho j?h CVC hE /" in a partially sound treated room and was recorded on a PC with a microphone at a sampling rate of 16 kHz. At the time of recording care was taken to keep the distance between microphone and speaker close to 20 cm. The speakers were asked to utter the lists twice. Fist test was treated as practice test and we had included their second recording to obtain 96 x 5 = 480 utterances for our acoustic studies.

3. PARAMETER MEASUREMENT

To measure the duration and frequency of acoustic features (burst, gap, voice onset time, initial formant transition of vowel, steady state of vowel, final formant transition of vowel) of stop consonants in CVC syllables, waveform and broad-band spectrogram have been used. The representative waveforms and spectrograms of the /CVC/ words have been shown in the figs. The arrows on the time axis in the figs. indicate the onset and/or offset of the acoustic features. The procedure for acoustic measurements is detailed below:

3.1 Voice Onset Time

The term Voice Onset Time (VOT) refers to the timing of the beginning of vocal cord vibration in CV sequences relative to the timing of the consonant release. Alexander, et.al. [12] compared five commonly used methods for determining the onset of voicing of syllable-initial consonants. Overall, the acoustic waveform provided the most accurate estimate of voicing onset. The time difference between release burst of stop consonant and the start of periodic activity (i.e., start of vocal cord vibrations) gives the VOT the VOT as shown in Fig. 1.

3.2 Burst frequency and duration

A speech burst has the form of impulse and is produced by the release of the closure in the vocal tract. While

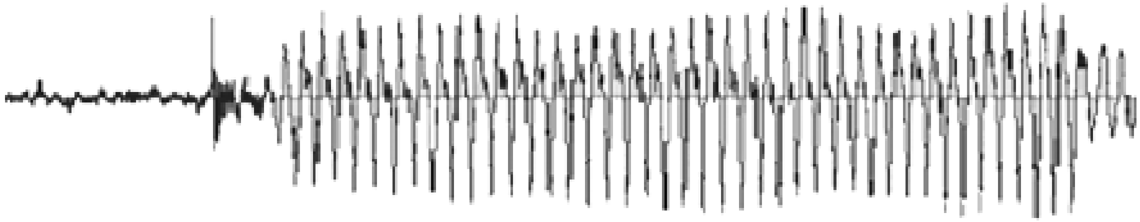

Fig. 1. VOT measurement from acoustic waveform. Time difference between A and B is equal to VOT

measuring the duration of the burst, onset of the burst is marked by fixing the points where pattern shows an abrupt change in the overall spectrum after occlusion. The offset of the burst is noted when energy ceases either at a frequency near second formant or higher. In unaspirated stops the offset of the burst has been noted as soon as regular glottal pulsing starts. In aspirated stops, the burst from aspirated noise could be separated either by the high frequency noise or by a brief period of silence before the onset of aspiration noise. The offset of the burst in unaspirated stops could be found easily by observing the absence of acoustic energy in the spectrogram. Burst frequency was measured from the spectra of each consonant. Spectra were obtained, taking the Fast-Fourier-Transform of the signal to determine the frequencies present. The burst frequency was chosen as the frequency corresponding to the highest amplitude present in the signal spectrum [15] as shown in the Fig. 2.

3.3 Formant transition

When the stop is adjacent to a vowel, the movement in the oral cavity to and/or from the closure results in rapid changes in the formant frequencies. These rapid changes in the vowel formants adjacent to a silence are known as transition and they are important cues for the identification of the different classes of stops [9]. Duration and formant frequency of formant transitions for second and third formants (F2 & F3) were measured from the spectrograph. The duration of formant transition was selected from the onset of the formant to the

Fig. 2. Frequency spectrum of initial burst in syllable / kat/. The x intercept corresponding to the arrow (showing maxima of the spectrum) gives the burst frequency.

steady state of vowel formant. The formant frequency was measured at their respective tip values. These measurements are shown in the Fig. 3.

The arrows on the time axis in the figure indicate the onset or offset of the acoustic features. From Fig. 3 we se that:

AB: initial burst duration
CD: initial formant transition of IInd formant
DE: vowel steady state of IInd formant
EF: final formant transition of IInd formant
FG: gap duration of final stop
GH: duration of final burst
F1, F2 & F3 on the frequency axis represent the Ist, IInd and IIIrd formants respectively

4. RESULTS

4.1 Acoustic Analysis

The acoustical study of 480 CVC syllables were carried out to measure various acoustic parameters such as

- Duration and frequency of initial burst
- Voice onset time (VOT)
- Duration and frequency of second formant for initial formant transition
- Duration and frequency of vowel's steady state portion
- Duration and frequency of final formant transition
- Gap duration, and
- Duration of final burst.

Measurements of the above parameters were carried out for all the words. This paper restricts the discussion only on the acoustic properties of initial stop consonants in CVC syllables. Important acoustic parameters for CV syllable (initial consonant - vowel) are duration of initial burst (BD), frequency of initial burst (BF), voice

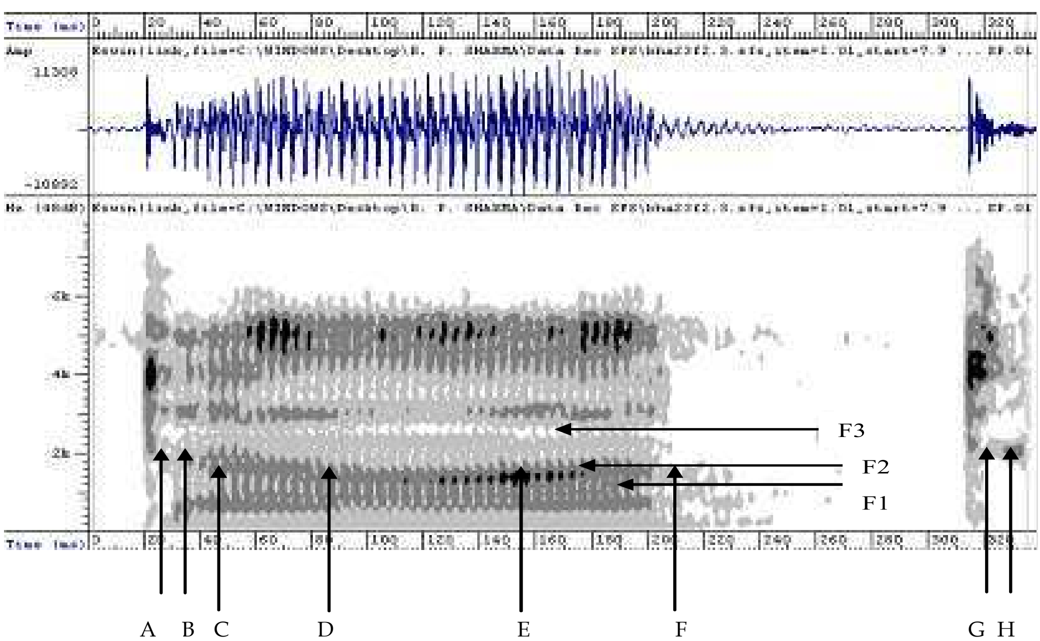

Fig. 3. Waveform and Spectrogram of ward /t.at /

onset time (VOT) duration, duration of second and third formant transition (F2D & F3D), and frequency of second and third formant transition (F2F & F3F). The average values of four parameters are shown in Table 1 for voiced and unvoiced stops according to their place of articulations.

The Table 1 shows the VOT durations for the unvoiced and voiced stop consonants. The VOT value, for voiced stop consonants is negative and large while for unvoiced stop consonants it is positive and small. For unvoiced stop consonants, the average VOT 's for /p, t, t., k / are 13.4msec., 13.1 msec., 8.5 msec., 31.7 msec. respectively. Thus the average VOT for different place of articulation is less than 15 msec., except for velars where it is about 30 msec. For voiced stop consonants, the average VOT 's for / b, d, d., g / are 111.6 msec., 121.4 msec., 109.9 msec., 97.1 msec. respectively. Thus the average VOT for different place of articulation is greater than 110 msec., except for velars where it is about 100 msec.

Table 1. Average values of various acoustic parameters measured for initial unvoiced and voiced stop consonants according to their place of articulations.

The Table 1 shows the average burst frequency of initial stop consonant in CVC syllable for the unvoiced and voiced stop consonants according to their place of articulation. No significant difference was found in burst frequency for voiced and unvoiced stop consonants but it is affected by the following vowel.

Labial stops, (i.e., /p/, /b/), have a primary concentration of energy in the low frequency range (910 - 2152.8 Hz) with an average of 1476.6 Hz. average frequency range for dental stops is 3647.0 to 4447.7 Hz with an average of 4116.4 Hz. For retroflex stops it is found to be from 2125.9 to 3807.3 Hz with an average of 3068.9 Hz, whereas for velar stops frequency range is from 1647.9 to 4139.9 Hz with an average value of 2580.0 Hz. Hence it can be concluded that the labial stops have lower burst frequency about 1500 Hz, and the dental stops have higher burst frequency about 4000 Hz, while the retroflex and velar stops have intermediate ranges of frequency about 3000 Hz and 2500 Hz respectively.

4.2 Recognition Results

The data was divided into training and test set with 60% of the data used for training and the rest 40% was used for testing the classifier. The acoustic parameters measured from the CVC context were VOT, burst frequency, burst duration and second formant transition duration, this give a total of four acoustic parameters.

Finally, above four acoustic parameters were given to a discriminant analysis based classifier using a quadratic discriminant function. The results obtained are show in the form of a confusion matrix in Table 2, which give the percentage classification of the eight stop consonants on the test data.

It may be observed from Table 2 that the stop consonants /k/ has maximum recognition score (i.e., 91.66 %). The recognition score for stop consonants /p/, /d/ and /t./ is 79.16%, 79.16% and 75.0% respectively. The recognition score for all stop consonants is greater than 50 %.

Table 1. Average values of various acoustic parameters measured for initial unvoiced and voiced stop consonants according to their place of articulations

POA	Stops	VOT (msec.)	BF (Hz)	BD (msec.)	F2D (msec.)
Labial	/ p /	13.4	1509.9	6.5	25.5
	/ b /	-111.6	1443.1	6.9	24.2
Dental	/ t /	13.1	3897.3	8.9	34.2
	/ d /	-121.4	4334.7	8.5	34.0
Retroflex	/ t. /	8.5	3085.1	8.1	31.3
	/ d. /	-109.9	3052.8	7.1	35.2
Velar	/ k /	31.7	2421.8	11.4	30.3
	/ g /	-97.1	2738.3	8.8	25.3

Table 2. Confusion matrix showing the percentage correct recognition of test stops consonants of Hindi

input output	/p/	/b/	/t/	/d/	/t./	/d./	/k/	/g/
/p/	79.16	0.00	8.33	0.00	0.00	0.00	12.5	0.00
/b/	0.00	50.00	0.00	8.33	0.00	8.33	0.00	33.33
/t/	12.50	0.00	54.16	0.00	20.83	0.00	12.50	0.00
/d/	0.00	0.00	0.00	79.16	0.00	8.33	0.00	12.50
/t./	8.33	0.00	16.66	0.00	75.00	0.00	0.00	0.00
/d./	0.00	16.66	0.00	25.00	0.00	50.00	0.00	8.33
/k/	4.16	0.00	4.16	0.00	0.00	0.00	91.66	0.00
/g/	0.00	16.66	0.00	12.50	0.00	16.66	0.00	51.16

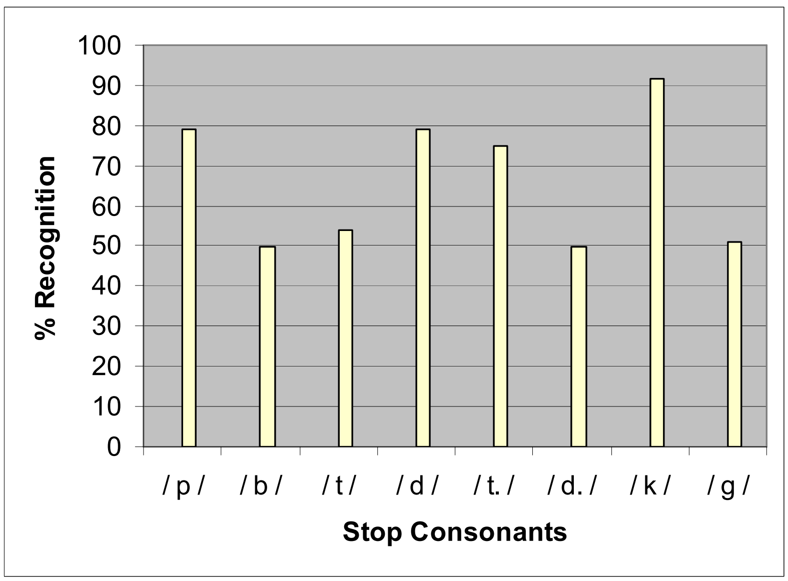

Fig. 4. Recognition performance of stop consonants

Also the recognition performance of various stop consonants is shown in Fig. 1, in the form of histogram.

5. CONCLUSION

The overall recognition of the stop consonants using the acoustic parameters is found to be 66.6% that is high considering the fact that only four features are used as compared to 13 features in MFCC [8] Further, the ratio of between classes to within class scatter shows that VOT provides the maximum discriminatory information between the four stop consonant classes. Thus the results from Table 2 indicate that acoustic parameters can be successfully used as features for the task of phoneme classification.

6. REFERENCES

[1] F.S. COOPER, P.C. DELATTRE and L.J. Gerstman, 1952. Some experiments on the perception of synthetic speech, *J. Acoust. Soc. Am.*, **24**, 597 - 606.

[2] M. HALLE, G.W. HUGHES and J.P.A. RADELY, 1957. Acoustic Properties of Stop Consonants, *Journal of Acoustical Society of America*, **29**, 107-116.

[3] L. LISKER and ABRAMSON, 1964. A cross study of voicing in initial stops: *Acoustical Measurements*, Word, **20(3)**, 384.

[4] L. LISKER and A. ABRAMSON, 1964. 'Some Effects of Context on VOT in English Stops', *Language Speech*, **10(1)**, 384.
[5] R.A. COLE and B. SCOTT, 1974. The phantom of the phonemes: Invariant cues for stop consonants, *Perception and Psychophysics*, **15**, 101 - 107.
[6] M. DORMAN, M. STUDDERT-KENNEDY and L. RAPHAEL, 1977. The invariance problems in initial voiced stops : release burst and formant transition as functionally equivalent context dependent cues, *Perception and Psychophysics*, **22**, 109 - 122.
[7] R.N. OHDE and D.J. SHARF, 1977. Order effect of acoustic segments of VC and CV syllables on stop and vowel identification, *J. of Speech and Hear. Research*, **20(3)**.
[8] H. WINITZ, C. LARIVIERE and E. HERRIMAN, 1975. Variations in VOT for English initial stops, *J. of Phonetics*, **3**, 41 - 52.
[9] A.S. ABRAMSON, 1996. Laryngeal timing in consonant distinctions, *Phonetica*, **34**, 295 -303.
[10] A. BONNEAU, L. DJEZZAR and Y. LAPRIE, 1996. Perception of place of articulation of French stop bursts, *J. Acoust. Soc. Am*., **100(1)**, 555 - 564.
[11] R.K. MANISH, K. JOSEPH, S. ANDREW and P.R. MICHAEL, 1999. Voice Onset Time and Burst Frequencies of four Velar Stop Consonants in Gujarati, *Journal of Acoustical Society of America*, **06(6)**, 3736 -3738.
[12] L.F. ALEXANDER, C. VALTER and M.C.U. JOJO, 2003. Accuracy and variability of acoustic measures of voicing onset, *Journal of Acoustical Society of America*, **113(2)**, 1025 - 1032.
[13] R. Ahmad and S.S Agrawal, 1969. Significant features in the perception of Hindi consonants, J. Acoust. *Soc. Am*., **45**, 758 - 763.
[14] O. Farooq and S. Datta, 2001. Mel filter-like admissible wavelet packet structure for speech recognition, *IEEE Signal Processing Letters*, **8(7)**, 196-198.
[15] K.N. Stevens, 1980. Acoustic correlates of some phonetic categories, *Journal of Acoustical Society of America*, **68**, 836 - 842.

Journal of Acoustical Society of India : Vol. 37, No. 2, 2010 (pp. 65-69)

Ultrasonic and Spectroscopic Studies of Binary Mixtures Ethyl Acetate + 2-Butanone and Ethyl Acetate + Hexane

A.J. Clement Lourduraj[1] and I. Johnson[2]
[1]*Lecturer in Physics, St. Joseph's College (Autonomous), Trichirappaali - 620 002*
e-mail : ajeevaclement @ yahoo.co.in
[2]*Reader in Physics, St. Joseph's College (Autonomous), Trichirappaali - 620 002*
e-mail : jnaadarsh @ hotmail.com

ABSTRACT

A deeper knowledge of mixing properties of multicomponent liquid systems is essential in many industrial applications, such as design calculation, mass transfer, fluid flow etc.

This paper reports the experimental densities, sound velocities and viscosities of the binary mixture Ethyl Acetate + 2-Butanone and Ethyl Acetate + Hexane which have been measured at 303.15K and 308.15K for the entire range of mole fraction. From these data, excess volume (VE) have been calculated. Experimental and computed results are used to study the type and nature of inter and intra molecular interactions between the mixing components. Even though these types of studies exist in the literature there is no confirmation for the observed excess properties through other non-ultrasonic techniques. For the confirmation of the excess properties FTIR spectra have been taken in the regions where VE is maximum negative in addition to some more regions and also for the participating pure liquid components. High-purity spectroscopic and HPLC grade chemicals of Ethyl Acetate and 2-Butanone were obtained from Qualigens fine chemicals. Their purities were 99.5 % or better and no further purification was done. The chemicals were stored over molecular sieves. The verification of the purity of the chemicals was realized by ascertaining the consistency of the values of density, viscosity and ultrasonic velocity at 298.15 K which was reasonably in accordance with the values found in the literature. FTIR spectra were taken for the liquid mixtures in a FTIR spectrum photometer (Perkin Elmer Co, model 1605) by using the KBr pellet method.

1. INTRODUCTION

The present work is a continuation of our earlier studies of thermodynamic and physico-chemical properties of non-aqueous binary and ternary liquid mixtures[1]. The present investigation is concerned with the study of the binary systems Ethyl Acetate + 2-Butanone and Ethyl Acetate + Hexane for their entire composition range. A deeper knowledge of mixing properties of such multicomponent liquid system is essential in many industrial applications, such as design calculation, mass transfer, fluid flow etc[3]. The present work reports densities, viscosities and speeds of sound for the system measured at 308.15K. From these data excess volume VE, have been calculated. FTIR spectra have been taken for some ranges of mole fractions of liquid mixtures and pure liquids.

2. EXPERIMENTAL MATERIALS

High - purity spectroscopic and HPLC grade chemicals of Ethyl Acetate, 2-Butanone and Hexane were obtained from Merck Co. Their purities were 99.5 % or better and no further purification was done. The chemicals were stored over molecular sieves. The verification of the purity of the chemicals was realized by ascertaining the consistency of the values of density, viscosity and ultrasonic velocity at 298.15K which were reasonably in accordance with the values found in the literature.

Table 1. Determination of mole fraction, velocity, viscosity and density for Ethyl Acetate + 2-Butanone

Mole Fraction (Ethyl Acetate)	AT 30^0			AT 35^0			Excess Volume (10^6 m^3)
	Viscosity (10^{-3} N.s/m^2)	Velocity (m/sec)	Density (10^{-3} kg/m^3)	Viscosity (10^{-3} N.s/m^2)	Velocity (m/sec)	Density (10^{-3} kg/m^3)	
1.0000	0.4046	1120.45	0.8891	0.4375	891.25	0.8789	0.0000
0.8885	0.4385	1132.85	0.8809	0.4565	1110.67	0.8721	-0.3901
0.7841	0.4114	1134.57	0.8699	0.4512	1115.37	0.8560	-0.3385
0.6793	0.4019	1140.67	0.8589	0.4373	1121.57	0.8511	-0.2411
0.5766	0.4063	1144.60	0.8529	0.4394	1125.30	0.8419	-0.7857
0.4773	0.4082	1145.51	0.8431	0.4441	1126.94	0.8362	-0.3225
0.3767	0.3943	1150.92	0.8369	0.4383	1132.74	0.8322	-0.4731
0.2801	0.3999	1163.33	0.8232	0.3812	1144.22	0.8100	-0.5008
0.1867	0.3779	1168.16	0.8106	0.4142	1148.96	0.8048	-0.5647
0.0932	0.3854	1173.67	0.8047	0.4193	1155.24	0.7957	-0.6449
0.0000	0.3916	1183.51	0.7934	0.4276	1164.96	0.7803	0.0000

Table 2. Observations of FTIR Spectrum of Ethyl Acetate + 2-Butanone

1 (EA) + 0(2B) cm^{-1}	0.9(EA) + 0.1(2B) cm^{-1}	0.8(EA) + 0.2(2B) cm^{-1}	0.7(EA) + 0.3(2B) cm^{-1}	*0.6(EA) + 0.4(2B) cm^{-1}	0.5(EA) + 0.5(2B) cm^{-1}	0.4(EA) + 0.6(2B) cm^{-1}	0.3(EA) + 0.7(2B) cm-1	0.2(EA) + 0.8(2B) cm^{-1}	0.1(EA) + 0.9(2B) cm^{-1}	0(EA) + 1(2B) cm^{-1}
3449.55	3449.85	3450.45	3755.77	3778.13	3768.93	3775.07	3765.76	3906.73	3920.45	3921.99
2991.58	2991.45	2990.51	3450.69	3447.05	3450.23	3448.38	3448.32	3769.93	3772.35	3778.25
2489.19	2369.39	2488.21	2990.49	2928.83	2990.28	2989.86	2988.64	3449.06	3449.47	3445.42
2362.08	2089.05	2365.16	2489.94	*2093.87	2378.86	2370.49	2368.72	2375.62	2988.97	2930.86
2088.87	1739.40	2089.01	2375.18	*1636.17	2091.95	2092.69	2094.28	2089.51	2380.41	2087.47
1763.76	1637.90	1762.32	2090.50	1418.32	1757.15	1757.83	1746.98	1636.11	2104.31	1815.01
1637.15	1409.82	1637.33	1761.48	1245.49	1637.35	1635.10	1635.26	1405.90	1740.66	1626.89
1378.64	1244.60	1376.73	1637.41	1113.89	1373.67	1373.15	1370.94	1243.50	1628.07	1409.75
1242.81	1110.28	1242.82	1375.96	1021.27	1242.87	1242.82	1242.92	1116.30	1367.68	1247.00
1056.51	1049.78	1164.40	1242.79	577.76	1168.70	1164.26	1114.23	1008.25	1243.00	1117.88
928.00	574.78	1056.35	1165.69		1056.34	1109.66	595.48	670.17	1167.31	1011.07
622.08		931.02	1056.63		935.24	1056.57			1008.88	563.25
		623.89	932.09		595.26	1005.30			586.32	
			622.77			938.26				
						594.26				

* Maximum shift in the frequency has been observed.

3. MEASUREMENTS

Densities of liquids and their mixtures were measured at 303.15K and 308.15K with specific gravity bottle method. The results of density are accurate to ± 0.0002 gcm^{-3}. An electronic digital balance is used to measure the mass of the liquids within an accuracy of ± 0.001g. The viscosities of the pure liquids and their mixtures were measured using an ostwald's viscometer. The flow times are measured within an accuracy of ± 0.01sec. The speed of sound in the mixture has been measured by an ultrasonic interferometer of frequency 2MHz. The speed of sound values is accurate to ± 2m.s-1. The measurements have been carried out in a constant temperature bath at 303.15K and 308.15K within an accuracy of ± 0.01K. FTIR spectra were taken for the liquid mixtures in a FTIR spectrum photometer (Perklin Elmer Co. model 1605) by using the KBr pellet method[4].

4. RESULTS AND DISCUSION

In the case of Ethyl Acetate + 2-Butanone mixture, the VE is maximum negative for 0.6 mole fraction of Ethyl Acetate. The maximum negative in excess volume is due to dipole-dipole interaction. It is also due to the interstitial accommodation of one type of molecule into other. In the case of Ethyl Acetate + Hexane mixture, the

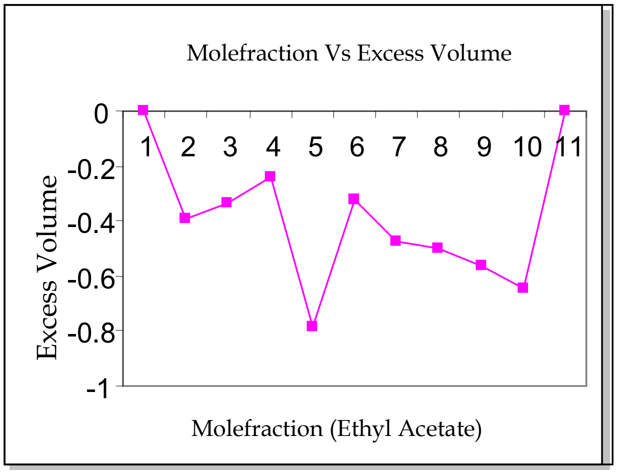

Fig. 1. Excess volume (ethyl acetate + 2-butanone)

Table 3. Determination of mole fraction, velocity, viscosity and density for Ethyl Acetate + Hexane

Mole Fraction (Ethyl Acetate)	AT 30^0			AT 35^0			Excess Volume (10^6 m^3)
	Viscosity (10^{-3} $N.s/m^2$)	Velocity (m/sec)	Density (10^{-3} kg/m^3)	Viscosity (10^{-3} $N.s/m^2$)	Velocity (m/sec)	Density (10^{-3} kg/m^3)	
1	0.5770	850.2	0.8891	0.5858	869.8	0.8658	0.0000
0.8996	0.5382	852.6	0.8612	0.5153	871.8	0.8525	-0.9771
0.7979	0.3653	867.8	0.8329	0.3757	867.2	0.8155	-4.4135
0.6973	0.3485	859.6	0.8001	0.3502	881.0	0.7869	-1.1964
0.5995	0.3338	886.0	0.7771	0.3227	887.0	0.7398	-1.0906
0.5004	0.3212	879.0	0.7529	0.3190	898.6	0.7414	-1.8497
0.3975	0.3063	867.2	0.7283	0.3004	917.4	0.7127	-2.0237
0.2901	0.2985	897.0	0.7360	0.2983	927.2	0.7180	-3.1648
0.1966	0.2754	913.4	0.6893	0.2694	920.0	0.6579	-1.0982
0.0980	0.2666	930.4	0.6724	0.2653	927.6	0.6623	-0.1531
0	0.2561	949.6	0.6507	0.2311	929.4	0.6134	0.0000

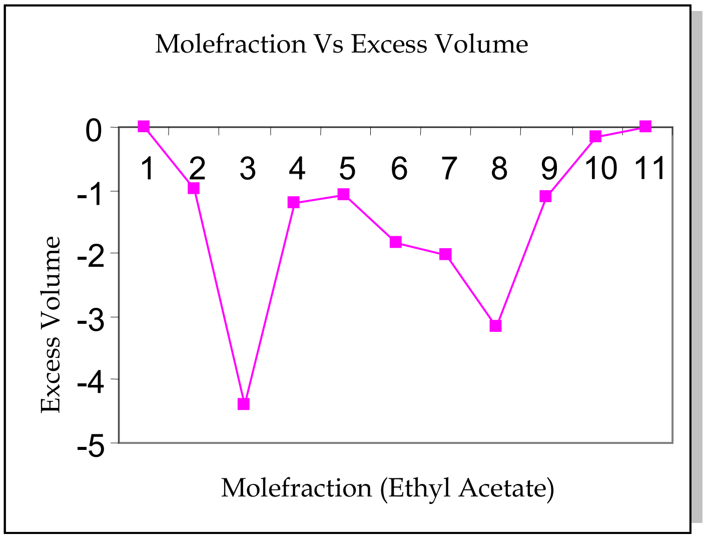

Fig. 2. Excess volume (ethyl acetate + hexane)

Table 4. Observations of FTIR Spectrum of Ethyl Acetate + Hexane

1 (EA) + 0(HEX) cm^{-1}	0.9(EA) + 0.1(HEX) cm^{-1}	*0.8(EA) + 0.2(HEX) cm^{-1}	0.7(EA) + 0.3(HEX) cm^{-1}	0.6(EA) + 0.4(HEX) cm^{-1}	0.5(EA) + 0.5(HEX) cm^{-1}	0.4(EA) + 0.6(HEX) cm^{-1}	0.3(EA) + 0.7(HEX) cm^{-1}	0.2(EA) + 0.8(HEX) cm^{-1}	0.1(EA) + 0.9(HEX) cm^{-1}	0(EA) + 1(HEX) cm^{-1}
3964.09	3917.93	3770.59	3972.80	3905.70	3855.32	3906.07	3964.69	3964.05	3964.48	3964.24
3772.12	3772.03	*3450.82	3774.67	3769.87	3768.40	3770.91	3773.07	3772.43	3772.97	3772.57
3449.31	3449.73	2988.62	3448.93	3448.68	3448.96	3448.84	3446.90	3447.13	3448.43	3437.12
2990.08	2928.11	*2493.14	2990.04	2928.17	2960.84	2964.89	2932.51	2929.40	2928.27	2928.11
2929.67	2859.61	*2384.79	2931.38	2859.60	2378.76	2491.89	2405.75	2110.78	2109.27	2119.44
2365.35	2098.42	2088.86	2087.94	2379.02	2093.17	2091.99	2091.46	1757.54	1627.09	
2091.73	1753.54	1760.91	1762.57	2092.59	1741.82	1763.72	1763.23	1625.96	1410.61	
1762.09	1628.57	1636.38	1634.83	1634.91	1636.66	1627.25	1627.46	1410.74	1115.31	
1629.98	1379.58	1378.06	1377.68	1381.22	1371.21	1378.57	1377.93	1245.29	608.91	
1378.55	1243.52	1243.04	1242.66	1242.46	1241.77	1242.87	1242.94	1116.49		
1242.99	1111.63	1054.23	1055.31	1110.54	1049.37	1056.01	1055.57	609.33		
1055.03	1050.10	*929.20	547.94	1049.25	931.21	930.32	621.67			
930.11	558.53	617.11		557.41	607.99	619.94				
616.31					533.17					

* Maximum shift in the frequency has been observed.

VE is maximum negative for 0.8 mole fraction of Ethyl Acetate also shows the presence of dipole-dipole interaction. The FTIR spectrum taken shows a change in the frequency value for 0.6 mole fraction of Ethyl Acetate (0.6 of Ethyl Acetate + 0.4 of 2-Butanone) and for 0.8 mole fraction of Ethyl Acetate (0.8 of Ethyl Acetate + 0.2 of Hexane). So, the FTIR spectrum study gives an additional evidence for the observed molecular interactions through excess volume study.

5. LITERARTURE CITED

Periodicals

[1] I.Johnson, M.Kalidoss and R.Srinivasamoorthy, September 2001, Acoustical investigation of some binary

and ternary liquid mixtures, Proceedings of the 17th International congress on Acoustics (ROME), Vol.I, Physical Acoustics - Part B, (12-13).

[2] Pandey J.D. and Ashok Kumar, 1994, Ultrasonic velocity in pure liquids, Journal of Pure and Applied Ultrasonics, 16(63-68).

[3] S. Viswanathan and M. Anand Rao, 2000, Journal of Chem. Eng. Data - 45 (764 - 770).

[4] A. Mukherjee, S. Kamila et al, 1999, Acoustics Letters (U.K)., 23(17 - 24).

[5] M. Kalidoss, I. Johnson, and R. Srinivasamoorthy, 1999, J. Acoust. Soc. Ind. 27(319).

[6] M. Kalidoss, and R. Srinivasamoorthy, 1997, J. Pure Appl. Ultrason. 19(9).

[7] C.V. Suryanarayana and S. Kuppusamy, 1979, J. Acous. Soc. Ind. 7,(131).

[8] R.J. Fort and W.R. Moore, 1965, Trans. Faraday society 61, (2102-2107).

[9] E. Zorebski and A. Zak -Z., 1999, Physikalische chemie.Bd. 210,S.(223 - 233).

Books

[1] Riddick.J.A., Bunger W.B., Sanako T.K., 1986, Organic solvents. Physical properties and methods of purification (Techniques of Chemistry) 4thed, Wiley-Interscience, New York.

[2] Weissberger, 1955, Technique of Organic Chemistry, Vol. VII, Organic solvents. Physical properties and methods of purification, 2nded, Inter-science publisher, New York.

[3] Handbook of Chemistry and Physics, 1984, The Chemical Rubber company, Cleveland, Ohio, USA.

[4] Robert M. Silverstein and Francis X. Webster, 1998, Spectrometric identification of organic compounds, John Wiley & Sons, Singapore.

Journal of Acoustical Society of India : Vol. 37, No. 2, 2010 (pp. 70-73)

Ultrasonic Investigation of Molecular Interactions in a Binary Mixture of DBP with Benzene at Different Frequencies

R. Paikaray and N. Mohanty
P.G. Deptt. of Physics, Revenshaw University, Cuttack-753 003, Orissa

ABSTRACT

The ultrasonic velocity (C) and density(ρ) at different frequencies (1MHz, 3MHz, 5MHz)in the binary mixture of DBP and Benzene at temperature 303K has been measured. The acoustic parameters like isentropic compressibility (β), intermolecular free length (L_f), acoustic impedance (Z) etc. have been computed using ultrasonic velocity and density. The trend of variation of these parameters shows the nature of molecular interaction in the binary mixture.

1. INTRODUCTION

Ultrasonic velocity is highly sensitive to structure and interactions present in the liquid system as it is fundamentally related to the binding forces between the constituents of the medium i.e. on the nature of clustering of molecules. Mixed solvents rather than pure solvents find practical applications in most chemical processes [1-2]. Parameters derived from ultrasonic velocity and corresponding parameters provide qualitative information regarding the nature and strength of interaction in liquid mixtures which is used in various industries and technology [3-5].

Further, ultrasonic investigation of liquid mixtures consisting of polar and non-polar components is of considerable importance in understanding component molecules and in gaining insight into structure and bonding of component molecules and other molecular processes. There are number of studies in liquid mixtures having Benzene as one of the components, but binary mixture with DBP as one of the components is at constant frequency are scarcely reported.

Din-n-butyl pathalate ($C_{16}H_{22}O_4$) (DBP) an odourless, colourless, viscous liquid does not occur in nature. It has a wide spread use throughout our society. The largest use of DBP is as a plasticizer (for nitrocellulose, ethyl cellulose, benzyl cellulose and for polyvinyl acetate and polymethyl metha crylate). It is added to hard plastics to make them soft. It used in printing ink, adhesives, paper coating, film coating, textile lubricating glass fibre, nail polish, hairspray, perfume solvent, fixative, antifoamer, mosquito repellant, etc. and above all it is used as a rocket fuel.

DBP is expected to interact with the non- polar molecule of Benzene differently at different frequencies. So a study is carried out in the binary mixture of DBP and Benzene at different frequencies. At present, ultrasonic velocity is measured and related parameters are calculated in the binary mixture of DBP and Benzene at different frequencies.

2. THEORY

The ultrasonic velocity and density of the binary mixture is measured using interferometer and is used to compute intermolecular free length (L_f), isentropic compressibility (β), acoustic impedance (Z) and their excess values [6] basing on the following relations.

Isentropic compressibility (β) = $1/\rho c^2$

Intermolecular free length (Ls) =K $\rho^{1/2}$

Acoustic impedence, Z= ρc

and the excess values are calculated as

$\beta^E = \beta - (X_A \beta_A + X_B \beta_B)$

$Z^E = Z - (X_A Z_A + X_B Z_B)$

$L^E_F = L_f - (X_A L_{fA} + X_B L_{fB})$

where X_A and X_B are mole fraction of DBP and Benzene respectively. β_A, β_B and ρ are isentropic compressibility of DBP, Benzene and binary mixture respectively. Z_A, Z_B and Z are acoustic impedance of DBP, Benzene and binary mixture respectively.

3. EXPERIMENTAL DETAILS

Binary mixtures of DBP and Benzene were prepared with varying fractions of DBP. Ultrasonic velocity was measured by a single crystal variable path interferometer at different frequencies of 1MHz, 3MHz and 5MHz. Density was determined with a Pyknometer before preparation of binary mixture.

4. RESULTS AND DISCUSSION

The experimental measured value of ultrasonic velocity (C) and density (ρ) at constant temperature and frequencies (1MHz, 3MHz and 5MHz) were used to calculate the β, Lf , z and excess values of β^E ,L^E_f and Z^E using given relations. The variation of ultrasonic velocity with mole fraction is shown in graph-1. The calculated values of isentropic compressibility β^E , intermolecular free length L^E_f and acoustic impedance Z^E for the mixture is shown in the graph and in Table 1 values of density (ρ) and velocity (c) at 303K for the mixture are shown.

It is observed from the graph that the ultrasonic velocity decreases gradually with increase of mole fraction

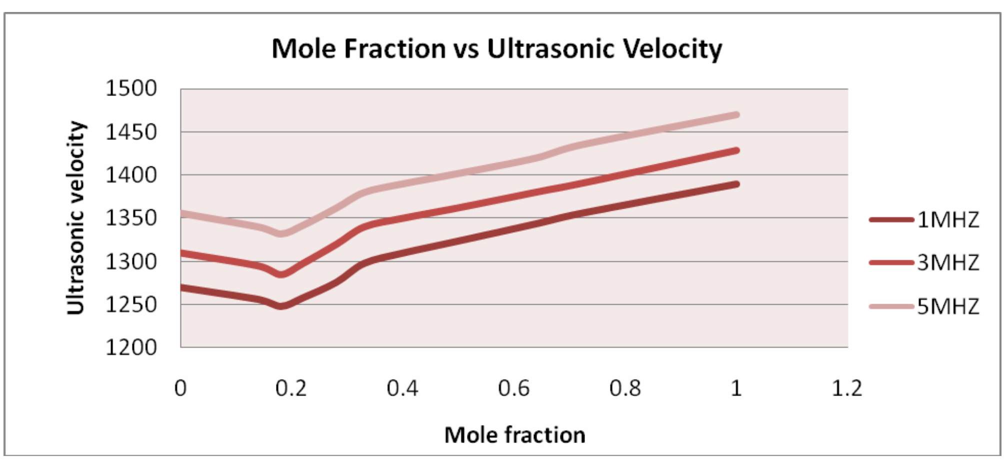

Fig. 1.

of DBP and again increases at DBP rich regions. Such variation of ultrasonic velocity with mole fraction is due to the different interactions present in the polar and non-polar liquid like DBP and Benzene respectively. DBP having hydrogen bonding is expected to give dipole - dipole interaction for which molecules move with high speed so, that ultrasonic velocity in DBP rich regions becomes high. When Benzene is added to DBP gradually the interacting molecules increases and can break the clustering of DBP and the dipole formation increases. Hence, the interaction between DBP and Benzene is strengthened due to formation of H-bonding. At a given concentration of DBP in benzene ultrasonic velocity increases with increase in frequency from 1MHz TO 5MHz. It is also observed that, with increase in frequency like 3MHz to 5MHz the interaction between DBP and benzene is decreased and ultrasonic velocity increases considerably.

Variation of excess isentropic compressibility (β) with mole fraction is shown in the graph. The negative excess compressibility suggests that the medium is highly packed, [7] β becomes increasingly negative. Further, when the frequency increases the interaction between liquid mixtures decreases for which the medium becomes loosely packed.

Variation of excess acoustic impedance is presented in the figure shows that more than one type of interaction may be presented in a given system. As the mixture is of polar and non-polar liquids the interactions

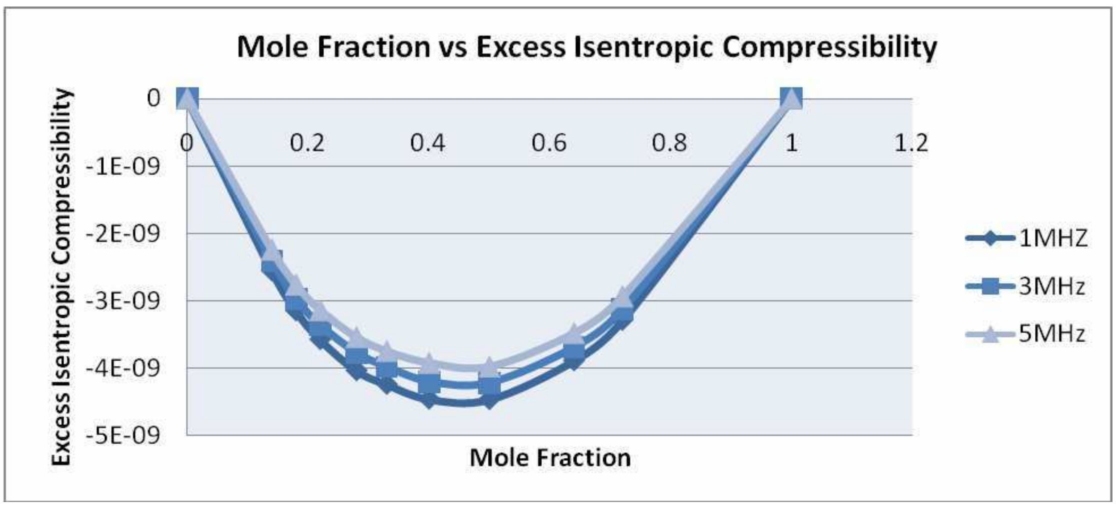

Fig. 2.

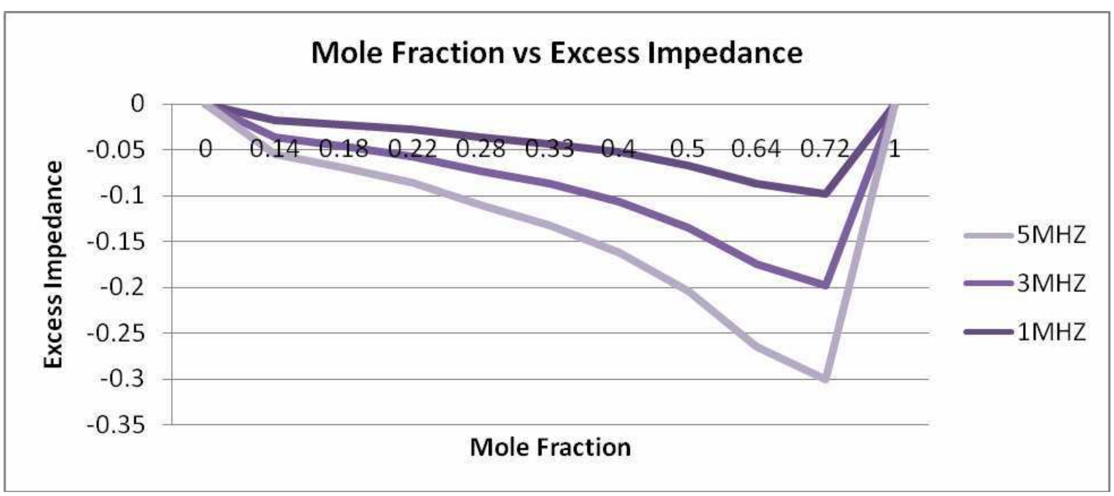

Fig. 3.

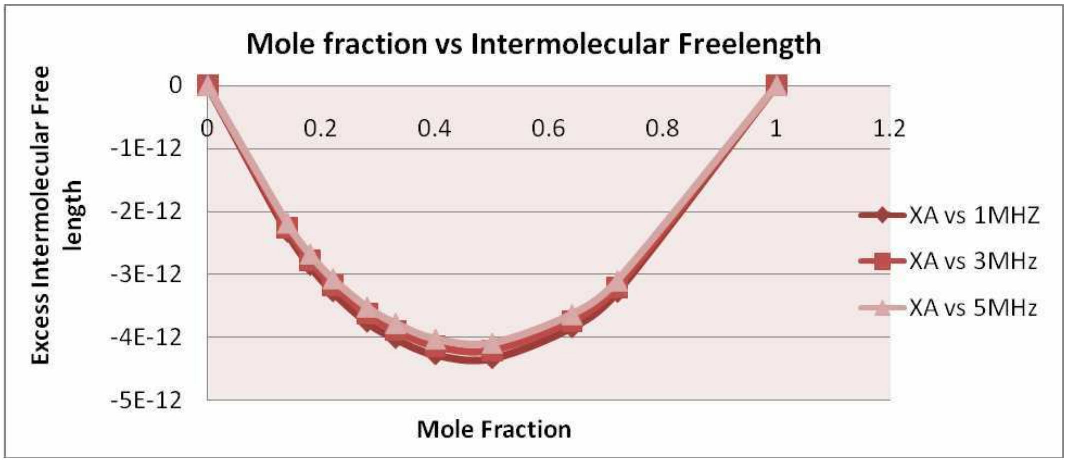

Fig. 4.

like dipole - dipole and dipole - induced dipole play an important role giving negative values. Further, with increase of frequency the excess value of Z decreases.

The variation of excess intermolecular free length LfE with mole fraction at different frequencies shows that the value of LfE decreases negatively and approaches a minimum and then increases at high concentration of DBP as intermolecular free length determines the nature of sound velocity in liquid mixture (8), such variation can be interpreted in terms of interaction between the different sizes of molecules. Due to dissociative nature of DBP and benzene the intermolecular free length decreases though interaction between molecules increases when the frequency increases (9, 10).

5. CONCLUSION

It is studied that acoustical parameters and negative excess values is due to the presence of H-bonding dipole - dipole, dipole induced dipole and dispersive force between the molecules in the mixture. It is also observed excess values are highly affected in high frequency range. Hence, acoustic parameters with variation of frequency play an important in polar and non-polar liquid mixtures.

6. REFERENCES

[1] J. D. PANDEY and A. K. SHUKLA, 1993. *J. Pure Appl. Ultrason.*, 15537.
[2] RIYAZUDDEN and NURUL ISLAM, 1997. *J. Pure Appl. Ultrason.*, 1916.
[3] S.L. OSWEL, P. OSWAL and R.P. PHALAK, 1998. *J. Sol. Chem.*, 2507.
[4] J. RAJASEKHAR and P.R. NAIDU, 1996. *J. Chem Engg. Data*, 41373.
[5] G. ARUL and L. PALANIAPPAN, 2001. *J. Pure and Appl Phys.*, 39561.
[6] B. RAVINDER REDDY and D LINGO REDDy, 1990. *Indian J. Pure and Appl. Phys.*, 37.
[7] B. GENCIA, R. ALCALDE, J. LEAL and J.S. MATON, 1997. *J. Chem. Soc. Foraday Trans.*, **93**, 1115.
[8] M.V. KAULGUD, 1963. *Z. Phys. Chem.*, **36**, 365.
[9] S. ACHARYA, R. PAIKARAY and G.C. MOHANTY, 2003. *Indian J Pure and Appl Phys.*, **41**, 855-857.
[10] T.N. SRIVASTAVA and R.P. SINGH, 1983. *Acoust. Lett.*, **6**, 53.

ISSN 0973-3302

JOURNAL OF ACOUSTICAL SOCIETY OF INDIA

Volume 37 Number 3 July 2010

A Quarterly Publication of the JASI
http://www.acousticsindia.org

JASI

Journal of Acoustical Society of India

The Refereed Journal of the Acoustical Society of India (JASI)

The Journal of Acoustical Society of India is a refereed journal of the Acoustical Society of India **(ASI)**. The **ASI** is a non-profit national society founded in 31st July, 1971. The primary objective of the society is to advance the science of acoustics by creating an organization that is responsive to the needs of scientists and engineers concerned with acoustics problems all around the world.

Manuscripts of articles, technical notes and letter to the editor should be submitted to the Chief Editor. Copies of articles on specific topics listed above should also be submitted to the respective Associate Scientific Editor. Manuscripts are refereed by at least two referees and are reviewed by Publication Committee (all editors) before acceptance. On acceptance, revised articles with the text and figures scanned as separate files on a diskette should be submitted to the Editor by express mail. Manuscripts of articles must be prepared in strict accordance with the author instructions.

All information concerning subscription, new books, journals, conferences, etc. should be submitted to Chief Editor:

Acoustics Section, National Physical Laboratory, Dr. KS Krishnan Road, New Delhi 110 012,
Tel: +91.11.4560.9319, Fax: +91.11.4560.9310, e-mail: mahavir@nplindia.org

Annual subscription price including mail postage is Rs. 2000/= for institutions, companies and libraries and Rs. 2000/= for individuals who are not **ASI** members. The Journal of Acoustical Society of India will be sent to **ASI** members free of any extra charge. Requests for specimen copies and claims for missing issues as well as address changes should be sent to the Editorial Office:

Acoustics Section, National Physical Laboratory, Dr. KS Krishnan Road, New Delhi 110 012,
Tel: +91.11.4560.9319, Fax: +91.11.4560.9310, e-mail: mahavir@nplindia.org

ISSN 0973-330

Printed at Alpha Printers, BG-2/38C, Paschim Vihar, New Delhi-110063 Tel.: 9811848335. JASI is sent to ASI members free of charge.

JASI

Journal of Acoustical Society of India (JASI)

A quarterly publication of the Acoustical Society of India

Volume 37, Number 3, July 2010

EDITORIAL

ARTICLES

INFORMATION

Sound Transmission Loss of Windows

The windows in your home do more than allow you to see outdoors, they also oblige you to listen to the bustle of the outdoors, like the not so calming drone of traffic and the neighbor dog's incessant barking. Standard windows easily transmit outdoor noise into your home, and likewise transmit noise from inside your home for all to hear outside. Sound reduction window treatments are often installed to alleviate noise traveling in both directions from sources such as traffic, home theaters, music rooms, loud neighbors and barking dogs, among others.

Windows pose several noise control challenges, including the free exchange of noise as described above as well as acoustic quality problems within the room. The characteristics of glass make it extremely reflective and resonant, allowing sound to both travel through it and resonate from it. These obstacles can be overcome through the implementation of an effective window soundproofing treatment, which does not require full replacement of your existing windows.

Regular double-pane windows, while marginally better than single-pane ones, are affixed within a common frame and vibrate together, making them ineffective at combating noise bleed. Soundproof windows can be easily installed in front of your existing windows, controlling noise transmission and avoiding the need to remove the windows already in place.

Soundproof windows incorporate advanced sound control technology, while being fitted in front of an existing window establishes a necessary isolation to further control sound reverberations. High quality soundproof windows consist of laminated glass with an inner layer of Polyvinyl Butyral (PVB) plastic to stop vibrations, and are housed within a frame that utilizes spring loaded seals for a tight grip. Soundproof window installation gives the supplementary benefit of extra insulation and draft control.

Some window sound control applications necessitate a more short-term remedy, as is the case when musicians seek to practice in a home without disturbing neighbors. Window plugs, or portable window covers designed to be affixed temporarily over a window to help block noise transmission through the window, can be easily removed, rolled up and stored when they are not in use. While window plugs do not control noise to the extent that a complete soundproof window installation would, they supply a popular cost effective alternative to meet specific needs.

A room with many windows, and thus many sound reflections, can benefit from sound control window blinds to absorb reflections and maintain sound quality within the room. These sound treatments are most effective when used in combination with ceiling and wall soundproofing treatments.

If you are interested in implementing window soundproofing treatments into your home or business, it is advised to consult a reputable soundproofing company to ensure that all variables are considered and that an effective solution is instated.

Mahavir Singh

Journal of Acoustical Society of India : Vol. 37, No. 3, 2010 (pp. 89-93)

Development of Quiet Aircraft Helmet: Active and Passive Approach

S. Veena[1], H. Lokesha, S.V. Narasimhan and R. Ranjit[2]
[1]*DSPS group, Aerospace Electronics Division*
National Aerospace Laboratories, Bengaluru - 560 017
[2]*Noise & Heat Control Systems Pvt. Ltd., RMV Extension, Bengaluru - 560 094*
e-mail: vveena@nal.res.in

[Received: 19.12.2009; Revised: 25.05.2010; Accepted: 21.06.2010]

ABSTRACT

For fighter aircraft, a new helmet has been designed and fabricated with very good passive and active attenuation techniques. The high frequency noise is attenuated using uniquely designed ear pods. However, the noise reduction by passive means will not be effective in the low frequency region. In view of this, Active Noise Control (ANC) is used to reduce the noise level in the frequency region up to about 1000Hz. Since fighter aircrafts are characterized by jet / broad band noise, a new algorithm based on Griffiths' cross correlation is used to improve ANC performance. This has resulted in a passive attenuation of about 34.7dB upto 10 KHz and additional 14dB reduction in the low frequency region upto 1 KHz due to ANC.

1. INTRODUCTION

The main sources of noise in the cockpit of fighter aircrafts are due to the airflow from the environmental control system (ECS), engine and structural vibration. However, the major contribution is due to the ECS[1]. There are many pilot helmets available in the market, however their passive attenuation may not be adequate to achieve sufficient attenuation. Further some of the helmets claim to have ANC in their ear cups and they are known as ANR helmets [2]. But the ANC systems present in most of these helmets are not capable of tracking the noise adaptively as they are designed using analog components. Also, since they utilize pilot communication speakers of the ear cup for generating the antinoise, their power rating and the frequency response may not be sufficient to generate antinoise of required power.

In ANC to achieve noise reduction, an antinoise (equal in magnitude and opposite in phase to that of noise to be reduced) is generated and superimposed on the existing noise. The antinoise generation has to be adaptive to take care of the variations in noise and the environmental characteristics. Therefore, antinoise is generated by the adaptive signal processing approach using feed forward technique based on gradient *filtered* -X LMS (FXLMS) algorithm. Many variants of this algorithm are present in the literature [3]. However, the fighter aircraft is characterized by broadband/jet noise and the performance of FXLMS algorithm for this scenario is poor due to modeling errors [3].

This paper gives a brief explanation regarding the development of a new prototype helmet with an unique ear cup design to achieve passive attenuation and an adaptive ANC system to cater for low frequency broadband noise, resulting in a good overall performance.

2. THE NEW HELMET

A new helmet with good passive attenuation is developed. The ear pods of the helmet are uniquely designed as hollow bellow shape using dense but flexible Poly Urethane rubber to give good passive attenuation. (Fig. 1). The rim of the pod is fitted with a soft ear seal that fits to the ear perfectly without any gap, for pilot's comfort. The flexible nature of the pod makes room for a heads of different size and at the same time gives a cushioning effect around the ear and a good acoustic seal.

The density of the pod and good fit (without any acoustic leak) of the ear seal around the ear help to cut down the high frequency noise to a large extent. The hollow area inside the pod offers sufficient space for the speaker system. An acoustic foam lining on the inside of the helmet shell not only holds the pod firmly in place but also adds to the passive attenuation significantly. The flexibility and cushioning effect of the pod enables the ear to be completely covered by the cup.

3. ANC SYSTEM DESIGN AND INTEGRATION

3.1 ANC Algorithm

In ANC, the input noise is picked up by the reference microphone and the antinoise is generated using feed forward approach (Fig. 2) and superimposed on the existing noise field by a loudspeaker. The noise cancellation takes place in the acoustic domain and is sensed by error microphone after it passes through the secondary path, . In view of this, the LMS algorithm cannot be applied directly and the presence of is accounted by FXLMS algorithm [3]. Here the filtered input is used for the adaptation of the controller.

The accuracy of the secondary path estimate determines the performance of ANC system [3,4]. The is identified on an on-line basis using LMS algorithm, by injecting a white noise into the system and its level has to be low, as it decides the floor noise level achieved by ANC. This identification has to be done in the presence of a strong primary noise . Further, the identification should be fast as it is required in advance for filtering the reference signal, calling for a larger adaptation step-size which results in a higher misadjustment. All these factors contribute to phase error and delay in , deteriorating the performance of ANC. Therefore an accurate is absolutely necessary for improving the performance of ANC, especially for broadband noise [4].

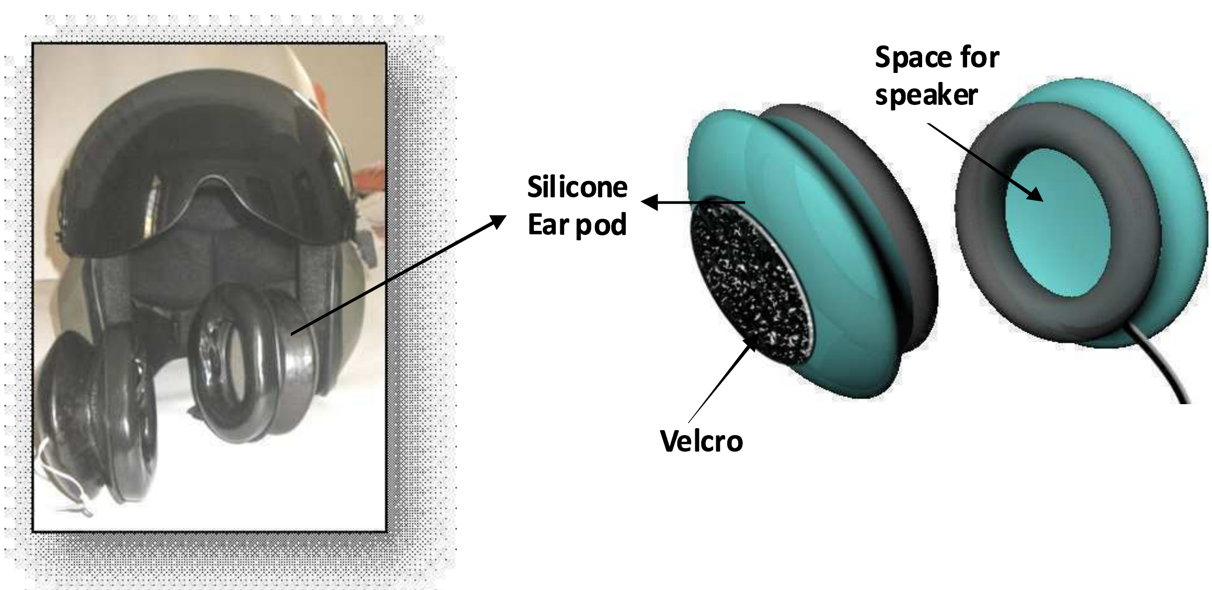

Fig. 1. Ear pods for the New designed helmet

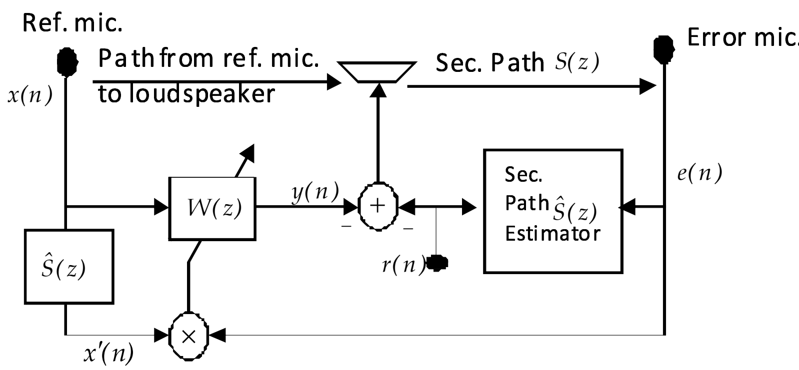

Fig. 2. Block schematic of Feed forward ANC using FXLMS algorithm

To remove the effect of the on identification, a new algorithm has been proposed [5] and is implemented for the helmet ANC. This algorithm is based on Griffiths' correlation computation [6], here the cross-correlation between and is computed and is averaged to remove the observation noise component in . This improves the and hence the ANC performance significantly.

3.2 ANC for helmet

The ANC is realized by two separate single channel ANC systems for each ear using single reference signal. The algorithm is developed in C language on TMS320C6701 processor. ANC system is designed to reduce the noise upto 1 KHz. The ANC system comprises of two parts. One is the transducer part which is integrated inside the helmet and the other is the control part, which houses the DSP processor and signal conditioning electronics. The signal conditioner consists of microphone preamplifiers, loudspeaker power amplifiers and associated anti-aliasing and reconstruction filters.

3.2.1 System configuration

Fig.3 shows the ANC configuration for pilot's helmet. A microphone for error signal is inserted into each of the ear cup. The reference microphone located in the cockpit picks up the noise signal to be cancelled and the

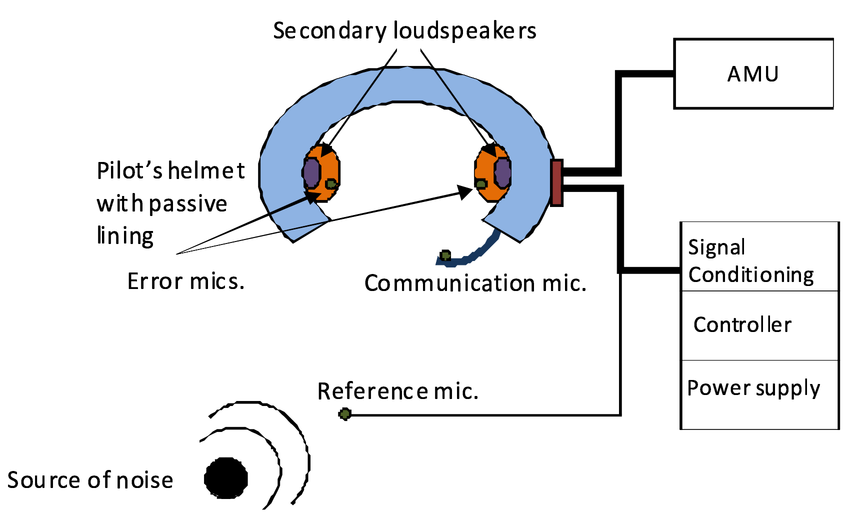

Fig. 3. ANC Configuration for TEJAS pilot helmet

processing unit generates the antinoise using this information. The antinoise is given out through the loudspeakers of the helmet, which are also used for pilot's communication and the error microphones gives feedback to the controller unit. The pilot communicates through a microphone attached to the helmet as shown in Fig. 2. Further, the pilot receives communication and warning signals from AMU (Audio Management Unit) through the same loudspeakers used for ANC. Since the feed forward technique will cancel only that noise, which is picked up by the reference microphone, these important signals are unaffected.

4. RESULTS

The performance of the new helmet is evaluated by recording microphone signals both outside and inside the helmet for a noise recording obtained from a typical fighter aircraft.

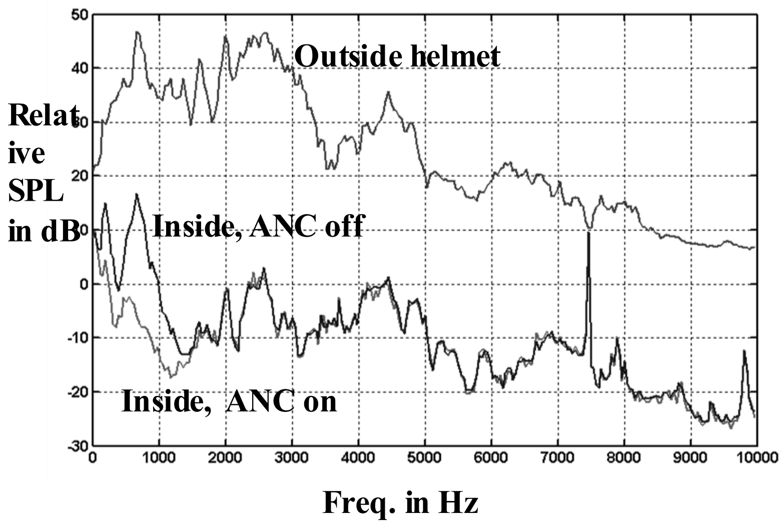

Fig. 4. Active and passive attenuation of the new helmet

For this helmet, the passive attenuation achieved upto 10 KHz is 34.7dB. However, in the frequency range upto 1 KHz, the passive attenuation achieved is only 28dB and ANC gives an additional attenuation of about 14dB over that of passive attenuation. The overall attenuation of the helmet upto 1 KHz is 42dB. Further, Fig.4 shows that very low frequency components below 100Hz are not sufficiently attenuated using ANC. This is due to the frequency response limitation of the transducers. However, as these frequency component's contribution to the audible noise is very limited, this not of major concern.

5. CONCLUSION

The development of a helmet with good passive and active noise suppression was considered. The passive attenuation achieved was 34.7dB upto 10 KHz. The ANC performance in the helmet is evaluated for a frequency range up to 1 KHz. The ANC system was able to reduce the noise by about 14dB in the laboratory environment. This noise reduction was achieved due to use of new Griffiths' algorithm which improves the ANC performance for a broadband noise. Further, the newly designed helmet gives a good passive attenuation owing to its unique design. The overall reduction achieved upto 1 KHz is 42dB.

6. ACKNOWLEDGEMENT

The authors would like to thank Dr. K. Vijayaraju, Co-ordinator, DISMAS, ADA for providing financial support to carry out this activity. They are also thankful to Prof. M.L.Munjal, FRITA, IISc for constant support in acoustical aspects of ANC and helmet design.

7. REFERENCES

[1] MICHAEL J. SMITH, 1989. Aircraft Noise", Cambridge Aerospace Series, Cambridge University Press, 1st Edition.

[2] Web link - "www.helmets.co.uk"

[3] S.M. KUO and D.R. MORGAN, 1996. Active Noise Control Systems, Algorithms and DSP implementation", John Wiley and Sons.

[4] M. KUO and DIPA VIJAYAN, 1997. A secondary path modeling technique for active noise control, *IEEE Trans. on Speech and Audio*, **5(4)**.

[5] S.V. NARASIMHAN, S.VEENA and H. LOKESHA, 2009. Variable Stepsize Griffiths' Algorithm for Improved Performance Of Feedforward/ Feedback Active Noise Control", Journal of Signal, Image and Video processing, Springer .

[6] L.J. GRIFFITHS, 1967. A simple adaptive algorithm for real time processing of in antenna arrays, *Pro*c. *IEEE*, **57**, 1696-1704.

Journal of Acoustical Society of India : Vol. 37, No. 3, 2010 (pp. 94-104)

Traffic Noise: 1/*f* Characteristics

K.B. Patangea[1], A.R. Khanb[2], S.H. Beherec[3] and Y.H. Shaikhd[4]
[1]*Dept. of Physics, Deogiri College, Aurangabad,-431 005, Maharashtra, India*
[2]*Maulana Azad College, Aurangabad, India*
[3]*Dept. of Physics , Dr. B.A. Marathwada University, Aurangabad, Indi.*
[4]*Shivaji College, Kannad, Aurangabad, India*
e-mail: patange_123@yahoo.com, subhash _behere@yahoo.com

[Received: 16.04.2010; Revised: 30.05.2010; Accepted: 08.06.2010]

ABSTRACT

Study of traffic noise is presented from the point of view of 1/*f* noise. Samples of Traffic Noise are collected from selected locations from busy roads of Aurangabad city in Maharashtra state (India) and data is analyzed. It is observed that in many cases the traffic noise possesses pink noise (1/f noise) prevailing over appreciable range of frequency. The log plot of noise power versus frequency results in a straight line with a slope approximately equal to unity confirming the presence of pink noise. After certain frequency, the noise power no more behaves like pink noise (1/*f* noise) and becomes more or less constant with random fluctuations. Plots of noise power versus frequency on log log basis for different locations studied are presented and the inferences are discussed.

1. INTRODUCTION

Traffic noise is considered as one of the important sources of noise pollution that adversely affects human health in residential urban areas [1-3]. Low frequency noise is common as background noise in urban environments arising due to many artificial sources like road vehicles, aeroplanes, industrial machinery, artillery and mining explosions and air movement machinery. This includes wind turbines, compressors, and indoor ventilation and air conditioning units etc. [4, 5]. Low-frequency noise or flicker noise has been found in many systems [6]. Intense low frequency noise may produce clear symptoms like respiratory impairment and aural pain [7]. The behavior generally persists over low frequencies [8]. The power spectra of large variety of complex systems exhibit 1/ *f* behavior at low frequencies. It is widely accepted that 1/*f* noise and self-similarity are characteristic signatures of complexity [9, 10]. Self-similarity, scale invariance and fractal nature are found to be characteristics of many natural phenomena [11, 12]. 1/*f* noise refers to the phenomenon of the spectral density, $S(f)$ of a stochastic process [13], having the form

$$S(f) = \text{constant}/f^{\alpha}$$

Where f is frequency, on an interval bounded away from both zero and infinity. Spectral density (power distribution in the frequency spectrum) is such a property, which can be used to distinguish different types of noise [14]. This classification by spectral density is given "color" terminology. The spectral density of white noise is flat ($\alpha = 0$), while pink noise has $\alpha = 1$, and brown noise has $\alpha = 2$. During last 80 years since the first observation by Johnson (1925), long-memory processes with long-term correlations and $1/f^{\alpha}$ (with $0.5 \leq \alpha \leq 1.5$) behavior of power spectra at low frequencies have been observed in physics, technology, biology, astrophysics, geophysics, economics, psychology, language and even music [15-24] and in traffic flow too [25].

The frequency spectrum of pink noise is flat in logarithmic space; it has equal power in bands that are proportionally wide [6, 16, 21, 24, 26]. This means that pink noise would have equal power in the frequency range from 40 to 60 Hz as in the band from 4000 to 6000 Hz. Since humans hear in such a proportional space, where a doubling of frequency is perceived the same regardless of actual frequency (40-60 Hz is heard in the same interval and distance as 4000-6000 Hz), every octave contains the same amount of energy and thus pink noise is often used as a reference signal in audio engineering. That is, the human auditory system perceives approximately equal magnitude on all frequencies. The power density, compared with white noise, decreases by 3 dB per octave (density proportional to $1/f$).

2. MATERIALS AND METHODOLOGY

To study the frequency distribution of the noise power, the noise recorded was analyzed using FFT (Fast Fourier Transform) technique. For the implementation of FFT, we used MathCAD 11. The audio files were opened in MathCAD for reading in the data and the characteristics of the recorded file such as sampling rate, number of channels, resolution etc were found. This is necessary for deciding the frequencies present based on sampling rate.

A program was written for this purpose, after reading in the data this displays the plot of amplitude versus time just like the wave representation of sound in any sound editing software like wave editor or wave pad. The amplitude data in time domain was then subjected to Fast Fourier Transform using the built in function FFT of MathCAD. We used 8192 (2^{13}) points for Fourier transform. Total number of frequencies resulting from the Fourier transform of the signal as described above is 4096. This allows a range of frequencies of up to about 22 KHz which is more than sufficient. In fact power at frequencies greater than about 10 KHz is marginal in general as compared to that at lower frequencies.

Fourier transform of the signal gives amplitude of noise at different frequencies. The amplitude resulting from the Fourier transform is a complex quantity with both real and the imaginary parts. Power can be found from the amplitude by taking its square, resulting data is written to text files for further use.

3. RESULTS AND DISCUSSION

Having analyzed plenty of data from wave files recorded at selected locations under different traffic conditions it was observed that the noise power is higher at lower frequencies in most of the cases and as one goes to higher frequencies, the noise power rapidly falls down. Later a stage is reached where the noise power is found to be more or less same with random fluctuations. A typical recording of noise level spectrum is shown in Fig 1. The noise was recorded at Highway near Baba Petrol Pump, Aurangabad for normal, general traffic conditions during busy hours. The traffic consisted of light vehicles such as cars, three wheelers, motorcycles and Buses. It is seen from the plot that the power level is on the higher side initially (at lower frequencies), with increase in frequency, the power level rapidly falls to a plateau like quasi steady state indicating more or less similar noise level over a wide range of frequencies. In addition to this, there are few sharp peaks and spikes seen at certain frequencies. These spikes or sharp peaks are characteristic of any typical sound like Horn etc being blown there. The sharp peak seen near 2.2 KHz in the fig 1 is due to blowing of horn of a bus and the broad burst near 1.4 KHz is due to blowing of horns by three wheelers.

The noise power spectrum shows fast falling trend with frequency, this exponential decrease in noise power suggests the presence of power law being valid; this also supports existence of 1/f noise. The study of large number of noise power spectra recorded under various conditions show that, not all the fast falling power spectra exhibit 1/f noise but very few of them show real 1/f noise in some frequency range and beyond that the noise ceases to behave like 1/f noise. The traffic conditions are general which in majority includes motorcycles, cars, buses and three wheelers. The percentage of heavy vehicles is around 7%.

It is seen from Fig 1 that the noise amplitude falls rapidly with frequency in the range 50 - 2000 Hz, however when the noise power level is plotted on log scale the shape is quite different as seen in Fig. 2 which is the plot of log of noise power level versus log of frequency for the data presented in Fig.1 for the initial part

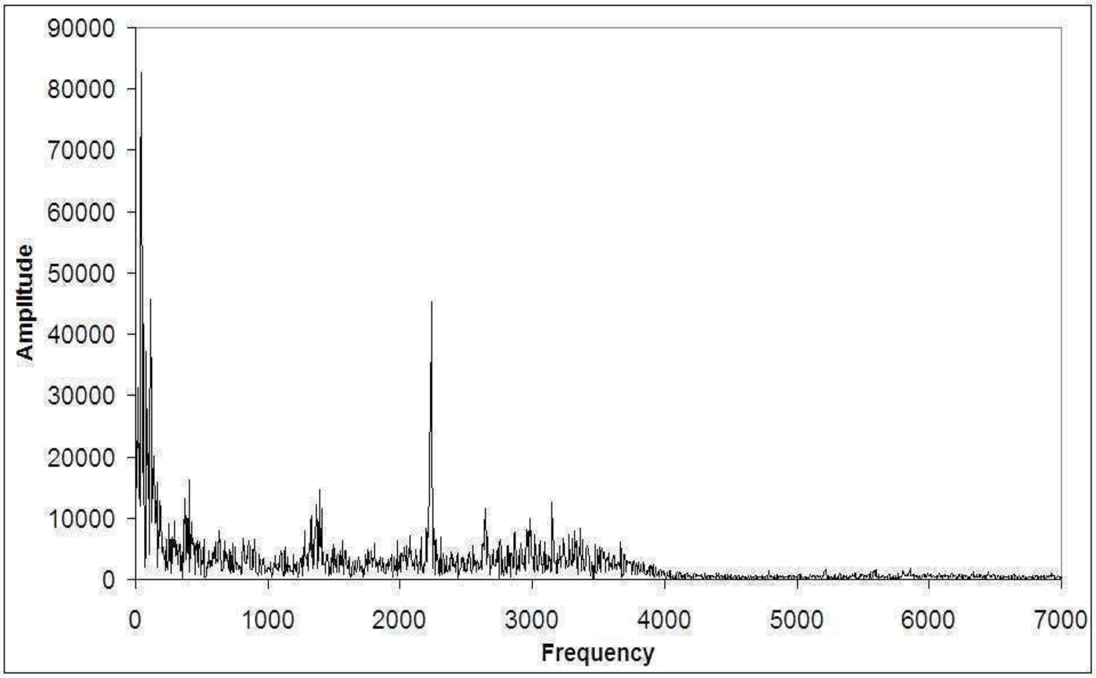

Fig. 1. Noise amplitude recorded at Highway near Baba Petrol Pump, Auranga bad for normal, general traffic conditions during busy hours

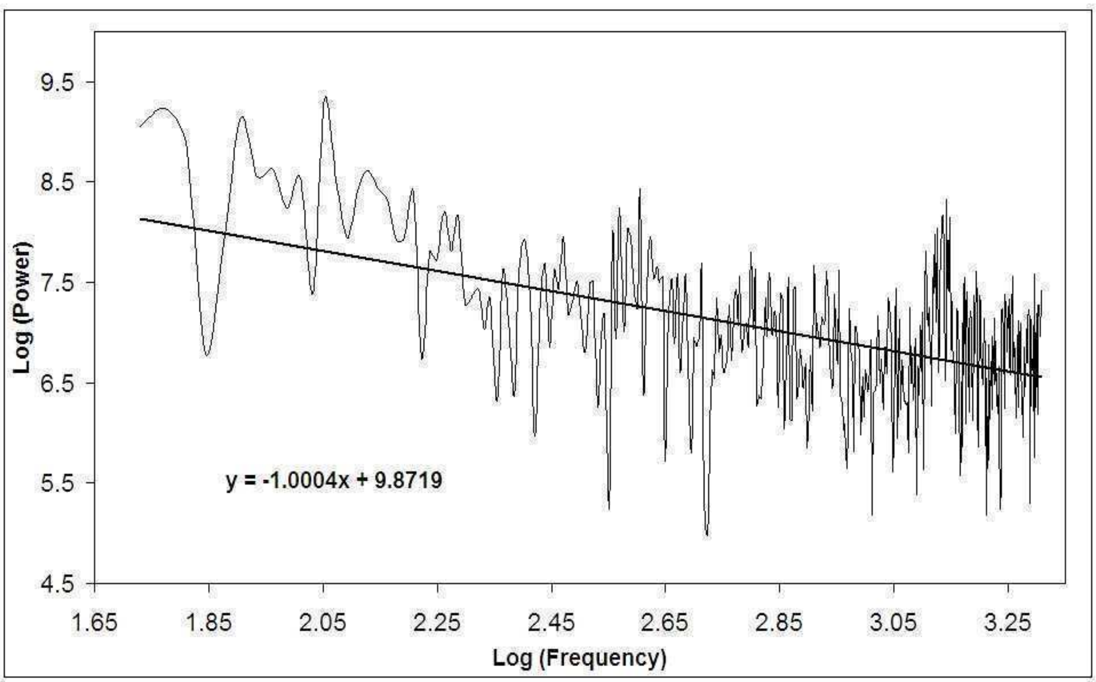

Fig. 2. Plot of log of noise power level versus log of frequency for the data presented in Fig.1 (50 - 2000 Hz)

of frequency. Thin line is the actual data plotted and the thick straight line is the least square fit applied to all these data points. Slope of the straight line fitting the data is found to be -1.0004 confirming that the noise power level follows 1/f trend and thus obeys 1/f law. As is seen from figure 2 that the power spectrum confirms presence of 1/f noise, the data from many other locations are found to exhibit the presence of 1/f noise in the initial part of frequencies. Few of such plots are shown in figures [3-14] which indicate the presence of 1/f noise in the initial part of the power spectrum. The noise samples were collected from different locations and under different noise conditions.

Figure 3 shows a plot of log of noise power versus log of frequency for the noise recorded near Baba Petrol pump when there was heavy traffic. 1/f noise is found to prevail over a limited range of frequencies i.e. 290 Hz to 3 KHz.

Figure 4 and 5 show plots for the noise recorded near Aakashwani and Figs. 6 and 7 are that for highway near Amarpreet Hotel for two different timings. Slope of the line fitting the data remains close to -1 confirming the presence of 1/f noise. Figure 8 also shows power law exponent close to -1 that confirms presence of 1/f noise over the range of frequencies plotted (See Table - 1)

Similarly, Figs. 9 to 14 shows the noise power spectrum plotted on log log scale for traffic noise recorded at six locations for traffic under free flow (without signals). The Noise power spectrum in this cases is found to have 1/f noise over wide rang of frequencies. In some of the plots sharp spikes are present in the power spectrum; however the 1/f nature remains persistent in these cases. It is confirmed from Figs. 2 - 14 and Table 1 that for traffic conditions presented, the noise power spectrum has 1/f noise during the initial part of the frequencies (50 Hz to 4 KHz) and the power law exponent is close to 1.

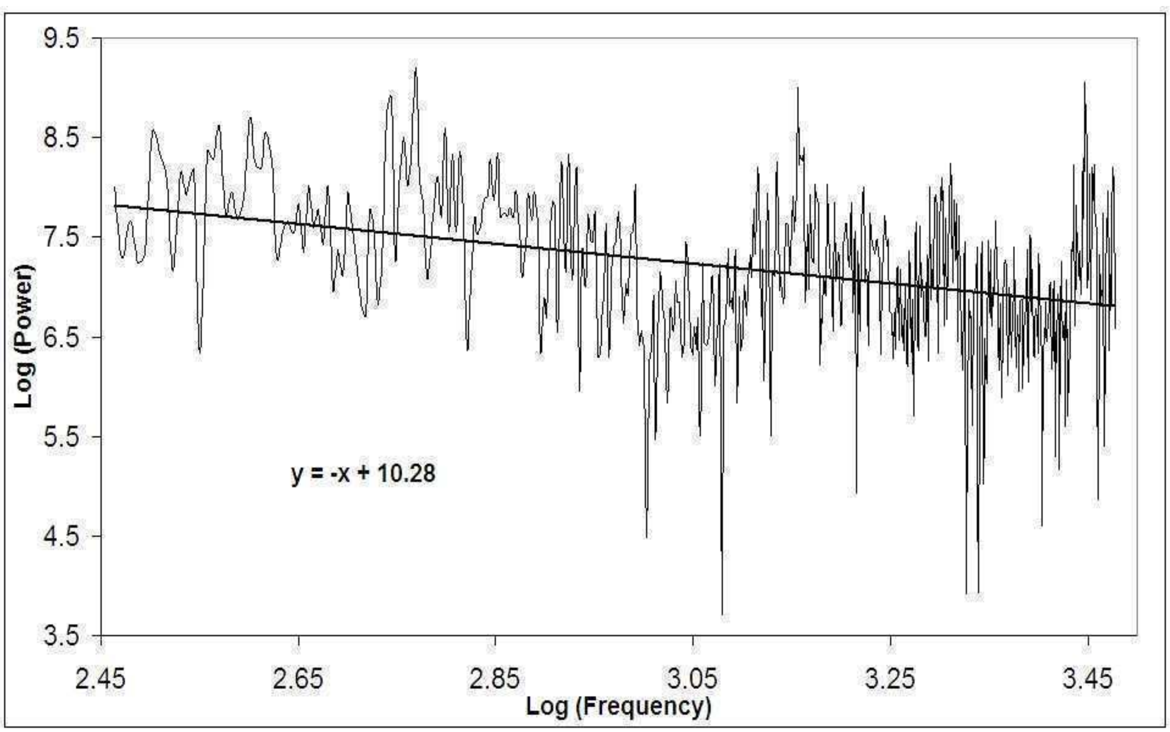

Fig. 3. Plot of log of noise power level versus log of frequency for Noise recorded at the highway near Baba Petrol Pump

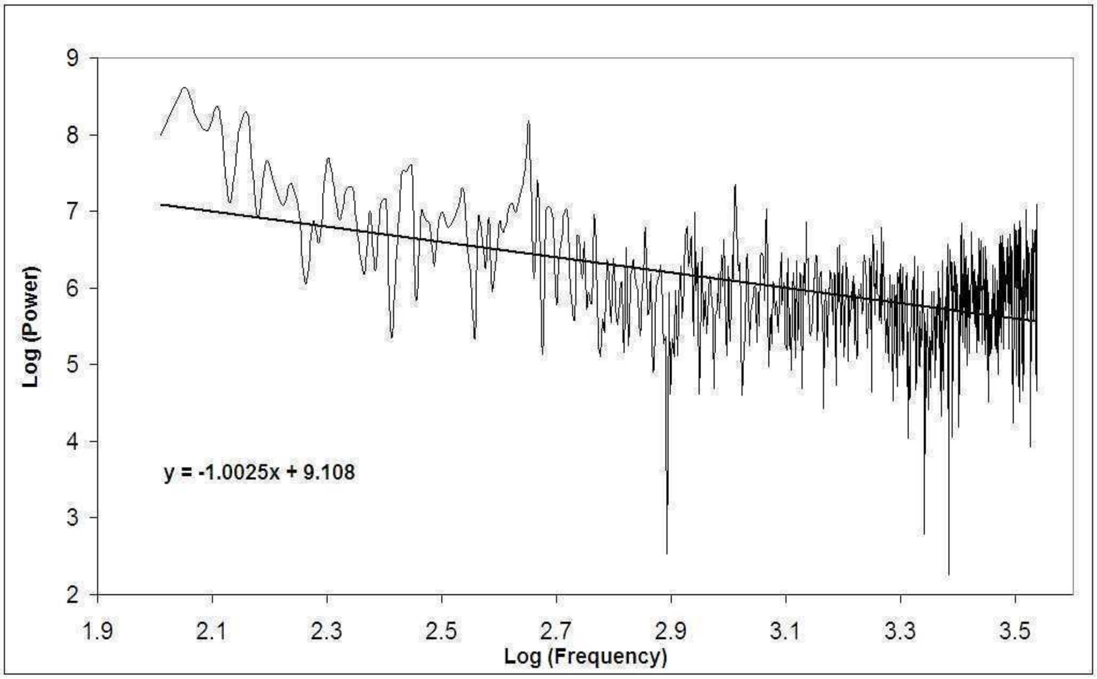

Fig. 4. Plot of log of noise power level versus log of frequency for Noise recorded at the highway near Aakashwani

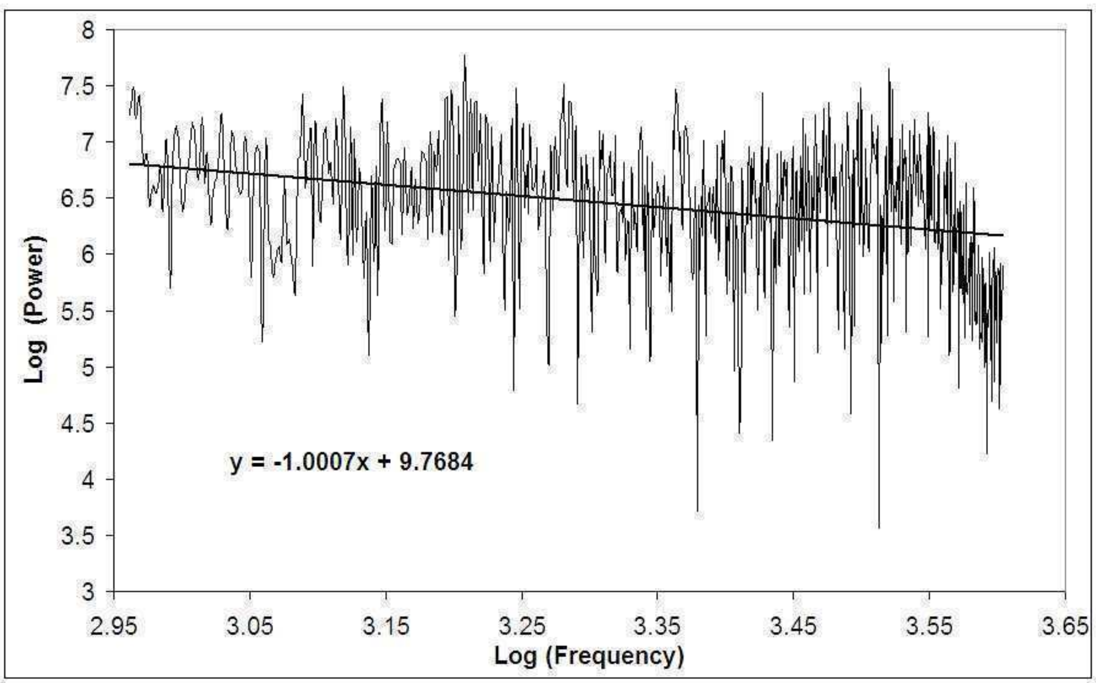

Fig. 5. Plot of log of noise power level versus log of frequency for Noise recorded at the highway near Aakashwani

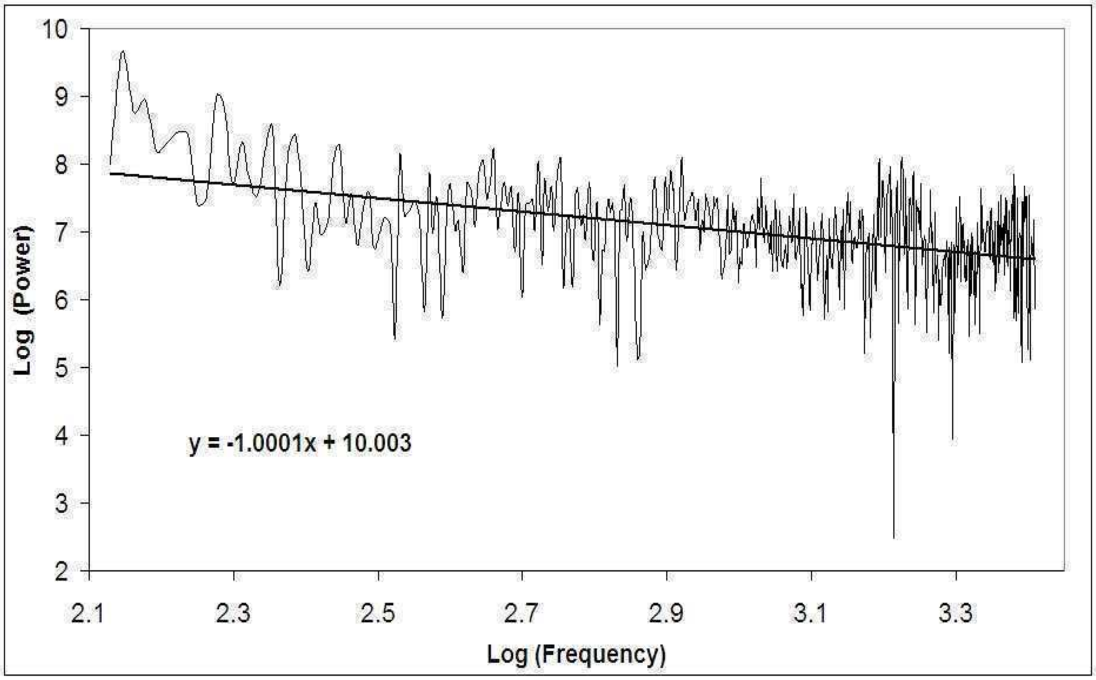

Fig. 6. Plot of log of noise power level versus log of frequency for Noise recorded at the highway near Amarpreet Hotel

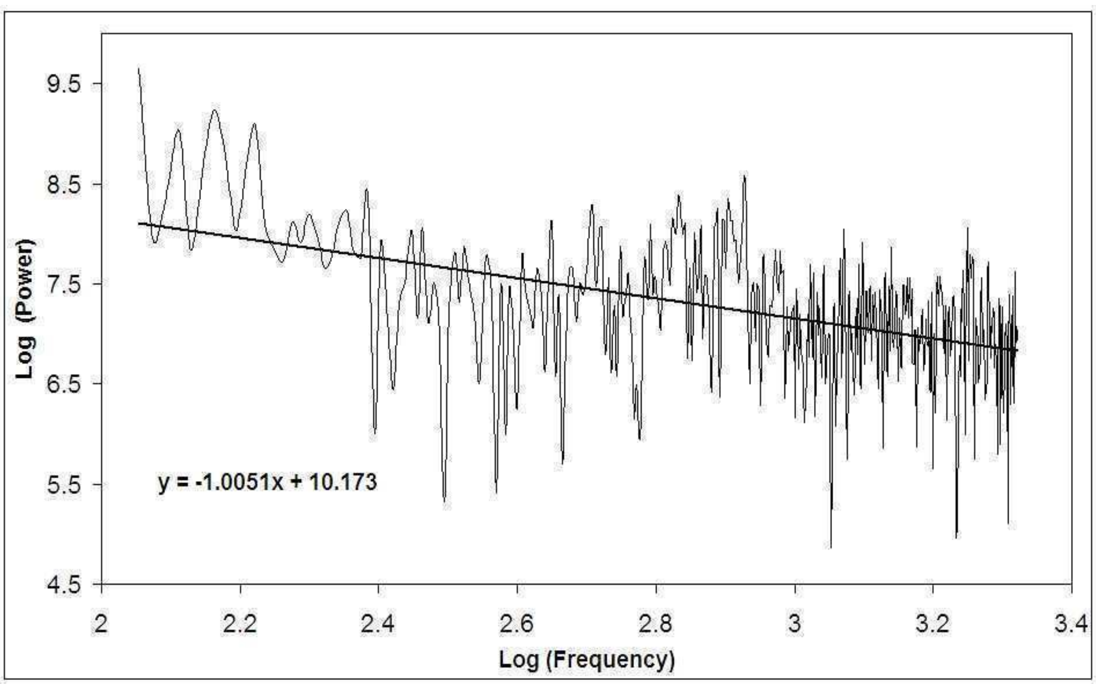

Fig. 7. Plot of log of noise power level versus log of frequency for Noise recorded at the highway near Amarpreet Hotel

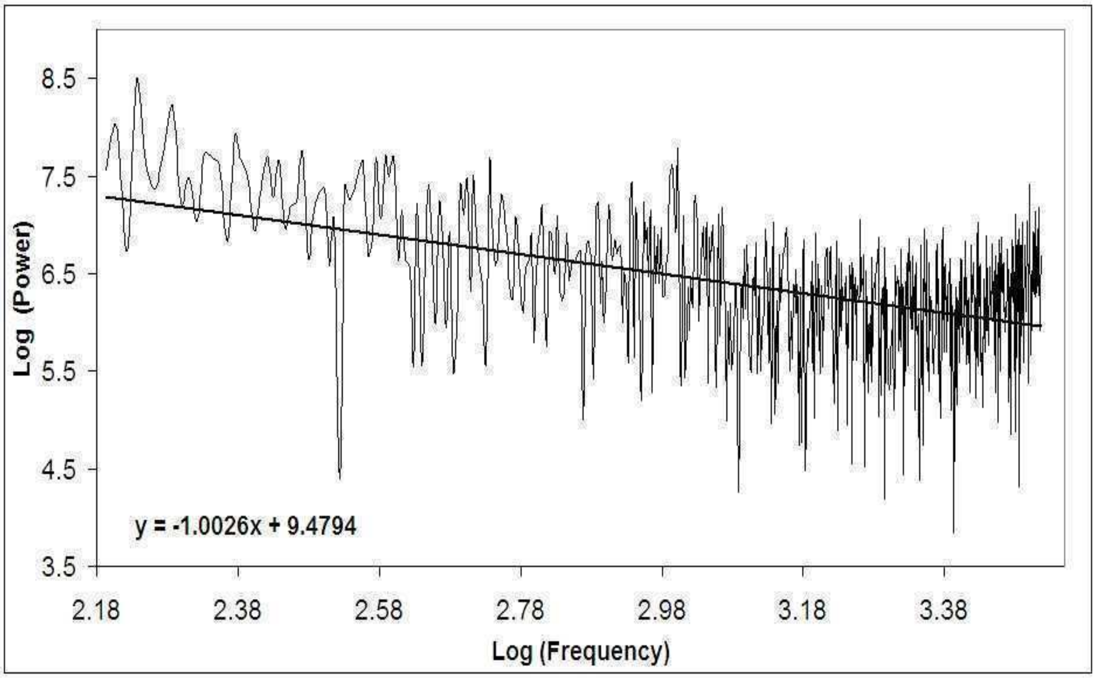

Fig. 8. Plot of log of noise power level versus log of frequency
for Noise recorded at the highway near Kranti Chowk

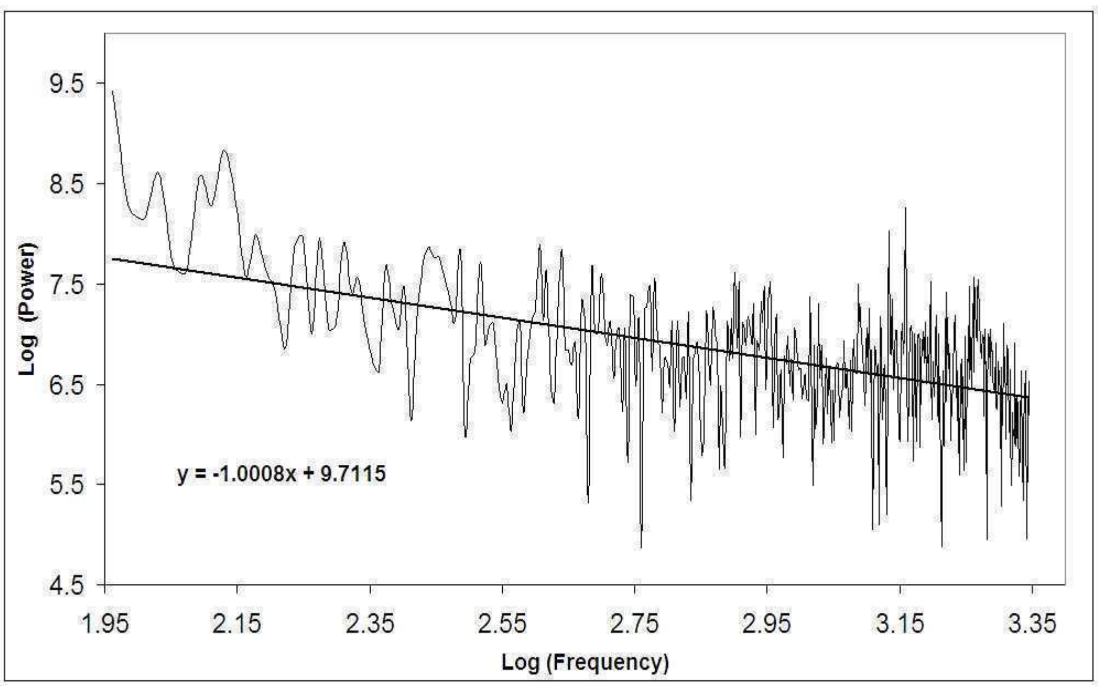

Fig. 9. Plot of log of noise power level versus log of frequency for
Noise recorded at the highway near Mondha Naka.

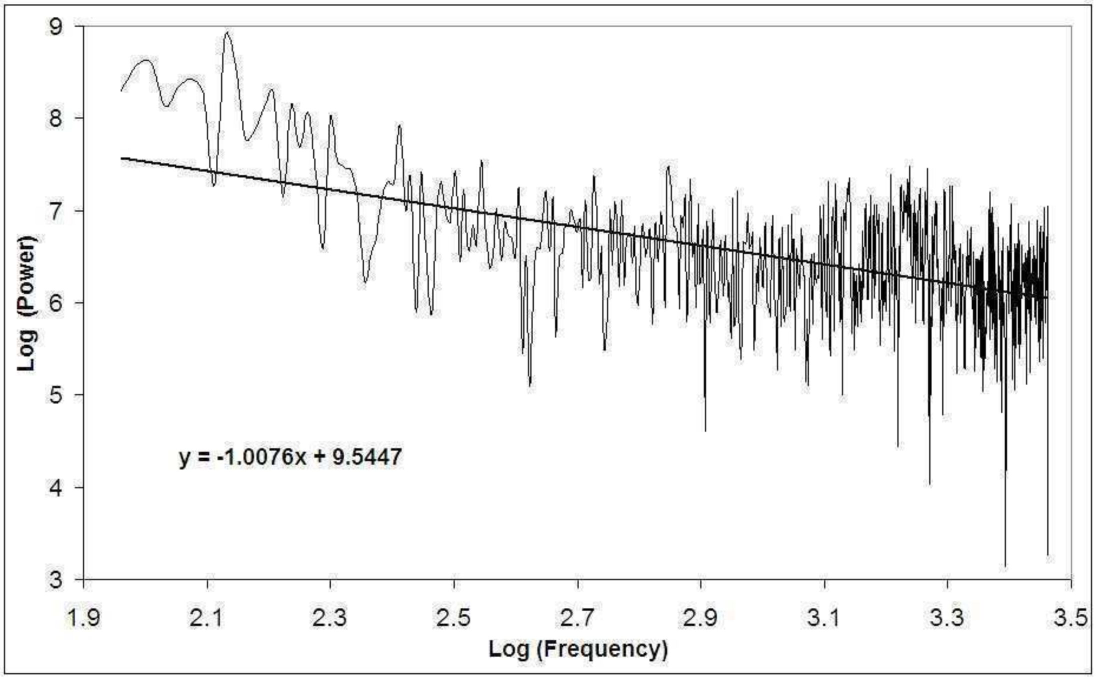

Fig.10. Plot of log of noise power level versus log of frequency for Noise recorded at the highway near Mondha Naka

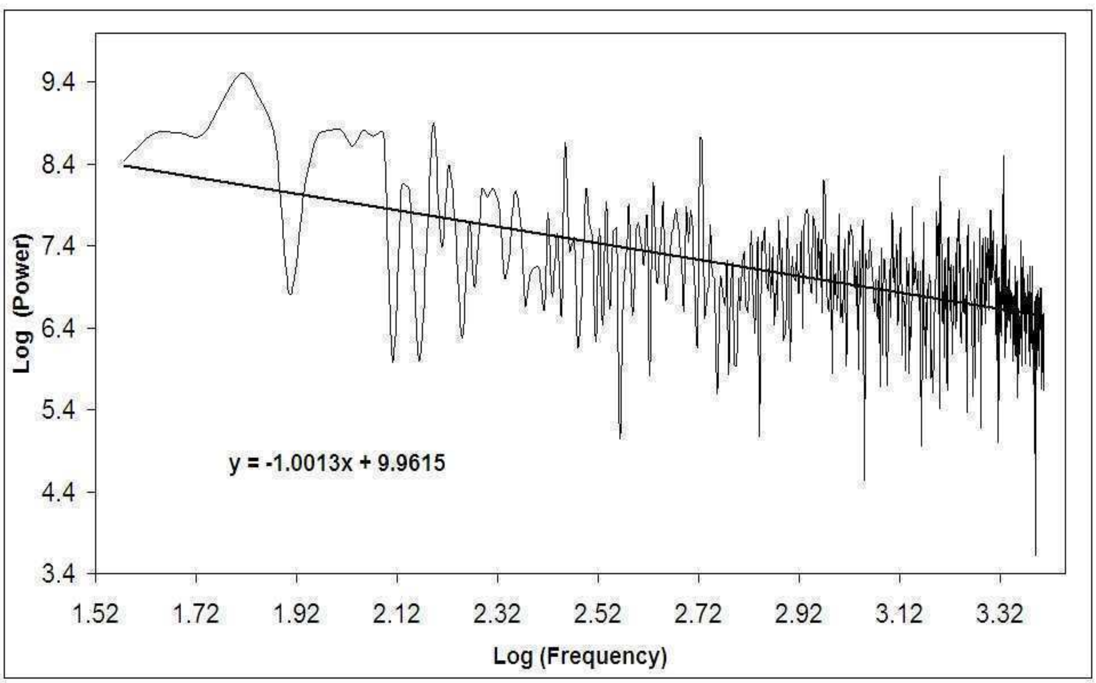

Fig. 11. Plot of log of noise power level versus log of frequency for Noise recorded at the highway near Rokdia Hanuman colony

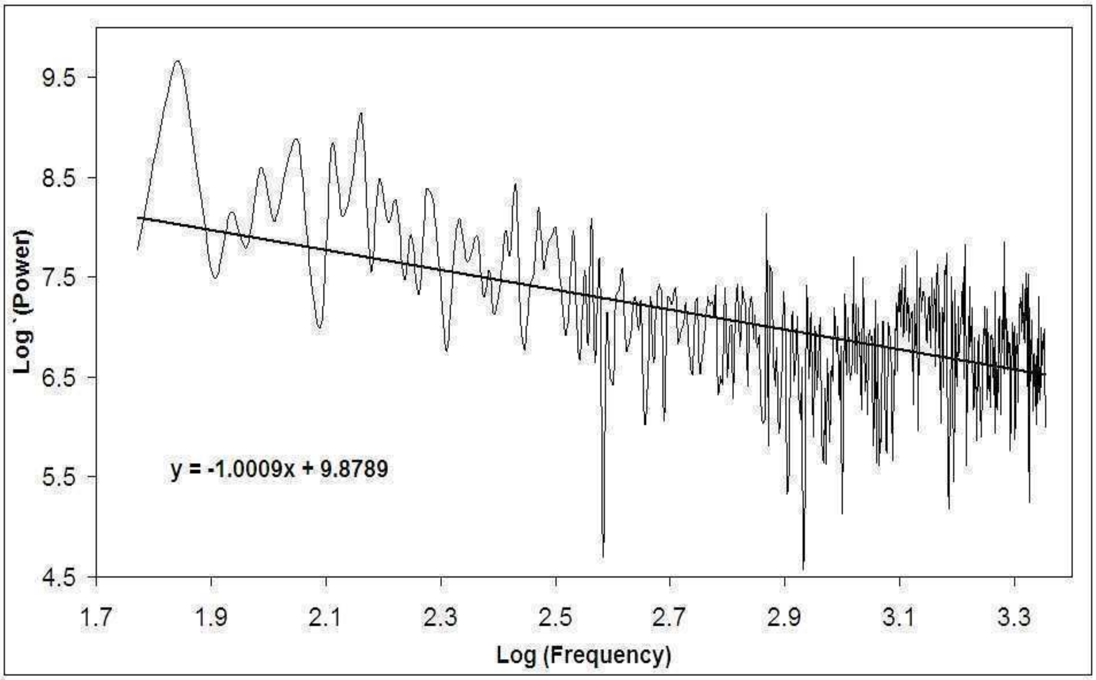

Fig. 12. Plot of log of noise power level versus log of frequency for Noise recorded at the highway near Rokdia Hanuman colony

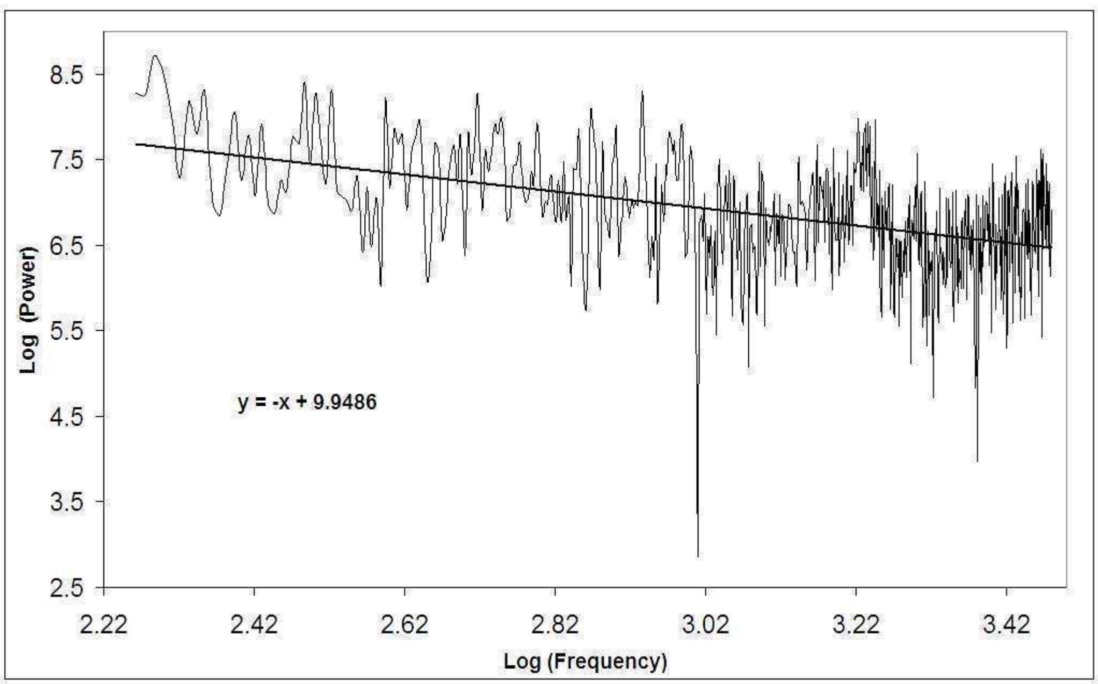

Fig. 13. Plot of log of noise power level versus log of frequency for Noise recorded at the highway near Rokdia Hanuman colony

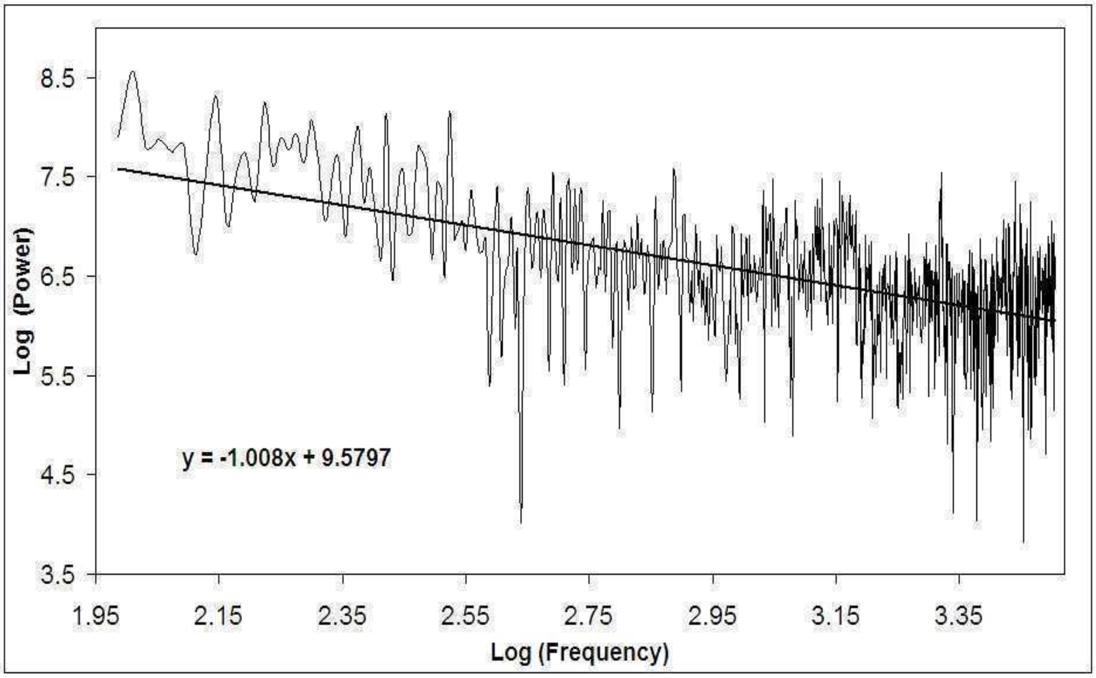

Fig. 14. Plot of log of noise power level versus log of frequency for Noise recorded at the highway near Rokdia Hanuman colony

Table. 1. Table showing Power law exponent and the range of frequencies for noise presented in Figure 2 to 14.

Figure No.	Location	Frequency Range Minimum	Maximum	Slope
2	Baba Petrol Pump	53.83	2035	1.0004
3	Baba Petrol Pump	290.7	3004	1.0000
4	Aakashwani	102.3	3445	1.0025
5	Aakashwani	915.2	4016	1.0007
6	Amarpreet Hotel	134.6	2562	1.0001
7	Amarpreet Hotel	113	2099	1.0051
8	Kranti Chowk	156.1	3284	1.0026
9	Mondha Naka	91.52	2213	1.0008
10	Mondha Naka	91.52	2902	1.0076
11	Rokdia Hanuman colony	37.68	2557	1.0013
12	Rokdia Hanuman colony	59.22	2256	1.0009
13	Rokdia Hanuman colony	183	3015	1.0000
14	Rokdia Hanuman colony	96.9	3192	1.0080

4. CONCLUSIONS

It is seen from Fig. 3 to 14 that noise originating from highway traffic under certain conditions exhibit the characteristics of pink noise over certain range of frequency. Table 1 summarizes the locations of study, the range of frequency and the power law exponent α. It is seen from the table that the value of α lie close to unity confirming the presence of pink noise (1/f noise) over the frequency range indicated. Most of the power spectra exhibit fast falling power with frequency, however few of them exhibit pink noise (1/f noise) characteristics with power law exponent α equal to unity.

5. REFERENCES

[1] M.U. ONUU, 2000. Road Traffic Noise in Nigeria: Measurements, Analysis and Evaluation of Nuisance. *Journal of Sound and Vibration*, **233,(3)**, 391-405.

[2] S.J. MARTIN, 2002. Numerical Modelling of Median Road Traffic Noise Barriers. *Journal of Sound and Vibration*, **251(4)**, 671-681.

[3] R. GAMBART, H. MYNCKE and A. COPS, 1976. Study of Annoyance by Traffic Noise in Leuven (Belgium). *Applied Acoustics*, **9(3**), 193-203.

[4] W. TEMPEST (ed.), 1985. The Noise Handbook. London: Academic Press.

[5] H.G. LEVENTHALL, 988, Low frequency noise in buildings-internal and external sources. *Journal of Low Frequency Noise and Vibration*, **7**, 74-85.

[6] http://www.nslij-genetics.org/wli/1fnoise/index.html

[7] H.E. VON GIERKE and C.W. NIXON, 1976, Effects of intense infrasound on man. In W. Tempest (ed.), Infrasound and Low Frequency Noise Vibration. London: Academic Press, **6**, 115-150.

[8] SUDESHNA SINHA, 1996. Transient 1/f noise. *Physical Review E*, 53.

[9] D.L. GILDEN, T. THORNTON and M.W. MALLON, 1995. *Science,* **267**, 1837-1839.

[10] H. WONG, 2003. Low-frequency noise study in electron devices: review and update. *Microelectron. Reliab.*, **43**: 585-599.

[11] SHAIKH YUSUF, A.R. KHAN, J.M.PATHAN J. M., PATIL ARUNA and S.H. BEHERE, 2009. *Fractal* pattern growth simulation in electrodeposition and study of the shifting of center of mass. Chaos, Solitons *and Fractals*, **42**, 2796-2803.

[12] H. SHAIKH YUSUF, A.R. KHAN, M.I. IQBAL, S.H. BEHERE and S.P. BAGARE, 2008. Sunspot Data Analysis using time series. *Fractal*, **16**(**3**), p. 259.

[13] LAWRENCE M. WARD and PRISCILLA E. GREENWOOD, 2007. *Scholarpedia*, **2(12)**, p. 1537.

[14] http://en.wikipedia.org/wiki/Colors_of_noise

[15] H. WONG, 2003. Low-frequency noise study in electron devices: review and update. *Microelectron. Reliab.*, **43**, 585-599.

[16] W.H. PRESS, 1978. Flicker noises in astronomy and elsewhere. *Comments on Astrophysics,* **7**, 103-119.

[17] F.N. HOOGE, T.G.M. KLEINPENNING and L.K.J. VANDAMME, 1981. Experimental studies on 1/f noise, *Rep. Prog. Phys.*, **44**, 479-532.

[18] P. DUTTA and P.M. HORN, 1981. Low-frequency fluctuations in solids: 1/*f* noise. Reviews of Modern Physics, 53: 497-516. doi:10.1103/*RevModPhys.*, **53**, p. 497.

[19] S.M. KOGAN, 1985. Low-frequency current 1/f-noise in solids, *Uspekhi Fizicheskikh Nauk*, **145**, 285-328; *Sov. Phys. Usp.*, **28**, p., 170.

[20] M.B. WEISSMAN, 988. 1/f noise and other slow, non exponential kinetics in condensed matter. *Rev. Mod. Phys.*, **60**, 537-571.

[21] B.J. WEST and M.F. SHLESINGER, 1990. The noise in natural phenomena, American Scientist, 78:40-45.

[22] Van Vliet C. M., 1991, A survey of results and future prospects on quantum 1/f noise and 1/f noise in general. *Solid-State Electron.*, **34,** 1-21.

[23] G.P. ZHIGALSKII, 1997. 1/f noise and nonlinear effects in thin metal films. *Uspekhi Fizicheskikh Nauk*,**167**, 623-648; *Phys. Usp.*, **40**, p. 599.

[24] E. MILOTTI, 2002. A pedagogical review of 1/f noise. e-print physics/0204033- arxiv.org.

[25] http://classes.yale.edu/fractals/CA/OneOverF/WhiteNoise.html

[26] M. GARDNER, 1978. *Sci. Am.*, **238(4)**, p. 16.

Journal of Acoustical Society of India : Vol. 37, No. 3, 2010 (pp. 105-111)

Study of Thermo Dynamical and Excess parameters of Binary and Ternary Mixtures by having Propanol as Common Component

M.M. Armstrong Arasu and I. Johnson*

Centre for Nano Science and Applied Thermodynamics

Dept. of Physics, St. Joseph's college, Trichy - 620 002, India

**e-mail: jnaadarsh@hotmail.com*

[Received: 21.12.2009; Revised: 27.04.2010; Accepted: 11.05.2010]

ABSTRACT

Industry demands reliable and accessible reference data on the physical and chemical properties of a wide variety of compounds. These data are required in the development of process design and efficiency and in the evaluation of possible environmental impacts.

1. INTRODUCTION

In this paper density, viscosity and speed of sound is measured for binary mixture of Propanol + Isopropyl acetate for temperatures 308.15K . The density , viscosity and speed of sound for ternary mixture of Propanol + Isopropyl acetate+ water were measured at 313.15K. The excess volume, Wada constant, ultrasonic relaxation time, deviations enthalpy, ultrasonic velocity, adiabatic compressibility viscosity, free length, internal pressure, acoustic impedance, free volume& Gibb's free energy were calculated for binary mixture at the constant temperature of 308.15K, for ternary mixture at the constant temperature of 313.15K

2. EXPERIMENTAL

The binary and ternary mixtures were prepared by mass, by mixing the calculated volumes of liquid components in airtight glass bottles. In all the measurements, INSREF thermostat with a constant digital temperature display accurate to ±0.01K was used. For all the mixtures and pure solvent triplicate measurements were performed and the average of all values were considered in the calculation. The mass measurements (± 0.0001g) were made using an electronic balance. The accuracy of density measurements was $0.0001 g.cm^3$. A set of 18 compositions was prepared for ternary mixtures and their physical properties were measured. Viscosity is measured by calibrated Ostwald's Viscometer. The speed of sound was determined using a constant frequency (2MHz) ultrasonic interferometer with an accuracy of $\pm 2\ m.s^{-1}$.

3. THEORY

The excess molar volume V^E was calculated from the density data by the relationship

$$V_E = V_M - \sum_i x_i V_i \quad (1)$$

where Vi represents the molar volume, x_i the mole fraction of the ith component and V_M is the molar volume of the mixture, given as

Journal of Acoustical Society of India : Vol. 37, No. 3, 2010 (pp. 112-120)

Transformation of Emotion Using Word Boundary Detection for Hindi Speech

Anurag Jain[1], S.S. Agrawal[2] and Nupur Prakash[1]*
[1]*School of I.T., GGSIP University, Delhi*
[2]*CDAC, Noida, India*
**e-mail: anurag_jain76@yahoo.com*

[Received: 17.03.2010; Revised: 20.05.2010; Accepted: 19.06.2010]

ABSTRACT

Emotion transformation is applied to synthesizing emotional speech from standard neutral speech. Emotion is an important cue to express the feeling of one's expression. It is also an important factor in expressive speech synthesis. If one wants to understand the meaning of an utterance, it must be in proper emotion otherwise semantically utterance will go to the wrong direction and give wrong result. Keeping the facts in view, an algorithm is proposed to transform a neutral utterance to target emotional utterance. The transformation adopts the concept of Linear Modification Model (LMM) model. The parameter used in the study are F0, Segmental duration and energy factor from the acoustic distribution analysis. As conversion target emotions, sadness, happiness and surprise are used. In the experiment, Segmental duration and F0 contours of neutral emotion are modified using the TD-PSOLA implementation. A word boundary detection algorithm is also proposed for Hindi and is implemented with the emotion conversion algorithm to find the word segments that are used as the input parameters for the emotion conversion algorithm. We have used Pitch and Intensity contours to word boundary detection algorithm.For performing experiments and verification of results, an emotion rich speech database is prepared with the help of 20 native speakers. Each speaker has been given 25 sentences and asked to generate utterances in five expressive states "neutral", "sadness", "anger", "surprise" and "happiness". These sentences are recorded in Normal laboratory conditions with 44.1KHz sampling rate and 16-bit precision with mono channel. Auto spectral subtraction and Multiband noise gating technique are used for noise reduction.

Two experiments are performed separately on Word Boundary detection and emotion conversion method and results are obtained. The results are analyzed and performance of the experiment is evaluated and it is found that word boundary detection algorithm has recognition accuracy is of 82% and emotion conversion algorithm is given the accuracy of 93.2% for surprise, 91.6% for sadness, 95.3% for anger and 88.6% for happiness as target emotion, where neutral is considered as source emotion. These results of emotion conversion algorithm are based on the subjective (perception) experiment performed on nearly 200 neutral speech corpuses distinct from the training set corpus.

1. INTRODUCTION

Emotion transformation is applied to synthesizing emotional speech from standard neutral speech. Emotion is an important cue to express the feeling of one's expression. It is also an important factor in expressive speech synthesis. To store all utterances of all the expressive styles require huge memory space and time. So there should an emotion conversion approach that minimizes the time and memory space for emotion rich database. In recent years, more efforts have been done for prosody conversion, voice conversion and emotion conversion using different techniques, among which emotion is an important parameter [1], [2]. Direct manual manipulation techniques are used by [3] to achieve the output of emotional speech. Speech synthesis markup language is also used to generate the expressive styles from neutral sentences [4], [5]. In [6] , various emotion and prosody conversion methods are performed on the acoustic distributions among emotions in Mandarian. LMM, GMM and CART methods were compared using Deviation of Perceived Expressiveness (DPE) to evaluate the expressiveness of output speech and suggest that these models give good results based on the size of the training set. GMM based spectral conversion was also applied in [7] and found that for required target emotion only spectral conversion method is not sufficient. HMM based modelling technique is also used to model context sensitive syllable F0 segments for each emotion alongwith the GMM method and codebook selection method [8], but resulted in more doubts when more substantial spectral and prosodic modifications occurred. HMM based data driven emotion conversion methods have also been implemented in [9], [10], [11]. In [11] due to prosodic parameter, prosody transformation is used within an emotion conversion framework.

In this paper, we presented a corpus based emotion conversion algorithm, which require only neutral speech of data to generate the desired target speech in different expressive style. Conceptually emotion conversion might be thought of as a form of prosody or voice conversion where a vocal tract spectrum has a major consideration whereas F0 and energy, intensity and duration patterns are of great concern with emotion transformation [12], [13].

In this paper, we have also proposed a word boundary detection algorithm for detecting word segments, which acts as the fundamental unit of speech during emotion conversion and duration conversion. Several Word boundary detection methods were also been explored and studied. For French analysis has been done by [14] and suggested the word segmentation using early rise in F0 starting at the beginning of content words. The results supports for auto segmental -metrical account of the intonational phonology of French. Several factors motivate the prosodic analysis for word boundary hypothesization. Duration, Intensity and Pitch reflects important cues for providing word boundary detection. According to [15] features of intonation like F0 contour rise/fall, F0 range and F0 rules represent important discourse information. Duration provides the syntactic relation between words [16]. Very few studies have been reported for Indian languages. In [17] Word Boundary detection algorithm is proposed and imposed on standard Colloquial Bengali speech and argued that Stress put its sign on suprasegmental parameters of the speech signal and based on Vowel duration, F0 differences and Periodic power of nucleus vowel, an algorithm was suggested. This algorithm is based on Pitch detection and Voice detection algorithm (PDA/VDA). Using F0 pattern and language dependent rules, [18] reported recognition rate for Hindi is about 70%, while as reported in [19] , 85% of the word boundary were correctly detected using F0 and word's pitch pattern (rise in a word and fall to the next word) behaviour. In [18], [19] only F0 is considered and other supra segmental features are not considered. Prosodic features like fundamental frequency, amplitude, duration and pause can be used as clues to detect word boundaries [20], while few language features can also be explored for locating word boundaries.

In this paper, we have proposed word boundary detection algorithm and emotion conversion algorithm for Hindi. First of all we try to check the number of words occurred in speech using word boundary detection algorithm and then emotion conversion algorithm, is implemented to transform the neutral speech to target speech emotion. The proposed algorithm of word boundary detection is based only two suprasegmental parameters (Pitch and Intensity) and gives the word boundary in most of the cases. We have tried to hide the syllable boundary information due to non-existence in emotion conversion algorithm. For emotion conversion, we proposed data driven emotion conversion module for Hindi, which require only neutral speech data to transform the emotion automatically. This algorithm is based on Linear Modification Model (LMM) where the neutral source utterance and neutral target utterance are analysed and on the basis of the prosodic differences between source and target utterance, Transformation takes place. In this paper, we have considered Neutral speech as source and sadness, happiness and surprise are considered as Target emotion. In such cases, the pitch pattern can be the input for emotion conversion module. A basic block diagram of the emotion conversion system is mentioned in Fig. 1.

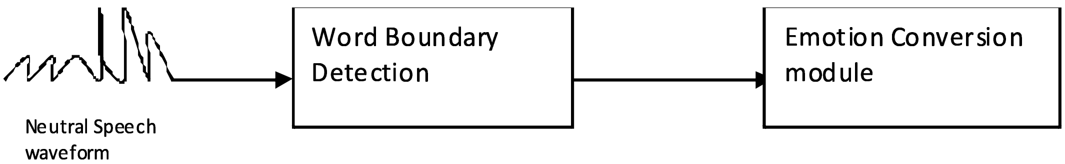

Fig. 1. Basic Block diagram of emotion conversion system

The rest of the paper is organized as follows. Section 2 details the emotional speech database used for evaluating F0 variations and emotion conversion. Section 3 describes the proposed algorithm for word boundary detection, which uses suprasegmental features to detect the word boundary. Section 4 proposes an algorithm, which are used to convert the emotion from "neutral" to emotional speech. Section 5 provides the results for word boundary detection and perceptual analysis for emotion conversion method. Section 6 provide the conclusion for this paper.

2. INTONATION BASED SPEECH DATABASE

To perform experiments and verification of results, an Intonation based Speech database is prepared. For the database, fifteen native speakers have been given 25 sentences to generate Hindi utterances in five expressive styles Neutral, Sadness, Anger, Surprise and Happy. These sentences are emotionally rich and can be spoken in all five emotions. Once in emotionally charged mood, each speaker was asked to record the sentences . These sentences are recorded in Normal laboratory conditions with 44.1KHz sampling rate and 16-bit precision with mono channel. After recording each speech file passed through optimization phase where Normalization of amplitude and noise reduction techniques are used.

There is another database which is directly associated with the main module of emotion conversion. The database is used to keep the pitch point values (Table 1) for tneutral utterances, already present in the Speech Database. We have computed 4 pitch points (F0min, F0max, F0beg and F0end) for each word segment present in the utterances among the numbers of pitch points. The total numbers of pitch points are based on number of words present in the utterance and resolution frequency (fr). The commonly available PRAAT analysis software tool [21] is used for this purpose. The target emotions are anger, surprise, happiness and sadness. These emotions are considered according to their different acoustic profiles [22]. Nearly two hundred utterances of neutral speech were carried out for training and rest of the utterances were kept reserve for testing. Other expressive style utterances are taken to choose the listeners for perception test. 30 listeners were appeared for the perception test and 1875 random utterances were given to them.

3. METHODOLOGY

Before proposing the algorithm for emotion conversion from neutral emotion to target emotion, speech corpora was analyzed on the basis of F0 contour and Intensity contour and their pitch values as table [1] are studied throughout the utterance. It is also observed that to get the word segments from the speech utterance, a word boundary detection is also required, which provide the number of word segments along-with the their segment duration, so that emotion conversion algorithm will be applied on segment basis.

In this way, the proposed emotion conversion methodology contains two algorithms

- Word boundary detection algorithm
- Word segment based emotion conversion algorithm.

3.1 Word Boundary Detection Algorithm

In general, three different kinds of waveform creates a speech signal, namely quasi-periodic, quasi random and the silence and Pitch detection algorithm (PDA) and Voice detection algorithm (VDA) are required in quasi periodic portion of the speech waveform [17]. Many PDA and VDA algorithms have been proposed based on short-term energy and zero crossing rate, and found that these features do not work in Noisy ambiance.

S. No	Sentence	Filename (.wav) (<Emotion> is replaced by "Neutral", "Anger", "Happy", "Surprise" and "Sad")
1	आज कालेज जाना है|	AajCollege <Emotion>
2	आज क्रिकेट मैच है|	AajCricket <Emotion>
3	मुझे आज काम करना है|	AajKaam <Emotion>
4	आज आफिस नही जाना है|	AajOffice <Emotion>
5	मैंने अपना काम कर लिया है|	ApnaKaam <Emotion>
6	दुकान बंद हो गई है|	DukaanBand <Emotion>
7	हम घर पँहुचने वाले है|	HumGhar <Emotion>
8	हम कल बाहर नही जाएंगे|	KalBaahar <Emotion>
9	मैनें कल उससे बात की थी|	KalBaat <Emotion>
10	कल मेरा ईगज़ाम है|	KalExam <Emotion>
11	कल सुबह घर पर मिलना है|	KalSubah <Emotion>
12	यह मुझसे नही होगा|	Mujhse <Emotion>
13	यँहा फूल तोड़ना मना है|	Phool <Emotion>
14	तुम गए और वह आ गई|	TumGaye <Emotion>
15	तुम्हारा फोन बज रहा है|	TumharaPhone <Emotion>
16	वह तुम्हारे घर में रहता है|	TumhareGhar <Emotion>
17	तुम पास हो गए हो|	TumPaas <Emotion>
18	उसका फोन नही आया है|	UskaPhone <Emotion>
19	उसकी गाड़ी छुट गई|	UskiGaadi <Emotion>
20	उसने परीक्षा दी और वह पास हो गया		UsnePareeksha <Emotion>

So a new method is proposed, where Intensity contour and Pitch contour are analyzed and based on the rules as proposed, word segments can be detected. For word boundary detection methodology, we have considered only three prosodic parameters "Defined Pitch contour " , "Undefined pitch on silence zone" and "Intensity contour".

Rules for Word boundary detection are as follows

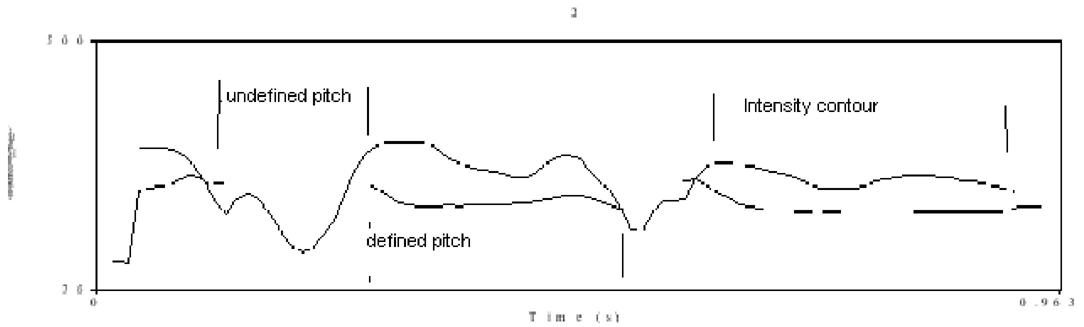

Rule 1: Intensity valleys above threshold value I0 are not considered as word segment boundary.
Rule 2: Intensity Valleys below I0 are considered as Word Boundary
Rule 3: Valleys on non- pitch range can be considered as word segment boundary
Rule 4: If there is no intensity point in undefined pitch pattern, there will not be any word boundary.
Rule 5: If there is more Intensity valleys on a pitch defined range and duration difference is less than 1.2 sec, only lowest intensity point will be considered as Word boundary.

3.2 Word segment based emotion conversion algorithm

Proposed emotion conversion methodology is based on Linear Modification model (LMM) . LMM model select prosody modification model from the prosody feature among emotions [6] .

$$Y_{n,i} = C_{n,i} X \quad (1)$$

Where "X" represents input parameter: F0, duration and intensity and "Y" represents the prosodic parameter of target emotions. "C" is used as the conversion scale to map source emotion to target emotion. The conversion scale is created from the training set of the speech database and "n" represents the expressive emotional style (happiness, sadness, anger and surprise) and "i" represents the emotion level.

Now we propose the model using the formula

$$Y_n = C_n X \quad (2)$$

In this method pitch points (Pi) were studied for the desired source emotion (Neutral) and target emotion and then conversion scale between corresponding pitch points were evaluated after normalization. This serves as an indicator of the values by which pitch points of source speech utterance must be increased or decreased to convert it to target utterance. When a sound file is selected, pitch analysis was performed, using timestamp and minimum and maximum pitch parameters. The information of the resulting pitch contour is used to posit glottal pulses where the original sound contains much energy and then pitch contour is converted to a pitch tier with many points. For pitch analysis step length is taken as .01 second and minimum and maximum pitch is taken as 75 Hz and 500 Hz. On comparison between source and target emotion training set, pitch points are divided in word segment group and set the initial frequency as xi's respectively. On the basis of observation of training set Cn is operated to the subsequent "x" values. All xi and yi are in Hz. To select Cn values, Conversion table is constructed. we have not calculated the mean of xi and Cn, these values are came out after the rigorous analysis of pitch patterns of falls neutral and emotional utterances.

Word segment based Emotion Conversion algorithm

Select desired sound wave form
Apply Word Boundary detection (WBD) algorithm
Convert speech waveform in pitch tier
// Stylization
For all Pis
Select Pi, that is more close to straight line and compare with resolution frequency (fr)
if distance between pi and straight line > fr
Stop the process
else
Repeat for other Pis
Divide the pitch points into word segments as produced by WBD
For each word segment's F0min, F0max, F0beg and F0end
Wordi,f= Cn,i,f XniI,f*
//Where n is emotional state, i denotes the word segment and f denotes the F0 values for various prosodic points..
Remove existing pitch points
Add newly calculated pitch points and duration in place of old pitch points.
Algorithm 1. Word segment based emotion transformation

Table 4: Pitch points (in Hz)

Pitch Points	Neutral	Surprise
Pt1.	276.4	349.5
Pt2.	319.7	389
Pt3.	205.7	244.5
Pt4.	211.3	217.9
Pt5.	331.7	255.6
Pt6.	262.3	414.1
Pt7.	246.9	261.7
Pt8.	141.8	492.1
Pt9.	171.3	324.2
Pt10	125.4	375.9
Pt11	205.2	399.2

Table 4 shows the list of pitch points involved (after normalization) in both emotions for a particular training set utterance as a showcase for "कल तुम्हें फासी हो जाएगी ". Figures 6 and 7 gives the idea about the pitch points involved in natural neutral emotion and natural surprise emotion respectively.

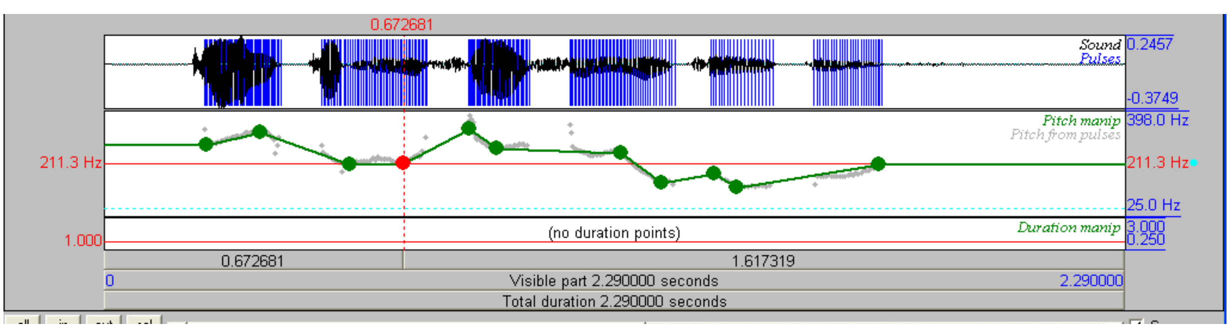

Fig. 6. Pitch points for natural neutral emotion

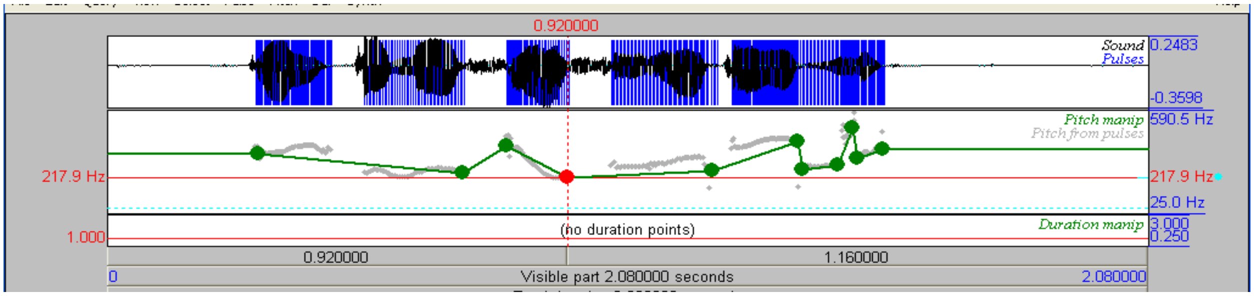

Fig. 7. Pitch points for natural surprise emotion

4. EVALUATION

The proposed algorithms were evaluated through Subjective and objective test. The objective test is conducted to measure the variation between target emotion and transformed speech converted from neutral speech using F0 variation word segment wise. On the other hand subjective experiments are performed by perception test with 20 Listeners and asked to perceive emotions of synthesized Transformed speech. They are carried out a force choice test among anger, sadness, surprise and happiness.

4.1 Objective Test

For this process, predefined speech training set are taken and randomly neutral utterance is selected. For example, "कल तुम्हें फासी हो जाएगी " were considered and their results are given in figure 10. In figure, upper picture shows the natural surprise utterance and lower part displays the transformed surprise utterance and display the differences between neutral and transformed surprise pitch point values, this is due to consider only the intonation and duration not other factors like stress and syllable position within the word. The experimental results are illustrated in figure. As a normal analysis, it is shown that difference of F0 between neutral and surprise is smaller than the other emotions. Although after carefully listening, listeners are very much comfortable with the emotion of transformed surprise emotion. It is easily verified in Perception test.

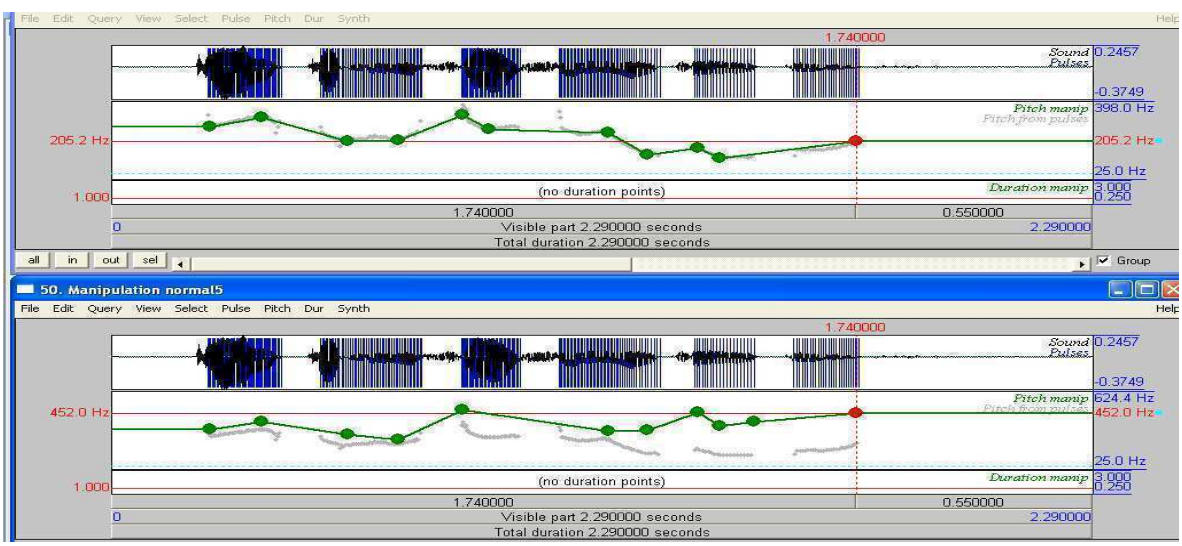

Fig. 10. Natural and transformed Surprise emotion utterance

4.2 Perception Test

In this part of experiment, utterances of all emotions are presented in front of listeners and asked to identify the emotions of those utterances. Listeners are divided into 3 groups of 5 candidates each. Table 8 presents the perception matrix on the original natural emotional data based on the F0 analysis of Intonation Patterns of Hindi. The matrix contains expressed emotions horizontally and perceived emotions vertically. Values are mentioned in percentage. As seen by perception matrix, "anger" is most accurately perceived emotion and least accurately perceived emotion is "happiness". Table does not depict 100% accuracy for each expressed emotion due to listener's confusion about the emotion. For some emotions it exceeds 100% and for some emotions it is below than 100%. It is because some times listener perceives more than one emotion for the same expressed emotion and sometimes he/she was unable to perceived the emotion under the mentioned category of emotions and assume it to be 0. It happened due to overlapped features of Pitch range and variation in all the emotions. It is concluded that no emotions has one to one mapping with particular pitch variation and other acoustic parameters. Afterwards listeners were again asked to predict the emotions of system generated transformed emotions to verify the performance of the system. Table 5 presents the perception matrix for the transformed emotional data from original neutral emotion speech. Listeners were provided full liberty to predict any emotion. In most of the cases sadness was only confused with neutral emotion and surprise was mostly confused with anger. So it may be assumed that if choice were only restricted to sadness and surprise, both the emotion would be identified correctly all the time.

Table 5. Transformed Perception matrix

Emotion	Surprise	Sadness	Neutral	Anger
Perception	93.2 %	91.6%	8.4%	6.8%

5. ACKNOWLEDGEMENT

This research was supported by Guru Gobind Singh Indraprastha University Delhi and Special thanks go to colleagues and post graduates students who participated in the perception test and speech recording.

6. REFERENCES

[1] I. MURRAY and J.L. ARNOTT, 1993. Toward the simulation of emotion in synthetic speech: A review of the literature on human vocal emotion, *J. Acoustic Soc. Amer.*, 1097-1108.

[2] R.M. STIBBIRD, 2001. Vocal expression of emotions in non-laboratory speech: An investigation of the reading/leeds emotion in speech project annotation data, Ph.D dissertation, Univ. Reading, U.K.

[3] J.E. CAHN, 1990. The generation of affect in synthesized speech, *J. Amer*. Voice I/O society. **8**, 1-19.

[4] M. SCHRODER and S. BREUER, XML represenation languages as a way of interconnecting TTS Modules, in *Proc. ICSLP*, Jeju, Korea, 889-1892.

[5] E. EIDE, A. AARON, R. BAKIS, W. HAMZA and J. PITRELLI, 2002.A corpus based approach to expressive speech synthesis, in Proc. IEEE Speech Synthesis Workshop , Santa Monica , CA, 79-84.

[6] T. JIANHUA and K. YONGGUO, 2006. Prosody conversion from neutral speech to emotional speech", in IEEE Trans on Audio, *Speech and Language Processing*, **14** , 1145-1154.

[7] H. KAWANAMI , Y. IWAMI, T. TODA, H. SARUWATARI and K. SHIKAMO, 1999. GMM based Voice conversion applied to Emotional Speech Synthesis, *IEEE Tran*s. *Speech and Audio Proc.* , 697-708.

[8] Z. INANOGLU and S. YOUNG S, A System for transforming the emotion in speech: combining data driven conversion techniques for prosody and voice quality.

[9] H. TSUZUKI, H. ZEN, K. TOKUDA, T. KITAMURA, M. BULUT and S. NARAYANAN, 2004. Constructing emotional speech synthesizers with limited speech database, *In Proc. ICSLP*, *2*, 1185-1188

[10] J. YAMAGISHI, K. ONISHI, K. MASUKO and T. KOBAYASHI, 2003. Modelling of various speaking styles and emotions for HMM-based speech synthesis, *In Proc. EUROSPEECH*, *3*, 2461-2464.

[11] Z. INANOGLU and S. YOUNG, 2009. Data Driven emotion conversion in spoken English, *in trans. Speech communication*, **51**, 268-283.

[12] Y. STYLIANOU, O. CAPPE and E. MOULINES, 1998. Continuous probabilistic transform for voice conversion", *IEEE Trans. Speech Audio and Process*, **6**, 131-142.

[13] A. Kain and M. Macon, 1998. Spectral voice conversion for text-to-speech synthesis, *In Proc. ICASSP*, **1**, 285-288.

[14] W. PAULINE, 2007. The role of early fundamental frequency rises and elbows in French word segmentation, *in Tans. Speech Communication*, **49**, 28-48.

[15] M. LIEBERMAN and J. PIERREHUMBERT, 1984. Intonational invariance under changes in pitch range and length, in Language Sound Structure, ed By M. Aronoff and R.T. Oehrle (M.I.T. Press) 157-233 1984.

[16] P. ESWER, 1990. A rule based approach for spotting characters from continuous speech in Indian Langauge, Ph.D , IIT Madras.

[17] S.K.D. MANDAL, B. GUPTA and A.K. DATTA, 2007. Word Boundary detection based on suprasegmental features: A case study on Bangla speech, *Int. J Speech Tec*., Springer, 17-28.

[18] C. SHAH and A.N. KHAN, Spoken document retrieval for broadcast news in Indian Languages", in IEEE's Intt. Conf. on acoustic, speech and signal processing (ICASSAP) Volume VI.

[19] G.V. RAMANA RAO and J. SRICHAND, 1996. Word Boundary Detection using pitch variations " , in fourth intt. Conf. on spoken language processing, Philadelphia .

[20] S. RAJENDRAN and B. YEGNANARAYANAN , 1996. Word Boundary hypothesization for continuous speech in Hindi based on F_0 Patterns, *Speech Communication*, **18(1)**, 21-46.

[21] http://www.fon.hum.uva.nl/praat

[22] R. BARRA, J. MONTERO, J.G. ARRIOLA, J. GUARAS, J. FERREIROS and J. PARDO, 2007. Onthe limitations of voice conversion techniques in emotion identification, in proc Interspeech.

Journal of Acoustical Society of India : Vol. 37, No. 3, 2010 (pp. 121-129)

A Preliminary Acoustic Study of Mizo Vowels and Tones

Priyankoo Sarmah[1] and Caroline R. Wiltshire[2]
[1]*Department of Linguistics and Cognitive Science Hankuk University of Foreign Studies*
202-1, 89 Wangsan-ri, Choein-gu, Mohyeon-myeon
Yongin, South Korea 449-791
e-mail: priyankoo@gmail.com
[2]*Department of Linguistics University of Florida 115454, Turlington Hall*
Gainesville, Florida, USA 32611
e-mail: wiltshir@ufl.edu

[Received: 12.04.2010; Revised: 27.05.2010; Accepted: 11.06.2010]

ABSTRACT

This paper provides quantitative measures of Mizo vowels and tones. The first two formants and durations of the five Mizo vowels were extracted, and their perceptual distances were measured. As F0 is the primary cue for the identification of Mizo tones, a quantitative parameter is built for instrumentally identifying the four Mizo tones namely, high, low, rising and falling tones using F0 as the major cue. While doing that, we also examined (a) if consonantal segments affect the pitch of Mizo tones in any way. In the presence of positive evidence for consonantal influence, this study will try to determine (b) how far into the F0 can the consonantal effects perturb. The results indicated that (c) in Mizo; consonantal segments in the onset do affect the pitch of the following tone in a significant manner. With the methodology adopted in this study it is concluded that the effects of consonants into the F0 may be highly predictable.

1. INTRODUCTION

Mizo is a Tibeto-Burman language spoken by over half a million people: approximately 539,000 in India, 1,000 in Bangladesh, and 12,500 in Myanmar. In India, it is spoken primarily in the state of Mizoram (Fig. 1). There has been descriptive work on its sound system in general [see 1-4], and its vowel inventory and tone system has been described and analyzed by native speakers [5-7]. However, none of the studies conducted on Mizo has based their conclusions on acoustic analysis.

Mizo is described as having five vowels with long and short distinction for each [5-7]. According to the same studies, the ten total vowels of Mizo are [i:, i, u:, u, ɛ:, ɛ, ⊃:, ⊃, a:,a]. The low vowels [a:, a] are described as central vowels. No other information about the Mizo vowel system is available from these studies.

The Mizo tone system is described as having an inventory of four tones: High (H), Low (L), Rising (R) and Falling (F) [5-7]. These studies do provide a few rules for the interactions of tones in suffixed or compounded words; however, both these researchers stress the desirability of acoustic analyses to support their descriptions.

The tones described in previous literature are more or less consistent with slight variations. For example, Bright is of the view that Mizo has H, F, L and an allophonic mid level tone sometimes realized as a mid to low

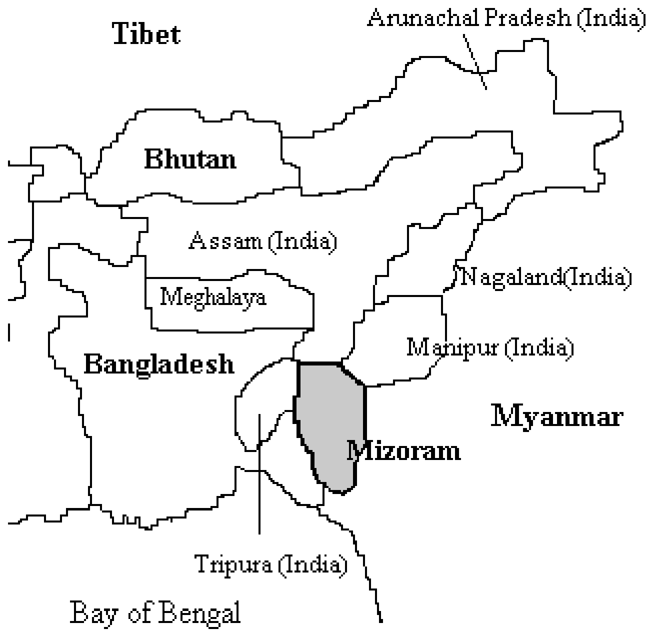

Fig. 1. Location of Mizoram in North-East India

falling tone [1]. Weidert describes the Mizo tones as high-level, high-falling, low-rising and low-level tones [4]. Chhangte describes the Mizo tone inventory as including H, R, F, and an unmarked tone, where the unmarked is phonetically mid or low [5]. Fanai also describes the four tones of Mizo as H, L, R and F where the L tone can also have an allophonic variation realized as an extra low tone that she marks as L [7]. As the L tones in Mizo are realized with a mid to low fundamental frequency (F0) movement, H is the only tone with a level F0 track [7]. The H and the L tones can occur on syllables with both long and short vowels, however; the R and the F tones can only occur with syllables with more than one sonorant in the rime (vowels and following consonants in a syllable). Hence, the four tones in Mizo can surface in monosyllabic, disyllabic and trisyllabic words as shown in Table 1.

Table 1. Tone distribution in Mizo syllables as in [7]

Syllable Types	Distributions								
Monosyllable	H	F	L	R					
Disyllable	HH	HL	HR	FL	LL	LH	LR	LF	RR
Trisyllable	LLL	LHH							

This work adds to the previous research on Mizo in various ways. First, this study provides the first acoustic analysis of the vowels in Mizo. Second, it provides the measures of perceptual difference (D_{ij}) between vowels in Mizo following Lindblom [8]. Third, this study provides an acoustic measure of the tones in words whose tones have been provided by previous researchers. Corresponding to the previous research findings it was confirmed that Mizo has four tones distinct tones namely, L, H, R and F. Fourth, the extent to which a syllable initial consonant affects the pitch of the part that hosts the tone or the tone bearing unit (TBU) in Mizo is examined, and some preliminary results about the differential effect of initial consonants are reported.

2. METHOD

2. 1 Data collection

One female native speaker of Mizo was recorded reading a list of target words in a frame sentence. The speaker was 25 years old, had been born and raised in Aizawl, Mizoram, and spoke Mizo, English, French, and a little Hindi. The speaker reported no developmental or acquired conditions that could lead to impaired speech or hearing. The frame sentence was "ka X ati", which translates to 'I said X' in English; the frame was used to keep the segmental and suprasegmental context consistent.

The word list was constructed by drawing on previous studies and included monomorphemic words representing all four aforementioned tones [4, 7]. For tone analysis 59 words appearing in minimal pairs were recorded. For vowel quality and temporal measurements 49 additional words were recorded resulting in a total of 108 words. To avoid any confusion for the speaker about which word was intended, English glosses were provided, as Mizo orthography contains no representation for tones [5]. The speaker was asked to produce the words four times each, each time embedded in the frame, and the fourth repetition was discarded to avoid list intonation effects. High quality recordings were made using a Sony TCD-D8 DAT recorder with a 44.1 KHz sampling ceiling, and a head-mounted Shure SM10A microphone, then digitized into a CSL model 4400. The data was acoustically analyzed using Praat 4.3.09 [9].

3. RESULTS

3.1 Vowels

3.1.1. Vowel quality and duration

The first and the second formant frequencies of vowels are argued to be the primary cue for identification of vowels [10]. Hence, the F1 and F2 for the Mizo vowels produced between two consonants were calculated. The formant frequencies were measured at the mid point of the vowels, following the methodology described in Abramson [11]. The F1 and F2 values for the Mizo vowels are presented in Table 2.

Table 2. Average formant frequencies (in Hz) and durations of Mizo vowels

Vowel	Long			Short		
	F1	F2	Duration (ms)	F1	F2	Duration (ms)
a	839	1418	178	781	1548	87
ɛ	617	2313	205	507	2218	99
⊃	779	1956	213	621	1416	96
i	NA	NA	NA	402	2490	85
u	548	1407	186	486	1208	82

As noticed from Table 2, the five vowels in Mizo are considerably distinct from each other at the mid point of the first two formants. In terms of vowel length, it is noticed that the long vowels are at least twice as long as the short vowels.

3.1.2 Perceptual distance

According to Lindblom [8] perceptual distinctiveness between vowels can be numerically expressed by calculating the Euclidean distance between two vowels. Hence, the perceptual spaces among the Mizo vowels were calculated using Eq. (1), where D_{ij} is the Euclidean distance between two vowel points and M1 and M2 are the frequency of F1 and F2 expressed in mels [8]. A higher D_{ij} value confirms that the two vowels i and j are highly distinct, for example in case of English, it has been noted that the average D_{ij} value is about 70.2 mels [12].

Journal of Acoustical Society of India : Vol. 37, No. 3, 2010 (pp. 130-138)

Nonlinear Acoustical Properties of Ternary Alloys

Giridhar Mishra*, S.K. Verma and R.R.Yadav
Physics Department, University of Allahabad, Allahabad-211 002, India
**e-mail: giridharmishra@rediffmail.com*

[Received: 08.04.2010; Revised: 19.05.2010; Accepted: 17.06.2010]

ABSTRACT

Using the interaction potential model we have calculated the higher order elastic constants and with the help of these elastic constants acoustical properties of ternary alloys Ni-Al-Fe and Ni-Al-Co are determined. Also Gruneisen numbers, acoustic coupling constants and acoustical anisotropy are calculated in order to discuss the acoustical properties of the ternary alloys. The temperature dependent ultrasonic wave propagation behavior is correlated with the microstructural phenomena during the wave propagation and thermal behavior of the ternary alloy. It is found that the thermal conductivity of the alloy plays important role in the ultrasonic wave propagation behavior inside the alloy. The results are in qualitative agreement with experimental trend.

1. INTRODUCTION

In the recent years, much basic and applied research has been dedicated to intermetallic alloys. Alloys based on the Ni-Al binary system are one of the most important and employed classes of intermetallic materials. [1-8]. NiAl is well known shape memory alloy having high thermal conductivity [9-13]. Due to the increase in ductility it builds up a starting point for the development of Ni-base super-alloys [14,15]. Due to their good magnetic properties, Fe-Ni-Al alloys have been employed as the basis of the Alnico permanent magnets. Later on, they were improved by major additions of Co and minor additions of Cu, Ti and traces of other elements. By alloying we can improve the interesting properties of NiAl. There are various features of nickel aluminides based ternary alloys [16-24] which make the ternary alloy very useful for various advanced applications such as in making gas turbine and aircraft engines [25,26]. In this paper we have established a theory for the evaluation of second and third order elastic constants (SOEC and TOEC) and ultrasonic attenuation in the $Ni_{50.0}$-$Al_{48.0}$-$Fe_{2.0}$ and $Ni_{50.0}$-$Al_{48.0}$-$Co_{2.0}$. Ternary alloys and we have correlated these nonlinear properties with the thermal conductivity of the alloys at high temperatures and the other microstructural features of the alloys [27-30]. The ultrasonic attenuation, thermal relaxation time, ultrasonic velocity and non linearity parameters are calculated in the temperature range 300-1000K along <100> direction.

2. THEORY FOR THE DETERMINATION OF HIGHER ORDER ELASTIC CONSTANTS AND ULTRASONIC ATTENUATION IN TERNARY ALLOYS

The elastic constant of the n^{th} order is defined as [31]:

$$C_{ijklmn}\ldots = (\partial^n F / \partial\eta_{ij}\partial\eta_{kl}\partial\eta_{mn}\ldots) \tag{1}$$

Here F is the free energy density of undeformed material and η_{ij} is lagrangian strain components tensor. The total free energy density F expanded in terms of strain η, can be written (using Taylor's series expansion) as:

Journal of Acoustical Society of India : Vol. 37, No. 3, 2010 (pp. 139-142)

Consonant Speech Recognition Based on Linear Predictive Coding Parameters and K-NN Algorithm

T.M. Thasleema and N.K. Narayanan
School of Information Science& Technology,
Kannur University, Kerala-670 567
e-mail: thasnitm1@hotmail.com, csirc@rediffmail.com

[Received: 11.12.2009; Revised: 17.04.2010; Accepted: 05.05.2010]

ABSTRACT

In articulatory phonetics, a consonant is a speech sound that is articulated with complete or partial closure of the upper vocal tract, the upper vocal tract being defined as that part of the vocal tract that lies above the larynx. Recognition methods for consonants contrast with vowels. There exists collection of techniques to extract the relevant features from the steady-state regions of the vowels and consonants both in time as well as in frequency domains in literature. However the error rate is highly notorious, that these methods are not reliable for building a practical speech recognition system. Hence the aim of the present work is to build a more promising method for consonant, -consonant vowel recognition. In recent years the technology for automatic speech recognition (ASR) has been progressing. Still needed way is to extract feature which is effective in any kind of environment, even a noise-distorted environment. In this paper we present a novel and accurate feature extraction technique for recognizing Malayalam spoken consonants based on Linear Predictive Coding method and wavelet packet decomposition method. Recognition is performed using k-NN pattern classifier. The classification is conducted for Malayalam consonant sounds (ka, kha, ga, gha, nga etc) using training and test set consisting of 75 (15 from each class) samples each. The overall recognition accuracy obtained for the vowel using LPC feature extraction method is 91%. The proposed method is efficient and computationally less expensive. The experimental results demonstrate the efficiency of the proposed algorithm.

1. INTRODUCTION

Phones are divided into two main classes as consonants and vowels. Both kind of sounds are formed by the motion of air through the mouth, throat or nose. Consonants are made by restricting or blocking the airflow in some way, and may be voiced or unvoiced. Because of this reason consonants can be distinguished by where this restriction is made[1]. The point of maximum restriction is called the place of articulation of a consonant. Consonants are also distinguished by how the restriction in airflow is made, for example whether there is a complete stoppage of air, or only partial blockage, etc. This feature is called manner of articulation of a consonant. The combination of place and manner of articulation is usually sufficient to uniquely identify a consonant. Consonants produce sounds that are more consistent and easier to identify than vowels. Therefore, they make a good starting point for learning to read.

The automatic recognition of speech, enabling a natural and easy to use method of communication between human and machine[2], is an active area of research as it still needed way to extract feature which is effective in any kind of environment, even a noise-distorted environment. In order to achieve high recognition accuracy the feature extractor is required to discover salient characteristics suited for classifications. Speech recognition system generally carries some kind of classification/recognition based upon speech features which are usually obtained via time-frequency representations such as Short Time Fourier Transform (STFT) or linear predictive coding (LPC) techniques [3]. LPC is a tool used mostly in audio signal processing and speech processing for representing the spectral envelope of a digital signal of speech in compressed form. It is one of the most powerful speech analysis techniques, and one of the most useful methods for encoding good quality speech at a low bit rate and provides extremely accurate estimates of speech parameters.

In this paper a linear predictive coding model is used for the recognition of spoken Malayalam consonant sounds. LPC determines the coefficient of a forward linear predictor by minimizing the prediction error in the least square sense. Then, we used k-nearest Neighbor classifier to classify the speech signals into sound classes. Also we compare the result with wavelet packet decomposition parameters.

2. LINEAR PREDICTIVE CODING

Linear prediction is a widely used and well-understood technique for the analysis, modeling, and coding of speech signals [4]. Parametric representation of a spectrum using linear prediction is a powerful technique in speech processing. For speech coding applications, LPC was introduced about 50 years ago [5] and it is still the main and effective tool in that field. In speech applications, the main advantage is usually attributed to the all-pole characteristics of vowel spectra. However, because the human ear is more sensitive to spectral poles than zeros[6], LPC also has advantages in terms of human hearing. In comparison with nonparametric spectral model techniques, LPC is also more powerful in compressing the spectral information into few filter coefficients which can be more efficiently quantized.

The LPC method considers a speech sample at time n, s(n) and approximates it by a linear combination of the past p speech samples in the following way.

$$s(n) \approx a_i s(n-1) + a_2 s(n-2) + ...a_p s(n-p) \quad (1)$$

where the coefficients a_1, a_2,……ap are assumed constant over the speech analysis frame.

The above equation can be transformed, by including an excitation term *Gu(n)*, to:

$$s(n) = \sum_{i=1}^{p} a_i s(n-i) + Gu(n) \quad (2)$$

where u(n) is a normalized excitation and G is the gain of the excitation. By expressing in the z-domain we get the relation

$$S(z) = \sum_{i=1}^{p} a_i z^{-1} S(z) + GU(z) \quad (3)$$

and consequently, the transfer function H(z) becomes

$$H(z) = \frac{S(z)}{GU(z)} = \frac{1}{1 - \sum_{i=1}^{p} a_i z^{-1}} = \frac{1}{Az} \quad (4)$$

This corresponds to the transfer function of a digital time varying filter. The main parameters that can be obtained with the LPC model are the classification voiced/unvoiced, the pitch period, the gain and the coefficients ai. It is important to note that the higher the order of the model is, the better the all pole model can represents spoken sounds.

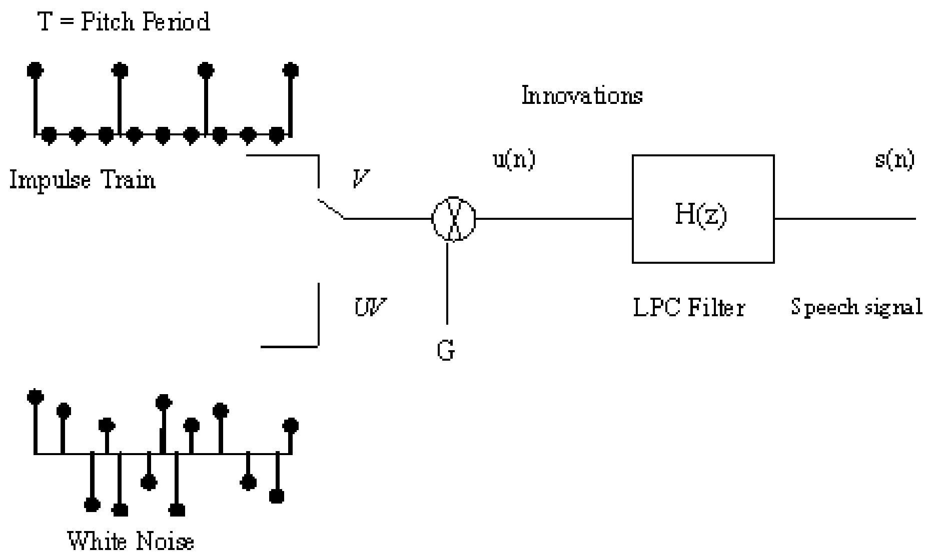

Fig. 1. Speech synthesis model based on LPC model

3. FEATURE EXTRACTION

We used Linear predictive coding method for developing feature vectors for representing a consonant sound. In this method the analysis was performed using 9th order LPC analysis. This contain enough information to represent the given input speech consonant sound without loss of much speech sound features. We used wavelet packet decomposition parameters for comparing the result.

4. CLASSIFICATION USING K-NN CLASSIFIER

Pattern classification [7] by distance functions is one of the earliest concepts in pattern recognition [8, 9]. Here the proximity of an unknown pattern to a class serves as a measure for its classification. A class can be characterized by single or multiple prototype pattern(s). The k-Nearest Neighbor method is a well-known non-parametric classifier, where a posteriori probability is estimated from the frequency of nearest neighbors of the unknown pattern. It considers multiple prototypes while making a decision and uses a piecewise linear discriminant function.

Let us consider the cases of m classes {Ci} where i=1:m and a set of N patterns {yi} where i=1:N whose classification is priory known. Let x denote an arbitrary incoming pattern. The nearest neighbor classification approach classifies x in the pattern class of its nearest neighbors in the set {yi} where i=1: N,

$$\text{i.e. if } \left\| x - y_j \right\| = \min \left\| x - y_j \right\| 1 \leq i \leq N \text{ then } x\, C\, Cj$$

This scheme (can be termed the 1-NN rule since it employs only the classification of the nearest neighbor to x) can be modified by considering the k nearest neighbors to x and using a majority-rule type classifier. The following algorithm summarizes the classification process.

The classification is conducted for 5 Malayalam consonant sounds using training and test set consisting of 75 (15 from each class) samples each. The recognition accuracies obtained for the each sound using the k-NN classifier based on the LPC parameters are tabulated in Table1.

Table 1. Recognition accuracies for 5 Malayalam vowel speech sound using k-NN classifier

S. No.	sounds	Recognition accuracy using LPC
1	ka [ ]	100
2	kha [ ]	100
3	ga [ ]	80
4	gha [ ]	90
5	nga [ ]	85

5. CONCLUSION

This paper presented a new approach to feature extraction of Malayalam spoken consonant sounds based on linear predictive coding for the computer recognition of human speeches. We used LPC coefficients for developing feature vectors for representing a consonant sound. Feature map drawn for consonant sounds shows markable class difference as well as good similarity among sounds of same person. Recognition is performed using k-NN pattern classifier. Compare to the wavelet packet decomposition method for wavelet feature extraction LPC feature extraction method is quite efficient. The overall recognition accuracy obtained for the consonant using wavelet packet decomposition method is 78% while the recognition accuracy obtained by using LPC feature extraction method is 91%. Even if the proposed k-NN classifier gives better recognition accuracy, the computational cost is high compared to other classifiers and to surpass such a problem we can go for faster k-NN methods. Effective implementation of multiple classifier system and other classifier like, ANN and SVM, are some of our future research directions and more research is needed to deal with building a fully functional system.

6. REFERENCES

[1] DANIAL JURAFSKY and JAMES H. MARTIN, 2004. An Introduction to Natural Language Processing, Computational Linguistics, and Speech Recognition', Pearson Education.

[2] L. RABINER and B. JUANG, 1993. Fundamentals of Speech Recognition', Pearson Education, pp 20-30.

[3] JIANG HAI and ER MENG JOO, 2003. Improved Linear Predictive Coding Method for Speech Recognition, I CICS-PCM.

[4] J. MAKHOUL, 1975. Linear prediction: a tutorial review, *Proceedings of the IEEE*, **63(4)**, 561-580.

[5] B. S ATAL and M R SHROEDER, 1967. Predictive Coding of Speech Signals, *Proceedings of IEEE Conf., Communication Processing*, pp. 360-361.

[6] M R SCHROEDER, Linear Prediction, Extremal Entropy and Prior Information in Speech Signal Analysis and Synthesis, *Speech Commun.*, (1), pp. 9-20.

[7] J.T. TOU and R.C. GONZALEZ, 1974. Pattern recognition Principles, Addison Wesley, London.

[8] SANKAR K. PAL and SUSHMITHA MITHRA, 1999. Neuro-fuzzy Pattern Recognition - Methods in soft computing , John Wiley & Sons, Inc.

[9] M. FRIEDMAN and A. KANDEL, 1999. Introduction to Pattern Recognition- Statistical, Structural, Neural and Fuzzy logic approach', World scientific.

Acoustical Society of India
(Regn. No. 65-1971)

Executive Council (2010-12)

Announcement

NSA 2010

Rishikesh . Uttarakhand . November 11-13
www.nsa2010.gpgcrishikesh.com

Important Dates

Important dates for NSA 2010

Call for Abstracts	April 2010
Submission of Abstract Deadline	15 May 2010 Extended to 30th May Late abstract submission till 15 June
Notification of Abstract acceptance	15 July 2010
Submission of Full Papers Deadline	15 September 2010
Registration Deadline	15 September 2010
Program Available	1 November 2010
NSA Symposia	11-13 November 2010

INFORMATION FOR AUTHORS

ARTICLES

The Journal of Acoustical Society of India (JASI) is a refereed publication published quarterly by the Acoustical Society of India (ASI). JASI includes refereed articles, technical notes, letters-to-the-editor, book review and announcements of general interest to readers.

Articles may be theoretical or experimental in nature. But those which combine theoretical and experimental approaches to solve acoustics problems are particularly welcome. Technical notes, letters-to-the-editor and announcements may also be submitted. Articles must not have been published previously in other engineering or scientific journals. Articles in the following are particularly encouraged: applied acoustics, acoustical materials, active noise & vibration control, bioacoustics, communication acoustics including speech, computational acoustics, electro-acoustics and audio engineering, environmental acoustics, musical acoustics, non-linear acoustics, noise, physical acoustics, physiological and psychological acoustics, quieter technologies, room and building acoustics, structural acoustics and vibration, ultrasonics, underwater acoustics.

Authors whose articles are accepted for publication must transfer copyright of their articles to the ASI. This transfer involves publication only and does not in any way alter the author's traditional right regarding his/her articles.

PREPARATION OF MANUSCRIPTS

All manuscripts are refereed by at least two referees and are reviewed by the Publication Committee (all editors) before acceptance. Manuscripts of articles and technical notes should be submitted for review electronically to the Chief Editor by e-mail or by express mail on a disc. JASI maintains a high standard in the reviewing process and only accept papers of high quality. On acceptance, revised articles of all authors should be submitted to the Chief Editor by e-mail or by express mail.

Text of the manuscript should be double-spaced on A4 size paper, subdivided by main headings-typed in upper and lower case flush centre, with one line of space above and below and sub-headings within a section-typed in upper and lower case understood, flush left, followed by a period. Sub-sub headings should be italic. Articles should be written so that readers in different fields of acoustics can understand them easily. Manuscripts are only published if not normally exceeding twenty double-spaced text pages. If figures and illustrations are included then normally they should be restricted to no more than twelve-fifteen.

The first page of manuscripts should include on separate lines, the title of article, the names, of authors, affiliations and mailing addresses of authors in upper and lowers case. Do not include the author's title, position or degrees. Give an adequate post office address including pin or other postal code and the name of the city. An abstract of not more than 200 words should be included with each article. References should be numbered consecutively throughout the article with the number appearing as a superscript at the end of the sentence unless such placement causes ambiguity. The references should be grouped together, double spaced at the end of the article on a separate page. Footnotes are discouraged. Abbreviations and special terms must be defined if used.

EQUATIONS

Mathematical expressions should be typewritten as completely as possible. Equation should be numbered consecutively throughout the body of the article at the right hand margin in parentheses. Use letters and numbers for any equations in an appendix: Appendix A: (A1, (A2), etc. Equation numbers in the running text should be enclosed in parentheses, i.e., Eq. (1), Eqs. (1a) and (2a). Figures should be referred to as Fig. 1, Fig. 2, etc. Reference to table is in full: Table 1, Table 2, etc. Metric units should be used: the preferred from of metric unit is the System International (SI).

REFERENCES

The order and style of information differs slightly between periodical and book references and between published and unpublished references, depending on the available publication entries. A few examples are shown below.

Periodicals:

[1] S.R. Pride and M.W. Haartsen, 1996. Electroseismic wave properties, *J. Acoust. Soc. Am.*, **100** (3), 1301-1315.
[2] S.-H. Kim and I. Lee, 1996. Aeroelastic analysis of a flexible airfoil with free play non-linearity, *J. Sound Vib.*, **193** (4), 823-846.

Books:

[1] E.S. Skudzryk, 1968. *Simple and Comlex Vibratory Systems*, the Pennsylvania State University Press, London.
[2] E.H. Dowell, 1975. *Aeroelasticity of plates and shells*, Nordhoff, Leyden.

Others:

[1] J.N. Yang and A. Akbarpour, 1987. Technical Report NCEER-87-0007, Instantaneous Optimal Control Law For Tall Buildings Under Seismic Excitations.

SUMISSIONS

All materials from authors should be submitted in electronic form to the JASI Chief Editor: Dr Mahavir Singh, Acoustics Section, National Physical Laboratory, Dr. K. S. Krishnan Road, New Delhi-110 012 (email: mahavir@nplindia.org Tel: +91-11-4560.9319, Fax: +91-11-4560.9310). For the item to be published in a given issue of a journal, the manuscript must reach the Chief Editor at least twelve week before the publication date.

SUMISSION OF ACCEPTED MANUSCRIPT

On acceptance, revised articles should be submitted in electronic form to the JASI Chief Editor (mahavir@nplindia.org)

ISSN 0973-3302

JOURNAL OF ACOUSTICAL SOCIETY OF INDIA

Volume 37 Number 4 October 2010

A Quarterly Publication of the JASI

http://www.acousticsindia.org

Journal of Acoustical Society of India

The Refereed Journal of the Acoustical Society of India (JASI)

The Journal of Acoustical Society of India is a refereed journal of the Acoustical Society of India **(ASI)**. The **ASI** is a non-profit national society founded in 31st July, 1971. The primary objective of the society is to advance the science of acoustics by creating an organization that is responsive to the needs of scientists and engineers concerned with acoustics problems all around the world.

Manuscripts of articles, technical notes and letter to the editor should be submitted to the Chief Editor. Copies of articles on specific topics listed above should also be submitted to the respective Associate Scientific Editor. Manuscripts are refereed by at least two referees and are reviewed by Publication Committee (all editors) before acceptance. On acceptance, revised articles with the text and figures scanned as separate files on a diskette should be submitted to the Editor by express mail. Manuscripts of articles must be prepared in strict accordance with the author instructions.

All information concerning subscription, new books, journals, conferences, etc. should be submitted to Chief Editor:

Acoustics Section, National Physical Laboratory, Dr. KS Krishnan Road, New Delhi 110 012,
Tel: +91.11.4560.9319, Fax: +91.11.4560.9310, e-mail: mahavir@nplindia.org

Annual subscription price including mail postage is Rs. 2000/= for institutions, companies and libraries and Rs. 2000/= for individuals who are not **ASI** members. The Journal of Acoustical Society of India will be sent to **ASI** members free of any extra charge. Requests for specimen copies and claims for missing issues as well as address changes should be sent to the Editorial Office:

Acoustics Section, National Physical Laboratory, Dr. KS Krishnan Road, New Delhi 110 012,
Tel: +91.11.4560.9319, Fax: +91.11.4560.9310, e-mail: mahavir@nplindia.org

ISSN 0973-330

Printed at Alpha Printers, BG-2/38C, Paschim Vihar, New Delhi-110063 Tel.: 9811848335. JASI is sent to ASI members free of charge.

JASI

Journal of Acoustical Society of India (JASI)

A quarterly publication of the Acoustical Society of India

Volume 37, Number 4, October 2010

EDITORIAL

ARTICLES

INFORMATION

Factors Affecting Speech Pickup in Buildings

To investigate the effects of room acoustics and noise on the performance of devices used for speech pickup, validate existing procedures for rating them, and make recommendations to improve their performance.

Examples of several devices commonly used for speech pickup in rooms (from top): hands-free conference phone, public-address microphone, computer microphone, clip-on lavaliere microphone

The performance of devices used for speech pickup (such as omni- or uni-directional microphones, and groups thereof) under real operating conditions in buildings may vary from expectations based on their laboratory ratings, due to such factors as noise, reverberation and mounting location. Research is needed to understand and help compensate for these effects.

- Performed measurements and recorded test speech material for each device in various physical conditions representing realistic combinations of speech signal levels, noise types and levels, and reverberation levels.
- Conducted listening tests by playing the test speech recordings for volunteers, who rated them on intelligibility and other subjective qualities of the signals.

A project report, which includes:

- Conclusions concerning the effects of noise, reverberation and mounting location on performance of the devices. The detrimental influence of noise and reverberation on speech intelligibility was quantified (using real fluctuating noise), and some mounting strategies that mitigate these degradations were indicated.
- Improved understanding of the relevance and applicability of laboratory ratings of devices for performance in real built environments.
- Results indicating how secondary properties such as quality and naturalness of sound influence the usefulness of the devices
- Discussion of the advantages of directional microphones and stereo pairs over omni-directional or monophonic microphones, particularly in rooms with significant reverberation.

Mahavir Singh

Acoustical Society of India
(Regn. No. 65-1971)

Executive Council (2010-12)

Factors Affecting Speech Pickup in Buildings

To investigate the effects of room acoustics and noise on the performance of devices used for speech pickup, validate existing procedures for rating them, and make recommendations to improve their performance.

Examples of several devices commonly used for speech pickup in rooms (from top): hands-free conference phone, public-address microphone, computer microphone, clip-on lavaliere microphone

The performance of devices used for speech pickup (such as omni- or uni-directional microphones, and groups thereof) under real operating conditions in buildings may vary from expectations based on their laboratory ratings, due to such factors as noise, reverberation and mounting location. Research is needed to understand and help compensate for these effects.

- Performed measurements and recorded test speech material for each device in various physical conditions representing realistic combinations of speech signal levels, noise types and levels, and reverberation levels.
- Conducted listening tests by playing the test speech recordings for volunteers, who rated them on intelligibility and other subjective qualities of the signals.

A project report, which includes:

- Conclusions concerning the effects of noise, reverberation and mounting location on performance of the devices. The detrimental influence of noise and reverberation on speech intelligibility was quantified (using real fluctuating noise), and some mounting strategies that mitigate these degradations were indicated.
- Improved understanding of the relevance and applicability of laboratory ratings of devices for performance in real built environments.
- Results indicating how secondary properties such as quality and naturalness of sound influence the usefulness of the devices
- Discussion of the advantages of directional microphones and stereo pairs over omni-directional or monophonic microphones, particularly in rooms with significant reverberation.

Mahavir Singh

Journal of Acoustical Society of India : Vol. 37, No. 4, 2010 (pp. 147-152)

Characterization of Sound Absorbing Materials for Noise Control

Paresh Shravage*, S.K.Jain, N.V. Karanth and S. Raju
NVH Lab, Automotive Research Association of India, Pune-411038
**e-mail: pareshshravage@gmail.com*

[Received: 05.12.2009; Revised: 30.06.2010; Accepted: 27.08.2010]

ABSTRACT

In recent years, sound absorbing materials are finding many applications in noise control abatement schemes. Sound absorbing materials are also used to improve the acoustics in indoor and outdoor situations. Poroelastic materials consist of continuous solid elastic material interconnecting pores generally referred as frame with interstitial fluid (i.e. air) inside them. Most porous material theoretical models are formulated in terms of macroscopically measurable physical properties of the frame and the fluid. Porous material characterization starts with classification of poroelastic materials according to their nature, then measurement of macroscopic physical parameters like porosity, flow resistivity, pore tortuosity, viscous length and thermal length as well as mechanical parameters like Young's Modulus, Poisson ratio and loss factor that determine the acoustical performance of the materials. The acoustical performance of the porous materials can be predicted with available porous models using these physical parameters. The paper presents a detailed review of characterization methods for sound absorbing materials. It also presents a discussion on advanced methods like inverse characterization methods used for getting physical parameters.

1. INTRODUCTION

Poro-elastic materials are formed from a continuous solid elastic material with open spaces or pores. The pores are saturated with a fluid. The most well known examples are probably sound absorbing foams. Sound absorbing foams are very soft materials that are characterized with a very high porosity. Viscous and thermal interactions between fluid and frame occur due to the acoustic wave propagation through the porous material. These interactions are the basis of the sound absorbing properties of the porous material. Most porous material theoretical models are formulated in terms of macroscopically measurable physical properties of the frame and the fluid (which may themselves be considered as separate components). The advantage of such an approach is that it enables the investigation of the influence of the various directly measurable physical properties of the porous material, so that a particular set of physical parameters can be identified that will result in a porous material having a specified performance. It should be noted, of course, that there is a direct link between the microscopic structure of a porous material and its macroscopic properties. To-date, however, there is little information linking the microscopic properties of a porous material to its macroscopic properties. The most important macroscopic physical properties of a porous material are: flow resistivity, porosity, pore tortuosity (these first three together constituting the fluid-acoustical properties), bulk density, in vacuo bulk density, shear modulus and loss factor (the latter four properties being the elastic properties of a porous material).

2. JOHNSON-CHAMPOUX-ALLARD MODEL

Open cell Poroelastic materials are very well described by Biot theory [1]. At the same time, in many situations when a material sample is excited by acoustical waves, the frame of this material behaves approximately as acoustically rigid (motionless) over a wide range of frequencies. In this case, the porous material can be replaced on a macroscopic scale by an equivalent fluid of effective density $\rho(\omega)$ and effective bulk modulus $K(\omega)$. The motionless frame condition can occur either because of high density or elasticity modulus, or because of particular boundary conditions imposed during the test. The dynamic density $\rho(\omega)$ and complex compressibility $K(\omega)$ for Johnson Model [2] are given by following equations.

$$\rho(\omega) = \rho_0 \alpha_\infty \left[1 + \frac{\sigma\phi}{j\omega\rho_0\alpha_\infty} \sqrt{\frac{4j\alpha_\infty^2 \eta\omega}{\sigma^2\Lambda^2\phi^2}} \right] \tag{1}$$

$$K(\omega) = \gamma p_0 \left[\gamma - (\gamma - 1) / 1 + \frac{8\eta}{j\Lambda' N_{pr}\omega\rho_0} \sqrt{1 + j\rho_0 \frac{\omega N_{pr}\Lambda'}{16\eta}} \right]^{-1}$$

where ρ_0 is density of fluid, ρ_0 is atmospheric pressure, γ is specific heat ratio N_{pr} is Prandtl number, η is coefficient of viscosity of air and is circular frequency. For a porous sample of thickness , backed by rigid wall specific acoustic surface impedance is given as

$$Z_s = -j \frac{Z_c}{\rho_0 . c_0} cot(kcd) / \phi \tag{3}$$

where Z_c and k_c are the characteristic impedance and the complex wave number of the porous specimen respectively. They are related to the effective properties of the porous medium by Eq. (4) and Eq. (5).

$$Z_c = (\rho(\omega) K(\omega))^{1/2} \tag{4}$$

and

$$k_c = j\omega . [\rho(\omega) / K(\omega)]^{1/2} \tag{5}$$

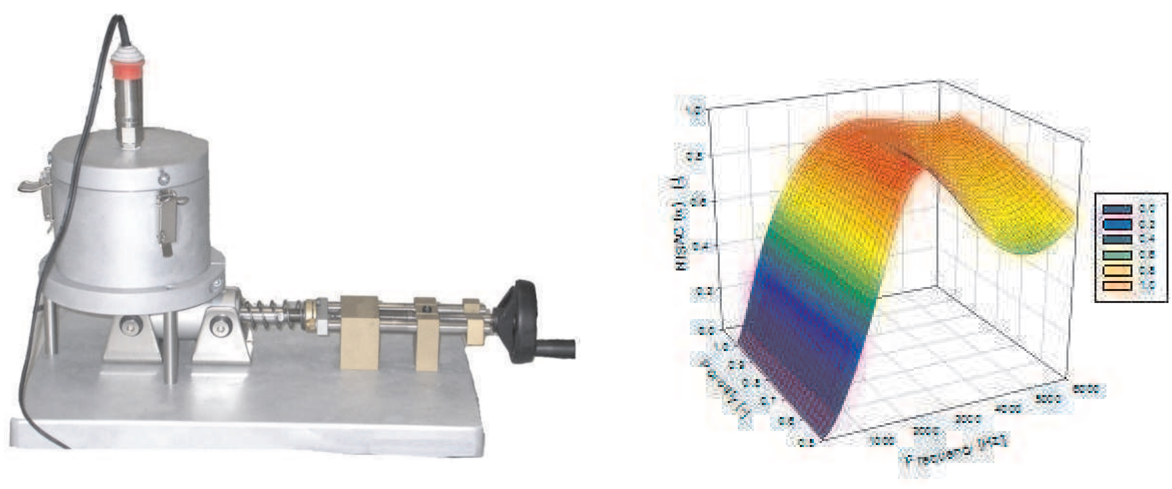

Fig. 1. Test rig for porosity measurement (ENDIF, Italy) and Effect of porosity on Sound Absorption

2.1 Porosity

It is the ratio of the fluid volume within the porous material to the total volume of material, on a unit-volume basis. Since the porosity quantifies the relative volume occupied is a key parameter in theories of sound propagation in porous materials [3, 4]. However, the porosity of typical acoustic materials such as foams and glass fibers is normally very high, i.e., greater than 0.90, and often greater than 0.98. Since the porosity is so large in most noise control materials, and because the variations in porosity tend to fall into a very narrow range, variations in porosity tend not to be very important when distinguishing between noise control materials. However, it should be remembered that much of the relative motion of the solid frame and the interstitial fluid, and that for this process to work, there must be continuous paths through the material. The most direct way of determining the porosity of a porous material is to measure the volume of air contained within the material. This method may be achieved using the apparatus developed by Champoux [5] shown in the figure 1. When the temperature of a rigid chamber containing a test sample is held very constant, a measurement of the change in air pressure that accompanies a known change in volume allows the volume of fluid within the sample to be determined if the change in air pressure accompanying the same volume change in a rigid, empty chamber of the same total volume is known. The figure below shows a porosity rig and effect of porosity on sound absorption coefficient.

2.2 Flow Resistivity

The specific flow resistance of any layer of porous material is defined as the ratio of the air pressure differential measured between the two sides of the layer to the steady state air velocity through and perpendicular to the two faces of the layer [6]. The flow resistivity is then the specific flow resistance per unit material thickness with SI units of MKS rayls/m. The flow resistivities of useful noise control materials vary widely, but typically fall in the range 103 rayls/m to 107 rayls/m.

The flow resistivity depends on the porosity of a material as well as its tortuosity, but for high porosity, low tortuosity fibrous materials, the flow resistivity is approximately inversely proportional to fiber radius squared at a constant bulk density: i.e., a large number of small fiber diameters results in a higher flow resistance than does a small number of larger fibers. At microscopic level, the flow resistance results from the formation of a viscous boundary layer as fluid flows over each fiber, and the amount of shearing in that boundary layer increases as the fiber radius decreases. The flow resistivity is thus usually taken to be a measure of the viscous coupling between the fluid and solid phases of the porous material, and so is a measure of the potential for viscous dissipation of sound. [7]

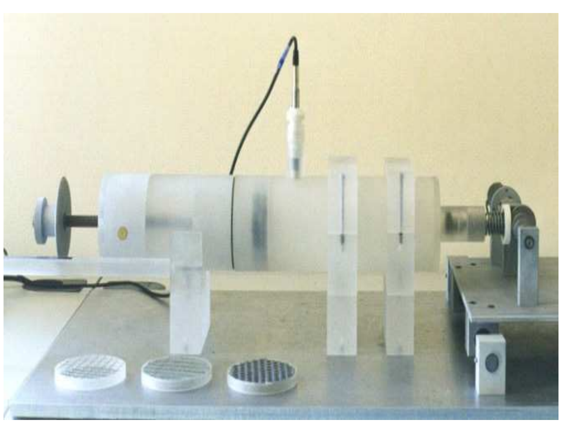

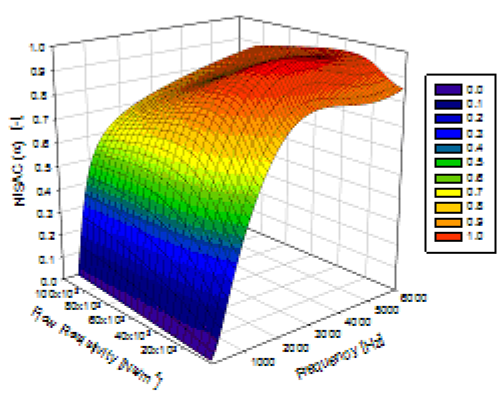

Fig. 2. Test rig for Flow resistivity measurement (ENDIF, Italy) and Effect of flow resistivity on Sound Absorption

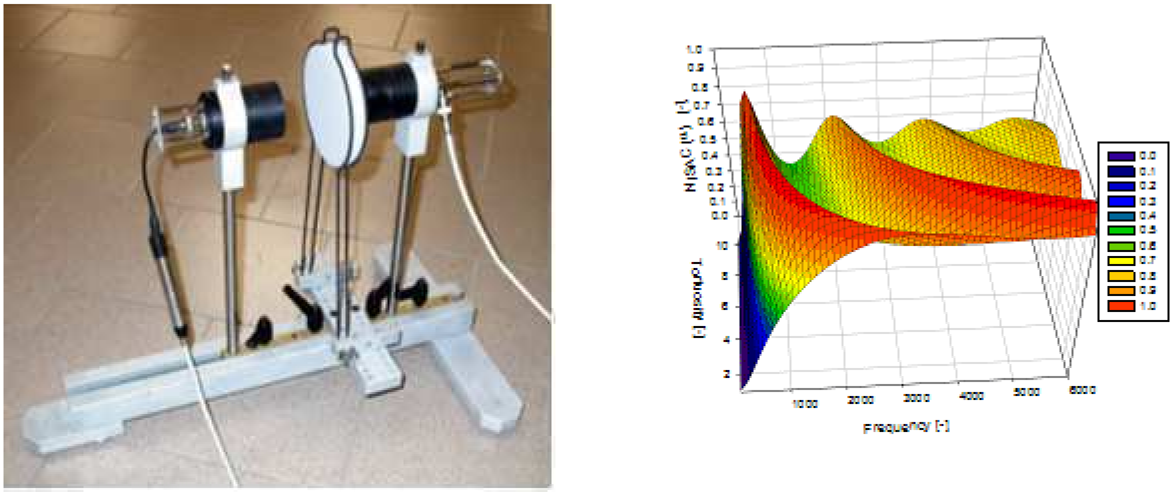

Fig. 3. Test rig for Tortuosity measurement (ENDIF, Italy) and Effect of tortuosity on Sound Absorption

2.3 Pore tortuosity

It is sometimes referred as structure factor and defined as defined as the ratio of actual path length through the material to the linear path length. It is a measure of deviation between the actual fluid flow path through the material and straight- line flow through the material. It results from inertial coupling between solid and fluid phases. The range of tortuosity is from 1 (low density fibrous material) to values of 10 (partially reticulated foams with any closed cells). Champoux and Stinson have developed an electrical conductivity technique to measure pore tortuosity. The voltage difference arising from passing a high voltage through a fluid-saturated (electrically conductive) sample is measured. With knowledge of the electrical transmitted waves. This method is based on measurement of reflected wave by the first interface of a slab of rigid porous material. This method is obtained from a temporal conductivity of fluid and fluid filled samples, a simple relation may be established to calculate the tortuosity when porosity is known. This method can not be used when material frame is conducting [8]. Recently Ultrasonic reflectivity method is proposed for measuring tortuosity of porous materials having a rigid frame. Tortuosity is a geometrical parameter which intervenes in the description of the inertial effects between the fluid filled the porous material and its structure at high frequency range. It is generally easy to evaluate the tortuosity from model of the direct and inverse scattering problems for the propagation of transient ultrasonic waves in a homogeneous isotropic slab of porous material having a rigid frame [9].

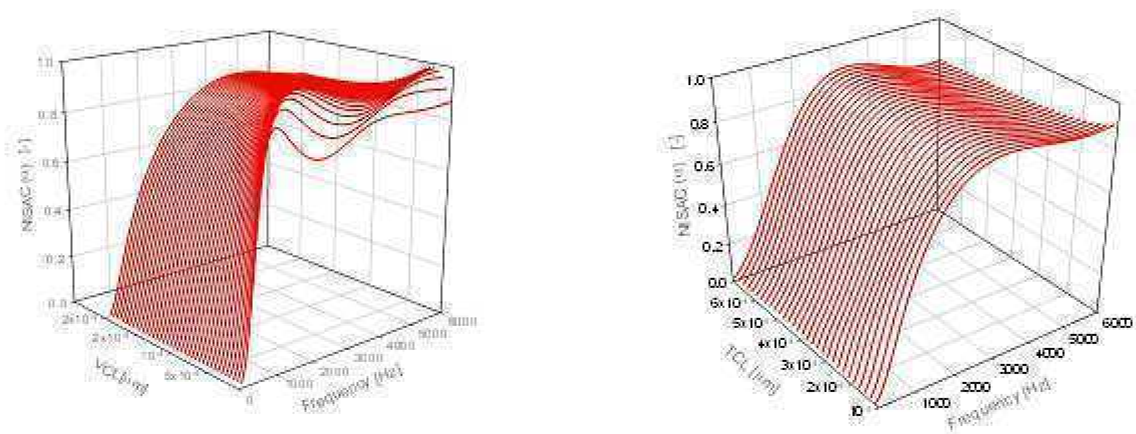

Fig. 4. Effect of characteristic lengths on Sound Absorption

2.4 Characteristic Lengths

The concept of viscous characteristic length is used to describe the acoustical behavior of fluid-saturated porous media in the high-frequency regime. A method to determine this parameter consists of measuring the wave attenuation in the high-frequency limit. This method has already been used for porous materials saturated by super fluid He. It is tested in the case of air-filled absorbent materials in a frequency range of 50-600 kHz. The thermal characteristic length is assumed to be known or measured independently [10]. Recently inverse characterization is becoming popular for predicting physical parameters using optimization techniques. In this paper characteristic lengths are predicted using genetic algorithm optimization. The effect of characteristics lengths on sound absorption is shown in Fig. 4.

3. RESULTS AND DISCUSSION

Porous materials of different typologies are tested and physical parameters are measured using specialized test rigs as discussed above. The physical parameters depicted in table 1. These measured parameters are fed to JCA model and sound absorption coefficient is simulated with compared with measured sound absorption coefficient using two microphone impedance tube.

Table 1. Physical Parameters

	Physical Parameters PET Felt 25 mm 24 Kg/m^3	Polyurethane foam-B 25 mm 40 Kg/m^3
Porosity	0.98	0.986
Flow Resistivity	6634	23367
Tortuosity	1.06	1.7
VCL	147	43
TCL	203	258

The comparison is shown in Fig. 5 for PET felt and in figure 6 for Polyurethane foam-B. From these figures it is clear that there is good correlation between measured sound absorption coefficient and simulated sound absorption using physical parameters of porous materials.

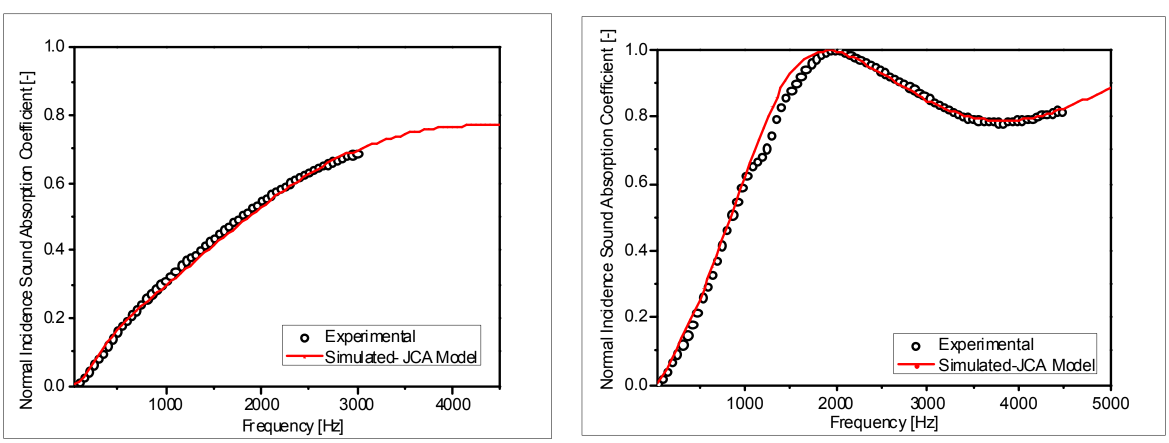

Fig. 5. Comparison of Sound Absorption coefficients with predicted sound absorption (5a): PET felt, (5b): Polyurethane foam

4. CONCLUSIONS

This paper presents a discussion on speclized test rigs for the measurement of physical geometrical parameters of porous materials. It also gives a comparison of measured sound absorption coefficient and simulated sound absorption coefficient using experimentally measured physical parameters of porous materials.

5. ACKNOWLEDGEMENT

The authors are also thankful to ENDIF, Italy for providing required test rig facility for the measurement of physical parameters.

6. REFERENCES

[1]. M.A. BIOT, 1956. Theory of propagation of elastic waves in a fluid saturated porous solid, I Low frequency range, II. High frequency range, *J. of Acoust. Soc. of Am.*, **28**,168-191.

[2]. J. F. ALLARD and Y. CHAMPOUX, 1992. New empirical equations for sound propagation in rigid frame fibrous materials, *J. of Acoust. Soc. of Am.*, **91(6)**, 3346-3353.

[3]. R. PANNETON and X. ONLY, 2006. Acoustical determination of the parameters governing viscous dissipation in porous media, *J. of Acoust. Soc. of Am.*, **119(4)**, pp. 2027-2040.

[4]. R.A. SCOT, 1946. The absorption of sound in a homogeneous porous medium, *Proceedings of Physical* Society, **58**, 165-183.

[5]. Y. CHAMPOUX, M.R. STINSON and G.A. DAIGLE, 1991, Air-based system for the measurement of porosity, *J. of Acoust. Soc. of Am.*, **89**, 910-916.

[6]. R.L. BOLT and R. BROWN, 1942. The measurement of flow resistance of porous acoustic materials, *J. of Acoust. Soc. of Am.*, **13(4)**, 337-342.

[7]. MICHAEL R. STINSON and GILLES A. DAIGLE, Electronic system for the measurement of flow resistance, *J. of Acoust. Soc. of Am.*, **83**, 2422-2428.

[8]. Y. CHAMPOUX, MICHAEL R. STINSON and GILLES A. DAIGLE, 1992. Acoustical models for sound propagation in rigid frame porous materials and influence of shape factors, *J. of Acoust. Soc. of Am.*, **92**, 1120-1131.

[9]. J.F. ALLARD, B. CASTAGNÈDE, M. HENRY and W. LAURIKS, 1994. Evaluation of the tortuosity in acoustic porous materials saturated by air, *Review of Scientific Instruments*, **65**, 7654-755.

[10] P. LECLAIRE, L. KELDERS, W. LAURIKS, M. MELON , N. Brown and B. CASTAGNÈDE, 1996. Determination of the viscous and thermal characteristic lengths of plastic foams by ultrasonic measurements in helium and air, *Journal of Applied Physics*, **80,** 2009-2012.

Journal of Acoustical Society of India : Vol. 37, No. 4, 2010 (pp. 153-160)

Design of a Single Cell of Captive Micro-Machined Ultrasonic Transducer (CMUT)

Aravind Kumar Pathak
DPD, Project MRSAM, RCI

[Received: 10.02.2010; Revised: 25.05.2010; Accepted: 27.07.2010]

ABSTRACT

Ultrasound plays a very important role as diagnostic tool in Human life as well as industrial characterisation. But the requirements of late have proven the limitations of the piezo transducers. This paper presents an attempt to design a Capacitive Micro-Machined Ultrasonic Transducer (CMUT), which can extend the uses of ultrasonic. The single cell of the CMUT has been designed considering electromechanical relaxation and pull-in effects. The driving mechanism for the transducer has been ascertained and then the dynamic response of the CMUT has been arrived at using MEMS modeling and analysis tool, Intellisuite. In the end the pressure generated by the transducer has been calculated using Rayleigh integral method.

1. INTRODUCTION

Currently, a vast majority of ultrasonic transducers are fabricated using piezo-electric crystals, ceramics, polymers and recently, piezo-composite materials [1]. But the requirement of a coupling media due to impedance mismatch of transducer and intermediate media has greatly restricted the use of conventional ultrasonic applications. For example, in air the generation of ultrasound by piezoelectric transducers is a challenge because the acoustic impedance of air (400 kg/m^2s), many orders of magnitude lower than the acoustic impedance of piezoelectric materials ($3\times 10^7 kg/m^2s$). This results in a very poor acoustic transmissibility in air. To improve the transmission efficiency, a matching layer, having the impedance value intermediate to the impedance of transducer and the impedance of the object of the consideration, is usually placed in between them. In many cases, when the impedance mismatch is very high such as air and metals, it is difficult to select an efficient matching layer material. In addition to impedance mismatch, the frequency range of operation for piezo-transducer is decided by geometry, size and required frequency of operation [2] that results in difficulty in getting a solution satisfying all the three requirements. Also the piezo-transducers are limited by very low strain levels limiting its effectiveness for certain applications in low frequency range. The more widely available piezoelectric ceramics gets depole, i.e. lose their piezoelectric properties, at relatively lower temperature (approximately 80 ºC), which prevents them from being used in high temperature environments.

Capacitive Micro-machined Ultrasonic Transducer (CMUT) may be an answer in future to overcome the problems encountered in piezo-transducers. Although the idea of using capacitive ultrasonic transducer is very old, the major reason for its unpopularity was the requirement of very high electric field at macro-scale, of the order of a million volt per centimeter to generate an electrostatic force as large as $1 kg/cm^2$[3]. But the recent advances in microfabrication technology, resulting from microelectronics and MEMS revolution, have made it possible to fabricate the transducer at micro scale and thus utilizing the advantage of scaling towards the electrostatic forces. For example, if we shall like to produce an electrostatic force of the order of $1 kg/cm^2$, we can compare the requirement of voltage at macro and micro scale. The electrostatic force [4] between two plates is given as

$$F = \frac{\in_0 AV^2}{2d^2}$$

Where

F - electrostatic force between the plates

$\in_0$ - permittivity

A - overlapping area of the plate

V - voltage applied

d - distance between two plates

If we keep the gap between the plates at 1mm, the voltage required to produce the force F of 1kg/cm^2 is 475383 V, but if we reduce the gap between the plates to 1µm, the required voltage is only 47 V. Also a CMUT obviates the requirement of any matching layer as it is able to produces ultrasonic waves in air efficiently. The miniaturization achieved through it and its fabrication as an array at much lower cost reflects the potential of this exciting technology [5]. The horizon of ultrasound sensors broadens with requirements like contactless operation for object detection, which paves the way towards various types of automations and surveillance activities.

The last decade has seen the evolution of a lot of activities towards micro-devices development based on semiconductor technology [7]. It has also given an impetus to technology development for capacitive micro-machined ultrasonic transducers. The development of CMUT has greatly benefitted from the development in technology for microphone and experience of development of capacitive transducers [8].

The first work reported on electrostatic ultrasonic transducer dates back to 1937 when Sell reported about his device with air between a membrane and a metal plate. In 1954, Khul et al [8] reported their detailed experiment on a capacitive transducer for airborne ultrasonics in which they used back plate with concentric grooves, which was similar to the principle of condenser microphone. In 1958, Matzuwa [9] reported another success with capacitive ultrasonic transducer. In 1979, Cantrell and Heyman [10] reported ?rst immersion version of CMUT application. In 1989,Suzuki, Higuchi and Tanigawa [11] reported development of micro-machined silicon array transducer in which they utilized back plate etched with pyramid shaped holes and studied the frequency response of the transducer.The 90's saw a rapid development in various aspects of CMUT. The detailed modeling of a CMUT was reported by Ladabaum et al. [2], in which they tried to develop an electro-acoustic model of the device, but they tried to consider the movement of the plate as a parallel plate capacitor. Ge [12] presented an improved model for CMUT by considering the diaphragm bending. Caronti et al [13] presented a more re?ned model in 2002, in which they tried to characterize quantitatively the e?ect of trapped air in the cavity resulting in the coupling between the modes of diaphragm and the air. All these models try to give a closed form solution by approximating the shape of the transducer to be circular. A detailed investigation of the radiated ?eld of a CMUT considering it as a rectangular planar piston has been reported by Hutchins et al [14] in 2003. Ladabaum et al. [15] have reported the micro-fabrication procedure adopted for their CMUT model. They have used surface micro-machining as the process and silicon nitride as the diaphragm material. They reported a dynamic range of 110 dB for the device operating in air at 2.3 MHz. X. jin et al [16] reported various improvements in fabrication methodology for optimizing the transducer performance which include membrane formation, vaccum sealing and electrode metallization. In 2003, Khuri-Yakub [17] reported fabrication of CMUT using wafer bonding technology. They reported an improvement in control over the gap height and the mechanical properties of the membrane.

Journal of Acoustical Society of India : Vol. 37, No. 4, 2010 (pp. 161-168)

Evaluation of Thermo Acoustical Parameters of Some Binary Mixtures from Volume Expansivity Data

M.M. Armstrong Arasu and I. Johnson*
Centre for Nano Science and Applied Thermodynamics
Department of Physics, St. Joseph's College, Trichy - 620 002, India
**e-mail: jnaadarsh@hotmail.com*

[Received: 13.04.2010; Revised: 21.06.2010; Accepted: 24.08.2010]

ABSTRACT

Researches have previously shown that the contribution of internal pressure and the temperature coefficient of volume to the sound velocity in the condensed phase is significant and that volume expansivity is the controlling factor for satisfactory description of the various parameter which describe the thermo-acoustic properties of polycrystalline solid ,metal, alkali halide salt, polyatomic ionic liquid and organic liquid mixtures. Such a description employs only volume expansivity data. From the volume expansivity data the isothermal , isobaric and isochoric acoustical parameters, Moelwyn-Hughes parameter, fractional free volume ,Huggin's parameter, sharma's parameters and repulsive exponent in Mie's potential have been evaluated in the mixtures of Ethyl acetate + 2 Butanone, Ethyl acetate +Hexane and Butyl acetate + Distilled water at 308.15K entire range of mole fraction.

1. INTRODUCTION

The volume expansively data is highly useful for evaluating Gruneisen parameter which is a useful quantity in studying the internal structure , molecular order and thermo acoustical properties of liquids and polymers. The important of volume expansively in evaluating various thermo acoustical properties has been amply demonstrated earlier. In this paper an attempt is made to analyze the relationship between different parameters that are used for system description like Moelwyn-Hughes parameter, fractional free volume, Huggin's parameter, sharma's parameters and repulsive exponent in Mie's potential have been evaluated in the mixtures of Ethyl acetate + 2 Butanone, Ethyl acetate +Hexane and Butyl acetate + Distilled water at 308.15K. It is interesting to note that all these thermo acoustical properties are liked to a single experimentally determinable quantity, volume expansivity.

2. EXPERIMENTAL

The binary were prepared by mass, by mixing the calculated volumes of liquid components in airtight glass bottles. In all the measurements, INSREF thermostat with a constant digital temperature display accurate to ±0.01K was used. For all the mixtures and pure solvent triplicate measurements were performed and the average of all values were considered in the calculation. The mass measurements (±0.0001g) were made using an electronic balance. The accuracy of density measurements was 0.0001g.cm-3. A set of 11 compositions was prepared for ternary mixtures and their physical properties were measured. Viscosity is measured by calibrated Ostwald's Viscometer. The speed of sound was determined using a constant frequency (2MHz) ultrasonic interferometer with an accuracy of ± 2 $m.s^{-1}$.

3. THEORY

The volume expansivity is given by

α = (1/V) dv/dT =1/ρ(dρ/δT) (1)

Let α, V and β respectively Volume expansivity, molar volume, and isothermal compressibility. If β ~ and V~ are the characteristic compressibility and volume (at absolute zero temperature and zero pressure), the their reduced values are given by ,

β=β/β=V ~c1 (2)

Where, the Moelwyn-Hughes parameter is

C1= dlnβ/dlnV (3)

The Sharma's parameters are expressed as ,

S_0 =((1+2αT)/ V ~c1)(3+4 αT) (4)

S = (1+ (4/3)αT (5)

S_0* =(1+2αT)/(1+ (4/3) αT) (6)

Huggin's parametr F is given in terms of Sharma's parameters given above as,

F = 2-S*+ So(So*-1)/αT (7)

Eqns.(1)-(2) demonstrate the importance of a in the evaluation of the parameters V,C1, S, S0,S0* and F, since all the parameters involved therein may be determined from the knowledge of a alone.

The volume dependence of sound speed in liquids at constant pressure and at constant temperature is represented isobaric and isothermal by acoustical parameters k and k' respectively, due to Rao, Carnevale and Litovitz. While examining the relationship between sound velocity u and density in liquids and determining the difference between k and k' in liquids, Aziz and Sharma have shown that the isochoric acoustical parameter k'' is given by.

k' = k=k''

In which

k' =k +k'' (8)

k= (dln u dlnV)P = 1/α (dln u dlnV) P (9)

k' = (dln u dlnV)T=1/ (dln u dlnV) T (10)

k''=1/α(dlnu dlnV)P-1/ (dlnu dlnV)T (11)

Using these calculated values of k and k'', the isothermal acoustical parameter k' can then be calculated for the binary liquid mixtures, using eqn(8).

The sound speed can be expressed as u2 =α/ s , where = Cp/Cv ,Cp and Cv are respectively the isobaric and isochoric heat capacity of the liquid.

The fractional free volume f which is a measure of disorder due to the increased obility of molecules in a liquid can be expressed as,

$f = Va/V = (k'+1)-1$ (12)

The repulsive exponent n in the Mie's potential is given by,

$n = 3(2k'-3)$ (13)

The equation (13) can be rearranged to give the dimensionless thermo acoustic parameters A* and B* as,

$A^* = 1 + f/k'$ (14)

$B^* = 1 + f/k$ (15)

The pseudo-Gruneisen parameter used for a structural study of liquids is usually expressed as

$\tau = \alpha V/\beta\ Cv = (y-1)/\alpha T$ (16)

The Gruneisen parameter is an important quantity of current interest because of its usefulness in studying the internal structure, molecular order and other thermo acoustic properties of polymers and liquids . We have a distinct relationship between the microscopic isothermal Gruneisen parameter τ' (as a measure of anharmonicity of the normal mode frequency v of the molecular vibrations), and the conventional thermodynamic Gruneisen parameter '(used for the structural study of liquids). There are two distinct modes are of low frequency and are anharmonic. They are characterized by high values of τ'. The low frequencies of these modes are determined almost entirely by the weak intermolecular forces. The intra molecular optical modes of vibration are of high frequency and are harmonic. They are characterized by low values of τ, and arise from the strong intra molecular forces which are altered little by pulling the molecules apart. The anharmonic (microscopic isothermal) Gruneisen parameter τ' is determined primarily by the intermolecular vibration, while τ is an average over all modes of vibration, including intermolecular and intra molecular vibrations which employ capacities of the liquid. As relatively little is known about the influence of the intermolecular vibration, while r is an average over all modes of vibration, including intermolecular and intra molecular vibrations which employ thermodynamic parameters such as the isochoric Cv and isobaric Cp heat the intermolecular vibrations on the heat capacity Cp in quasi spherical molecular liquids and fluorocarbon fluids, the analysis of the theoretical foundations of the relationship between τ' and t is essential for this class of liquids. The ratio of the Gruneisen parameters (τ/τ') is utilized to measure the intermolecular isobaric heat capacity and the adiabatic bulk modulus due to the molecular vibrations in these liquids.

Much confusion has existed in literature to recognize the difference between r' and t for liquids. It may be clearly pointed out that the concept of t' and t is appropriate to all the solids, molten metals, liquids, liquefied gases and polymets which show anharmonicity of molecular vibrations. However, Swamy overlooked the basic conceptual aspect that t and t' may not have the same values for different substances. It was shown that t' and t in case of organic liquids differ from one another. For organic molecules, experimentally it is observed that τ'>τ which implies that a certain fraction of the molecules in a molecular liquid has a finite and common fractional frequency dependence on the volume at a constant temperature and the remaining modes are unaffected by volume changes. Following Hart-mann, this fact can be explained by noting that not all the normal mode contributions to heat capacity Cp also contribute to the volume change of the sound speed (moleuclar rotation, for example). The analogous situation in the case of polymeric materials has already been noted . In order for to be as large as ', only a fraction Cp' of the total Cp that is taken up by the molecular vibrations which interact with volume, should be used in eqn.(12).

Thus $\tau' = u^2\alpha/Cp'$ (17)

From eqns. (16) and (17) it follows that

$X^{-1} = \tau/\tau' = Cp'/Cp$ (18)

Eqn(18) shows that the quantity X = τ/τ' is of some interest since it gives a simple method to measure the ration Cp/Cp for a complex liquid and hence Cp which refers to that part of the isobaric heat capacity taken up by molecular vibrations which interact with volume.

The B/A is a particular combination of the temperature and pressure derivation of the sound of speed is a given by

$$B/A = (B/A)' + (B/A)'' \quad (19)$$

where $(B/A)' = y(Cp-1)$ (20)

$$(B/A)'' = -(y-1)\ (\delta-1) \quad (21)$$

leads to a way to determine the Beyer's nonlinear parameter theoretically.

4. RESULTS AND DISCUSSION

In the table 1, 2 and3 give the calculated values of , V ~ β~s, C, ,S, So, S*, F, k, k", F, N, A*, B* and k / k' for binary liquid mixtures- Butyl Acetate + water , Ethyl Acetate + 2 Butanone and Ethyl Acetate + Hexane at 308.15 K using only the experimental data of density at three different temperatures.

It may be absorbed from table 1,2 and 3 that C values vary from 6.6 to 15.3 for the liquid mixture studied in agreement with the value of C ,in other non- associated of the liquids . This signifies the non -linear variation of volume expansivity of the liquids with mole fraction.

The value of reduced compressibility βs~ ranges from 3.32 to 14.8 as compared to the range from about 5 to 8 for the molen alkali halides and 4 to 6 for polymers.

The value of So remains fairly constant within the experimental error. The estimated values of So are on the average , lie the range 1.05 to 1.28. The Sharma's parameter So may be termed a molecular constant which varies its constancy for a wide verity of binary mixtures for investigating thermo acoustic and an harmonic properties.

The calculated values of S* are around 1.04 to 1.99 for the binary mixture as compared to 1.5 for polymers .It may be interesting to note that So* is equal to 1.04 to 1.99 similar ranges to that of poly crystalline solids.

The Value of the Huggin's parameter range from about 0.5 to 1.5 which are of the same order as observed for polymers. Crystalline and molten alkali halids, liquid alkali metals and ionic liquids.

The Calculated acoustical parameter k range from 2.9 to 7.1 in the mixtures , the value of the ratio k/k' are close to about unity , for liquid. The value of n is found to 13.4 to 14.9 with different mole fraction, which is the same order as reported by Sockiewies.

The isochoric acoustical parameters k" has the range of 0.72 to 1.2.

The average values of the dimensionless parameters A* and B* for the liquid mixtures examined have the value 1.02to 1.05 respectively in the case of fluorocarbon fluids. This means that on the average the approximate relationship A* = B* = 1.05 for holds for these liquids mixtures as compared to A* =B* =1.05 for fluorocarbon fluids.

Table 4, 5 and 6 gives the calculated values of δ, y, (B/A)' , (B/A)" and (B/A) for all the liquid mixture studied. The calculated values of (B/A) are the range of 7.6 to 10.5 when comparer with the range of 7.14 to 8.71 for some quasispherical molecular liquids observed by Sharma .Generally there is a slight variation in the non - linear parameters for the case of Butyl Acetate + water , Ethyl Acetate + 2 Butanone and Ethyl Acetate + Hexane . The reason is attribute to the presence of h-bond type and dipole -dipole interaction.

Table 1. Nonlinear parameter of Butyl Acetate + water (Temp at 30 °C, 35 °C and 40 °C)
Note: x(1) is Mole fraction of Butyl Acetate

X(1)	1.0	0.9	0.8	0.7	0.6	0.5	0.4	0.3	0.2	0.1	0.0
$a10^{-3}K^{-1}$	1.073	1.642	0.934	1.611	2.046	1.255	1.268	2.366	1.025	0.501	0.332
V ~	1.269	1.375	1.24	1.369	1.438	1.306	1.308	1.483	1.259	1.139	1.095
C	7.797	6.983	8.188	7.008	6.759	7.434	7.412	6.676	7.918	11.01	14.23
β	6.436	9.251	5.849	9.079	11.69	7.263	7.326	13.93	6.23	4.228	3.677
S	1.115	1.093	1.118	1.094	1.067	1.11	1.109	1.043	1.117	1.12	1.117
S	1.44	1.675	1.384	1.662	1.84	1.515	1.521	1.972	1.421	1.206	1.136
S*	1.153	1.201	1.138	1.199	1.228	1.17	1.171	1.246	1.148	1.085	1.06
F	1.075	0.76	1.154	0.776	0.546	0.972	0.965	0.38	1.102	1.413	1.518
K	3.399	2.991	3.594	3.004	2.88	3.217	3.206	2.838	3.459	5.005	6.617
K^{-}	0.609	0.785	0.532	0.778	0.846	0.684	0.688	0.879	0.585	0.52	0.595
K*	4.008	3.776	4.126	3.783	3.726	3.901	3.895	3.717	4.044	5.009	6.017
f	0.199	0.209	0.195	0.209	0.211	0.204	0.204	0.211	0.198	0.166	0.142
N	15.05	13.66	15.76	13.7	13.36	14.4	14.37	13.3	15.26	21.02	27.1
A*	1.049	1.055	1.047	1.055	1.056	1.052	1.052	1.057	1.049	1.033	1.023
B*	1.057	1.069	1.054	1.069	1.073	1.063	1.063	1.074	1.057	1.033	1.021
K/K′	0.847	0.792	0.871	0.794	0.772	0.824	0.823	0.763	0.855	1.000	1.099

Table 2 . Nonlinear parameter of Ethyl Acetate + 2 butanone (Temp at 30 °C,35 °C and 40 °C)
Note: x(1) is Mole fraction of Ethyl Acetate

X(1)	1.0	0.9	0.8	0.7	0.6	0.5	0.4	0.3	0.2	0.1	0.0
$a10^{-3}K^{-1}$	2.064	1.257	0.942	9.084	0.641	0.932	1.133	0.62	0.429	0.296	1.246
V ~	1.441	1.306	1.242	1.235	1.174	1.24	1.281	1.169	1.125	1.086	1.303
C	6.753	7.43	8.164	8.278	9.658	8.196	7.661	9.817	12.05	15.38	7.449
β~	11.81	7.273	5.879	5.741	4.716	5.84	6.703	4.642	3.989	3.567	7.22
S	1.066	1.11	1.118	1.119	1.121	1.118	1.114	1.121	1.119	1.116	1.11
So	1.848	1.516	1.387	1.373	1.263	1.383	1.465	1.254	1.176	1.121	1.512
S*	1.229	1.17	1.139	1.135	1.104	1.138	1.158	1.101	1.075	1.054	1.169
F	0.536	0.971	1.15	1.170	1.328	1.156	1.041	1.340	1.457	1.541	0.977
K	2.876	3.215	3.582	3.639	4.329	3.598	3.330	4.408	5.529	7.194	3.224
K^{-}	0.848	0.685	0.537	0.514	0.251	0.53	0.637	0.221	0.196	-0.81	0.681
K*	3.725	3.900	4.119	4.154	4.58	4.129	3.968	4.630	5.332	6.386	3.905
f	0.211	0.204	0.195	0.194	0.179	0.194	0.201	0.177	0.157	0.135	0.203
n	13.35	14.40	15.71	15.92	18.48	15.77	14.80	18.78	22.99	29.29	14.43
A*	1.056	1.052	1.047	1.046	1.039	1.047	1.050	1.038	1.029	1.021	1.052
B*	1.073	1.063	1.054	1.053	1.041	1.054	1.060	1.040	1.028	1.018	1.063
K/K′	0.772	0.824	0.869	0.876	0.945	0.871	0.839	0.952	1.036	1.127	0.825

Table 3. Nonlinear parameter of Ethyl Acetate + Hexane (Temp at 30 °C,35 °C and 40 °C)
Note: x(1) is Mole fraction of Ethyl Acetate

X(1)	1.0	0.9	0.8	0.7	0.6	0.5	0.4	0.3	0.2	0.1	0.0
$a10^{-3}K^{-1}$	2.064	1.317	3.26	4.317	0.216	2.369	2.293	2.439	2.428	1.164	2.224
V ~	1.441	1.317	1.589	1.686	1.063	1.484	1.473	1.493	1.491	1.288	1.464
C	6.753	7.337	6.668	6.858	19.42	6.676	6.69	6.665	6.667	7.597	6.706
β~	11.81	7.562	12.98	13.02	3.324	13.95	13.4	14.49	14.4	6.844	12.9
S	1.066	1.108	0.96	0.845	1.113	1.043	1.049	1.037	1.038	1.113	1.054
So	1.848	1.541	2.339	2.773	1.088	1.973	1.942	2.002	1.997	1.478	1.914
S*	1.229	1.175	1.286	1.319	1.04	1.246	1.242	1.25	1.249	1.161	1.238
F	0.536	0.937	0.005	0.572	1.592	0.379	0.417	0.343	0.348	1.023	0.453
K	2.876	3.168	2.834	2.929	9.21	2.838	2.845	2.832	2.833	3.298	2.853
K^-	0.848	0.704	0.931	0.961	1.553	0.879	0.872	0.885	0.884	0.65	0.866
K*	3.725	3.873	3.766	3.891	7.654	3.717	3.717	3.718	3.717	3.949	3.719
f	0.211	0.205	0.209	0.204	0.115	0.211	0.211	0.211	0.211	0.202	0.211
n	13.35	14.24	13.59	14.34	13.92	13.3	13.3	13.3	13.3	14.69	13.31
A*	1.056	1.052	1.055	1.052	1.015	1.057	1.057	1.057	1.057	1.051	1.056
B*	1.073	1.064	1.074	1.069	1.012	1.074	1.074	1.074	1.074	1.061	1.074
K/K′	0.772	0.818	0.752	0.752	1.203	0.763	0.765	0.761	0.762	0.835	0.767

Table -4: Nonlinear parameter of Butyl Acetate + water (Temp at 30 °C,35 °C and 40 °C)
Note: x(1) is Mole fraction of Butyl Acetate

X(1)	δ	y	τ	(B/A)'	(B/A)"	(B/A)
1.0	7.798	1.692	2.092	11.502	-4.704	6.797
0.9	6.983	1.656	1.297	9.914	-3.930	5.983
0.8	8.188	1.622	2.161	11.665	-4.476	7.188
0.7	7.009	1.589	1.185	9.548	-3.539	6.008
0.6	6.760	1.554	0.879	8.955	-3.195	5.759
0.5	7.434	1.518	1.341	9.772	-3.338	6.434
0.4	7.412	1.484	1.240	9.521	-3.108	6.412
0.3	6.677	1.450	0.618	8.236	-2.559	5.676
0.2	7.915	1.414	1.312	9.788	-2.869	6.918
0.1	11.011	1.380	2.460	13.817	-3.805	10.01
0.0	14.235	1.345	3.368	17.801	-4.566	13.231

Table 5. Nonlinear parameter of Ethyl Acetate +2Butanone(Temp at 30 ºC,35ºC and 40ºC)
Note: x(1) is Mole fraction of Ethyl Acetate

X(1)	δ	y	τ	(B/A)'	(B/A)"	(B/A)
1.0	6.753	1.692	1.0875	9.734	-3.981	5.753
0.9	7.430	1.656	1.6952	10.655	-4.224	6.430
0.8	8.164	1.622	2.1447	11.626	-4.461	7.164
0.7	8.278	1.589	2.1040	11.566	-4.287	7.278
0.6	9.658	1.554	2.8074	13.460	-4.802	8.658
0.5	8.196	1.518	1.8055	10.930	-3.734	7.196
0.4	7.661	1.484	1.3878	9.891	-3.229	6.661
0.3	9.817	1.450	2.3578	12.793	-3.975	8.817
0.2	12.05	1.414	3.1315	15.646	-4.587	11.059
0.1	15.38	1.380	4.1555	19.857	-5.468	14.388
0.0	7.449	1.345	0.8984	8.674	-2.225	6.449

able -6: Nonlinear parameter of Ethyl Acetate + Hexane (Temp at 30 ºC,35 ºC and 40 ºC)
Note: x(1) is Mole fraction of Ethyl Acetate

X(1)	δ	y	τ	(B/A)'	(B/A)"	(B/A)
1.0	6.753	1.692	1.0875	9.734	-3.981	5.753
0.9	7.337	1.656	1.6175	10.501	-4.163	6.337
0.8	6.668	1.622	0.6197	9.197	-3.529	5.668
0.7	6.858	1.589	0.4427	9.309	-3.450	5.858
0.6	19.42	1.554	8.3195	28.638	-10.21	18.426
0.5	6.676	1.518	0.7107	8.621	-2.945	5.676
0.4	6.690	1.484	0.6858	8.449	-2.758	5.690
0.3	6.665	1.450	0.5998	8.220	-2.554	5.665
0.2	6.667	1.414	0.5543	8.018	-2.350	5.667
0.1	7.597	1.380	1.0588	9.105	-2.507	6.597
0.0	6.706	1.345	0.5031	7.674	-1.968	5.706

4. ACKNOWLEDGEMENT

The authors are thankful to DST for the FIST Programme.

5. REFERENCES

[1] B.K. SHARMA and R.R. REDDY, 1987. *Temperature invariance of so-parameter of polymers pramana*, **28** p. 197.

[2] S.A. TIWARIAND S. RAJAGOPALAN, 1990. Thermoacoustcal parameters in Ethyl and Propyl Benzoates at 228 K-293K *Acoustic Letters*, **14**, p. 92.

[3] REDDY, REDDY and MURTHY, 1987. Simple expressions for the Moelwyn-Hughes parameters and Thermo Acoustical parameters of polymers, *Acoustics Letters*, **10** , p. 128.

[4] J.A. REDDICK, W.B. BUNGER and T.K. SANAKO, 1986. Organic solvents. Physical properties and Methods of purification. Techniques of chemistry 4th ed., Wiley-interscience: New York.

[5] B.K. SHARMA, REDDY and R.R. SHARMA, 1985. Constant and some Thermo-acoustic properties of polycrystalline Rare Earth metals, Alkali metals, alkali Halides and Polyatomic Ionic Liquids, *Indian J. Pure and Appl. phy.*, **23,** p. 396.
[6] B.K. SHARMA, 1986. Isochoric Temperature Coefficient of Surface Tension and So-parameter of Quasi-spherical molecular liquids, *Pramana*, **26**, p. 223.
[7] R.A. AZIZ, D.H. BOWMAN and C.C. Lim, 1972. Relation between Beyers non linear parameter and other physical parameters, *Can. J. phys.*, **50**, p. 646.
[8] B.K. SHARMA, 1983. Nonlinear acoustical parameters of liquids. *J. Acoust. Soc. Amer.*, **73**, p. 106.
[9] B.K. SHARMA, 1988. Relationship between the Rao's Acoustical parameter, gruneisen parameter and Beyer's nonlinearity parameter of quasi-Spherical Molecular liquids from thermo-acoustic data Acustica. **67,** p. 52.
[10] A.B. COPPENS, R.T. BEYER, M.B. SEIDEN, J. DONOHUE, F. GUEPIN, R.H. HODSON and C.J. TOWNSEND, 1956. Thermodynamical parameters of liquid mixtures. *J. Acoust. Soc. Am.*, **38**, p. 797.
[11] O. NOMOTO, Theory of liquids. *J. Phys. Soc. Japan*, **21**, p. 569.
[12] E. SOCZKIEWICZ, 1977. Nonlinear acoustical parameters of some liquids Archiv Acoust (poland),**2**, p. 325.
[13] E. SOCZKIEWICZ, 1978. Inter relationship among various non linear and isochoric parameters Acustica (Germany), 39, p. 189.
[14] B.K. SHARMA, Thermo-Acoustic and Nonlinear properties of Quasi spherical molecular liquids through internal pressure-temperature data, *J. Pure Appl. Phys.*, **23**, p. 247.

Journal of Acoustical Society of India : Vol. 37, No. 4, 2010 (pp. 169-179)

Case Study on Uncertainty Estimation of Acceleorometer Calibration System as per ISO 16063-21

A. Tamil Chandran, P. Surendran* and S. Saseendran
Fluid Control Research Institute,
Kanjikode west,Palakkad, Kerala, India- 678 62
**e-mail: p.surendran@fcriindia.com*

[Received: 12.12.2009; Revised: 27.07.2010; Accepted: 21.08.2010]

ABSTRACT

In practice, traceability leads to improve the accuracy and agreement among the results obtained using different means of measurement. However, in every calibration within the traceability chain there is a certain increment of the uncertainty of measurement. The uncertainty of measurement gives an idea of the length of the traceability chain and the accuracy of the methods used to calibrate the measurement standard. It highlights that an important portion of system uncertainty related with these reference standards depends on two factors, their traceability chain to basic standards and the measurement accuracy achieved within the traceability chain. ISO 16063-21/2003 discusses different components of expression of uncertainty of measurement in accelerometer calibration. This paper presents the results and methodology adopted in determining the uncertainty budget of a new accelerometer calibration system installed at FCRI as per ISO 16063 requirements. The basic requirement of the accelerometer calibration system to comply with ISO 16063 is also discussed. The results discussed in this paper are from three case studies undertaken employing.

a) Comparison calibration between two primary (laser) calibrated accelerometers.
b) Comparison calibration between primary (laser) calibrated accelerometer and a working standard accelerometer with different mounting conditions simulated.
c) Comparison calibration employing 'RED STONE' check as suggested by the manufacturer of the system.

1. INTRODUCTION

In the past, the values of measurement uncertainty of a calibration system or a calibration service were absolutely incomparable. Most of the calibration system manufacturers gave no information or only one best value of one component that was part of the calibration system. These technical data had been neither serious nor comparable. Now the awareness and necessity for quality calibration system demand for minimizing the system uncertainty. ISO also had taken major part to improve the uncertainty estimation. In recent years the older standards concerning the calibration of vibration and shock transducers ISO 5347 have partly been revised. Results of these activities is a new series called "Methods for calibration of vibration and shock transducers, ISO 16063-xx" [2-7].

This paper discuss about the basic requirements for accelerometer calibration and different components of expression of uncertainty of measurement as given in ISO 16063-21/2003. Results of three case studies undertaken employing different procedures using comparison calibration method are discussed. Based on these studies, the uncertainty budget is prepared as per ISO 16063 requirements.

2. NEED FOR CALIBRATION

The use & application of vibration and shock sensors continues to grow at an exponential rate. Vibration sensors are used from aerospace labs to automotive test rigs, to smart systems providing condition monitoring systems and active vibration control.

While these sensors continue to improve the performance of people, products and processes, this growing needs of test and automation is also demanding a calibration liability. At sometimes, during a sensor's product life cycle, either at time of manufacture or in test, a sensor must be calibrated. Without calibration to a known acceleration standard, an accelerometer's output cannot be absolutely verified and trusted. When an accelerometer fails during calibration (due to mechanical or electrical problems), all scaled data measured by that sensor are invalid since the time of last valid calibration. Often it is impossible to tell exactly when a sensor has failed; therefore, test data taken during the full calibration interval must be revalidated or scrapped - wasting time and money. This is why the most critical and costly measurement applications require sensor calibration both immediately before and immediately after each test, to validate the data [1].

3. RESULTS AND CONCLUSION

Traceability is achieved through an unbroken link of reference calibrations back to a physical constant or national or international standard. In many cases in India, The National Physical Laboratory, New Delhi (NPL) is the custodian of different reference standards. Traceability is important to ensure the validity of the overall calibration system results. Typical calibration techniques utilize a back-to-back or reference sensor with which the test accelerometer signal is compared. In calibrating the system reference accelerometer, each step in the link of these reference calibrations adds more uncertainty into the end calibration performed. In India NABL is authorized to accredit different laboratories and suggest for inter comparison between laboratories for increase of the confidence level in calibration.

4. INTERNATIONAL STANDARDS FOR VIBRATION SENSOR CALIBRATION

In recent years the ISO has introduced new series of standards for vibration sensor calibration. These standards describe basic concepts, different methods of calibration and details the about uncertainty estimation. Table 1 gives the list of current ISO standards available on calibration of vibration sensors.

Table 1. ISO 16063 summary

ISO 16063-1	Basic concepts [2]
ISO 16063-11	Primary vibration calibration by laser interferometry [3]
ISO 16063-12	Primary vibration calibration by reciprocity method [4]
ISO 16063-13	Primary shock calibration using laser interferometry [5]
ISO 16063-21	Secondary vibration calibration [6]
ISO 16063-22	Secondary shock calibration [7]

Primary calibration facilities are normally held at custodian laboratories like NPL in India & PTB in Germany etc. FCRI has recently commissioned a vibration sensor calibration system by comparison to a reference transducer complying with requirements of ISO 16063-21/2003 standard.

4.1 ISO 16063 Part 21

This standard describes the comparison calibration of vibration transducers over the frequency range from 0,4 Hz to 10 kHz. The content of the standard covers the uncertainty estimation of measurement, apparatus requirements and ambient conditions required for calibration Preferred amplitudes and frequencies are also stipulated. Attainable uncertainties of calibration for magnitude and phase shift are also indicated in the text.

4.2 Calibration System Description [8]

The calibration system consists of an air bearings shaker with a force rating of 25lbs and frequency range upto 20 kHz and also a flexure shaker with a force rating of 40lbs meant for low frequency requirement, which starts from 2Hz. This is also used for linearity check. Both the shakers are run by a common power amplifier. A signal conditioner is available to connect the reference accelerometer and the sensor to be calibrated. A dedicated software is available for running the system and for automated report generation. The signal conditioner has the capability of accepting various inputs of charge, ICP, capacitance and voltage mode sensors. The block schematic of the arrangement is shown in Fig. 1.

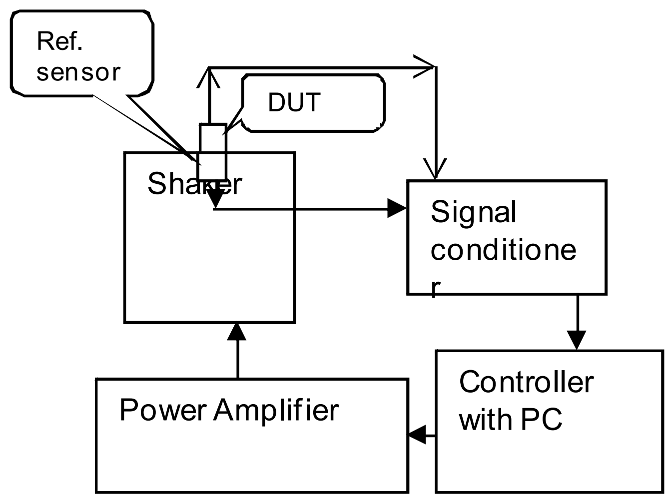

Fig. 1. Schematic of the calibration setup

5. EXPANDED UNCERTAINTY AS PER ISO 16063 PART 21: 2003 [6]

The uncertainty of measurement in calibration shall be expressed by the "expanded uncertainty" 'U'. The purpose of 'U' is to provide an interval 'y-U' to 'y+U' with in which the value of 'Y', the specific quantity subject to calibration and estimated by 'y', can be expected to lie with high probability. To confidently assert that $y-U \leq Y \leq y+U$, the expanded uncertainty U has to be actually determined.

The estimation procedure is explained in subsequent sections.

5.1 Standard Uncertainty Estimation

Each component of uncertainty that contributes to the uncertainty of the measurement shall be represented by a standard deviation u_i, terms standard uncertainty, equal to the positive square root of the variance u_i^2. Some standard uncertainties can be obtained as statistically estimated standard deviations by the statistical analysis of observations (type A evaluation of standard uncertainty). Other standard uncertainties shall be evaluated as the standard deviation of a probability distribution describing the scientific judgment of all possible values of the respective quantity (Type B evaluation of standard uncertainty). In particular, if there is no specific information about the possible values of a quantity responsible for systematic effects that these values are within the bounds b- and b+, a uniform distribution over the interval [b-;b+] has to be used to represent this information. It has a standard uncertainty $b/\sqrt{3}$. If an influence quantity can be considered uniformly distributed but is known to be transferred into the measurement results with a specific non - liner function, this information shall be taken into account by choosing the associated distribution model. The associated standard uncertainty is $b/\sqrt{2}$.

5.2 Combined Standard Uncertainty

The combined standard Uncertainty u_c, as the standard uncertainty of the measurement of Y, shall be determined by combination of the individual standard uncertainties using the law of propagation of uncertainty. For the cases where no significant correlations are present, equation for combined standard uncertaintyis $u_c(y) = \sqrt{\sum_{i-1}^{N} \left(\frac{\partial f}{\partial x_i} \right)^2 u^2(x_i)}$ the symbols $\partial f / \partial x_i$ are often referred to as sensitivity coefficients c_i,

5.3 Expanded Uncertainty

The "expanded uncertainty" U shall be determined by multiplying u_c by a coverage factor k. $U=ku_c$ where a value of k=2 should preferably be used for a confidence level of 95%.

5.4 Calculation of the Relative Expanded Uncertainty $U_{rel}(S)$ for the Sensitivity Magnitude

The relative expanded uncertainty of measurement of the magnitude of the complex sensitivity $U_{rel}(S)$, for each of the applied frequencies, accelerations and amplifier gain settings (if an amplifier is part of the calibrated transducer) is calculated from the following formulae. $U_{rel}(S) = ku_{c,rel}(S)$.

5.5 Calculation of the Expanded Uncertainty U($\Delta\varphi$) for the Phase Shift

The expanded uncertainty of measurement of the phase shift ' $\Delta\varphi$ ' of the complex sensitivity S, at each of the applied frequencies, accelerations and amplifier gain settings is calculated from the following formula

$U(\Delta\varphi)=ku_c(\Delta\varphi)$

5.6 Uncertainty Parameters

The following parameters are involved in uncertainty estimation as per ISO 16063 part 21.

Sensitivity

a) Calibration of reference standard accelerometer set
b) Linearity of reference standard accelerometer set
c) Drift for 3 Year, 0.05% per year
d) Effect of non linearity of transducers
e) Voltage ratio specification
f) Effect of calibration at < REF amplitude
g) REF Signal to noise effect
h) Sensitivity of condition amplifier calibration
i) Influence from temperature variation, Reference standard accelerometer sensitivity, 23 ± 3 C, 0.02%per C. Max 4 C used
j) Max allowed difference between reference level before and after the measurement
k) Influence of mounting parameters on unknown, cable, plug and torque, max 0.05%
l) Influence from acceleration distortion. Difference in freq. Slope typically 2%/decade 2nd and 3rd harmonics less than 2% m) Influence from transverse acceleration. Transverse vibration aT for shaker max. 10% Transverse sensitivity ref. Std. Accelerometer, SV,1 max 2%
n) Influence from base strain. Estimated to be less than
o) Influence from relative motion Estimated to be less than
p) Influence from non -linearity of amplifier to be less than
q) Influence from gravitation. Estimated to be less than
r) Influence from magnetic field from exciter. Estimated to be less than
s) Influence from other environmental effects. Estimated to be less than
t) Influence from residual effects (e.g. random effect in repeated measurement, experimental standard deviation of arithmetic mean.)

Phase

a) REF primary laser calibration
b) Conditioning amplifier Phase Vs Gain
c) Conditioning amplifier frequency response
d) Transducers frequency response (theoretical)
e) Amplitude effect on amplifier phase
f) Amplitude effect on transducer phase
g) Instability amplitude phase / source impedance effect
h) Instability of transducer phase sensitivity
i) Environmental effects on amplifier phase
j) Environmental effects on transducer sensitivity phase
k) Mounting / cabling effects
l) Effect of calibrating at < ref amplitude
m) REF signal to noise effects

6. UNCERTAINTY ESTIMATION PROCEDURES

FCRI's calibration system 'VWIN' supplied by MB Dynamics USA make [8], is a fully automated calibration system complying to ISO 16063/21.

To estimate the standard uncertainty of the system, three different techniques as detailed below were attempted.
a) Comparison calibration between two primary (laser) calibrated accelerometers.
b) Comparison calibration between primary (laser) calibrated accelerometer and a working standard accelerometer with different simulated mounting conditions.
c) Comparison calibration employing 'RED STONE' check as suggested by the manufacturer of the system.
Based on above case studies, the uncertainty budget is prepared as per ISO 16063 requirements

6.1 Comparison Calibration Between Primary (Laser) Calibrated Accelerometers

For the comparison calibration two numbers of NIST traceable primary laser calibrated accelerometers were used. Both accelerometers are of make PCB Piezotronics. One accelerometer was primarily calibrated for the frequency range of 5 to 20000Hz and the second sensor was calibrated in the range of 1 to 10000Hz. The first accelerometer was used as the reference transducer for the comparison calibration and was kept below the shaker table. The second sensor was kept on top of the shaker table. Both accelerometers have a nominal sensitivity of 100mv/g. The calibration was performed for the frequency range of 5 to 10000Hz. Ten trials were taken as part of system uncertainty estimation. From the ten trials standard deviation in sensitivity and phase was calculated.

6.2 Comparison Calibration between Primary Calibrated Accelerometer and a Working Standard Accelerometer

This calibration was done as same as section 6.1 except that a working standard accelerometer was used as a sensor to be calibrated. This calibration was done in the same frequency range of 5 to 10000Hz with two different mounting conditions ie., stud mounded and adhesive mounted. Standard deviation observed in both cases was computed.

6.3 Comparison Calibration Employing 'Red Stone' Check

'RED STONE' [9] check is the manufacturers standard recommendation practice for verifying the system performance and to find the deviation from the other calibration.

For RED STONE check, two accelerometers are to be used. Both laser calibrated reference accelerometer were mounted back to back on to the shaker table. Initial calibration uses the bottom accelerometer as a reference and the top sensor as the device under test (DUT). For further calibration trials, the initial DUT was used as a reference sensor, which in turn is used to verify the laser calibrated sensor. Any differences in sensitivities between initial values and after the RED STONE check are the error due to the calibration system. This can be considered as the system uncertainty of the calibration system.

7. RESULTS

Results comprising the measured & reference sensitivity, phase, standard deviation between trials and uncertainty between trials are reported in this section for the three set of calibrations.

7.1 Comparison Calibration between Laser Calibrated Accelerometers

Sensitivity

Freq. in Hz	Sensi-tivity in mv/g	Stan dard devi- ation	Uncer tainty in %	Laser cal sensi tivity in mv/g	Devi. from laser cal. values in %
5	101.63	0.37	0.26	101.02	-0.61
10	100.65	0.14	0.10	100.50	-0.15
20	99.94	0.03	0.02	99.98	0.05
50	99.27	0.15	0.11	99.31	0.03
100	98.64	0.06	0.04	98.68	0.04
159	98.29	0.06	0.04	98.26	-0.04
160	98.30	0.07	0.05	98.26	-0.05
300	97.64	0.06	0.04	97.69	0.05
500	97.25	0.03	0.02	97.28	0.03
1000	96.61	0.03	0.02	96.59	-0.02
2000	96.10	0.03	0.02	96.10	-0.01
4000	95.86	0.04	0.03	95.74	-0.12
6015	95.96	0.02	0.02	95.94	-0.02
8000	96.90	0.03	0.02	96.98	0.08
10000	96.90	0.05	0.03	96.54	-0.38

Phase

Freq. in Hz	Phase (Deg.)	Standard deviation	Uncer tainty in %	Laser cal Phase (Deg.)	Devi. from laser cal. values in %
5	0.9	0.17	0.12	1.0	0.03
10	0.1	0.02	0.02	0.1	0.02
20	-0.5	0.05	0.04	-0.4	0.07
50	-0.7	0.06	0.04	-0.7	0.00
100	-1.0	0.04	0.03	-0.9	0.07
159	-1.0	0.01	0.01	-1.0	0.02
300	-1.4	0.03	0.02	-1.4	0.00
500	-1.8	0.01	0.00	-1.7	0.03
1000	-2.6	0.00	0.00	-2.6	0.03
2000	-4.4	0.01	0.00	-4.4	0.01
4000	-8.0	0.01	0.01	-8.0	-0.01
6015	-11.7	0.01	0.01	-11.5	0.14
8000	-15.0	0.01	0.01	-15.1	-0.05
10000	-18.1	0.01	0.01	-19.3	-0.73

7.2 Comparison Calibration between Laser Calibrated Accelerometers and Working Standard Accelerometer Stud mounted- sensitivity

Frequency in Hz	Sensitivity in mv/g	Standard deviation	Uncertainty in %
5	98.21	0.52	0.37
10	98.19	0.25	0.18
20	98.07	0.11	0.08
100	98.11	0.09	0.06
159	98.13	0.09	0.06
160	98.28	0.12	0.08
300	98.19	0.10	0.07
500	98.29	0.09	.06
1000	98.29	0.09	0.06
2000	98.47	0.07	0.05
4000	97.84	0.10	0.07
6504	98.86	0.07	0.05
8000	99.52	0.03	0.02
10000	101.63	0.15	0.11

Stud mounted -Phase

Frequency in Hz	Phase (Degree)	Standard deviation	Uncertainty in %
5	3.83	0.77	0.55
10	1.94	0.37	0.26
20	0.83	0.18	0.12
100	-0.11	0.04	0.03
159	-0.19	0.02	0.01
300	-0.64	0.02	0.01
500	-1.11	0.02	0.01
1000	-2.28	0.00	0.00
2000	-4.58	0.00	0.00
4000	-9.96	0.15	0.10
6504	-14.65	0.04	0.03
8000	-17.69	0.12	0.08
10000	-21.06	0.06	0.04

Adhesive mounted - Sensitivity

Frequency in Hz	Sensitivity in mv/g	Standard deviation	Uncertainty in %
5	97.78	0.60	0.43
10	97.87	0.15	0.11
20	97.77	0.09	0.06
100	97.83	0.11	0.07
160	98.11	0.14	0.10
300	97.90	0.11	0.08
500	98.00	0.10	0.07
1000	98.04	0.10	0.07
2000	98.27	0.10	0.07
4000	98.07	0.12	0.09
6504	99.20	0.17	0.12
8000	100.43	0.04	0.03
10000	102.07	0.26	0.18

Adhesive mounted - Phase

Frequency in Hz	Phase (Degree)	Standard deviation	Uncertainty in %
5	4.25	0.39	0.28
10	2.15	0.08	0.06
20	0.93	0.04	0.03
100	-0.19	0.15	0.11
159	-0.15	0.05	0.04
300	-0.64	0.01	0.00
500	-1.10	0.01	0.01
1000	-2.27	0.01	0.01
2000	-4.57	0.01	0.01
4000	-9.85	0.06	0.04
6504	-14.71	0.05	0.03
8000	-18.29	0.01	0.01
10000	-21.32	0.03	0.02

7.3 Red Stone' Check

Sensitivity

Freq. in Hz	Sensitivity in mv/g	Standard deviation	Uncer tainty in %	Laser cal sensi tivity in mv/g	Devi. from laser cal. values in %
5	102.71	0.79	0.56	102.34	-0.36
10	102.03	0.28	0.20	101.87	-0.15
20	101.48	0.09	0.06	101.35	-0.13
50	100.85	0.07	0.05	100.72	-0.13
100	100.26	0.12	0.08	100.19	-0.07
159	99.88	0.08	0.06	99.78	-0.10
160	99.82	0.04	0.03	99.77	-0.05
300	99.32	0.10	0.07	99.25	-0.07
500	98.93	0.03	0.02	98.89	-0.04
1000	98.34	0.03	0.02	98.04	-0.31
2000	97.95	0.02	0.01	97.90	-0.05
4000	97.81	0.03	0.02	97.74	-0.08
6015	98.30	0.04	0.03	98.21	-0.09
8000	99.26	0.02	0.02	99.15	-0.12
10000	100.99	0.05	0.04	100.88	-0.11

Phase

Freq. in Hz	Phase (Deg.)	Standard deviation	Uncertainty in %	Laser cal. phase (Deg.)	Devi. from cal. laser in %
5	-0.32	0.27	0.19	0.60	0.51
10	-0.30	0.08	0.06	0.00	0.17
20	-0.70	0.04	0.03	-0.50	0.11
50	-0.54	0.04	0.03	-0.60	-0.04
100	-0.83	0.06	0.04	-0.80	0.01
159	-0.81	0.02	0.01	-0.70	0.06
300	-0.77	0.08	0.06	-0.80	-0.01
500	-0.86	0.01	0.00	-0.80	0.03
1000	-0.86	0.01	0.00	-0.80	0.03
2000	-0.79	0.00	0.00	-0.80	-0.01
4000	-0.81	0.01	0.01	-0.90	-0.05
6015	-0.97	0.03	0.02	-1.00	-0.02
8000	-1.18	0.01	0.00	-1.10	0.05
10000	-1.07	0.02	0.02	-1.10	-0.02

8. DISCUSSION ON THE STANDARD UNCERTAINTY

Standard uncertainty computed by various methods is plotted in Figs. 2 and 3. The study had indicatmaximum uncertainty of around 0.6 % at 5Hz. Sensitivity & Phase obtained by back to back calibration are well comparable with primary calibrated values as indicated in Figs. 4 & 5.

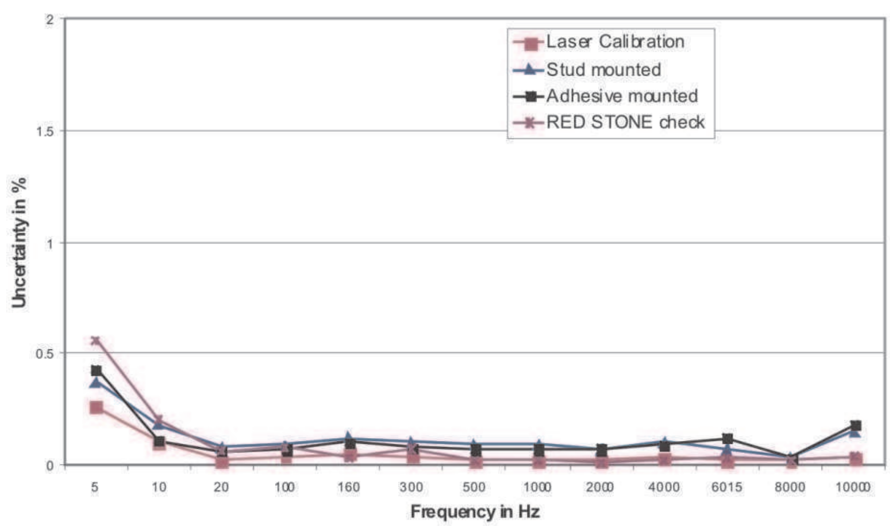

Fig. 2. Uncertainty in sensitivity

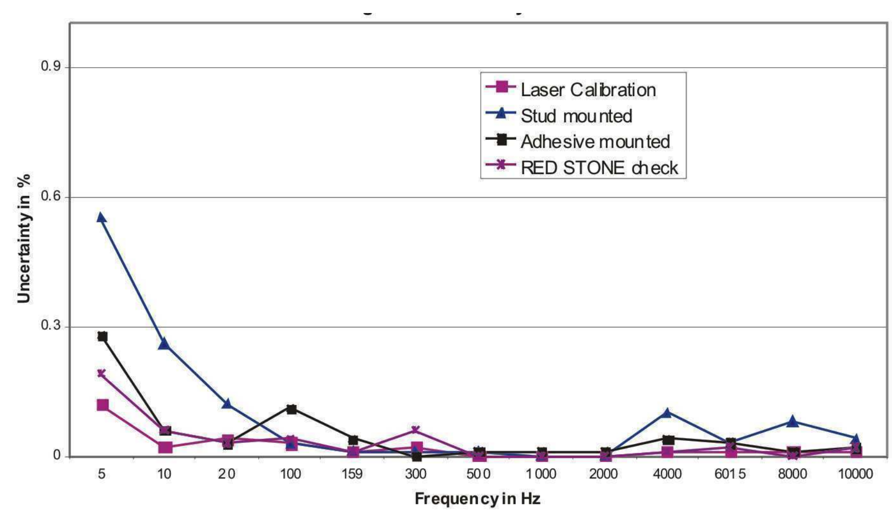

Fig. 3. Uncertainty in Phase

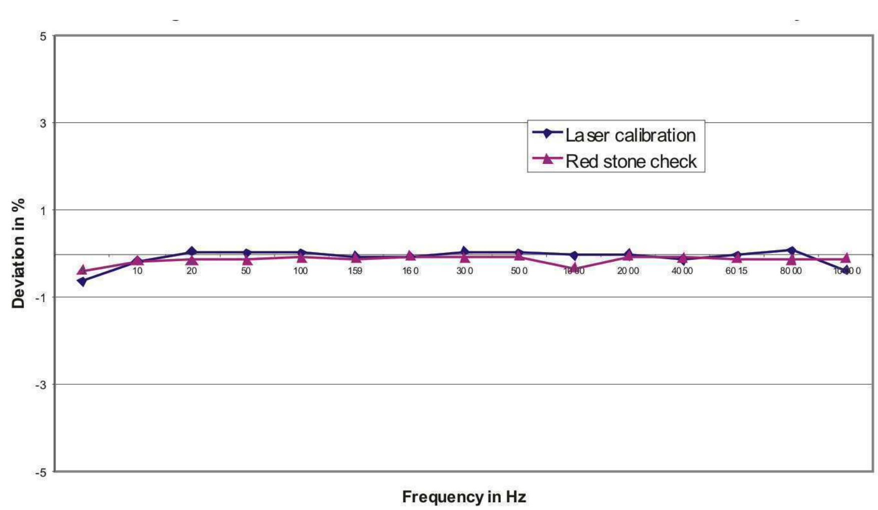

Fig. 4. Deviation between Lase Calibration & FCRI calibration - Sensitivity

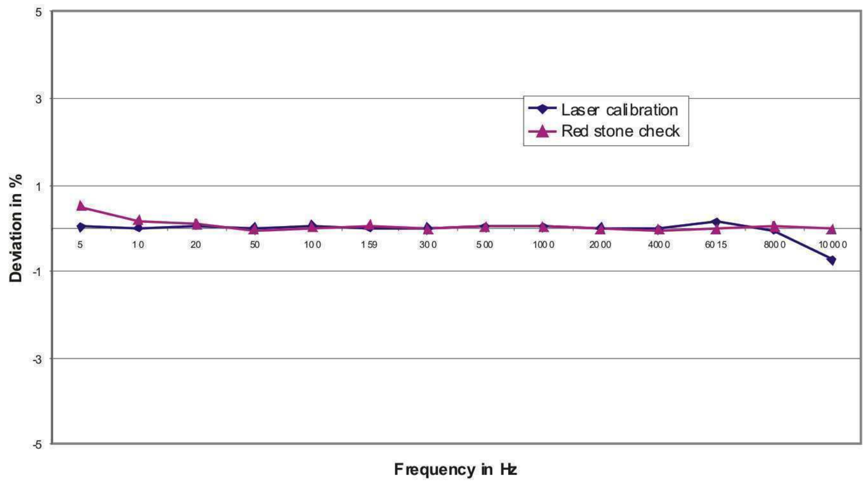

Fig. 5. Deviation between Lase Calibration & FCRI calibration - Phase

9. REFERENCES

[1] HOLGER NICKLICH, 2004. Calibration of Sound and Vibration Sensors and vibration testing systems', Proceedings of the 5th International symposium on Environmental testing for space programmes, pp. 481-485

[2] ISO 16063-1:1998. Ed. 1, Methods for the calibration of vibration and shock transducers - Part 1: Basic concepts.

[3] ISO 16063-11:1999. Ed. 1, Methods for the calibration of vibration and shock transducers -- Part 11: Primary vibration calibration by laser interferometry.

[4] ISO 16063-12:2002, Ed. 1, Methods for the calibration of vibration and shock transducers -- Part 12: Primary vibration calibration by the reciprocity method.

[5] ISO 16063-13:2001, Ed. 1, Methods for the calibration of vibration and shock transducers -- Part 13: Primary shock calibration using laser interferometry.

[6] ISO 16063-21:2003, Ed. 1, Methods for the calibration of vibration and shock transducers -- Part 21: Vibration calibration by comparison to a reference transducer.

[7] ISO 16063-22:2005, Ed. 1, Methods for the calibration of vibration and shock transducers -- Part 22: Shock calibration by comparison to a reference transducer.

[8] MB WIN 475 Calibration system manual, 'MB Dynamics'.

[9] MB dynamics application notes AN163.

[8] MB WIN 475 Calibration system manual, 'MB Dynamics'.

[9] MB dynamics application notes AN163.

Journal of Acoustical Society of India : Vol. 37, No. 4, 2010 (pp. 180-185)

Study of Thermodynamical Properties of Sodium Fluride in Aqueous Medium at Different Temperature

K. Rajagopal[1] and S. Edwin Gladson[2]
[1]*Department of Physics, Government College of Engg., Tirunelveli-627 007, Tamilnadu*
e--mail; krpal 25 @ yahoo.com
[2]*Department of Physics, St. Xavier's Catholic College of Engg.,*
Chunkankadai - 629 807, Tamilnadu
e-mail: aseg_win @ rediffmail.com

[Received: 15.02.2010; Revised: 17.07.2010; Accepted: 22.08.2010]

ABSTRACT

Density, viscosity and ultrasonic velocity measurements have been carried out on Sodium Fluoride (0.1 to 0.9) M in aqueous medium at T = (303.15, 308.15, 313.15 and 318.15)K. Several thermo dynamical parameters such as Gibbs free energy (ΔG), attenuation constant (α), relaxation time (τ), relative association (RA) and apparent molal volume ($V\varphi$) have been calculated from the measured data on density, viscosity and velocity. These parameters have been used to analyse the interaction between the molecules in the solution and structure making/ breaking ability of the solute in the given solution.

1. INTRODUCTION

In biophysical chemistry, drug-macro molecular interaction is an important phenomenon involving a complex mechanism. Since most of the biochemical processes occur in aqueous media the studies on the thermodynamic and transport properties of drugs in the aqueous phase provides useful information in Pharmaceutical and Medicinal Chemistry. The drug water molecular interaction and their temperature dependence play an important role in the understanding of drug action. Measurement of ultrasonic velocity and its related parameters gives important information about the physicochemical behaviour of the solution [1-3]. In this paper we report the data of density, ultrasonic velocity and viscosity of sodium fluoride in water at different temperatures. Sodium fluoride is colourless crystalline salt used in the treatment of tooth decay. From literature we find that sodium fluoride acts as structure breaker in water and D_2O [4]. Gathimathi et al [5] has determined acoustic parameters such as adiabatic compressibility, Rao's constant Wada's constant, internal pressure, free volume of NaF in aqueous medium for the temperature range of 35ºC to 55ºC. They have suggested that NaF acts as structure maker in water. In this paper we report new parameters like Gibb's free activation energy, relaxation time, apparent molal volume and limiting partial molal volume from the density, velocity and viscosity data for the temperature range of 303.15 K to 318 .15K . Since the second derivative of limiting partial molal volume ($\partial^2 V_\varphi^0 / \partial T^2$) gives better idea about the structure making/breaking of the solute [6], it has been calculated.

2. EXPERIMENTAL

Sodium fluoride (AR grade 99% assay S.D fine Chem Ltd Mumbai) was used as such without any pre-treatment. Aqueous sodium fluoride solutions of 0.1M, 0.3M, 0.5M, 0.7M and 0.9M were prepared using double distilled deionised water with a conductivity of 1.5 $\mu\Omega^{-1}cm^{-1}$. The weighings were done on a high precision AND electronic balance (Model HR 300, Japan) with a precision of ± 0.1mg. The densities of the solutions were measured using a single stem pycnometer. Viscosity was measured by means of a suspended level Ubbelohde viscometer with a flow time of 204 s at 303.15K. The time of flow was measured with a stop watch capable of recording ± $2ms^{-1}$. The ultrasonic velocity was determined using a single crystal ultrasonic interferometer (Mittal make, India) at a frequency of 2MHz and the reproducibility of the velocity values are within ±2 ms-1. The temperatures of the solutions were maintained to an accuracy of ± 0.01k in an electronically controlled thermostatic water bath [7].

3. RESULTS AND DISCUSSION

The experimental values of the densities, ultrasonic velocity and viscosity of (0.1 to 0.9) M aqueous sodium fluoride solutions at T= (303.15, 308.15, 313.15 and 318.15) K are measured. The variation of these parameters with concentration and temperature are shown in Fig. 1, Fig. 2 and Fig. 3, respectively.

Relaxation time, ultrasonic attenuation, relative association, surface tension and other parameters are calculated

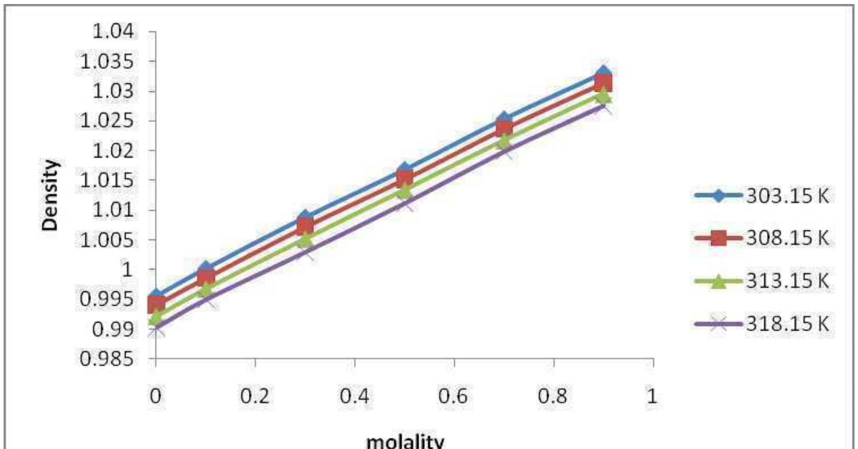

Fig 1

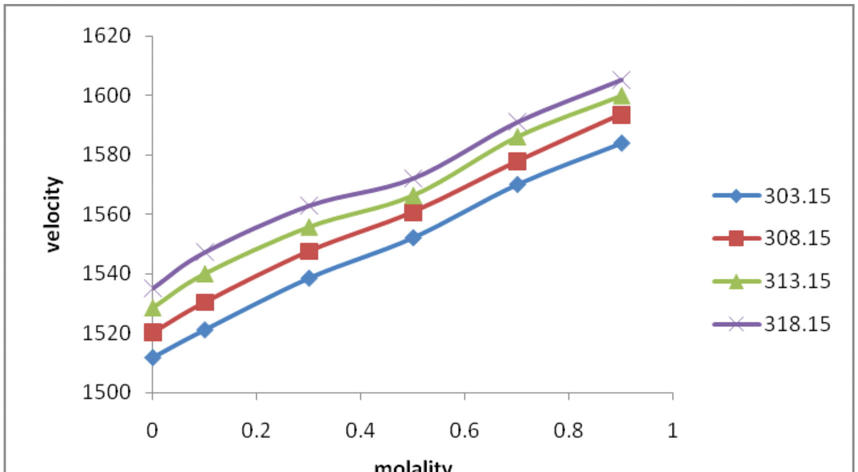

Fig 2

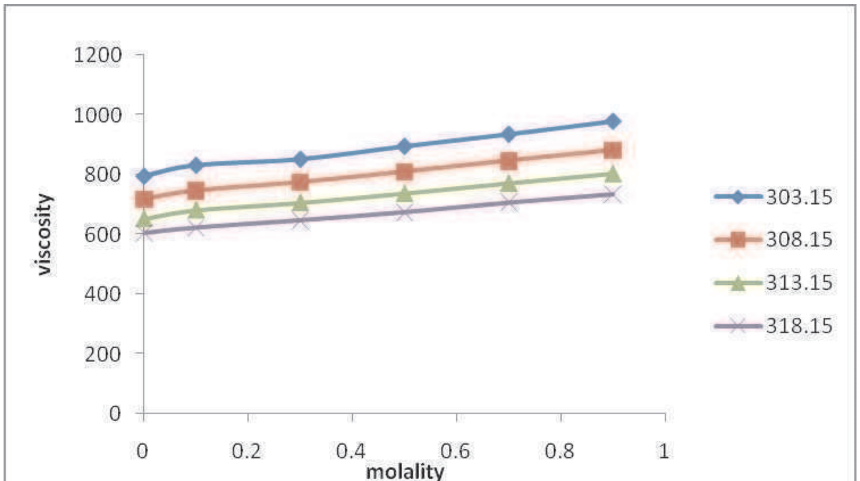

Fig 3

using following relations.

Relaxation time, $\tau = 4\eta / 3\rho u_s^2$ (1)

Ultrasonic attenuation, $\alpha = \omega^2 \tau / 2u$ (2)

Relative association, RA = $\rho / \rho 0[u0 / u]^{1/3}$ (3)

Surface tension, $\sigma = 6.3x10^{-4} \rho u^{3/2} N / M$ (4)

Gibb's free energy, $\Delta G = RT \ln(\eta V / hN) kJmol^{-1}$ (5)

where R-universal gas constant, T-temperature, V- molar volume, h-Planck' constant, N-Avagadro number,η-viscosity, ρ-density and u-ultrasonic velocity. The values of these parameters under different temperatures are given in Table 1.

Acoustical relaxation time is directly proportional to adiabatic compressibility and viscosity[8]. Relaxation time of aqueous sodium fluoride solutions is found to be increase with increase in concentration and decreases with increase in temperature. Ultrasonic attenuation of solution is found to be increase with increase in concentration and decrease with increase in temperature shows a trend similar to that of acoustical relaxation time.

Relative association of solution is found to be increase with increase in concentration and decrease with increase in temperature. Surface tension of solution is found to be increase with increase in concentration and temperature.

The Gibbs free energy is found to be increase with increase in concentration and decrease with increase in temperature The Gibbs free energy of activation ΔG was also verified from the graph (Fig. 4), using Eyring equation

Table 1. Relaxation time, Attenuation constant, Relative association, Surface tension and Gibb's free energy of aqueous sodium fluoride at different temperatures

Temperature	Molality	Relaxation time	Attenuation constant	Relative association	Surface tension	Gibbs free energy
303.15	0.1	0.48	0.0249	1.003	37.39	9.15
	0.3	0.476	0.0244	1.007	38.36	9.2
	0.5	0.488	0.0248	1.012	39.178	9.31
	0.7	0.494	0.0248	1.017	40.191	9.41
	0.9	0.504	0.0251	1.022	41.031	9.52
308.15	0.1	0.426	0.0219	1.002	37.669	9.02
	0.3	0.428	0.0218	1.007	38.632	9.11
	0.5	0.437	0.0221	1.012	39.438	9.21
	0.7	0.443	0.0222	1.017	40.419	9.32
	0.9	0.449	0.0222	1.021	41.337	9.41
313.15	0.1	0.385	0.0197	1.002	37.955	8.94
	0.3	0.387	0.0196	1.007	38.862	9.02
	0.5	0.396	0.0199	1.013	39.58	9.12
	0.7	0.401	0.0199	1.017	40.659	9.23
	0.9	0.407	0.0201	1.022	41.506	9.33
318.15	0.1	0.349	0.0178	1.002	38.149	8.85
	0.3	0.353	0.0178	1.007	39.039	8.94
	0.5	0.36	0.0181	1.013	39.706	9.04
	0.7	0.365	0.0181	1.018	40.772	9.15
	0.9	0.37	0.0182	1.022	41.631	9.25

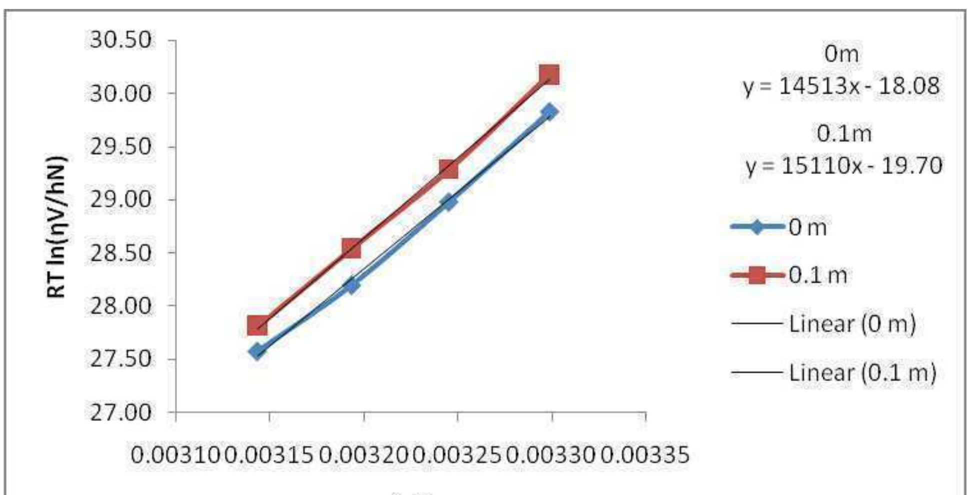

Fig 4

$$\Delta G = \Delta H + T\,\Delta S \qquad (6)$$

where ΔH is enthalpy and ΔS is entropy.

The apparent molal volumes, V_ϕ were calculated from density data using the equation

$$V\varphi = (M/\rho) - 1000(\rho - \rho_0)/M\rho_0 \qquad (7)$$

where ρ and ρ_0 are the densities of solution and solvent (aqueous sodium fluoride), respectively, m is the molality of the solute and M is its molar mass. The calculated values of V_ϕ are also included in Table 2. The magnitude of negative values of V_ϕ for the solution indicates weak solute-solvent interactions.

The standard partial molal volume and its temperature dependence provide valuable information of the solute- solvent interactions[9,10].The variation of the apparent molal volumes, V_ϕ with the concentration can be represent by the equation

$$V_\phi = V_\phi^0 + S_v\, m \qquad (8)$$

where V_ϕ^0 is the limiting value of apparent molal volume and S_v is the experimental slope. The values of V_ϕ^0 and S_v obtained by least squares fitting of the V_ϕ values of Eqn (1) are reported in Tables 3. The plots of V_ϕ against m were linear in all cases. It is evident from Table 3 that the values of V_ϕ^0 are negative indicating weak solute solvent interaction and the slope S_v for sodium fluoride are positive suggesting strong solute-solute interactions in the system [11].

The variation of V_ϕ^0 with temperature can be expressed as

$$V\varphi = a + bT + cT^2 \qquad (9)$$

where T is the temperature in Kelvin. The coefficients a,b and c are determined Fig. 5 and the following equation is obtained.

Table 2. Apparent molal volume of aqueous sodium fluoride at different temperatures

Molality ms m mol.kg^{-1}	303.15K	V_ϕx10^6 3mol^{-1} 308.15K	313.15K	318.15K
0.1	-4.212	-3.287	-4.386	-5.503
0.3	-2.185	-1.927	-1.675	-0.76
0.5	-0.588	-0.458	-0.733	-0.221
0.7	-0.611	-0.538	-0.474	-0.7
0.9	0.243	0.286	0.213	0.132

Table 3. Limiting partial molal volumes (V_ϕ^0) and experimental slopes (Sv) of sodium fluoride in water at different temperatures.

Temperature K	V_ϕ^0x106 m3.mol^{-1}	Svx106 m3.mol^{-1}
303.15	-4.091	5.242
308.15	-3.318	4.267
313.15	-4.01	5.199
318.15	-4.243	5.664

Journal of Acoustical Society of India : Vol. 37, No. 4, 2010 (pp. 186-200)

Sinusoidal Wavelet for Perception of Audio Signals Applied to Indian Classical Music

Charu[1], V.G. Das[2], V. Prem Pyara[3], V. Prem Kumari[4] and Meena Sachdeva[5]
[1]*Dept. of Electronics and Communication Engineering,*
Galgotias College of Engineering and Technology, Greater Noida, India
e-mail: charup123@gmail.com
[2]*Dayalbagh Educational Inst (Deemed Univ.), Agra, India*
e-mail: vgdas@rediffmail.com
[3]*Dept. of Electrical Engg, Dayalbagh Educational Institute (Deemed Univ.), Agra, India*
[4]*Dept. of Music, Dayalbagh Educational Institute (Deemed Univ.), Agra, India*
[5]*Dept. of Computer Application, Galgotias College of Engineering and Technology, Greater Noida*

[Received: 23.04.2010; Revised: 25.06.2010; Accepted: 25.07.2010]

ABSTRACT

Fast Fourier Transform is a computationally efficient tool used for the spectral analysis of signals. Simultaneously Wavelet Transforms provide a constant 'Q' factor. Here, a wavelet is developed for the estimation of frequency of audio signals. This wavelet provides resolution comparable to human auditory system. This is applied to frequency estimation in Indian Classical Music. In case of Indian Classical Music, the task of frequency estimation is comparatively difficult as the note frequencies are not fixed but vary at fixed ratios with respect to base frequency chosen by the performer. The results observed were found accurate and almost match the expected frequencies calculated theoretically.

1. INTRODUCTION

Fourier series and transform methods are useful for transforming time domain information to frequency domain and are commonly used for spectral estimation. Fourier series gives the amplitude spectrum in frequency domain for any periodic function specified in time domain. The Fourier Transform gives the amplitude density spectrum of periodic signals. This transform gives a one to one mapping from time domain to frequency domain and the time domain function can be recovered exactly from the frequency spectrum. Though no information is lost, the Fourier Transform suffers from the drawback that information about time of occurrence of an event remains hidden in the phase component of the spectrum. It is not possible to know which period of time the value of the coefficient of a certain frequency belongs. The Short Time Fourier Transform (STFT) solves this problem by dividing the signal into smaller segments in time domain and analyzing each segment individually. The resolution in frequency domain obtained by STFT is of uniform frequency width in the entire frequency band. The frequency domain behavior of audio signals is logarithmic in nature. Therefore, the per unit resolution $\Delta f / f$ is a more reasonable measure for analyzing audio information. The spectral components obtained by STFT are at equal intervals of frequency (Δf). Thus, the STFT gives a better per unit resolution at high frequencies as compared to low frequencies. On the other hand, the Wavelet Transform deals with the signals logarithmically. The per unit resolution obtained by this transform is the same both at high and low frequencies. This transform is evaluated as a function of time at different scale factors. The scale may be considered to be the inverse of the frequency. This gives a three dimensional view of frequency distribution. Two dimensions are time and scale. The amplitude forms the third dimension. Several researchers have applied wavelets for speech and music signal analysis [1]-[19]. The problem of pitch determination of music signals requires exact spectral estimation with a high resolution. This resolution should match with the resolving capabilities of an expert musician. Here, an estimation of the resolution obtainable by various wavelets is studied, so that we may identify the wavelet that extracts exact spectral amplitudes and simultaneously gives a high resolution.

2. WAVELET AS A BAND PASS FILTER

The Wavelet Transform of a signal is obtained by finding the cross correlation of the Wavelet with the signal. The frequency resolution is a measure which gives the minimum difference between the frequencies of a signal, which can be recognized as separate entities. The logarithmic frequency behavior of audio signals causes this resolution to be measured as the ratio of this frequency difference with its central frequency. A measure of this resolution by a certain wavelet can be obtained by finding the spectrum of the particular wavelet. The frequency spectrum of these wavelets invariably has a band-pass characteristic. This behavior is exploited in building multi-resolution filters using Wavelet Transforms. The ratio of the width of the 3dB pass-band (Δf), to the central frequency f_0 is a good indicator of how well a wavelet can resolve two adjacent frequencies. Therefore, it is proposed to measure $\Delta f/ f_0$ for different wavelets. There is no effect of scaling factor on $\Delta f / f_0$ as both the numerator and the denominator change by same ratio on scaling. The Quality factor Q of a band-pass filter is defined as $Q = f_0 / \Delta f$. A measure of Q of different Wavelets is a good indicator of the resolution power of that Wavelet. Higher the value of Q, better the resolution. The minimum value of Q required by the Wavelet in order to meet the requirements of resolution of pitch for the particular case of music is established in the following section.

3. VALUE OF Q FACTOR FOR PITCH ESTIMATION OF MUSIC SIGNAL IN INDIAN CLASSICAL MUSIC

The ears of experienced musicians identify small deviations in tune quite easily. The scale of Indian Music divides an octave into seven swaras and further divides them into srutis. The swaras differ from one another by 2, 3 or 4 srutis. There Are 22 srutis in one octave and an error by even one sruti is considered to be going out of tune. The interval of one sruti is expressed as frequency ratio. These srutis are not equal. According to Dr. S.S. Bhave, a scientist cum musician working with CSC group at TIFR, Mumbai there are three intervals that are represented by a sruti in Indian Music system [20].

The intervals are 81/80, 25/26, 256/243. The smallest of the sruti ratios so identified is 81/80. This is similar, as resolving 1.25Hz in 100Hz. Thus, if the machine recognition is to match the needs of Indian Music system, the desired resolution should be better than 1:25 Hz at 100 Hz. The resolution power of good musician is considered to be equal to 1 Hz at 100 Hz [21]. This is equivalent to a per unit resolution of 0.01. The desired Q factor of the wavelet should be equal to 100 so that it may behave like a tunable band pass filter of the required Q value. A wavelet is designed here considering these requirements.

4. WAVELET DESIGN FOR MUSICAL PITCH ESTIMATION

In fourier analysis, pure sine and cosine functions are used for extracting the frequency spectrum. These functions have an impulse response given by the Dirac Delta function. The Dirac Delta function $\delta(\omega-\omega_0)$ has the following property.

$$\delta(\omega-\omega_0)=0 \qquad \text{for } \omega \neq \omega_0 \tag{1}$$

and,

$$\int_{\infty}^{\infty} \delta(\omega-\omega_0)\,d\omega = 1. \tag{2}$$

Journal of Acoustical Society of India : Vol. 37, No. 4, 2010 (pp. 201-205)

Fundamental Frequency and Perturbation Changes Under Voince Loading

R. Rajasudhakar and S.R. Savithri
Dept of Speech-Language Sciences, All India Institute of Speech & Hearing, Mysore-6.
e-mail: rajasudhakar82@yahoo.co.in ; savithri_2k@yahoo.com

[Received: 17.05.2010; Revised: 19.07.2010; Accepted: 21.08.2010]

ABSTRACT

Voice problems are known to be common among voice professionals worldwide. Teachers form a large group of voice professionals where females are a majority in that profession and are known to have more voice problems than males. The present study investigated the working day (vocal loading) effect on acoustic parameters like phonation fundamental frequency (pF0), standard deviation of fundamental frequency (SD pF0), frequency and amplitude perturbation and speaking fundamental frequency (sF0) on a single working day. Five female primary school teachers in the age range of 22 to 42 years participated in the study whose average professional teaching experience was 8 years. The teachers were asked to phonate vowel /a/ for 5 seconds at their comfortable pitch and loudness and recorded a standard reading passage in Kannada. These recordings were made at four different times of a single work day - Monday. i.e., (a) before the first class, (b) after the first class, (c) after lunch, and (d) after the last class. The light-weight, portable digital audio tape (DAT) recorder was used to collect the voice and speech sample. The pF0, SD pF0 and perturbation measures like jitter and shimmer were extracted from phonation of vowel by using PRAAT software and sF0 was measured from the reading text by using the same software. The pF0 increased by 2 Hz between the two conditions i.e., before first class and after last class; SD pF0 increased by 0.34 Hz, jitter increased by 0.20% and sF0 increased by 5 Hz due to prolonged teaching effect and the same trend was not noticed for shimmer. Fundamental frequency and frequency perturbation measures (except amplitude perturbation) are sensitive measures which undergone changes because of prolonged voice use (vocal loading).

1. INTRODUCTION

In this modern society, speech and voice professions are very common. The occupational voice problems in such professions are caused due to the basic reason of vocal loading. Vocal loading is defined as a combination of vocal loading time and factors affecting voice production such as the acoustic conditions at work (size of work space, reverberation properties, background noise) as well as the size of the characteristics of speech communication (size of groups) [1]. Most of the studies have investigated teachers as they exposed to various loading factors. Noise is a very common and relatively well-known factor in the working environment of professional voice users. As many as 50% to 80% of teachers experience or have experienced voice problems according to questionnaire studies [2, 3].

A very few studies were reported on voice changes induced by vocal loading. Most of the studies have used rather short loading times, the shortest being 15 to 20 minutes [4, 5] and the longest from 45 minutes to 2 hours [6, 7]. Variables like fundamental frequency, sound pressure level, perturbation values and long-time average spectrum have been used for measuring voice changes. These studies reported contradictory results and revealed individual differences. However, the most common result is that fundamental frequency (F0) rises after loading [8, 9]. It has been found that the fundamental frequency depends on the circumstances i.e. lower in reading samples in laboratory condition than in teaching speech in a classroom condition [10]. The problem in laboratory condition is that the difficulty of simulating the real-life situation. The sound pressure level values and shimmer increased after loading [11]. It was reported that the fundamental frequency of text-reading sample was increased after a vocally loading workday in a group of primary school teachers [12]. Interestingly, studies have shown that the jitter value increased [8], or decreased [9] and/or shown no essential changes [13] due to vocal loading. The results of the effects of prolonged vocal use on voice function are quite scant and far from conclusive. There are very few studies on the voice changes due to vocal loading in Indian primary school teachers. The present study aimed to document the effects of prolonged teaching on acoustic measures like fundamental frequency and perturbation changes on a single workday in five school teachers at primary level.

2. METHOD

Participants: Five primary school teachers (females) in the age range of 22-42 years (average age was 32.2 years) volunteered to participate in the experiment. Their teaching experience ranged from 2-20 years (average teaching experience: 8.6 years). They taught Science, Kannada, Social science and English to third and/or fourth grade students. The average number of students in each grade was about 30 to 35. The number of classes taken by the teachers per day was around five and the duration of each class was 45 minutes. The participants were free from hypertension, high blood sugar, allergies, asthma and gastro-esophageal reflux disorder and did not report of any speech, language, hearing or voice problems at the time of the study.

Instruments used: A portable, light-weight digital audio tape (DAT) recorder (Olympus digital voice recorder WS-100, Japan) was used. The recorder had in-built condenser microphone (ME 15) and the weight of the device was about 54 grams (including battery). The overall frequency response of the microphone was 100 Hz to 5000 Hz and size of the DAT recorder was about 94(L) x 40(W) x 15.1(T) mm. The sampling frequency was 12 kHz and the maximum power consumption of the DAT recorder was 100mWatts. PRAAT [14] software was used to extract fundamental and perturbation measures.

Recording procedures: The teachers in the study were ensured about the research objectives. The recording of voice samples was done on a regular workday (Monday) after a relaxed week end. The teachers were instructed not to over use the voice on the previous day (Sunday) and spend the day with more voice rest and adequate sleep. The DAT recorder was worn around the neck of the subject. The distance between microphone and mouth was 10-12 cm. The subjects were instructed to phonate the vowel /a/ for 5-6 seconds in their comfortable (habitual) pitch and loudness at four different time intervals of a workday - (1) before the first class i.e. condition 1, (b) after first class i.e. condition 2, (3) after lunch i.e. condition 3, and (d) after the last class i.e. condition 4. Also, the subjects were instructed to read the standardized Kannada passage (42 words). Both oral and written instructions for using the tape recorder and tasks to be performed were given to the subjects in advance.

Acoustic analyses: PRAAT software was used to extract fundamental frequency of phonation (pF0), standard deviation of fundamental frequency of phonation (SD pF0), jitter, shimmer and speaking/reading fundamental frequency (sF0). The measures like pF0, SD pF0, jitter and shimmer were measured from vowel /a/ phonation and sF0 from the Kannada reading passage. Statistical analysis: The mean and standard deviation of pF0, SD pF0, jitter, shimmer and sF0 were calculated from five teachers at four conditions. Non-parametric Friedman test was administered to check the differences between conditions. Wilcoxon signed ranks test was used to find out the pair-wise comparison.

3. RESULTS AND DISCUSSION

The mean fundamental frequency of phonation was 201 Hz at starting of the day i.e. before the first class. It rose to 212 Hz after the first class (condition 2) and after lunch, it dropped to 199 Hz. After the last class it increased to 203 Hz. Table 1 shows the mean and standard deviation of acoustic parameters measured across different conditions.

Table 1. Mean (M) and standard deviation (SD) of F0 and perturbation measures of teachers

SI No	Parameters	Condition 1 (Before I class)		Condition 2 (After I class)		Condition 3 (After lunch)		Condition 4 (After last class)	
		M	SD	M	SD	M	SD	M	SD
1	pF0 (Hz)	201	24	212	16	199	22	203	25
2	SD pF0 (Hz)	1.63	0.47	1.96	0.86	2.37	2.23	1.97	1.07
3	Jitter (%)	.30	0.1	0.30	0.12	0.34	0.16	0.50	0.22
4	Shimmer (%)	11.09	3.95	6.77	2.95	9.69	3.87	10.09	3.30
5	sF0 (Hz)	208	25	224	19	216	32	213	26

The SD pF0 was increased gradually from 1.63 Hz (condition 1) to 1.96 Hz (in condition 2), to 2.37 Hz (in condition 3) and decreased to 1.97 in condition 4. Though the SD pF0 decreased from condition 3 to 4, but it was higher when compared to condition 1. The jitter value was same in condition 1 and 2 (0.30%), then it rose to 0.34% (condition 3) and 0.50% (condition 4). It was noticed that the jitter value increased from condition 2 and was maximum in condition 4. The shimmer value was 11.09% in condition 1 and dropped down to 6.77% in condition 2. It was increased gradually from 9.69% (in condition 3) to 10.09% (in condition 4). Before the first class, the fundamental frequency of reading text (sF0) was 208 Hz and was increased to 224 Hz (condition 2). After lunch and after the last class, it was decreased to 216 Hz and 213 Hz, respectively.

Results of Friedman test revealed that there was a significant difference between conditions on pF0 values ($p<0.05$). No significant difference was noticed between conditions on SD pF0, jitter, shimmer and sF0 ($p>0.05$). Results of Wilcoxon signed ranks test revealed a significant difference between conditions 1 and 2 in pF0 ($p<0.05$). The pF0 was significantly higher in condition 2 compared to condition 1. The increased pF0 in condition 2 can be attributed to vocal warm-up. It was reported that vocal warm-up is a normal phenomenon that happens about 10-30 min after talking has begun [10]. In vocal warm-up, some adaptation of the voice apparatus obviously takes place and vocal and physical changes follow. However, the physiology behind the warm-up phenomenon is not well-known. Also, there was a significant difference between conditions 2 and 3 ($p<0.05$) on pF0. The pF0 was significantly higher in condition 2 compared to condition 3. After lunch, the value of pF0 dropped (condition 3) and it can be because of vocal resting during the lunch hour of 45 minutes where the teachers did not engage in louder talking. This finding was in consonance with the findings of Vilkman et al. [11] who reported a dropped F0 after lunch break. Figure 1 shows the graphical representation of changes in phonation fundamental frequency (pF0) across four conditions.

Comparison of beginning (condition 1) and end of the day (condition 4) samples revealed that the parameters pF0, SD pF0, jitter and sF0 were higher in condition 4 compared to condition 1. Increase in these values can be

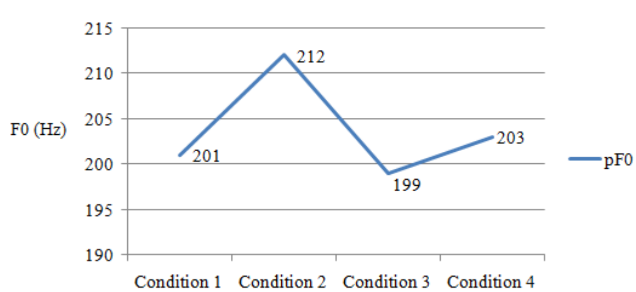

Fig. 1. Phonation F0 changes across different conditions

attributed to the prolonged voice use (workload) of teachers in a single regular workday. Except shimmer, other parameters increased from condition 1 to condition 4. Table 2 shows the mean and standard deviation of F0 and perturbation measures of teachers in condition 1 and 4.

Table 2. Mean (M) and standard deviation (SD) of F0 and perturbation measures of teachers between condition 1 and 4

SI No	Parameters	Condition 1 (Before I class)		Condition 4 (After last class)		Differences (Con4-Con1)	
		M	SD	M	SD	M	SD
1	pF0 (Hz)	201	24	203	25	2	1
2	SD pF0 (Hz)	1.63	0.47	1.97	1.07	0.34	0.6
3	Jitter (%)	0.30	0.1	0.50	0.22	0.20	0.12
4	Shimmer (%)	11.09	3.95	10.09	3.30	-1	-0.65
5	sF0 (Hz)	208	25	213	26	5	1

The standard deviation of fundamental frequency of phonation (SD pF0) increased from condition 1 to condition 4 by 0.34. Hammarberg [15] examined the relationship between voice disorders and SD F0, who found that larger than normal SD F0 accompanied a hyperfunctional, rough or unstable voice. Thus, increased SD F0 may indicate instability of laryngeal function and one possible reason for this could be impaired coordination of VF movements, which is a symptom of fatigue. Also, this result is in agreement with the findings of Rantala et al. [3] who reported increased SD F0 after loading. The jitter value also increased from starting of the day to end of the day. It was 0.30 % in condition 1 (before the first class) and increased to 0.50% in condition 4 (after the last class). The same findings was reported by Rantala et al. [3] and Gelfer et al. [8] who reported increased jitter value after vocal loading.

Unlike jitter, the shimmer did not show the same trend. There was a gradual reduction in shimmer value from condition 1 to 4. Vilkman et al. [11] and Rantala et al. [16] found increased shimmer after loading, but the present finding did not support their results. This could be due to less number of subjects or some methodological differences. The speaking/reading fundamental frequency (sF0) was high in condition 2 when compared to condition 1. Increase in F0 could be interpreted as a warm-up change connected with the initial adaptation of the apparatus to the loading. Resting of the apparatus pulls down the F0 value (condition 3) after lunch. Though, the sFo was less in condition 4 when compared to condition 3, but it was higher than in condition 1. The sF0 increased around 5 Hz between the beginning of the first class and end of the last class. The obtained result is in partial agreement with the results of Rantala et al. [3] who reported that the F0 increased about 9.7 Hz between the first and last lesson; also, the F0 increased about 7.24 Hz between the first class recording and last class recording [17].

4. CONCLUSION

The 'trend' followed at four intervals of time for pF0, SD pF0, jitter and sF0 (except shimmer) was same and uniform. There was an increase in pF0, SD pF0, jitter and sF0 after first class, followed by a reduction in these values after lunch. It can be inferred that vocal warm up has taken place after beginning of teaching. Then, the system learned to adjust with the demands of the classroom requirements. This laryngeal adjustment depends on the classroom situations. Hence there was a reduction in the afternoon. At the end of the day, the acoustic measures like- pF0, SD pF0, jitter and sF0 had higher values compared to the starting of the day. These observations were made on a single workday of five primary school teacher. Larger number of sample is warranted to generalize the results.

The pF0 increased by 2 Hz between the two conditions i.e., before first class and after last class; SD pF0 increased by 0.34 Hz, jitter increased by 0.20% and sF0 increased by 5 Hz. The frequency parameters which increased may be a consequence of the normal physiological adaptation of the vocal apparatus to loading and hence, a sign of healthy voice. But the perturbation measures like jitter and shimmer did not follow the trend as like frequency measures. Jitter shown increased value because of prolonged teaching, but shimmer did not. Hence, the frequency and perturbation measures (except shimmer) are sensitive enough to document the changes on voice in a single workday. Further investigation on vocal health of teachers and other professional voice users is warranted.

5. ACKNOWLEDGEMENT

This is a part of an outcome of the doctoral research of the first author. The authors would like to thank Dr. Vijayalakshmi Basavaraj, Director, All India Institute of Speech & Hearing, Mysore for granting permission to carry out this study. Also, authors extend their thanks to the subjects who participated in the study.

6. REFERENCES

[1] E. VILKMAN, 1999. Voice problems at work: A challenge for occupational safety and health arrangement. *Folia Phoniatrica Logopaedica*, **52**, 120-125.

[2] C. GOTAAS and C.D. STARR, 1993. Vocal fatigue among teachers. *Folia Phoniatrica Logopaedica*, **45**, 120-129.

[3] L. RANTALA, E. VILKMAN and R. BLOIGU, 2002. Voice changes during work: Subjective voice complaints and objective measurements for female primary and secondary school teachers. *Journal of Voice*, **16(3)**, 344-355.

[4] R.E. STONE and D.J. SHARF, 1973. Vocal changes associated with the use of atypical pitch and intensity levels. *Folia Phoniatrica Logopaedica*, **25**, 91-103.

[5] S.E. LINVILLE, 1995. Changes in glottal configuration in women after loud talking. *Journal of voice*, **9**, 57-65.

[6] R.L. NEILS and E. YAIRI, 1987. Effects of speaking in noise on vocal fatigue and vocal recovery. *Folia Phoniatrica Logopaedica*, **39**, 104-112.

[7] M.P. GELFER, M.L. ANDREWS and C.P. SCHMIDT, 1996. Documenting laryngeal change following prolonged loud reading: a videostroboscopic study. *Journal of voice*, **10**, 368-377.

[8] M.P. GELFER, M.L. ANDREWS and C.P. SCHMIDT, 1991. Effects of prolonged loud reading on selected measures of vocal function in trained and untrained singers. *Journal of voice*, **5**, 158-167.

[9] J.C. Stemple, J. Stanly and L. Lee, 1995. Objective measures of voice production in normal subjects following prolonged voice use. *Journal of voice*, **9**, 127-133.

[10] L. RANTALA, P. LIMDHOBA E. VILKMAN, 1998. F0 change due to voice loading under laboratory and field conditions: a pilot study. *Logopedics Phoniatrics Vocology*, **23**, 164-168.

[11] E. VILKMAN, E.R. LAURI, P. ALKU, E. SALA and M. SIHVO,1999. Effects of prolonged reading on F0, SPL, subglottal pressure and amplitude characteristics of glottal flow waveforms. *Journal of voice*, **13 (2)**, 303-315.

[12] A.M. LAUKKANEN, I. ILOMAKI, K. LEPPANEN and E. VILKMAN, 2008. Acoustic measures and self reports of vocal fatigue by female teachers. *Journal of voice*, **22(3)**, 283-289.

[13] J. VERSTRAETE, G. FORREZ, P. MERTENS and F. DEBRUYNE, 1993. The effect of sustained phonation at high and low pitch on vocal jitter and shimmer. *Folia Phoniatrica Logopaedica*, **45**, 223-228.

[14] P. BOERSMA and D. WEENINK, 2009. Institute of phonetic sciences, University of Amsterdam. Retrieved from http://www.praat.org/

[15] B. HAMMARBERG, 1986. Perceptual and acoustic analysis of dysphonia. [doctoral dissertation]. Stockholm, Sweden: Huddinge University Hospital.

[16] L. RANTALA and E. VILKMAN, 1999. Relationship between subjective voice complaints and acoustic paramerters in female teachers' voice. *Journal of Voice*, **13(4)**, 484-495.

[17] R. RAJASUDHAKAR and S.R. SAVITHRI, 2009. Voicing periods in a primary school teacher. *Journal of All India Institute of Speech & Hearing*, **28**, 36-41.

Acoustical Society of India
(Regn. No. 65-1971)

Executive Council (2010-12)

INFORMATION FOR AUTHORS

ARTICLES

The Journal of Acoustical Society of India (JASI) is a refereed publication published quarterly by the Acoustical Society of India (ASI). JASI includes refereed articles, technical notes, letters-to-the-editor, book review and announcements of general interest to readers.

Articles may be theoretical or experimental in nature. But those which combine theoretical and experimental approaches to solve acoustics problems are particularly welcome. Technical notes, letters-to-the-editor and announcements may also be submitted. Articles must not have been published previously in other engineering or scientific journals. Articles in the following are particularly encouraged: applied acoustics, acoustical materials, active noise & vibration control, bioacoustics, communication acoustics including speech, computational acoustics, electro-acoustics and audio engineering, environmental acoustics, musical acoustics, non-linear acoustics, noise, physical acoustics, physiological and psychological acoustics, quieter technologies, room and building acoustics, structural acoustics and vibration, ultrasonics, underwater acoustics.

Authors whose articles are accepted for publication must transfer copyright of their articles to the ASI. This transfer involves publication only and does not in any way alter the author's traditional right regarding his/her articles.

PREPARATION OF MANUSCRIPTS

All manuscripts are refereed by at least two referees and are reviewed by the Publication Committee (all editors) before acceptance. Manuscripts of articles and technical notes should be submitted for review electronically to the Chief Editor by e-mail or by express mail on a disc. JASI maintains a high standard in the reviewing process and only accept papers of high quality. On acceptance, revised articles of all authors should be submitted to the Chief Editor by e-mail or by express mail.

Text of the manuscript should be double-spaced on A4 size paper, subdivided by main headings-typed in upper and lower case flush centre, with one line of space above and below and sub-headings within a section-typed in upper and lower case understood, flush left, followed by a period. Sub-sub headings should be italic. Articles should be written so that readers in different fields of acoustics can understand them easily. Manuscripts are only published if not normally exceeding twenty double-spaced text pages. If figures and illustrations are included then normally they should be restricted to no more than twelve-fifteen.

The first page of manuscripts should include on separate lines, the title of article, the names, of authors, affiliations and mailing addresses of authors in upper and lowers case. Do not include the author's title, position or degrees. Give an adequate post office address including pin or other postal code and the name of the city. An abstract of not more than 200 words should be included with each article. References should be numbered consecutively throughout the article with the number appearing as a superscript at the end of the sentence unless such placement causes ambiguity. The references should be grouped together, double spaced at the end of the article on a separate page. Footnotes are discouraged. Abbreviations and special terms must be defined if used.

EQUATIONS

Mathematical expressions should be typewritten as completely as possible. Equation should be numbered consecutively throughout the body of the article at the right hand margin in parentheses. Use letters and numbers for any equations in an appendix: Appendix A: (A1, (A2), etc. Equation numbers in the running text should be enclosed in parentheses, i.e., Eq. (1), Eqs. (1a) and (2a). Figures should be referred to as Fig. 1, Fig. 2, etc. Reference to table is in full: Table 1, Table 2, etc. Metric units should be used: the preferred from of metric unit is the System International (SI).

REFERENCES

The order and style of information differs slightly between periodical and book references and between published and unpublished references, depending on the available publication entries. A few examples are shown below.

Periodicals:

[1] S.R. Pride and M.W. Haartsen, 1996. Electroseismic wave properties, *J. Acoust. Soc. Am.*, **100** (3), 1301-1315.

[2] S.-H. Kim and I. Lee, 1996. Aeroelastic analysis of a flexible airfoil with free play non-linearity, *J. Sound Vib.*, **193** (4), 823-846.

Books:

[1] E.S. Skudzryk, 1968. *Simple and Comlex Vibratory Systems*, the Pennsylvania State University Press, London.

[2] E.H. Dowell, 1975. *Aeroelasticity of plates and shells*, Nordhoff, Leyden.

Others:

[1] J.N. Yang and A. Akbarpour, 1987. Technical Report NCEER-87-0007, Instantaneous Optimal Control Law For Tall Buildings Under Seismic Excitations.

SUMISSIONS

All materials from authors should be submitted in electronic form to the JASI Chief Editor: Dr Mahavir Singh, Acoustics Section, National Physical Laboratory, Dr. K. S. Krishnan Road, New Delhi-110 012 (email: mahavir@nplindia.org Tel: +91-11-4560.9319, Fax: +91-11-4560.9310). For the item to be published in a given issue of a journal, the manuscript must reach the Chief Editor at least twelve week before the publication date.

SUMISSION OF ACCEPTED MANUSCRIPT

On acceptance, revised articles should be submitted in electronic form to the JASI Chief Editor (mahavir@nplindia.org)